MOLECULAR MECHANISM OF COLD INDUCING RBM3

By

Min ZHANG

A Thesis Submitted to

the Department of Biology, Chemisty, Pharmacy

of Freie Universität Berlin

To obtain the Academic Degree

Doctor rerum naturalium (Dr. rer. nat.)

August 2022, Berlin

The work presented in this dissertation has been performed between September 2018 to August 2022 under the supervision of Prof. Dr. Florian Heyd at the Free University of Berlin, Department of Biology, Chemistry, Pharmacy, and under the supervision of Prof. Dr. Wei CHEN in Southern University of Science and Technology, Department of Biology. I hereby declare that this dissertation was written and prepared by me independently. Furthermore, no sources and aids other than those indicated have been used. Intellectual property of other authors has been marked accordingly. I also declare that I have not submitted the dissertation in this or any other form to any other institution as a dissertation.

First reviewer: Prof. Dr. Florian Heyd

Second reviewer: Prof. Dr. Wei CHEN

Disputation on: Feb. 7, 2023

ACKNOWLEDGEMENTS

First, I would like to thank my mentor Prof. Dr. Florian Heyd for his support and appreciate him to give me the opportunity to study in the Free University of Berlin. His knowledge, preciseness, straightforwardness and hard work impress me a lot, and I learn a lot from him including science and other aspects. Especially, he suggests me to perform the fantastic RBM3 project, which perfectly matches with my previous background, and I like it so much.

Second, my great appreciations will be given to Prof. Dr. Wei CHEN in the Southern University of Science and Technology. With his guidance, I performed an interesting project regarding alternative polyadenylation in his lab, which I didn't show in the thesis as it is totally different topic from the stories I wrote here.

I also want to express my great gratitude to Dr. Marco Preußner, who initiates RBM3 project. His constructive discussion and suggestion help the projects go well. He also helped me a lot to address some problems of my daily life in berlin. I will not forget him all my life.

Further, my friend, Dr. Bin ZHANG, an expert in bioinformatics analysis, helped for the bioinformatics analysis part in the thesis. Without his help and useful discussion, I couldn't make the G4 thermo-sensor story to a genome-wide scale mechanism. Hope our future collocation also goes well.

The lab manager Dipl. Ing. Antje Grünwald and technician Bobby Viet Draegert should be greatly appreciated for helping me daily work in the FU Heyd lab. When I had some problems not only regarding scientific research not also my life, they always kindly helped me in time. Without their help and understanding, I couldn't finish my PhD thesis within the short time.

Further, thank all the lab mates in Heyd lab and Chen lab. Without their help, my thesis could not be finished. My great appreciation will be given to all my friends for their encouragement and help during my study in Berlin.

Great appreciations next will be given to my mother, my father, mother-in law, and father-in law as they always support me a lot and help me to take care of my little kid, Shuhan, when I am not in China. My big brother always trusts me and supports me when I confronted difficulties in both research and life.

Last, but not least, my special great appreciations will be given to Dr. Xiaofei WU, my husband, for his continuous encouragements in my life. Dr. WU spends a lot of time playing with and looking after our little son after work even though as a computer scientist, he is also busy with his work. Due to the Corona pandemic, it is very difficult for me to travel back home in China. Thank him for what he has done for our little kid, Shuhan WU. With his support, I can confidently insist on my dream and do the scientific research, which I love very much. I hope that the Dr.rer.nar.thesis is not the final destination of my research career.

Min ZHANG

August 2022, Berlin

Table of Contents

Summary

Alternative splicing is a prominent and sophisticated molecular machinery in gene regulation. It is well-known that temperature, as a crucial factor, can influence alternative splicing to further modulate gene expression.

In this thesis, we first focused on the RNA binding motif protein 3 (RBM3), a well-known cold-induced protein, to decipher the molecular mechanism how cold induces RBM3 expression. A "poison" exon, exon 3a, in the RBM3 mRNA isoforms was successfully identified to be responsible for the degradation of RBM3 transcripts at normal and high temperature. Briefly, the "poison" exon 3a containing premature termination codons (PTCs) can elicit non-sense mediated decay (NMD) of the transcripts. At normal and high temperature, the "poison" exon is substantially included, which induces the NMD of RBM3 transcripts, and RBM3 expression is downregulated; at low temperature, exon 3a is majorly exclusive, resulting that RBM3 transcripts escape from the NMD, and RBM3 expression increases. Next, two strong exonic splicing *cis*-regulatory enhancer (M2 and M4) were determined via mutagenesis screening to potently promote exon 3a inclusion at normal and high temperature. Antisense oligonucleotides (ASOs) (2'-O-MOE and morpholino chemistry modification), targeting M2, M4 motif and 5' splice site (SS) in the exon 3a RNA, efficiently increase endogenous RBM3 expression at both mRNA and protein levels in both HEK293T and neuroblastoma N2a cells. Given that the evolutionary conservation of "poison" exon 3a of RBM3 between humans and mice, it is conceivable that the effective ASOs can be potentially and therapeutically used in clinic, such as cardiac arrest, moderate or severe neonatal encephalopathy or even some neurodegenerative diseases, as RBM3 has been well demonstrated to protect neurons in *vivo* through mediating structural plasticity in mice before.

Next, for the first time we report that in mammalian cells RNA itself can directly sense temperature alterations though "spliceswitch", G-quadruplex (G4) structures to modulate alternative splicing and further regulate gene expression. Utilizing RNA sequencing data of human cells at different temperatures, we found that RNA G4 (rG4) motifs are significantly enriched around splice sites of cassette exons repressed upon cold shock. We further validated that formation/stabilization of rG4 indeed effectively mask splice sites, which decreased exon inclusion in several cold-repressed exons of several different genes, showing that G4 stabilizer ligand (PDS) could decrease the inclusion of cold-repressed exons at four temperatures. Taking RBM3 as an example, we found that stabilizing G4 through PDS can significantly decrease the

inclusion of RBM3 exon 3a in cells. Meanwhile, the putative G4 motifs (G1) of RBM3 is manifested to form real rG4 *in vitro* by biophysical assays. Under low KCl condition, G4 signal is temperature sensitive, showing higher signal at low temperature; while under high KCl condition, its temperature sensitivity is not significantly obvious. Intriguingly, the stability of G4s across different temperatures is reversible, presenting that rG4 signal gradually decreases from 33°C to 40°C, and then if the temperature goes back to 33°C from 40°C it returns to the signal level at 33°C. Furthermore, stabilizing rG4s in RBM3 exon 3a is also capable of increasing endogenous RBM3 expression at both mRNA and protein levels at only high temperature, but not at low temperature. In conclusion, rG4s are stable enough at low temperature to mask splice sites, thereby promoting "poison" exon 3a exclusion, so stabilizers are less effective for the stabilization of rG4s in this scenario; while at high temperature rG4s are predominantly unstable to make the G4 stabilizers present their effects more easily. Our results unveil an unexpected mechanism how temperature perturbations are directly sensed by RNAs and integrated into gene expression programs via spliceswitch, which might provide a novel avenue to treat disease caused by splicing defects.

Finally, considering that both *cis*-regulatory enhancer elements M2 and M4 and repressive G4 motifs can modulate the alternative splicing of RBM3 "poison" exon 3a, we asked how these elements cooperate each other, and further whether there exist other *cis*-regulatory element networks to be involved in the regulation of alternative splicing. Systematic CRISPR-dCasRx perturbation sliding on the "poison" exon 3a and its flanking introns clearly show that several gRNA clusters targeting M2, M4, 3'SS (G1), G3 and 5'SS, increase endogenous RBM3 expression with higher fold-changes at high temperature than that at low temperature. This indicates that M2, M4 enhancer and G4 structure (G1 and G3 motif) may be the strongest *cis*-regulatory elements modulating exon 3a inclusion. By virtue of the relatively low resolution of CRISPR-dCasRx screening, to further deeply dissect the *cis*-regulatory network regulating exon 3a inclusion, we sequentially mutated the sequence surrounding alternative splice site in the exon 3a and its flanking intronic region. An exonic *cis*-regulatory element in the proximity to the downstream of alternative splice site was successfully identified to inhibit the usage of alternative splice site. Meanwhile, several intronic *cis*-regulatory elements in vicinity to each other in distance were determined to be involved in enhancing or repressing exon 3a inclusion. To further understand the coordinated network of *cis*-inhibitory and -enhancing regulatory elements in achieving the regulation of temperature sensitive RBM3 exon 3a inclusion and simplify the model as well, we took enhancer M4 and repressive motif G1 and G3 as

representative examples to build a working model which manipulates RBM3 exon 3a inclusion. At low temperature (33°C) both G1 and G3 repressive activity are dominant, while the enhancer activity of M4 is more powerful than the repressive activity of G3 at high temperature (40°C). At 37°C, repressive activity of G1 and G3 is almost identical to the enhancer activity of M4. Finally, we showed that both phosphatase and CLK inhibitor influenced the inclusion of "poison" exon 3a just at high temperature, but not at low temperature, suggesting that G4 activity is indispensable of phosphorylation, and M2 and M4 function dependently on the phosphorylation status of *trans*-acting factors.

In summary, three independent and connected stories with high novelty in the dissertation were successfully conducted: 1) discovered the mystery how RBM3 expression is cold-induced in a post-transcription level and developed ASOs to boost RBM3 expression, which may potentially protect neurons at normal temperature in clinic; 2) proposed and demonstrated RNA serves as physiologically direct thermo-sensors via spliceswitch formed by G-quadruplex in mammalian cells. Importantly, the "poison" exon 3a of RBM3 is one of the cold-repressed exons (CRE) candidates with G4 near splice sites. This illuminates that stable RNA G4s at low temperature in the splice sites of exon3a, which influence the utilization of splice sites, are one of the reasons that cold represses "poison" exon 3a inclusion; 3) fine-tuned mapping *cis*-regulatory elements , that modulate RBM3 exon 3a inclusion and deciphered the coordinated *cis*-regulatory network of alternative splicing of exon 3a.

Key words: temperature-sensitive alternative splicing, non-sense mediated decay, *cis*-regulatory element, antisense oligonucleotide, RNA G-quadruplex

Introduction

1 Molecular mechanism of alternative splicing

Substantial studies have shown that splicing is one of the most essential cellular events in gene regulation. A gene is conventionally composed of multiple exons and introns, introns in the precursor mRNA (pre-mRNA) are efficiently co-transcriptionally or post-transcriptionally excised out, and exons are ligated together to produce mature mRNA. Meanwhile, most of the excised-out introns are debranched and degraded within seconds[1-5]. The process is termed as splicing. If the intron is not effectively spliced out, it is intron retention. Correct recognition of exons and removal of introns are quite conserved and crucial cellular machineries. Most of the processes in splicing are catalytically achieved by the spliceosome comprised of stepwise assembled protein complexes at different splicing stages. Briefly and canonically, a couple of splicing consensus elements and splicing complex proteins are involved in splicing. U1 snRNP (U1) recognizes approximately conserved 5'splice site (SS) (AGGTAAGT), which is also called donor of splicing; U2AF35 binds to AG site of 3'SS named as acceptor; U2AF65 interacts with polypyrimidine; SF1 is associated to branch point; and the complex in the stage is called E complex. Then, SF1 dissociates with branch point, and U2snRNP (U2) binds to branch point, promoting U1 to interact with U2 and U2AF. Here, the assembled complex on the pre-mRNA is named A complex. Next, U2AF35 and U2AF65 leave pre-mRNA, and U4, U5, and U6 come to associate with U1 and thus B complex is composed of U1, U2, U4, U5 and U6. Subsequently, U1 and U4 disassociate with B complex, leading active B* complex formation. B* complex is further rearranged into C complex, which catalyzes the exon ligation and intron lariat removal[6] (**Fig. 1.1**).

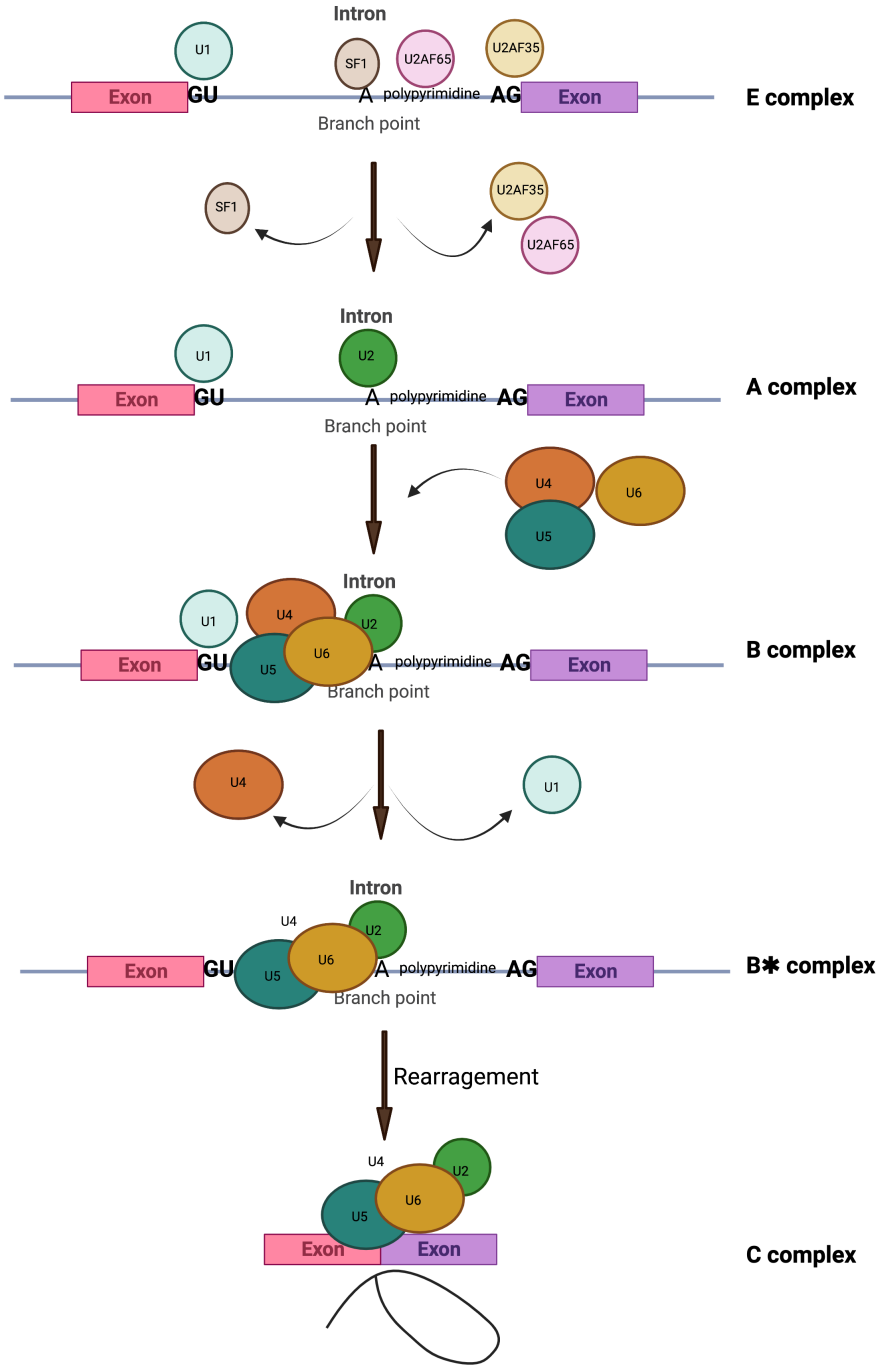

Figure 1.1 Schematic for different stages of splicing machinery. U1 to U6 bind to sequences of pre-mRNA to catalytically initiate the chemical reactions step by step, resulting that both 3' splice site and 5' splice site are ligated together, and intron lariats are removed. U1, U2, U4, U5, U6 represent U1 snRNP, U2 snRNP, U4 snRNP, U5 snRNP and U6 snRNP, respectively.

In the splicing machinery, most of exons are constitutively included, while some are alternatively spliced in various scenarios. This phenomenon is referred as alternative splicing, which is one of the major molecular mechanisms to accomplish the complex of transcriptome

in multicellular organisms[7]. It was estimated that at least 60% of human genes undergo alternative splicing[6,8], and 70% to 90% of alternative splicing influence the coding capacity of a gene[9]. In a particular gene, its splicing pattern is possibly distinct in differential tissues, presenting even more than thousands of splicing patterns. Also, the alterative splicing pattern can significantly change in different cellular conditions or stresses, which adds more layers of complexity in the regulation of alternative splicing. Accordingly, splice site selection must be intricately modulated at different molecular layers in cells. In myriads of studies have reconciled that, except for the loose consensus of 5'SS, 3'SS, branch point, polypyrimidine tract and their corresponding core splice factors (U1 to U6), the fine-tuning alternative splicing is highly dependent on the auxiliary factors, such as *cis*-regulatory element and its relevant *trans*-acting binding factor, RNA secondary structure, even transcription rate, chromatin structure and RNA modification. These factors together contribute to the complex of transcriptome repertoire to further produce complicated proteome[10]. It's too ambitious to discuss all the aspects in the thesis, and I will just summarize how alternative splicing is modulated by the following three major factors: *cis*-regulatory element and *trans*-acting factor, RNA secondary structure and transcription rate.

1.1 *Cis*-regulatory element and *trans*-acting factor

The RNA sequence responsible for the U1 to U6 recognition is centrally predominant in the process of alternative splicing, but their recognitions are also influenced by other additional *cis*-regulatory elements. These elements can enhance or repress the whole splicing reaction circle through various mechanisms. In accordance with their genetic locations and functions in splicing, they are classified as exonic splice enhancer (ESE), intronic splice enhancer (ISE) and exonic splice silencer (ESS) and intronic splice silencer (ISS). These *cis*-regulatory elements are identified via in silico sequence alignment and/or experimental demonstration in the wet lab and are usually relatively conserved across species. Additionally, a plenty of potential *cis*-regulatory elements have been identified to be *cis* elements of a specific *trans*-acting factor with in *vitro* assays, such as SELEX[11] and various CLIP methods[12]. It appears that they mechanically act differentially in the splicing machinery.

U1 to U6 are key *trans*-acting factors to associate with RNA sequence modulating alternative splicing, and meanwhile other *trans*-acting factors also can be recruited to the auxiliary *cis* elements to influence splicing machinery. These *trans*-acting factors are usually RNA binding proteins. In general, SR family act as enhancers[13], while hnRNP family serve as repressors[14].

Of course, their functions are not absolutely settled as SR family also can repress alternative splicing and hnRNP family can promote splicing as well in some settings. One of the most interesting aspects in *trans*-acting factors involved in splicing, is their phosphorylation-dependent activities, showing that both hyper- and hypo-phosphorylation can inhibit or enhance splicing. Additionally, *trans*-acting factor also can be non-RNA binding proteins, which are lacking RNA binding domain, and they must be cooperatively assembled with other proteins to target the RNA sequences[15-17].

1.1.1 Genome-wide high-throughput analysis

5'SS and 3'SS are not absolutely conserved in the differential exons across species, instead that they are degenerate in many cases. Alexander B. Rosenberg *et al*. constructed a library with millions of synthetic 5'SSs and 3'SSs in several gene contexts. With this comprehensive screening, they concluded that *cis*-regulatory elements acted addictively rather than cooperatively. Referring to the RNA-seq data, they further trained a model to predict the influence of single nucleotide polymorphisms (SNP) in the exon inclusion with high accuracy[18]. To examine the complexity of 5'SS determining the selection of splice site*s*, Mandy S Wong *et al*. developed three libraries containing thousands of minigenes with differential 5'SSs and found the major determinant of 5'SS usage was the intrinsic sequence. Gene context also had tremendous influence in splice site usage, showing that a weak upstream 3'SS induced the context dependence of 5'SS activity in IKBKAP minigene[19].

Auxiliary splicing element networks are complicated in the regulation of splicing. To identify potential ESE, randomized 18-nt library was inserted into downstream of an exon from a *Drosophila* doublesex gene (*dlx*), and then functional enhancers were enriched in multiple rounds of *in vitro* splicing. Ultimately, six classes of recurring degenerate sequence motifs, which were capable of being activated by specific serine/arginine (SR)-rich splicing factors, were identified. This study also implicated that SR protein could interact with a broad spectrum of degenerated RNA sequences[20]. Bioinformatically, RESCUE-ESE was developed to predict the ESE in human genome, and 10 ESE motifs were successfully predicted with the algorithm, demonstrated by abolished enhancer activity after point mutation[21]. Zefeng Wang *et al.* inserted random 10 mer into a chimeric minigene reporter, which was composed of exon 2 of the Chinese hamster dihydrofolate reductase (DHFR) gene, its flanking introns, and split GFP exons, to systematically screen ESS modulating the alternative splicing of DHFR exon 2. The screening produced 141 ESS decamers, which could be clustered into 7 putative ESS motifs,

and some of them belonged to hnRNPH and hnRNPA1[22]. Although this is artificially gene context, it demonstrated that ESS could dominantly affect the exon inclusion in some contexts.

In a genome-wide scale, *trans*-acting factors synergistically or antagonistically regulate the complicated alternative splicing events. Using splicing-sensitive arrays and CLIP-seq in mouse embryo fibroblasts (MEFs), Shatakshi Pandit *et al*. showed that both SRSF1 and SRSF2 could not only promote, but also repress exon inclusion *in vivo*, and their binding pattern couldn't explain the opposite effects. Further detailed analysis demonstrated that the response caused by loss of SRSF1 or SRSF2 was accompanied with synergetic loss or compensatory gain of other proteins in the affected exons[23]. Therefore, the effect of one SR protein on the splicing regulation is highly dependent on the complicated interplaying with other proteins. Genome-wide CRISPR-Cas9 screen was also used to identify the potential *trans* to modulate alternative splicing of neuronal microexon in MEF2D gene. Around 200 regulators, including protein turnover, chromatin, and RNA processing factors, were identified to contribute to the alternative splicing event. Overexpression of SRSF1 and RNPS1 strongly enhanced the microexon inclusion. Importantly, this study identified an entire signaling pathway involved in the microexon regulation and suggested that the splicing regulation of microexon is a complicated process[24]. Jernej Ule *et al*. deciphered the molecular mechanisms of Nova regulating alternative splicing through combining bioinformatics, biochemistry, and genetics assays. They showed that Nova genome-widely binding to the exonic YCAY clusters strongly inhibited the exon inclusion through blocking the U1snRNP recruitment, whereas exon inclusion would be enhanced when Nova was associated with intronic YCAY cluster because the binding promoted the spliceosome assembly[25]. This study demonstrated that the binding position of *trans*-acting factor influenced its activity of splicing regulation.

1.1.2 Mechanism study in an individual gene

With the tremendously increasing studies, numerous *cis*-regulatory elements and *trans*-acting factors have been individually uncovered to be involved in the regulation of alternative splicing. Here, the neuronal alternative splicing is mainly focused on as the target gene of the thesis, RBM3, is related to hypothermia and functions to protect neurons. Also, just some of the classical *cis* and *trans* are classified into ESE, ESS, ISE, and ISS groups to discuss here (**Fig. 1.2**).

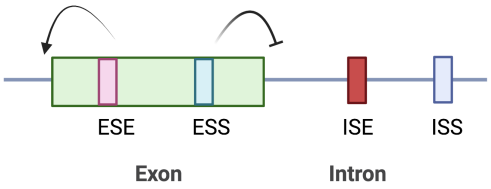

Figure 1.2 Position diagram of different *cis*-regulatory elements in the exon and intron. ESE: exonic splicing enhancer, ESS: exonic splicing silencer, ISE: intronic splicing enhancer, ISS: intronic splicing silencer.

ESE

The best characterized ESEs in neurons are serine-arginine-rich SR or SR-like family[26,27]. The RNA association of SR enhancer protein usually promotes the recruitment of U1snRNP or U2snRNP or counteracts with repressor protein to block/inhibit their binding to RNA. The C to T mutation in SMN2 gene tremendously inhibits the exon 7 inclusion, and Luca Cartegni *et al*. revealed that the mutation site was the position of ESE, and the binding of SRSF1 was abolished by the single base mutation[28]. Additionally, Htra2-β1, a SR-like protein, was also demonstrated to promote exon 7 inclusion of SMN2 through binding to the exonic AG-rich motif[29].

ESS

The negative regulation factor in the exon is mainly the protein of hnRNP group. In exon 4 of the CD45 gene, mutation of the ESS1 dramatically decreases the binding of hnRNPL to RNA, and depletion of hnRNPL caused the increasing of exon 4 inclusion. Thus, hnRNPL was identified to specifically bind to the ESS1, thereby inhibiting the exon 4 inclusion[30]. Similarly, several nucleotides at the 5′ end of exon 7 was identified as *bona fide* ESS to repress exon 7 inclusion via directly binding to hnRNP H, and it was further demonstrated by the increased exon 7 inclusion caused by partial depletion of hnRNPH via antibody against hnRNPH in the *in vitro* splicing reaction and the rescued inhibitory effect after addition of purified hnRNPH[31].

ISS

In adenovirus L1 mRNA, SRSF1 interacts with the elements adjacent to branch point to block 3'SS in the early infection stage, while the dephosphorylated SRSF1 disassociates with RNA, thereby unblocking the 3'SS in the late stage of infection[32-34]. The RNA binding protein Sex lethal (Sxl), which is specifically expressed in female flies, dramatically inhibits the male

specific splicing pattern. Sxl binds to the 9-nt U-rich element of the target transcripts, such as Transformer (Tra) and Male-specific lethal 2 (Msl2). In Tra pre-mRNA, Sxl binds to the U rich element in vicinity to proximal 3'SS of exon 2 to block the recognition of U2AF, thereby leading to the usage of distal 3'SS. In this case, the exon containing stop codon is excluded in the presence of Sxl, producing active Tra protein in female files. For the Msl2 transcripts, Sxl protein directly binds to the polypyrimidine near the 3'SS and the U rich element adjacent to 5'SS in the intron 1, resulting in the dramatical inhibition of both 5' and 3'SS utilization, and thereby Sxl causes intron 1 retention[35].

As a famous splicing repressor family, polypyrimidine tract binding protein 1 (PTBP1) doesn't express in mature cells, such as neurons and muscle cells, but in neuronal stem cells; whereas PTBP2 is found in neurons and muscles, and PTBP3 is in liver cells[36,37]. PTBP family was shown to bind CU rich in the intron to repress splicing. Inhibition of PTBP1 strongly converts fibroblasts into the neurons[38] or astrocytes into neurons[39,40], showing that different astrocytes from distinct brain regions can be converted into different subtypes of neurons. One of the interesting targets of PTBP1 is exon 10 of PTBP2, and PTBP1 significantly represses exon 10 inclusion of PTBP2. The exclusive exon 10 causes translational frameshift and is coupled with non-sense mediated decay (NMD) of PTBP2, thereby reducing PTBP2 expression[37,41]. PTBP1 and PTBP2 also repressed the exon 18 inclusion of PSD95, and the exon 18 exclusive transcript is coupled with NMD of PSD95 transcripts as well. During neuronal development, the decreasd expression of PTBP1 and PTBP2 makes exon 18 inclusion isoform dominant in a time dependent manner, resulting that more PSD95 production in mature neurons. In non-neuronal cells, high expression of PTBP1 dramatically represses exon 18 inclusion, so the PSD95 is subject to NMD, leading to almost no PSD95 expression. In contrast, in neurons, less PTBP cannot sufficiently inhibit exon 18 inclusion, more exon 18 containing isoforms are produced, and thus PSD95 highly expresses in neurons[42].

NOVA2 binds to the YCAY clusters in the flanking intron region of Dab1 exon 7b and 7c in the time window from E10 to P0, thereby strongly inhibiting the exon inclusion. As Dab1 is important in neuronal migration, overexpression of exon 7b and 7c inclusion isoform causes abnormal neuronal migration, suggesting that Dab1-7b/7c isoform may has antagonizable role with WT Dab1, and balance between these isoforms is critical for neuronal migration[43].

ISE

Some 5'SSs are found to be activated by the adjacent intronic U-rich elements. In Msl2[44] and K-SAM[45], TIA2 binds to the U-rich elements at the downstream 5'SS to activate spliceosome assembly, thereby promoting splicing machinery. Another ISE is UGCAUG, which is in the downstream intron of c-src, fibronectin, non-muscle myosin heavy chain (NMHC) exon, calcitonin and several neuronally regulated exons[46-48]. Mutagenesis analysis shows the intronic hexamer is essential to strongly promote splicing machinery. However, when the UGCAUG appears in the upstream intron of exon, it represses exon inclusion. Thus, the regulatory activity of UGCAUG in alternative splicing also seems to depend on its position[49]. Later, the corresponding binding protein of UGCAUG was demonstrated as RBFOX family[49]. SRRM4, a neuronal specific protein, binds to the UCG-rich region between polypyrimidine tract and 3'SS[50], and is associated with early spliceosome components, indicating its important role in early spliceosome assembly[51]. siRNA knock-down of SRRM4 significantly reduces exon inclusion, suggesting the function of SRRM4 in promoting the exon inclusion[50]. It has shown that the most frequent motif surrounding SRRM4 binding site is PTBP binding motif, and this illustrates that SRRM4 may antagonize with PTBP[51]. The evidence that around 1/3 *in vivo* targets of SRRM4 overlap with PTBP1 also demonstrates their antagonistic effects on alternative splicing modulation[52].

In summary, the alternative splicing is a complicated cellular process, and the fact that transcripts of *trans*-acting factors also undergo alternative splicing adds another more sophisticated layer to the regulation. Deeply uncovering the molecular mechanisms will help to find more therapeutic targets in clinic.

1.2 RNA secondary structure

1.2.1 Genome-wide high-throughput analysis

When we discuss RNA secondary structure *in vivo*, the first essential question we need to ask is: does RNA secondary structure exist *in vivo*? Genome-wide RNA-secondary structure mapped with dimethyl sulfide (DMS) demonstrated that RNA is indeed less folded *in vivo* than *in vitro*. For example, a stem loop structure in RPL33A predicted by algorithm was strongly supported by *in vitro* structure data, while the *in vivo* DMS-seq showed almost little structure there[53]. RNA secondary structure *in vivo* is possibly determined not only by its own

thermodynamics' stability but also by the presence of RNA binding protein and ATP-dependent helicase*s*. It has shown that RNA structure remarkably increases after ATP depletion *in vivo*[53]. Importantly, Natalia Sanchez de Groot *et al.* showed that RNA structure could drive the interaction with proteins because a dearth of double-stranded regions of RNA correlate with numerous protein contacts[54]. Although active unfold RNA occurs *in vivo* due to some factors, RNA secondary structure indeed exists with increased signal in some scenarios *in vivo* beyond all doubts.

The association of RNA secondary structure with splicing has been presented by several groups in plants. In *Arabidopsis thaliana* seedlings, Structure-seq, which firstly shows the detailed *in vivo* genome-wide analysis information of RNA structure, has determined that strong RNA secondary structure at the proximity region of 5'SS in the exon is positively correlated with non-spliced transcripts, whereas no obvious signal at both 3' and 5' SSs in the spliced transcripts[55,56]. This gives us implication that the RNA secondary structure at 5'SS may inhibit splicing events although the possibility of protein protection effect cannot be ruled out to lead the low DMS reactivity, thereby resulting in high structure signal. Indeed, Sager J. Gosai *et al*. used a ribonuclease-mediated protein foot printing approach to simultaneously observe RNA binding protein (RBP) binding and secondary structure profile in 10-day old seedling nuclei (around 40% mRNA are pre-mRNA). They found the landscape of RNA protein binding had anti-correlation with that of secondary structure, indicating that the RBP can protect the RNA from the accessibility of structure profile reagents, leading to ablation of the structure signal[57]. Thus, this further demonstrated that the structured signal in common structure mapping, such as DMS, is also probably single stranded RNA with RBP binding[58]. Of course, we need to consider that single stranded RNA may also form secondary structure *in vitro* due to some unknown mechanisms, such as temperature change, in Sager J. Gosa's method. Importantly, they found higher structure score in both 5' and 3'SS surrounding regions (within splice site 30 bp) and introns compared to exonic regions, suggesting that RNA secondary structure may contribute to alternative splicing. Also, the intron retention transcripts were identified with more structured and occupied by RBPs within this region[57], and this indicates that intron retention is possibly attributable to the hinderance of spliceosome assembly by RBP binding and RNA secondary structures although whether it is the direct cause or the cause-result relationship needs to further determined. Zhenshan Liu *et al*. constructed *in vivo* nuclear RNA structurome in plants and identified significantly higher SHAPE reactivity at the upstream of 5'SS in spliced transcripts than non-spliced ones. Artificial insertion of stem loop to the 5' ss

extraordinarily disrupts the splicing event, while mutants, which loosened the stem loop with mutation at the complementary base of splice site AG, strongly reduces the repression activity of stem loop in splicing machinery[59].

In *Drosophila melanogaster*, phylogenetic comparisons identified 202 conserved pairs, which can form stable stem loop structure, among 12 *Drosophila* genomes. These elements are in the alternatively spliced introns, long introns and adjacent to weak splice sites. Thus, the base paired sequence can loop out the intron to shorten the distance of 3'SS and 5'SS, contributing to intron definition. Also, they can potentially mask the splice sites, and mutagenesis indeed shows that the mutation, destabilizing the stem loop structure, promotes the usage of adjacent splice sites[60].

Some strong and novel structured introns have been identified to be capable of bypassing the necessity of U2snRNP and relative *trans*-acting factor in the splicing machinery as these structured introns loop out the intron and bridge the splice sites together to promote the splicing reaction in fish. In eukaryotes, the self-splicing group II intron is a mitochondrial RNA tertiary structure that is absent in vertebrates but essential for respiration in plants, fungi, and yeast. If the RNA structure is destroyed by small molecules, the growth of fungi will be significantly inhibited[61].

A natural RNA aptamer (some small molecules and usually cellular metabolites) specifically binding to a particular conformation of "riboswitch" can influence the availability of splice sites and branch points, so splicing machinery can be altered in this case. Modulating alternative splicing through riboswitch has been characterized in bacteria[62], filamentous fungi[63,64], green algae[65], and higher plants[66,67]. The RNA sequence sensing riboswitch is relatively conserved in fungi, and bioinformatics analysis has showed that 23 genes cross 11 species of filamentous fungi remain riboswitch. Fungal TPP (Thiamin pyrophosphate) riboswitch from *Neurospora crassa* shows that the RNA structure masks the intronic 5'SS at low TPP concentration, while the structure changes to release the internal splice sites at high TPP concentration. Therefore, the splice site selection is distinct at different TPP concentrations[68]. For example, in green algae, the riboswitch TPP can influence the accessibility of branch points to regulate alternative splicing in THIC and THI4 genes; 5'SS accessibility also can be modulated by TPP through RNA secondary structure in NMT1, TH14 and NCU01977.1 gene of Filamentous fungi[64]; in higher plants, THIC gene is the only gene, whose 5'SS is masked or not in different concentrations of TPP[67], to be identified so far. In

humans, few riboswitches are reported, but it is possible that there are riboswitches in human genome recognized by some small molecules. G4 probably can be regarded as riboswitch given that potassium can stabilize it.

In humans, with the PARS (Parallel Analysis of RNA Structure) method, it has been identified that the acceptors are occupied with more structured motifs, whereas the donors are less structured in the exon-exon junction region in human lymphoblastoid cell lines[69], indicating that these structure signatures may contribute to the splicing machinery. More interestingly, single nucleotide variants cause genome-wide structural change (riboSNitches) in a human family trio (mother, father, and their child) shown with 1907 riboSNitches events determined from 20,000 SNPs. For example, the SNP of MRPS21(a single base change from A to C) significantly changes its RNA structure[69]. Svetlana Kalmykova *et al.* bioinformatically identified a dearth of pairs of conserved complementary regions (PCCRs) and found CCR was more enriched in the cryptic and inactive splice site groups than active splice site group. This indicates that the potential base-pairing group could mask the splice site to repress splicing machinery[70]. Alternative exons have more *Alu* elements in their flanking intron than constitutive exons[71], indicating that *Alu* elements may mediate the splicing types of their flanking exons. Elana Miriami *et al.* in *silico* identified two highly enriched conserved groups of *cis* elements (pyrimidines: mostly C residues; purines: mostly G residues) in the relative conserved positional order of upstream and downstream flanking introns of skipped exons. Surprisingly, these two groups are complementary and can be base paired each other well, and thus one hypothesis comes out that the stem loop-like secondary structure can loop out the exon, resulting in its exclusion[72].

Although many *trans*-acting factors have consensus binding motifs from the *in vitro* SELEX enrichment or in cell profiling (such as iCLIP, PAR-CLIP *etc.*), not all enriched *cis* elements are associated with the splicing factors. Additionally, these high-throughput methods also give us some degenerate RBP binding motifs. The evidence indicate that the *cis* elements are necessary but are not sufficient for the *trans*-acting factor binding in some cases. RNA secondary structure may be another layer to be involved in the intricated splicing modulation. RNA modification also can affect alternative splicing through altering the RNA structure. Combining PAR-CLIP (hnRNPC) and M6A-immunoprecipitation, Nian Liu *et al.* identified more than 39,060 site, in which more than 2,500 sites of HNRNPC-binding signal significantly decreased when the adenine methylation at position 6 dramatically reduced after

methyltransferase knock-down, and the signal of these binding sites was also coupled with alternative splicing, showing less methylation, more exon exclusion. The genome-wide mechanism is termed "m6A-switch" as PolyU elements, that hnRNPC bind to[73], are enriched in the stem region of RNA structure, and the methylated adenine in this structure leads the stem loop more loose, thereby promoting the accessibility of hnRNPC to polyU[74] to influence the efficiency of alternative splicing machinery.

It has been discussed and demonstrated that *cis*-regulatory elements cooperated with RNA secondary structure to regulate splicing reactions[75]. Robert C. Spitale *et al.* found the computational prediction of RBFOX2 binding site was improved if they combined the known UGCAUG consensus of RBFOX2 binding sequence with icSHAPE (*in vivo* click selective 29-hydroxyl acylation and profiling experiment), an RNA secondary structure profiling method, with the reference of iCLIP RBFOX2 dataset[76]. This study also implicates that combination of binding consensus and local RNA secondary structure to develop algorithms is feasible and achievable direction to predict the binding site of a particular *trans*-acting factor.

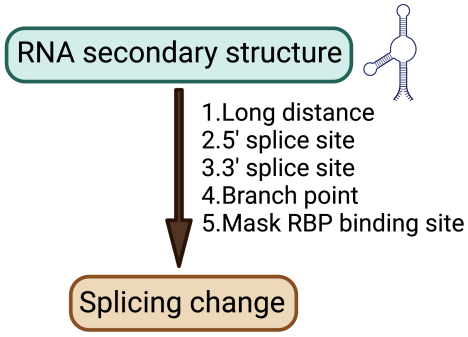

Figure 1.3 Brief overview how RNA secondary structure influences splicing. 1. RNA sequences within a long distance can interact with each other to affect splicing machinery; 2. RNA secondary structure can mask 5' splice site to inhibit splicing event; 3. Formation of RNA secondary structure is capable of masking 3'splice site to constrain splicing reaction; 4. If branch point region forms RNA secondary structure, the accessibility of branch point puts on brakes; 5. RNA secondary structure formation can influence the RBP binding site, which potentially enhance or repress splicing reaction, to manipulate splicing events.

1.2.2 Mechanism study in an individual gene

The influence of RNA secondary structure in splicing is a wide phenomenon across different species. In the following part, some individual cases, that how RNA secondary structure is

involved in the splicing regulation, will be discussed in accordance with the influence of RNA secondary structure in long distance, 5'SS, 3'SS, branch point and RBP binding site, in different species from viruses to humans (**Fig. 1.3**).

Long distance

RNA secondary structure formed by base-pairing of two sequences within long distance is capable of widely influencing alternative splicing in many species from viruses to chickens. In duck hepatitis B virus, the splicing efficiency of a RNA derived from pregenomic RNA is inhibited by two regions of *cis* elements, which can base-pair to mask the 5'SS and 3'SS, showing that the impair of secondary structure dramatically enhances its splicing machinery[77]. In yeast YL8A, a pair of complementary *cis* elements in the intron can base-pair to shorten the distance between 5'SS and 3'SS, thereby promoting exon inclusion[78]. D. LIBRI *et al.* identified a series of base-paired *cis*- elements, which promote splicing, in the 325-nt yeast (*Saccharomyces cerevisiae*) rp5lb intron using random N selection, suggesting that the base pairing contributes to the process of spliceosome assembly through improving intron definition[79]. *Drosophila* Dscam gene produces variable 38,016 axon guidance receptors through mutually exclusive alternative splicing of 95 distinct exons. Brenton R. Graveley identified one docking site in the downstream flanking intron of exon 5, and a series of selector sequence, which are perfectly complementary to the docking site, in the upstream introns of each exon 6 variants. Thus, the model was proposed: once the docking site base-pairs with selector sequence, the exons will be looped out and exclusive as the secondary structure abolishes the repressor activity at the adjacent splice site with unknow mechanism, leading to the efficient utilization of the splice site and the others remaining inhibition[80]. Similarly, Yun Yang *et al.* demonstrated the model also worked in 14-3-3ζ and Mhc pre-mRNA to contribute the mutually exclusive splicing event in *Drosophila* species[81]. In the chicken P-tropomyosin pre-mRNA, the upstream intronic region of exon 6B can form stable secondary structure with exon 6B and part of downstream intronic region of exon 6B, and this structure represses exon 6B inclusion. Disruption of the secondary structure significantly promotes the splicing machinery of exon 6B, indicating that the sequester caused by secondary structure can block the recruitment of *trans* to exon 6B, thereby remarkably inhibiting splicing event[82].

In mammals, the earliest report regarding the role of RNA secondary structure in alternative splicing possibly is in 1985 by David Solnick[83]. This paper shows that the exon will be excluded when it is in the loop of the hairpin in both *in vitro* assays and in cells. Another paper

reported that a base-paired RNA secondary structure in the region of 5'SS and branch point formed before the spliceosome assembly in exon 18 of neuronal cell adhesion molecule (NCAM) gene, and thereby inhibiting the splicing event[84]. Two repressive *cis* regulatory elements in the flanking introns, that hnRNPA1 bind, efficiently inhibit exon 7B inclusion, but the glycine-rich C-terminal domain of hnRNPA1, which activates the distal 5'SS, is indispensable for the inhibition. Further, considering that hnRNPA1 can simultaneously bind to two *cis*-regulatory elements, the researchers proposed the model that hnRNPA1 could concurrently interact with the upstream and downstream flanking introns of its exon 7B to loop out the exon 7B, thereby inhibiting splicing of exon 7B[85]. It is well-known that an evolutionally conserved RBFOX2 binding site is in the intronic distal site to modulate alternative splicing. Michael T Lovci *et al.* took *KIF21A* and *ENAH* gene as examples and found that the conserved stem loop was formed through base-pairing to bridge the distal RBFOX2 binding site nearby the 5'SS[86]. In non-neuronal cells, PTB can bind to two intronic CUCUCU elements flanking the exon N1 to exclude the c-src exon N1, while its interaction with upstream intronic elements was disrupted by unknown mechanism in neurons, leading to exons N1 efficiently spliced[87].

RNA secondary structure within a long distance is also related to human diseases. Alternative splicing of the proteolipid protein 1 gene (PLP1) produces two isoforms, PLP1 and DM20, through alternative usage of proximal and distal 5'SS in the exon 3. If the utilization of proximal and distal 5'SS is unbalanced, it will cause the X-linked leukodystrophy Pelizaeus-Merzbacher disease (PMD). Jennifer R. Taube *et al.* showed that the secondary structure from long-distance base-paring in the intron 3 contributed to the selection of 5'SS, and people with intron 3 mutations, which can destroy the secondary structure, indeed have abnormal ratio of PLP1 to DM20, resulting in PMD[88].

5' splice site

In murine leukemia virus, the accessibility of 5'SS is modulated by the upstream RNA stem-loop, and the influence of stem-loop sequence is negligible as almost all the stem-loops functionally have the similar effects. Further mutagenesis experiment demonstrated that the differential access of U1snRNP to 5'SS causes the intricated splicing regulation in retrovirus[89]. In *Nicotiana plumbaginifolia*, H X Liu *et al* have shown that insertion of 18 or 24 bp sequence, which potentially form stem loop structure, into the region close to 5'SS in the middle of short intron significantly inhibited splicing event, but the splicing was not influenced if the insertion occurred nearby the 3'SS.[90]

In mammalian fibronectin EDA exon, both ESE and ESS modulate the splicing machinery together[91]. The interaction of SR protein-RNA complex is lost after the ESS mutation is introduced in the mouse Fibronectin EDA exon, while the splicing efficiency change is indistinguishable in human ESS mutation of Fibronectin EDA exon. This controversial splicing behavior can be explained as the whole RNA secondary is different between humans and mouses in ESS mutated RNA. In humans, ESS mutation cannot induce huge change of the RNA secondary structure, while the "looped out" ESE in mouse WT EDA exon base-pairs with *cis* elements to become stem region, thereby resulting that the ESE is fully masked[92,93]. Exonic terminal stem loop 2 that is close to the 5'SS in SMN2 exon 7 shows the inhibitory impact on splicing machinery, and destabilization of the structure via point-mutation significantly enhances splicing efficiency[94]. Additionally, another intronic *cis*-acting element representing enhancer activity, also can form stem loop structure, showing that less SMN exon 7 inclusion after the structure is disrupted[95]. The evidence strongly suggest that RNA secondary structure is complicatedly and intricately involved in the splicing modulation.

Genomic point mutation can alter RNA secondary structure to dysregulate alternative splicing, leading genetic disorders. In the premature aging disorder Hutchinson-Gilford Progeria Syndrome, a *de novo* C1824T point mutation activates a cryptic alternative 5′ splice site of exon 11 in the LMNA gene. With SHAPE-MaP and mutagenesis analysis, Asaf Shilo *et al.* demonstrated that RNA secondary structure, splice site position and sequence cooperated to decide which splice site was used. The mutant bears the advantage of splice site position and sequence (due to C1824T in the splice site). Antisense oligonucleotides targeting the *cis* element, which is complementary to 5'SS surrounding sequence, dramatically enhance the alternative 5'SS usage, indicating that 5'SS is sequestered in the secondary structure, which destroys the recruitment of U1snRNP[56]. Christine P. Donahue *et al.* showed that the mutation in microtubule-associated protein Tau (MAPT) exon 10, destabilized the stem loop, and antisense oligonucleotide treatment of targeting the stem loop region significantly increased exon 10 inclusion, while the mutants, that stabilize the stem loop dramatically reduced PSI, suggesting the stem loop structure may mask the 5'SS[96]. Physiologically, several mutations of MAPT exon 10 in humans, which destabilize or stabilize the secondary structure surrounding 5'SS[96-98], cause frontotemporal dementia with Parkinsonism linked to chromosome-17 (FTDP-17)[99-102]. Hamideh Yadegari *et al.* showed that a point mutation in the distal intron caused remodeling of RNA secondary structure to sequester 5'SS, thereby leading to intron retention

in the VWF gene. This intron retention isoform generates a truncated protein that lacks the carboxy-terminal end of the VWF protein, which results in type 1 von Willebrand disease[103].

Interestingly, RNA secondary structure nearby 5'SS is also demonstrated to enhance splicing. In *Saccharomyces cerevisiae*, *in vivo* DMS probing shows that the RNA stem loop, containing two complementary sequences near 5'SS and branch point, acts as an early step of spliceosome assembly to promote splicing machinery. This finding indicates that the secondary structure formation is earlier than 5' spliceosome complex recruitment[104].

3' splice site

Combining DMS-MaPseq data with the DREEM algorithm, Phillip J. Tomezsko *et al.* could effectively detect alternative RNA structures of HIV-1 and found an RNA transcript might have more than one RNA conformations. Then, they experimentally validated that HIV-1NL4-3 structure had two dominant conformations. In one of them, the 3'SS is masked by base-pairing, and the 3'SS is fully exposed in another one. Mutants destabilizing the RNA structure remarkably augment the utilization of 3'SS[105]. In *Saccharomyces cerevisiae* COF1 intron, G to A substitution between branch point (BP) and 3'SS region disrupts the RNA stem loop, which potentially shortens the distance of BP to 3'SS, and sterically masks the splice sites. Importantly, this working mechanism also works in UBC13 intron[106]. To investigate whether RNA hairpin can sequester splicing signal, VALERIE GOGUEL *et al*. inserted a series of small sequence elements, which can potentially generate RNA hairpins between the 3'SS and branch point region, to the short intron of RPSJ5A in yeasts. Both in *in vitro* and in cellular assays, spliceosome assembly and splicing process are consistently hindered, showing that even 6-nucleotide hairpin manifests efficient inhibition, and a 15-nucleotide hairpin almost abolishes the splicing event[107]. James O. Deshler found that several randomly induced point mutations could activate a silent 3'SS in the intron of budding yeast actin gene in a genetic screen. Further analysis shows these mutations disrupt a stem-loop secondary structure located in this region. These results indicate that the stem loop structure can sequester the cryptic 3'splcing site in WT intron[108].

In the human growth hormone transcript, a stem loop masks the 3' acceptor and its branch point of exon 3B to promote this exon skipping[109]. In ATM gene, a pseudo-splice site in the intronic region cooperates with enhancer, repressor, and RNA secondary structure to modulate the splicing events[110].

Branch point

In the *Drosophila melanogaster* Adh gene, a stem loop exists at the upstream of branch point. Disruption of the stem region in the secondary structure remarkably reduces the activity of splicing machinery, and the difference between mutants restoring the base paring of the stem and WT is indistinguishable in terms of the splicing efficiency. Surprisingly, mutants with higher stability of stem loop also reduces splicing efficiency, indicating that the stem loop structure is evolutionally meaningful[111].

RBP binding site

In general, *trans*-acting factors just can recognize single-stranded RNA in a sequence-dependent manner. Indeed, Michael Hiller *et al.* demonstrated that the enhancer and repressor region in the mRNA favor single-stranded conformation, while the others bear more RNA secondary structures[112]. The RNA secondary structure formed by base-paring can hide the consensus *cis*- regulatory elements to influence the recruitment of their *trans*-acting factors, and the secondary structure also can destroy the interaction between RNA and *trans*-acting factors. However, the increasing evidence show that some specific RNA secondary structures can be specifically recognized by corresponding *trans*-acting factors, such as MBNL[113]. Furthermore, it has been demonstrated that the binding sequence of many RBPs, such as HuR, is degenerate and relatively loose. In this case, it is possible that linear loose *cis* sequence is just one of layers for RBP recognition, and RNA secondary structure serves as further well-defined signal for the specific interaction between the RNA and RBP. In fact, recently computational prediction of the putative RBPs of a particular *cis* element has demonstrated the hypothesis mentioned above at some points. They showed that the ability and accuracy of prediction is higher if considering surrounding RNA secondary structure together with the expected consensus. Since the importance of RNA secondary structure in the recognition between RNA and protein cannot be ignored, there is a high possibility that alternative splicing process also can be affected through RNA secondary structure, eg. influencing the accessibility of RBP binding sites.

The involvement of RNA secondary structure in the recognition of RBP has been demonstrated in several species. HnRNP A1 is demonstrated to control alternative splicing of HIV-1 mRNA via cooperatively binding to intronic and exonic splicing silencers within a conserved RNA secondary structure[114]. Similarly, SRp55, a member of the *Drosophila melanogaster* SR

protein family, is showed to bind a conserved consensus motif, which contains a secondary structural element in a pool of random RNA sequence. Mutagenesis defines a 20 nucleotide hairpin loop structure as the binding site[115]. RONALD J. BUCKANOVICH *et al.* identified a series of long stem-loop RNA oligos, which can bind to Nova-1 with extremely high affinity from a pool of 10^{15} random 52-mer. These oligos hold an around 15bp consensus [UCAU(N)0–2]X3 for Nova binding. Interestingly, mutation of base pairing in the stem sequence to disrupt the secondary structure with unchanged loop region significantly reduces three-fold binding with Nova-1, indicating that both consensus and stem loop structure contribute to this specific interaction[116].

In summary, RNA secondary structure has been experimentally demonstrated to intricately cooperate with primary *cis*-regulatory elements to determine the alternative splicing in many individual genes. In a view of evolution, RNA secondary structure may act to set an upper limit to control alternative splicing besides the enhancer and repressor.

1.3 Transcription rate

As about 80% of splicing events are co-transcriptional[117], it is conceivable that transcription rate can influence the process of alternative splicing. Indeed, slow RNA polymerase II dramatically increases exon 18 inclusion of NCAM, which was proposed to correlate with chromatin modification[118]. If the transcription rate is fast, the availability of adjacent 3' weak splice site and 3' strong splice site is similar, and thus the 3' strong splice site will be utilized; if the transcription rate is slow, the proximal 3' splice site will be more available, resulting in "first served, first committed" and the selection of 3' proximal splice site[119-123].

Interestingly, it seems that the influence of transcription rate in splicing is coupled with RNA secondary structure. As a matter of fact, *in vitro* results regarding the influence of RNA secondary structure in splicing aren't reproduced in live cell systems in some settings. Thus, a hypothesis is proposed: it is conceivable that RNA secondary structure of pre-mRNA is coupled with transcription together given that the only difference between *in vitro* and live cell experiments is that the transcription exists in live cells. If we go back to basic concept that RNA is widely coated by RNA binding proteins, such as hnRNP family, which are ubiquitously expressed in the cells, the true setting is more potentially complicated. These coated RBPs on RNA can prevent from RNA folding into stable RNA secondary structure. Therefore, there is just very limited timespan for RNA to form secondary structure, and this hypothesis perfectly

matches with the experimental results. If the loop length of two putative base-pairing *cis* elements is more than 110 bp, RNA secondary structure cannot be formed in cells as RBPs associate with RNA, which block RNA secondary structure formation in advance. If the loop length is short, stable secondary structure can be found earlier before RBP binding[124]. Additionally, slow pol II remodels the RNA secondary structure of Alu regions and exons to influence splicing, and it was observed that more structured introns at their 3'splice sites were efficiently removed in the slow pol II setting.[83]

In summary, alternative splicing is not a single isolated reaction, but is coupled with other cellular events. Ultimately, which splice site is selected is coordinately determined by all the factors together.

2 Temperature sensitive alternative splicing

At the macroscopic level, many biological phenomena are related to temperature, such as the body temperature increasing in sickness, homothermic *vs* heterothermic animals *etc.* At the molecular level, alternative splicing, as an essential mechanism of gene regulation, has been shown to be one of the essential cellular events in response to temperature changes. To date, a plethora of studies regarding temperature sensitive alternative splicing have been focused on the plants possibly by virtue of the huge body temperature change of plants in a day. Conceivably, temperature remodels alternative splicing through acting on the factors, which influence the molecular process of alternative splicing.

2.1 Phosphorylation of *trans*-acting factor

The phosphorylation status of SR proteins determines their functions and distributions during pre-mRNA splicing[13,14,125,126]. Both hyper- and hypo-phosphorylation can inhibit alternative splicing, so it is great of importance to balance the phosphorylation state of SR proteins for the action of SR protein kinase and phosphatase. If the phosphorylation is distinct at different temperatures, phosphorylation should be one of the mediators to modulate temperature sensitive alternative splicing. Indeed, Marco Preußner *et al.* showed that the circadian rhythm of body temperature drives SR protein phosphorylation in cycles to control alternative splicing events[127]. James Manley group also revealed that dramatic dephosphorylation of SRSF10 after heat shock[128]. Later, Tom Haltenhof *et al.* further demonstrated that evolutionarily conserved CLK kinases were the key kinases in response to temperature alternations for the phosphorylation of SR proteins from reptiles to mammals. CLK kinases present higher kinase

activity at lower temperature, while its activity dramatically decreases at high physiological temperature[129].

In principle, the phosphorylation state of other *trans*-acting factors, such as hnRNP family[130], should also influence alternative splicing. Unfortunately, to my knowledge, so far, few studies show whether and how temperature changes affect their activities coupled to alternative splicing machinery.

2.2 RNA secondary structure

RNA secondary structure changes its conformation in response to temperature changes. Experimentally, Yue Wan *et al.* obtained relative melting temperatures (Tm) for RNA structures of over 4000 transcripts from yeasts with Parallel Analysis of RNA structures with Temperature Elevation (PARTE) from 23 °C to 75 °C *in vitro*. Their studies show that different classes of RNA bear different propensity to melt, presenting that mRNA with the lowest Tm and ncRNA with the highest Tm[131]. The sensitivity of RNA secondary structure to temperature provides sessile plants with an opportunity to sense the temperature changes. Silvi Rouskin *et al.* showed that temperature at 95 °C disrupted RNA secondary structure, and RNA was less structured at higher temperature, while more structured RNA regions were observed at lower temperature[53]. As increasing temperature tends to unfold RNA, temperature has been used as a factor in some RNA structure prediction program, such as RNAstructure[132], ViennaRNA[133] and RNAtip[134]. Indeed, Andrey Chursov *et al.* developed an algorithm to predict the RNA secondary structure in response to different temperatures. With the algorithm, the structural difference of two RNAs with several base mutations can be predicted at different temperatures[134]. Although they didn't mention whether RNA can be a thermometer to modulate alternative splicing, it is conceivable that it can as RNA secondary structure is coupled with splicing regulation.

It has been shown that the inhibitory effect of RNA stem loop, which potentially shorten the distance of BP to 3'SS, thereby sterically masking the splice site, on splicing is highly dependent on the temperature with *in vitro* assays in COF1 intron *of Saccharomyces cerevisiae*[106]. Markus Meyer showed that in yeasts around 70% of the recognition of 3'SS is mediated by RNA secondary structure as the density peak of available annotated 3'SS overlaps with that of non-structured sequence proximity to 3'SS, not that of structured sequence predicted by RNAfold. Then, they hypothesized that one of these RNA secondary structures

could act as thermo-sensor to mask 3'SS, thereby controlling the accessibility of 3'SS and modulating alternative splicing. Finally, they successfully validated the hypothesis in RPS23B intron[135]. In plants, the 3'SS of intron 2 in HsfA2 pre-mRNA has been demonstrated to present two conformations at different temperatures. At high temperature, an RNA conformation with single-stranded polypyrimidine tract (PPT) is dominant, and thus the PTBP binds to the PPT, strongly repressing splicing; at low temperature, the PPT is sequestered by base pairing with another element, and thus the accessibility of PTBP to PPT is inhibited, promoting the U2AF recruitment and splicing machinery[136]. In human cells, it has shown that hyperthermia can increase full-length of SMN2 mRNA even though the researcher claimed that it was due to the upregulation of the enhancer protein TRA2 beta[137]. However, if we consider that it has been shown a stem loop exists nearby 5'SS of exon 7 in SMN2, which inhibits the inclusion of exon 7,[94] heat treatment will potentially disrupt the RNA secondary structure. Thus, the disrupted inhibitory stem loop in hyperthermia may also contribute to the increased exon 7 inclusion.

In a word, RNA secondary structure changes may contribute to temperature sensitive alternative splicing since RNA secondary structure originally plays a role in the modulation of alternative splicing.

2.3 Transcription rate

Since most of the alternative splicing events are coupled to the transcription, modulation of alternative splicing by temperature changes can be mediated by transcription rate. Indeed, it has been shown that moderate high temperature significantly increased transcription rate[138]. Therefore, theoretically there will be more intron retentions at high temperature due to higher transcription rate in those genes, whose splicing is highly dependent on the transcription rate and have more intron retention at high temperature. More substantial investigations in this field need to be done in the future.

3 RNA G-quadruplex

As the development of high-throughput sequencing and bioinformatics analysis, a plethora of RNA secondary structures have been computationally and/or experimentally identified, such as stem-loops (hairpins)[139], internal loops[140], bulges[141], pseudoknots[142], kink-turns[143], complex multibranch loops[144], and G-quadruplex (G4), in both prokaryotic and eukaryotic cellular transcriptome[145]. These RNA structures are highly involved in the modulation of alterative splicing as aforementioned. Here, rG4 is focused to discuss in detail.

3.1 Definition and property

Typically, the RNA structure, that two or more sequential guanines are stacked into 4-runs with divergent sequences of loops, is named as a classical RNA G-quadruplex (rG4) as shown in **Fig. 1.4**. Simply, the G4 consensus is defined as $G_{\geq 2}(N_{1-7}G_{\geq 2})_{\geq 3}$ (**Fig. 1.4a**). It has been shown that shorter loops provided greater stability of G4[146], while longer loops in reducing the stability of G4 structure will reach a relatively unalterable plateau with the increasing length[147]. The interaction force of each G in the G4 structure is Hoogsteen base paring (**Fig. 1.4b**), instead of Watson-Crick, and each stack of bases has extensive network of H bonds and π–π interactions with the nearby stack layer of bases. Compared to DNA G4, rG4 is more stable as the difference of sugar phosphate. Firstly, the hydroxyl group of RNA makes rG4 have more intramolecular interactions within RNA, which promotes rG4 stability; Second, the hydroxyl group also sterically stabilize the conformation of rG4 through orientationally preventing the *syn*-conformation; third, hydroxy group favors to bring more water into the hydroxy groove to further stabilize the structure. These factors together contribute to the parallel conformation of rG4, that is all 4 strands are in the same orientation (**Fig. 1.4c**), while DNA G4 has several kinds of conformations. Finally, the uridine base also contributes to the stability of rG4 at some points[148]. High-throughput sequencing of DNA G4 structure in the human genome has shown that DNA G4 is highly enriched in the promoters, 3′ UTR and 5′ UTR, exons, introns, and splicing junctions[149]. To make it simple, all the "G4" below mentioned is "rG4" unless explicitly stated.

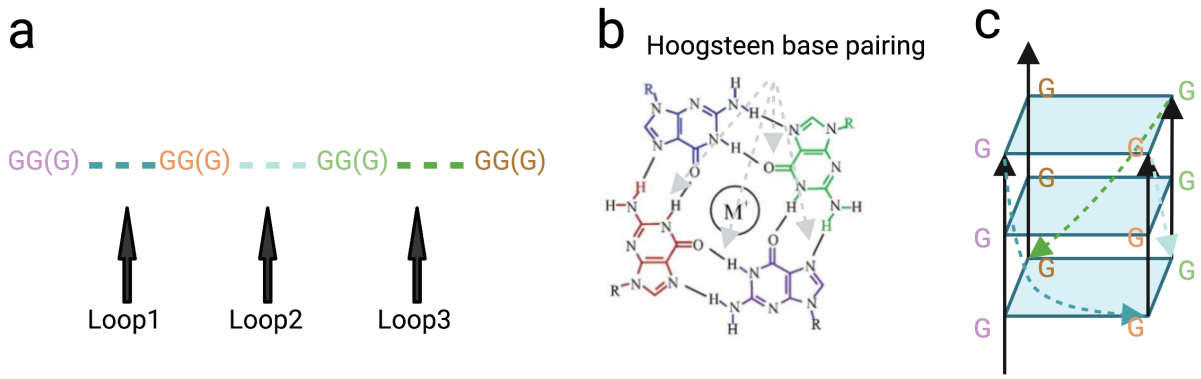

Figure 1.4 Typical G4 sequence and topology. **a**, Typical G4 sequence with G runs and loops. **b**, Hoogsteen base pairing in G4 and metal in the core of G4 structure. **c**, Canonical G4 structure in parallel conformation.

Besides the regular G4 structure, current mounting G4-transcriptome data also suggests some non-canonical G4s, such as a long loop of 8 to 15 nt, a burge of one non-G in one of the G-runs and a G-vacancy in one of the G-tracts[150,151]. Interestingly, G4s can not only exist intramolecularly, but also intermolecular G4s can be formed within different RNA or even DNA molecules[152]. For instance, in the R loop, DNA and newly transcribed RNA can form hybrid G4s, which function in many cellular events[153,154].

Another interesting characteristic of G4s is that some ions, small molecules, and proteins can stabilize or unwind them. Among them, potassium is the best stabilizer ion for G4s as its unique ionic radius can perfectly enter G4 channels to interact with other atoms within G4s. The ability of ion stabilizing G4 is K^+>Na^+>Li^+[155,156]. Also, some small molecules have been identified and synthesized to bind and stabilize G4s, such as pyridostatin (PDS) and its derivates, and they are called G4 stabilizer ligand[157]. Additionally, several RNA helicases have been reported to contribute to G4 unwinding, such as DHX36[158], RHAU[159,160] and DHX9[161]. Meanwhile, some proteins have been identified to bind G4s, and they don't dissolve them, but function in cellular events[162].

However, the direct evidence to support RNA G4s *in vivo* is limited. So far, to my knowledge, immunostaining with G4 specific antibody is one of the methods to directly observe intracellular G4s[163].

3.2 Genome-wide distribution of G4s

It has been shown that G4s widely distribute in the genome. The intermolecular G4s between DNA and RNA have been identified[164] in the R loop. Also, genome-wide analysis has shown that putative hybrid G4s are highly enriched within the downstream regions of transcription start site (TSS) in more than 97% of the human genes[165]. G4 structure is highly enriched in the beginning and end of the genes, that is in the 5'UTR[166] and 3'UTR region[167], indicating that G4s may be involved in the modulation of translation and alternative polyadenylation process.

In 2016, Chun Kit Kwok *et al.* reported a genome-wide rG4 profiling through comparing the RT stop signal in different treatments of K^+, K^++PDS and Li^+ using purified polyadenylated RNA from Hela cells, and concluded that G4s were widespread in the transcriptome[151]. The main argument for this paper is that they used pure RNA to map the G4 signal *in vitro* and cannot truly convey the true G4 formation in cells. Concurrently, David P Bartel lab took advantage of the specificity of DMS modification on guanine (G) to distinguish *in vitro* folding

and *in vivo* folding of G4s[168]. In details, DMS can methylate A and C to disrupt the Watson-Crick base paring of modified A and C with other bases (T and G). Meanwhile, DMS also can modify G at N7 position[169], and the G4 refolding will be affected although the modification does not influence the Watson-Crick base paring. Thus, with the DMS treatment in cells, if G4 is formed *in vivo*, G4 structure can protect G residue from the DMS modification, the G4 can refold *in vitro* under high KCl condition, and thereby RT stop signal appears; if the G4 doesn't exist *in vivo*, G can be modified by DMS, thereby preventing the G4 from refolding *in vitro* and resulting in no RT stop signal. With this method, they found that G4s were widespread unfolded in mammalian cells. Then, they claimed that microorganisms evolutionally delete G rich element from their genomes as they are lacking unwinding proteins, while mammalian genome has numerous G rich elements, potentially forming G4s, but mammalian cells have a robust and effective system (e.g., helicase) to dissolve the G rich structures in cells. Admitting the reasonability of the explanations, we still need to ask the following question: if G4s are not useful or redundant in a genome-wide scale, why evolutionally they have not been deleted from mammals so far and an energy consuming system (helicase *etc*.) is developed to dissolve it? In contrast, in lower organisms, such as bacteria, G rich elements are lacking in their genomes. One more conscientious statement is that G4s are functionally necessary in mammals as evolutionally they are remained. Their formation *in vivo* is modulated by many factors, such as unwinding factor[170,171], ion concentration *etc*., although so far not so many helicases unwinding G4 have been well characterized. Additionally, G4s may form in a particular time of RNA life, such as pre-mRNA and RNA transportation stage, or in a unique cell condition (cell cycle, cell stress, disease condition *etc.*). It also cannot be excluded that G4 formation is cell-type specific. Additionally, David P Bartel lab used polyA enriched mRNA, which dramatically dilutes pre-mRNA and other non-polyA RNA signal. Finally, as they mentioned in the paper, they couldn't map the G4 in the small RNA, such as microRNA, due to the length limitation in the library construction. Using *in vivo* SHALiPE-Seq, Xiaofei Yang *et al.* demonstrated that G4s existed and functioned in *Arabidopsis* transcriptome[172]. Another group developed G4RP-seq, which utilizes biotin-linked G4 stabilizer to pull down the G4 from the fixed RNA samples, to profile the G4 landscape, showing that G4s are widely distributed in the mammalian transcripts[173]. Recently, Ilias Georgakopoulos-Soares *et al.* showed that G4 signal is highly enriched near splice sites through analyzing the DNA G4 signal, and the G4 may promote exon inclusion through recruiting some potential RBPs[174].

3.3 Validated G4s modulating alternative splicing

How G4s regulate splicing is still in its infancy, and here the majority of the validated G4s involved in the alternative splicing are summarized according to their different influences in splicing.

Masking 5'SS: Jean-François Fisette *et al.* showed that RNA G4 in proximity to a minor 5'SS of BACE1 exon 3 dramatically inhibited the minor 5'SS as G4 deletion exaggerated the minor splice site usage[175] through preventing hnRNPH recruitment. This finding indicated that G4s may sterically mask its adjacent splice sites to constrain the spliceosome assembly. In EWSR1 exon 8, two G4s are in vicinity to 5'SS, recruiting hnRNPH1 to efficiently repress exon 8 inclusion[176].

Enhancing intron removal: A G4 of PAX9 intron 1 was reported to dramatically enhance the splicing efficiency of intron 1, showing that mutant with G4 disruption bared more intron retention[177]. The fully transcribed TP53 encodes full-length of TP53, and the transcripts with intron 2 retention generate N-terminal truncated TP53 protein, which is lacking first 39 N-terminal residues corresponding to the main transaction domain. Virginie Marcel *et al.* showed that a G4 structure in the intron 2 contributed to the intron removal as mutagenesis of G4 dramatically increased the retention of intron 2[178].

Splicing enhancer: G4 I-8 located at the downstream of exon V8 in CD44 efficiently promotes exon V8 inclusion through interacting with hnRNP F. Importantly, this exon switch can regulate cancer epithelial–mesenchymal transition (EMT)[179]. In FRM1 transcripts, a G4 is also demonstrated as a potent exonic enhancer[180].

3.4 Other functions

G4s can influence the alternative polyadenylation, and mRNA transport and the formation of RNA granules. Individually, RNA G4s have been biophysically demonstrated to exist in FMR1 and BCL mRNA[181,182]. G4s in LRP5 and FXR1 genes have been shown to promote alternative polyadenylation, producing more short transcripts[183]. G4s also exist in the 3'UTR of around 30% of dendritic mRNA, including PSD95 and CAMKII. λN-GFP labelled 3′ UTR RNA of PSD95 was observed to rapidly transport in neurites, indicating that G4s may act as "zip-code" signal to contribute to mRNA transport in the neurites[184]. G4s from the G4C2 repeats in ALS/FTD-Associated C9ORF72 RNA contribute to the phase separation of RNA granules[185].

HnRNPH can associate with the G4 repeats in the C9ORF72, leading to the sequester of hnRNPH, and thus the alternative splicing related to hnRNPH is dysregulated in ALS brain[186].

Messenger RNA translation is also influenced by G4s. Andrew L. Wolfe *et al.* reported that EIF4A is responsible for the translation of those transcripts with G4 rich in the 5'UTR to drive tumor growth[187] although how G4s act in the process need to be further determined. The human CCHC-type zinc finger nucleic acid-binding protein (CNBP/ZNF9) was reported to bind the G4 in the 5'UTR, thereby promoting mRNA translation[188]. G4s in the 5'UTR of proto-oncogene NRAS was demonstrated to inhibit its translation as both deletion and mutation of the G4 structure dramatically enhance translation in the reporter[189]. Interestingly, Markus Wieland *et al.* showed that G4s influenced translation in a temperature dependent manner in the *E. coli* system of artificial overexpression of plasmids with G4s. Higher temperature destabilizes G4, thereby promoting translation. Furthermore, the sensitivity of inhibitory effect of G4s on translation also depends on the stability of G4. If G4s are stable enough, the G4 dependent translation regulation are not temperature sensitive; If G4s are less stable, the translation is temperature sensitive[190].

4 NMD

Non-sense mediated decay (NMD) is an RNA surveillance pathway, and it is coupled with translation to limit the synthesis of truncated or harmful protein in all eukaryotes. Many studies have shown that NMD is a conserved proofreading pathway, which is essential for vertebrate survival, but not for bacteria and *C.elegans*[191].

4.1 Enhancer and repressor of NMD

In the sophisticated pathway, UPF protein family is essential to distinguish NMD-targeted transcripts and non-NMD targets[192]; SMG proteins as kinases, are also prominent through mediating the phosphorylation status of UPF proteins to control UPF activity[193,194]. Some NMD enhancers, and repressor proteins have been determined. If a premature termination codon (PTC) occurs at more than 50-nt and less than 400-nt upstream of EJC (exon-exon junction complex), which is composed of Y14, MAGOH, eIF4A3 and MLN51, and deposits at exon-exon junction, the EJC will promote the recruitment of UPF proteins to initiate NMD[195,196]. It is also clear, at least to some extent, that SR proteins can enhance NMD machinery, illustrating that overexpression of SR protein promotes NMD efficiency[197]. Given that not all the transcripts with PTCs are subjected to NMD, systematically bioinformatic

analysis also tends to identify some *cis* elements, which potentially repress NMD. Indeed, some *cis*-regulatory elements, which are in proximity to the stop codons, are shown as inhibitory elements[198]. For instance, binding of PTBP1[199] and hnRNP family proteins[200] adjacent to stop codons is capable of inhibiting UPF protein recruitment.

4.2 Gene feature of NMD targeting transcripts

So far, there have been several gene features identified to be recognized by NMD machinery. First, the introduction of a PTC not only shortens open reading frame (ORF), but also lengthens the 3'UTR. Indeed, it is determined that a transcript with longer average 3'UTR can be naturally recognized by NMD machinery[201], albeit not always. Second, the transcripts with mutations or differential mRNA isoforms, which alternative splicing generates to introduce PTCs at upstream of exon-exon junctions, also can be targeted by NMD pathway[202-205]. In this scenario, some "rules" have been discovered and summarized through analyzing the high-throughput sequenced cancer samples with dozens of mutations and experimental validations[206]. The "last exon rule", that generally PTC occurring in the last exon cannot elicit NMD, presenting that transcripts with mutations to produce PTC in last exon have identical expression level with non-mutants[207]. "55-nt boundary rule", the distance of PTC to EJC must be more than 50-nt to efficiently induce NMD, while PTC, that is in proximity to start codon, fails to produce NMD[208]. It is also difficult to induce NMD for the PTC in a long exon with more than 400-nt in length[207]. Next, 3'UTR intron[209] and uORF transcript [210]also can be NMD targets. Although these summarized "rules" can explain most of the NMD events, still around 30% of NMD events cannot be explained with the current gene features[211]. More deep investigations need to be done in this aspect in the future.

4.3 Degradation of NMD transcripts

The initiation or premise of NMD is the recognition of PTCs, once the PTCs were recognized by NMD pathway, the targeted transcripts can be degraded through two pathways: one is exonucleolytic decay through SMG5/7 to associate with CCR4/NOT and DCP2/XRN1; another one is mainly dependent on the SMG6 to degrade the targets via endo-cleavage by exosome and XRN1[212].

4.4 Diseases related to NMD

NMD plays a crucial role in the regulation of physiological expression level of transcripts in many cellular events, such as stem cell development[213,214], cell-cycle progression[215] and embryonic development[216]. Meanwhile, it can cause a number of diseases once it is dysregulated, such as β-thalassemia due to 5' PTC of β-Globin (HBB), inherited blindness caused by 5' or 3' PTC in Rhodopsin (RHO) and inherited bleeding tendency from 5' or 3' PTC of Coagulation factor X (F10)[217]. This raises a possibility that modulating NMD is an achievably therapeutic strategy to treat diseases[211].

5 RBM3

5.1 Discovery and expression of RBM3

5.1.1 Structure and evolution

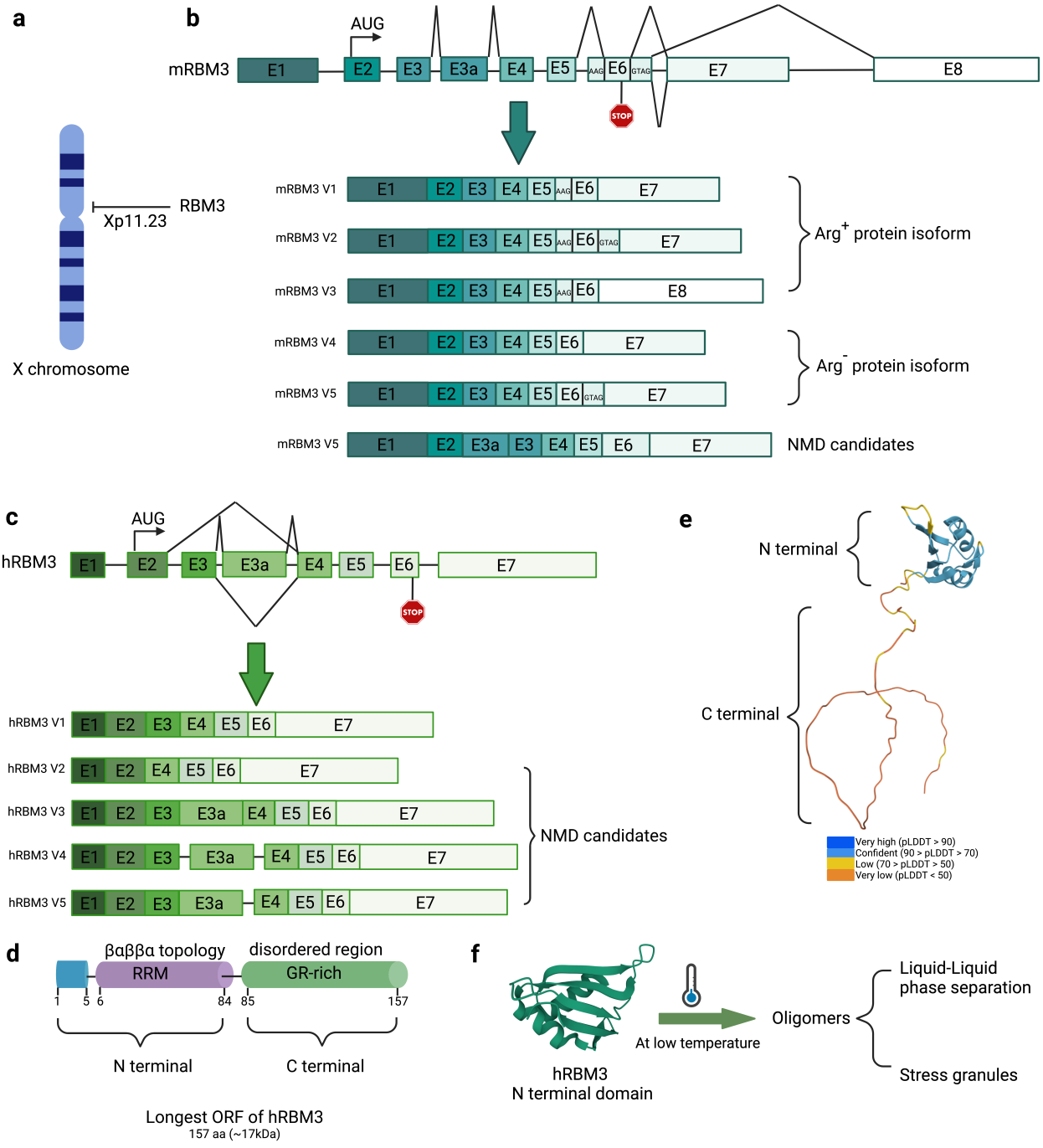

Figure 1.5 Isoforms of RBM3 RNA and sturcture of RBM3 protein. **a**, RBM3 gene in the Xp11.23 of X chromosome. **b and c,** mRNA and hRBM3 isoforms of mRBM3 and hRBM3 gene generating from alternative splicing, respectively. hRBM3 contains 8 exons with alternatively spliced

E3 and E3a. mRBM3 is composed of 8 exons with alternatively spliced of 5' and 3' exon 6, producing two protein isoforms with or without arginine. Each rectangle represents a exon, and the solid line is intronic region. Fold line links the ligated exons together. **d**, Strcuture of the longest ORF of hRBM3. Human RBM3 is around 17kDa containing the longeste open reading frame of 157 amino acids with N termimal beta and alpha topology and C termianl disordered region. **e**, Protein structure of hRBM3 predicted by AlphaFold. C termial of RBM3 is higly flexible. **f,** Response of N-terminal of hRBM3 protein to low temperature. N terminal of RBM3 forms oligomers, resulting in phase-phase separation and producing stress granules. All the isoform information of mRBM3 and hRBM3 are obtained from NCBI. NMD: non-sense mediated decay. hRBM3 V1: NM_006743; hRBM3 V2: NM_001017431; hRBM3 V3: NM_001017430; mRBM3 V1: NM_001293658; mRBM3 V2: NM_001166409; mRBM3 V3: NM_016809; mRBM3 V4: NM_001166410; mRBM3 V5: NM_001166411.

In 1995, the RNA-binding motif protein 3 (RBM3) was identified as a novel gene located between OATL1 and GATA1/TFE3 in human sub-band Xp11.23[218](**Fig. 1.5a**). Human RBM3 generates at least three alternatively spliced transcripts, and two of them are thought as non-sense mediated candidates referring to the NCBI annotations. Human RBM3 protein expresses in a variety of fetal tissues with the longest open reading frame (ORF) encoding a 17 kDa protein with 157 amino acids (**Fig. 1.5c**). In mice, mRBM3 gene produces at least five different isoforms, and exon 6 is alternatively spliced at the 5'splice site (SS) and 3'SS due to the GTAGGTGA and NAGNAG sequence, respectively[219]. The 3'SS variants of exon 6 encode two protein variants (+/- Arg) with only one amino acid distinction (**Fig. 1.5b**). In the hRBM3, a "g" to "a" point mutation exists, showing ag|aag|CCAGGG in mice and ag|aaaCCAGGG in humans at the 3'SS, thereby lacking NAGNAG tandem acceptors in humans. Similarly, at the 5'SS, there also exists a "g" to "a" point mutation with "gtag|gtga" in mice and "atag|gtga" in humans, resulting in no alternative splicing event there in humans. These differences between human and mouse are likely cis-driven species-specific alternative splicing events. So far, it remains elusive why mice generate these particular mRNA and protein isoforms, and whether these species-specific isoforms function distinctly. Additionally, the NMD targeting isoforms, exon 3a inclusion and exon 3 exclusion, might also exist in mice since sequence identities between humans and mice are quite high with 91% identity in exon 3a and its flanking region as well as 85% similarity of exon 3 and its flanking sequences. So far, it remains unknown why the cells generate these NMD targeting transcripts.

Evolutionally, RBM3 gene is quite conserved from mice to humans, and less conserved from snakes to mice, shown in the phylogenetic tree of RBM3 gene (**Fig. 1.6a**). With reference to

alternative splicing events, the exon 2 to exon 5 of RBM3, encoding N-terminal of the RBM3 protein, is the most conserved region. Strikingly, the alternative splicing process of RBM3 seems more complex in low species, especially the region from exon 6 to the transcript end (**Fig. 1.6c**). A comparison of all annotated isoforms reveals more alternative splicing events in the 3'UTR of avian and reptiles than in rodents, monkeys and primates. NAGNAG alternative splicing of exon 6 emerges from the chickens to mice, and then vanishes in the monkeys and humans. In contrast, the GTAG/GTGA alternative splicing of exon 6 at 5'SS, is found only from mice to monkeys, but is absent in humans. Apparently, alternative splicing process of RBM3, is least complicated in humans – lacking almost all types of alternative splicing in the 3'UTR.

In opposition to alternative splicing, alternative polyadenylation (APA) of RBM3 appears more elaborate in high developed eukaryotes. From chickens to humans, only the major polyadenylation signal is conserved, revealing that humans have 2-times more detected APA events than chickens (**Fig. 1.6b**). In humans, even coding and intronic regions of RBM3 contain APA sites, suggesting the importance of APA to fine-tune RBM3 transcript expression in humans. This is consistent with the finding that the number of polyadenylation factors tend to increase in higher eukaryotes through phylogenetic analyses of eukaryotic polyadenylation factors in several organisms[220].

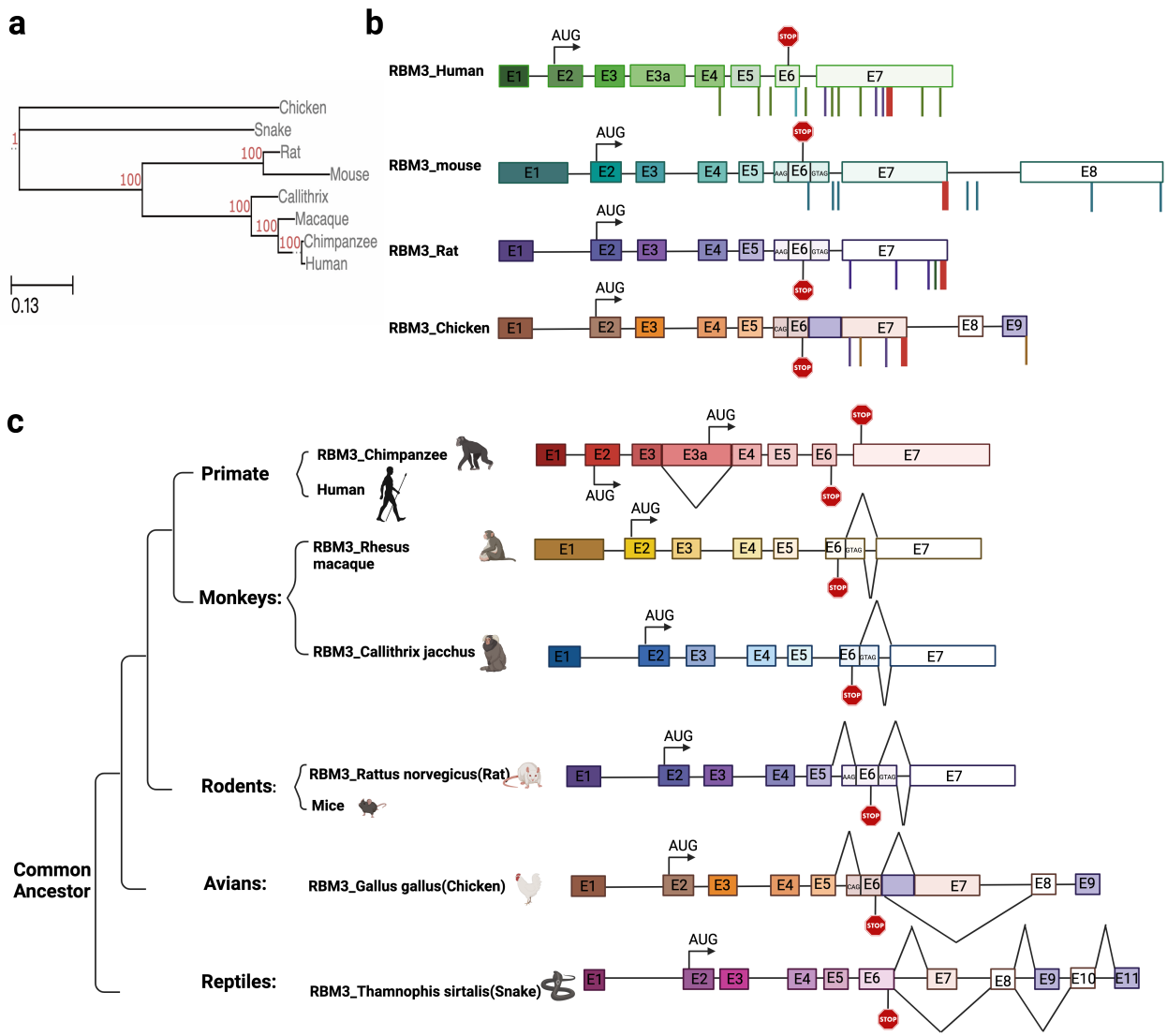

Figure 1.6 Evolution of alternative polyadenylation and splicing of RBM3. a, Phylogenetic tree of RBM3 gene. The number represents bootstrap value. **b**, Alternative polyadenylation signal of RBM3 in different species from PolyA-DB database. Each polyA signal is marked by a vertical line. The bold red vertical line indicates the major polyA site. **c**, Differential alternative splicing processes of RBM3 in divergent species. Each rectangle represents a exon, and the solid line is intronic region. Fold line links the ligated exons together.

Evolutionally, RBM3 gene is quite conserved from mice to humans, and less conserved from snakes to mice, shown in the phylogenetic tree of RBM3 gene (**Fig. 1.6a**). With reference to alternative splicing events, the exon 2-5 of RBM3, encoding N-terminal of the RBM3 protein, is the most conserved region.

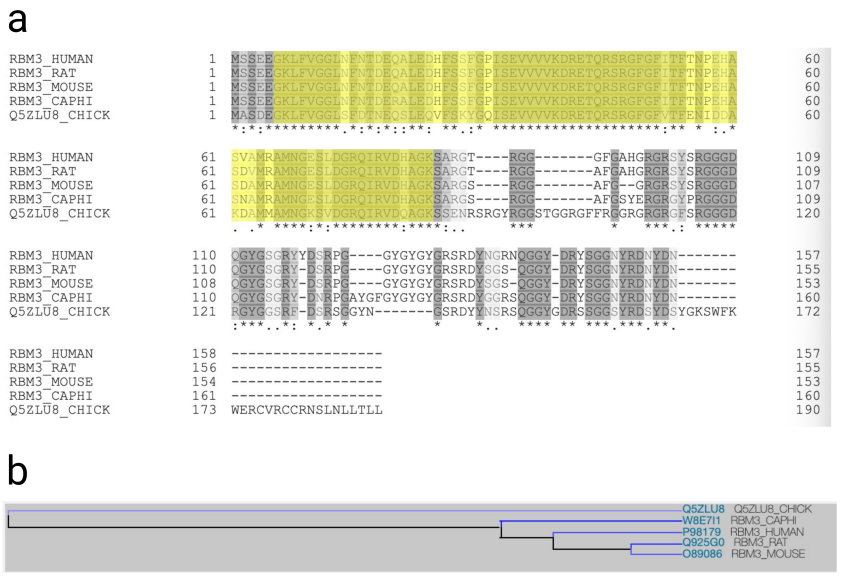

Figure 1.7 Evolutional conservation of RBM3 protein. a, Sequence alignment of RBM3 protein across different species from humans to chickens**.** N terminal of RBM3 is evolutionally conserved, and C terminal of RBM3 is less conserved. **b**, Phylogenetic tree of RBM3 protein. Rat and mouse is closer to humans in comparison to chimpanzees. CAPHI indicates chimpanzee.

RBM3 protein is also evolutionarily conserved from chickens to humans, showing a similar size and high conservation in amino acid sequence especially in the N-terminal domain (**Fig. 1.7a**)[221]. RBM3 belongs to the glycine–arginine (GR)-rich RNA-binding protein (RBP) family, containing one *beta*-sheet packed N-terminal RNA-binding domain (RRM), a highly flexible disorder C-terminal GR-rich region composed of a stretch of RGG/RG repeats and a low sequence complexity YGG-rich region (**Fig. 1.5c, d** and **e**). The RRM domain, as a widespread protein structure in high organisms, usually binds 2-6 nucleotides, and clustered copies of this domain can further facilitate its binding affinity and specificity[222]. Both truncated minimal RRM domain and sequences consisting of several arginine–glycine (RG) motifs of RBM3 are capable of forming oligomers in solution via nonspecific interactions on the grounds that the minimal RRM domain has multiple 'sticky' patches on its surface, which drive the formation of the asymmetric oligomers. Interestingly and importantly, the oligomerization favors at low temperature. The molecular basis of its temperature-dependent oligomerization potentially accordingly links it to its function as a cold-shock protein[223]. This temperature dependent oligomerization may also result in liquid–liquid phase separation and might trigger the formation of stress granules under cold-shock conditions (**Fig. 1d**). RBM3–RNA complex also possibly exists in a dynamic equilibrium of monomeric and oligomeric forms as the chemical

shift perturbation doesn't fit to a 1:1 binding model (**Fig. 1.5d**). If RBM3 favors phase separation at low temperature, it will be totally different from the basic concept that increased temperature may accelerate phase separation of proteins due to the thermodynamical driven[224].

5.1.2 Spatial and temporal distribution

At a cellular level, RBM3 protein is predominantly found in the nucleus, but can undergo nuclear-cytoplasmic shuttling[225]. For example, RBM3 shuttles to endoplasmic reticulum (ER) during ER stress[226]. In *ex vivo* cultured rat neurons, RBM3 is in the nucleus and in a heterogeneous population of granules within dendrites. NAGNAG RBM3 protein isoforms, that differ by a single Arg, are identified in neurons with identical expression. The variant lacking Arg tends to accumulate in the dendrite and cytoplasm in neurons, while in astrocytes it is the only isoform (**Fig. 1.8a**). Meanwhile, Arg^+ variants exhibit higher signal in the nucleus[227]. So far, it remains elusive that 1) whether these two isoforms have a similar function in different physiological conditions; 2) why and how cells produce two isoforms with just one amino acid difference; 3) why they differentially distribute in neurons; 4) whether they are differentially expressed in other cell types and 5) whether the spatial distribution of these different mRNA isoforms of mRBM3 is also divergent in cells.

RBM3 broadly expresses in multiple tissues *in vivo*. In rat brains, RBM3 expression is developmentally regulated, peaking in the first to second postnatal (P) weeks, followed by a decline in most brain regions. Meanwhile, its subcellular distribution shifts from nuclear to more soma-dendritic distribution from P13. RBM3 expression is the highest in cerebellum, olfactory bulb, proliferating cell fields and other regions with high translation rates. RBM3 mRNA and protein express in both glutamatergic and GABAergic cells, showing strong dendritic labeling signal[228]. Similarly, in mouse olfactory bulb, cortex, and cerebellum, RBM3 expression significantly decreases at both RNA and protein levels in an age dependent manner. Immunohistochemistry staining showed that spatial-temporal distribution of RBM3 expression is consistent with doublecortin, a marker of neuronal precursor cells, indicating that RBM3 may function in neuronal precursor cells[229]. Differential RBM3 expression is also observed in different stages of mouse Sertoli cells, and interestingly its expression decreases in Sertoli cells of cryptorchid testis, indicating a potential function in the development of germ cells[230]. In both male and female mice, RBM3 expression in the reproductive organs (testis and ovary) is higher than in other organs, such as heart, liver and kidney, and its expression seems to be correlated with the reduced temperature of these organs[231]. Additionally, mRNA expression of RBM3 is

higher (around 2 folds) in the sexually dimorphic nucleus of the preoptic area (SDN-POA) of male mice compared to that of female mice. Pharmaceutical inhibition of NMDA results in downregulation of RBM3 in male mice, but not in female mice. Why RBM3 mRNA shows differential expression between male and female mice in SDN-POA region remains unclear. More studies need to be done to check whether the difference is due to X chromosome inactivation. It is also unknown whether RBM3 is involved in neuronal survival of SDN-POA during development and how NMDA receptor activation regulates RBM3 expression. Lastly, it is noticed that in humans, like mice, RBM3 protein expression is significantly higher in infants (<1 year) than that in older years (1, 4, 34 years) in prefrontal cortex, hippocampus, and hypothalamus (**Fig. 1.8b**)[232].

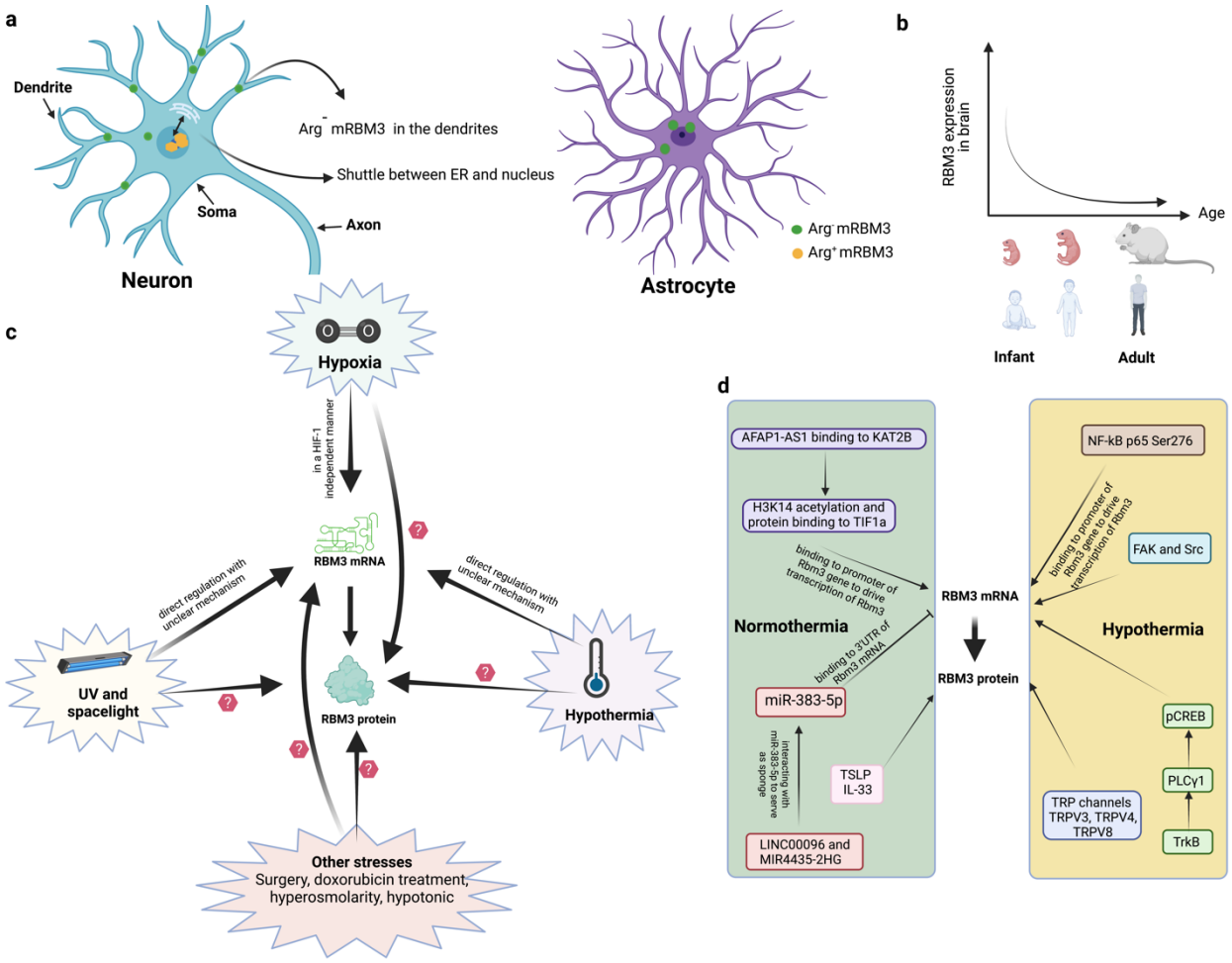

Figure 1.8 Expression, induction and molecular regulation of RBM3. a, Distribution of two isoforms of mRBM3 in neurons and astrocytes. mRBM3 without arginine is mainly located in the dendrites, and mRBM3 containing arginine primarily distributes in soma and can shuttle between ER and nucleus. Green dot indicates mRBM3 with arginine, and yellow dot represents mRBM3 without arginine. **b**, Age-dependent expression of RBM3 in human and mouse brain. RBM3 expression

significantly decreases with the increasing ages in human and mouse brain from infants to adults. **c**, Induction of RBM3 at mRNA and protein level. Question mark means the induction remains elusive. **d**, Molecular mechanisms of RBM3 induction under hypothermia and normothermia.

5.1.3 Hypothermia induction

In 1997, Danno *et al.* firstly reported that RBM3 transcripts strongly increased at low temperature (32°C) in a variety of human cell lines. Meanwhile, the group found that RBM3 was upregulated at RNA level with cycloheximide treatment, but wasn't upregulated at RNA level with other stresses, such as cadmium chloride, H_2O_2, ethanol, and osmotic shock, arguing against a general induction by cellular stress[233], and also indicating that non-sense mediated decay may be involved in regulating the expression of RBM3 RNA. Later, mRBM3 cDNA was cloned, and it was found that mRBM3 expression is temperature sensitive at both RNA and protein levels[230]. In cultured young rat neurons and astrocytes, RBM3 protein expression is ultra-sensitive to temperature alternations, and even 1°C reduction can result in the upregulation of RBM3[234]. In the hibernating ground squirrel, RBM3 is elevated during pre-hibernation and hibernation in both hypothalamus and cerebral cortex[235]. Taken together, the expression of both RBM3 RNA and protein is highly responsive to temperature, and this phenomenon is conserved in mammals. It has been shown that the activity of CLK1/4 kinases, which globally control alternative splicing and gene expression as a thermo-sensor, is sensitive to physiological temperature changes from 33°C to 40°C[236]. Additionally, temperature-driven alternative splicing also has been reported to be coupled with mRNA decay[237]. This suggests a potential role of CLK1/4 kinases as thermo-sensor modulating cold-induced RBM3 expression. Additionally, some other inducers also have been demonstrated to induce RBM3 at mRNA level or protein level (summarized in **Fig. 1.8c**)

5.2 Molecular mechanism of RBM3 induction

Twenty years ago, an RBM3 leader sequence, mediating cap-independent translation via an internal ribosome entry site (IRES), was seemingly identified, showing a higher activity at 33°C compared to that at 37°C in some cell lines[238]. Later, discrete *cis*-regulatory elements including a 22-nt IRES module, a 10-nt enhancer, and 2 inhibitory sequences, were dissected within the 720bp 5' leader of the RBM3 mRNA[239]. Unfortunately, the 5' leader was subsequently demonstrated as a cloning artifact because it was mapped to mouse chromosome 18, rather than chromosome X, where the RBM3 gene is located[240].

One effect of cooling is the activation of TrkB via PLCγ1 and pCREB signaling, which increases RBM3 protein expression *in vivo* in mice. Blocking of TrkB activation abolishes cooling-induced structural plasticity in neurons, suggesting that the non-canonical TrkB/PLCγ1/pCREB signaling pathway connects cooling with neuroprotection caused by RBM3[241]. Ushio *et al.* reported that phosphorylated NF-kB p65 Ser276 could bind to a putative promoter region of RBM3 to drive RBM3 transcription under hypothermia. This connection is strengthened by the finding that CAPE (caffeic acid phenethyl ester), preventing the translocation of NF-kB p65 from the cytoplasm to the nucleus, repressed RBM3 expression at low temperature[242]. Recently researchers found that both knock-down of FAK (focal adhesion kinase) and Src via siRNA and pharmaceutical inhibition of FAK can abrogate RBM3 expression and its neuroprotection against rotenone, thereby indicating that the FAK/Src signaling axis regulates the transcription of RBM3 gene in human SH-SY5Y neuroblastoma cells, HEK293 and PC12 cells[243].

Under hypothermia, TRPV family, a well-known thermo-sensor, is involved in RBM3 induction in the protein level. At 37°C, both RN1747 (a TRPV4 agonist) and GSK1016790A (a more specific and potent TRPV4 agonist) inhibits RBM3 protein expression in U-2 OS cells[244]. Under hypothermia (32°C), shRNA against TRPV4 suppresses RBM3 protein expression[244]; Gd^{3+} (a broad TRPV channels inhibitor), Ruthenium red (a broad inhibitor of nonselective cation channels including all TRP channels) and RN1734 (a selective TRPV4 antagonist) also abolish RBM3 protein induction[244], but RN1734 cannot repress RBM3 expression in the cell lines derived from TRPV4-KO mice[245], suggesting that the hypothermia induction of RBM3 is dependent on TRPV4. As TRPV4 functions as a nonselective cation channel with moderate calcium selectivity that mediates heat-induced calcium influx[246], the researchers further investigated whether Ca^{2+} contributed to the induction of RBM3 under hypothermia. However, both A23187 (a calcium ionophore) and BAPTA-AM (a cell-permeant chelator) inhibited RBM3 expression at 32°C as well as 37°C[244]. Taken together, it seems that both TRPV4 activation at 37°C and inactivation at 32°C could inhibit RBM3 expression, and its effect on RBM3 expression is independent on the ion channel activity on the grounds that both up-regulation and down-regulation of intracellular calcium repress RBM3 expression. Given that BAPTA-AM has broader effect in cells and it significantly reduces free intracellular calcium, thereby generating more other cellular events[247], we possibly can just focus on the a calcium ionophore effect on RBM3 expression. It seems that at 37°C increasing intracellular calcium will repress RBM3 expression, while the inhibitory effect of TRPV4 on RBM3

expression is dispensable of its activity that mediates calcium influx at 32°C. At 37°C, increased intracellular calcium will activate calcium-activated potassium channel, suggesting that RBM3 expression may be coupled with intracellular potassium concentration.

Furthermore, Takanori Fujita *et al*. found the induction of RBM3 under hypothermia was still observed in the TRPV4-KO cells, indicating that other TRP channels may compensate the effect of TRPV4. TRPV3 and TRPM8, but not other TRPV ion channel family proteins, were identified to be necessary for RBM3 expression through specific inhibition via S408271 and AMTB (TRPV3 and TRPM8 specific inhibitor) at both 32°C and 37°C and siRNA against TRPV3 and TRPM8 at 32°C. However, unexpectedly, camphor and WS-12, which specifically activate TRPV3 and TRPM8 channels respectively, do not enhance RBM3 expression, but down-regulate RBM3 expression at 37°C. In summary, TRPV3, TRPV4 and TRPV8 may have other unknown functions, which are not related to its ion channel activity, to modulate RBM3 induction. More work need to be done to demonstrate how TRPV family modulate RBM3 expression at hypothermia, normal or high temperature, whether calcium is the direct mediator in the regulation need to be further investigated and whether calcium is the direct effector to modulate RBM3 expression and if so, how it orchestrates RBM3 expression.

Non-coding RNAs, such as lncRNA and microRNA, are also involved to regulate RBM3 expression at normal temperature. In nasopharyngeal carcinoma cells, TIF1a (Transcription intermediary factor 1-alpha) is identified as a nuclear transcriptional coactivator to drive RBM3 transcription from RNA-seq datasets, and then it is validated by CHIP-seq[248]. AFAP1-AS1 (Actin filament-associated protein 1-antisense 1) was also demonstrated to bind KAT2B (Lysine Acetyltransferase 2B), to promote acetyltransferase activation, thereby enhancing H3K14 acetylation and protein binding to the bromo domain of TIF1a, further increasing transcription level of RBM3. Rui Ma *et al.* reported that miR-383-5p, which is down-regulated in NPC tissues and cells, directly targeted 3'UTR of RBM3 predicted by Target Scan, and overexpression of miR-383-5p decreased the expression of RBM3 protein[249]. Furthermore, it was reported that miR-383-5p interacts with lncRNA LINC00096 triple-negative breast cancer and MIR4435-2HG in head and neck squamous cell carcinoma, which can serve as a miRNA sponge to regulate RBM3 expression[250,251].

Although it has been demonstrated that several mechanisms are involved in the regulation of RBM3 induction at low temperature (summarized in **Fig. 1.8d**) , how is the specificity of cold-induced protein expression narrowed down to RBM3 (and/or other few cold induced proteins)?

Despite of a lot of ongoing research, it is still not clear how RBM3 is selected to increase its expression under hypothermia even though the overall protein synthesis is significantly reduced at low temperature. Open questions are: 1) identification of other specific transcription factors (in addition to NF-kappa B) driving RBM3 transcription, 2) whether alternative splicing or polyadenylation events of RBM3 significantly change in various induction conditions, 3) what key *cis*-regulatory elements and *trans*-acting factors contribute to the post-transcriptional regulation of RBM3 and 4) whether these *cis* and *trans* factors are responsible for the RBM3 induction under various stress conditions. RNA modification patterns and RNA degradation may also be involved in RBM3 induction, and modulation at the protein level also may contribute to control RBM3 expression. It is known that cooling can globally repress translation, but it is still elusive whether translation efficiency and protein degradation of RBM3 alter in different cellular circumstances.

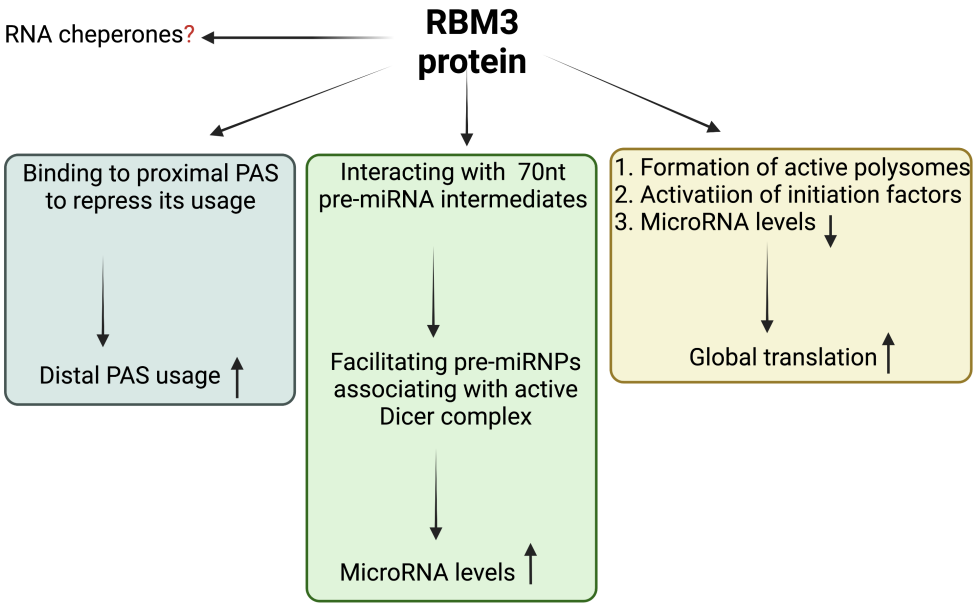

Figure 1.9 Functions of RBM3 in gene regulations. RBM3 is capable of regulating gene expression in different levels including promoting distal PAS usage, increasing microRNA level, and enhancing global translation.

5.3 Functions of RBM3

RBM3 plays an important role in different cellular conditions, but the molecular details how RBM3 functions in numerous stress conditions are not fully understood. Here, I first discuss how RBM3 is involved in different layers of gene regulation and then describe its potential role as RNA chaperone (summarized in **Fig. 1.9**).

RBM3 is involved in post-transcriptional regulation of gene expression. Liu *et al.* reported that RBM3 regulates circadian gene expression by controlling alternative polyadenylation, binding to proximal alternative polyadenylation sites to repress PAS usage, and thereby facilitating distal PAS usage.[252-254] Increasing evidence has shown that alternative polyadenylation is essential in development, cellular differentiation and proliferation and neuronal activity, and its dysregulation is involved in cancers and other diseases related to the nervous system[254]. It has been reported that cancer cells tend to globally shorten 3′UTRs of mRNA, while neurons prefer to use distal polyadenylation site which may in part be influenced by RBM3[253].

In the B104 neuronal cell line, more than 60% of miRNAs are significantly downregulated after RBM3 knockdown, while overexpression of RBM3 restores miRNAs level. Furthermore, it was shown that Dicer activity and transport of pre-miRNAs from the nucleus to cytoplasm weren't affected by RBM3 reduction. Rather, RBM3 can directly bind to 70 nt pre-miRNA intermediates and facilitate their integration into larger ribonucleoproteins (pre-miRNPs), which can then be further processed by activated Dicer.[255] How RBM3 choses its miRNAs target and how this activity relates to cellular functionality remains to be discovered.

RBM3 enhances global translation in B104 cells through facilitating the formation of active polysomes, activating initiation factors in N2a cells and counteracts FMRP (Fragile X mental retardation protein) function at the level of translational regulation[227]. Overexpression of RBM3 at both 37°C and 32°C increases protein synthesis by 3 folds possibly through its binding to 60S ribosomal subunits in an RNA-independent manner. However, overexpression of RBM3 does not alter the ratio of monosomes to polysomes, suggesting that a similar percentage of mRNAs is actively translated. Subsequently, it is suggested that RBM3 may affect protein synthesis by a post-translational mechanism, that RBM3 alters microRNA levels to influence the stability of the nascent peptide[256]. Current research has shown that RBM3 is involved in the regulation of alternative polyadenylation, miRNA biogenesis and translation, and now it will be interesting to determine whether RBM3 also specifically participates in the modulation of other layers of gene regulation, such as transcription, alternative splicing, or mRNA turnover.

Here, we proposed that RBM3 probably serves as an RNA chaperone. First of all, PAR-CLIP datasets indicate that the RNA binding specificity of RBM3 is relatively broad, showing that several thousand binding sites are distributed in the CDS, intronic regions and UTRs with an enrichment in 3′UTRs within 100 nucleotides upstream of the polyadenylation sites[257]. A G-

rich binding motif was identified, which however was only present in around 60% of the exonic binding sites and was not very significant, suggesting its broad binding specificity. Furthermore, transcriptomic analysis by RNA-sequencing of RBM3-/- lung innate lymphoid cells (ILCs) shows increased type 2 cytokines and IL17A as well as global expression differences in critical cytokines, receptors, transcription factors, and survival transcripts compared with WT ILCs. These transcript changes do not correlate with the presence of AU-rich elements (AREs), which RBM3 has been suggested to bind[225,258]. This again indicates that RBM3 may interact with RNAs in a sequence-nonspecific manner although these changes may be an indirect effect of RBM3.

Single-stranded RNAs are highly flexible macromolecules and can take a wide variety of alternative conformations. RNA folding, especially that of large RNAs, must be assisted for the RNA to reach the biologically relevant conformation and not be trapped in one of the many potential and incorrect structures. There are many RNA-binding proteins that recognize RNA with a broad specificity, also termed nonspecific nucleic acid-binding proteins. These proteins have a biological role as RNA chaperones and are thought to directly assist folding of RNA by preventing and resolving misfoldings. Some RNA-binding proteins are highly specific for an RNA motif or RNA structure. Others are less sequence-specific and can bind to RNA with high affinity, whatever its sequence, by a highly cooperative mode of interaction. However, these latter proteins may also have high-affinity binding for sequence-specific sites, which can then be used as nucleation sites for RNP formation. Once the the RNA has been folded, the RNA chaperone can be removed without altering the RNA conformation. Moreover, RNA chaperones do not need ATP or GTP hydrolysis to achieve their function[259]. We here speculate that RBM3 acts as an RNA chaperone, which will be addressed in future research. It is especially interesting to speculate that this function is required at lower temperature, where the tendency of RNAs to form intra- and intermolecular secondary structures is increased. Also, the potentials of RBM3 oligomerization at low temperature may also implicate its RNA chaperon role.

Both Hfq[260], a stress response protein in bacteria, and CspA[261], the major cold-induced protein expressed in *Escherichia coli* upon temperature downshift, are known to be global post-transcriptional regulators that chaperone small RNAs[262]. In bacteria, it is well-known that most of the translation machinery is repressed at cold stress, and one of the mechanisms is that 5′-UTR of mRNAs tends to form stable secondary structures upon cold stress, thereby masking

the Shine–Dalgarno sequence of mRNAs from the ribosome or interfering with subsequent translation elongation steps. In analogy, RBM3, as a stress and cold induced protein, like CspA in bacteria, may serve as an RNA chaperon to modulate the secondary structure of mRNA, which may thus contribute to fine-tune translation efficiency[142]. In line with this idea, RBM3 enhances global protein synthesis at both physiological and mild hypothermic temperatures. In sucrose gradient assays, RBM3 cofractionates with heavy mRNA granules and multiple components of the translation machinery, further indicating an involvement of RBM3 in controlling translation[256]. However, the mechanism that RBM3 modulates RNA secondary structures and translation remains to be discovered. We hypothesize that the RNA to RBM3 ratio in cells will determine the role and binding mode of RBM3 to RNA. At high temperature, RNA binding may be limited to some high affinity binding sites, whereas at low temperature RBM3 levels increases, which may allow spreading of RBM3 along RNAs from high affinity nucleation sites. This could result in many cellular RNAs covered with RBM3 al low temperature and could point to a general role of RBM3 as RNA chaperone that could control formation of intra-and inter-molecular secondary structures, the formation of aggregates and phase separation. However, such functions remain speculative at present.

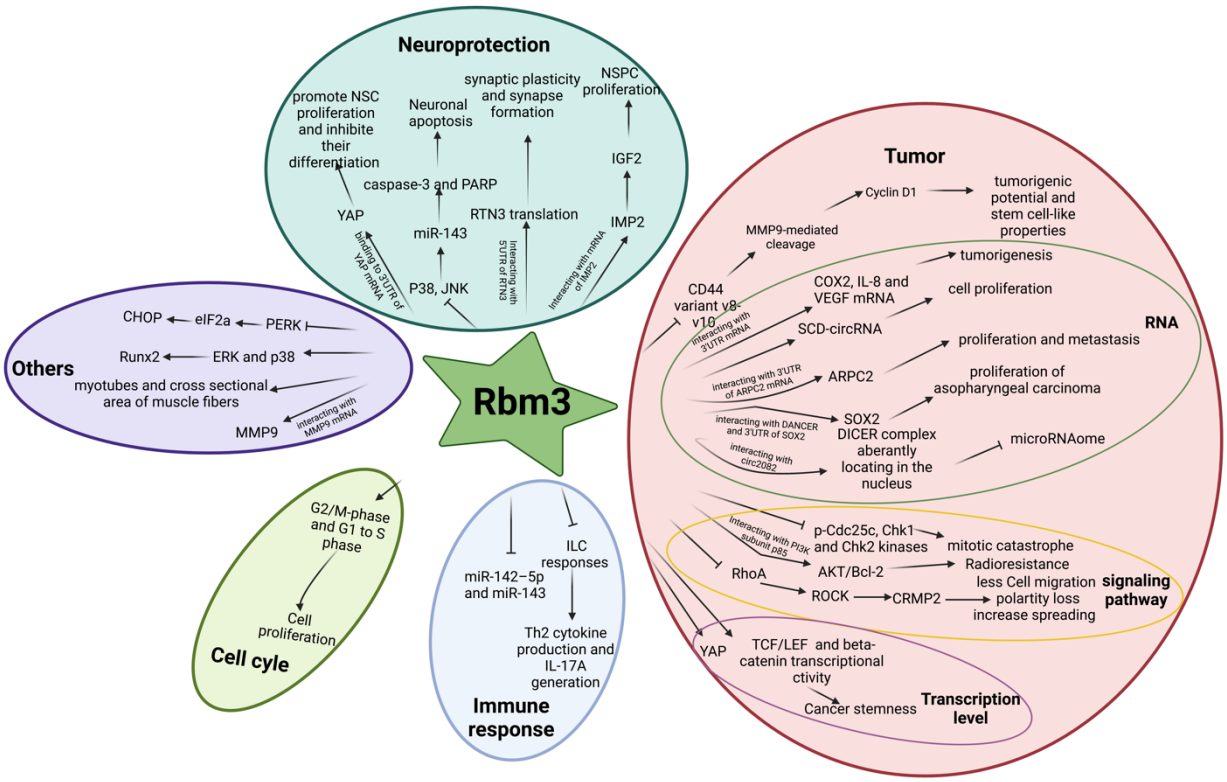

Figure 1.10 Functional molecular mechanisms of RBM3 in different cellular settings. RBM3 functions in a cellular level in different scenarios including 1) tumor through regulating RNA metabolism, signaling pathway and manipulating transcription; 2) neuroprotection via regulating distinct signaling pathways; 3) inhibiting immune response; 4) promoting cell proliferation through cell cycles; 5) others.

5.3.1 Neuroprotection

RBM3 is thought to mediate, at least partially, the profoundly neuroprotective function under hypothermia, which has been used for several decades in clinic although it remains some controversies[263]. RBM3 is ubiquitously expressed in the brain, but there is no obvious abnormality in brain development in RBM3 KO mice, probably due to other unknown compensative effects[264]. Peretti *et al.* reported that cooling could increase synapse numbers and restore neuronal structural plasticity in both prion-infected and 5XFAD Alzheimer's disease mouse models. Indeed, lentiviral-mediated RBM3 expression in brain prolongs survival time of disease mice, while knockdown of RBM3 via shRNA decreases survival time[265]. A potential downstream target of RBM3 is RTN3 (Reticulon 3), which is directly involved in synaptic plasticity and synapse formation. In this scenario, RBM3 could act as a *trans*-acting factor, which promotes RTN3 translation through interacting with the 5'UTR of RTN3 mRNA. This link is strengthened by the finding that lentiviral-mediated downregulation of endogenous RTN3 partially abolishes cold-induced neuroprotection mediated by RBM3 in prion-disease mice, indicating that RTN3 is required for RBM3-mediated neuroprotection[266]. Another paper also demonstrated the neuroprotective roles of RBM3 in maternal cooling stress. RBM3 associates with the 3'UTR of Yap1, thereby increases the stability of Yap1, and finally enhances the proliferation rate of neural stem cells and inhibits their differentiation[236]. A similar finding was made in an siRNA-mediated knock-down of RBM3 in neuronal cells, which significantly diminishes the neuroprotective effect of hypothermia, while over-expression of RBM3 attenuates cleavage of PARP and prevented inter-nucleosomal DNA fragmentation and apoptosis[229]. RBM3 can also block the activation of p38 and JNK signaling pathways, and thus can decrease levels of cleaved caspase-3 and PARP, which promotes cell survival after UV irradiation in neuronal SH-SY5Y cells[267]. Additionally, Yang *et al.* showed that overexpression of RBM3 prevented SH-SY5Y cells from NO-induced apoptosis through suppressing NO-induced miR-143 production in a P38-dependent manner, while RBM3 silencing abolishes neuroprotective effect of mild hypothermia[268].

RBM3 has also been suggested to play a beneficial role in several *in vivo* models for acute brain injury. For example, it has been reported that more neurons are generated in the CA1 region of rats, which are exposed to hypothermia (32–33°C) for 2hrs immediately after resuscitation from 5 min of asphyxia cardiac arrest, and the neural production is coincided with an upregulation of RBM3. However, a direct role of RBM3 was not shown as other cold-induced proteins may be responsible for the neuronal protection[269]. Zhu *et al*. reported that RBM3 facilitated neurogenesis in a niche-dependent manner in adult hypoxic ischemia (HI) injury mouse model. In this scenario, RBM3 interacts with IGF2 mRNA binding protein 2 (IMP2), enhances its expression by an unknown mechanism[270] and thereby stimulates IGF2 release specifically in neural stem cells in the subventricular zone (SGZ). The mechanism what makes RBM3 function specifically in the SGZ remain elusive, but it may be related to the response to IGF2.

5.3.2 Immune response

In both heterozygous and homozygous RBM3 KO mice, both eosinophilic lung inflammation and Innate lymphoid cells (ILC) activation tend to increase, showing elevated Th2 cytokine production and IL-17A generation. Transcriptomic analysis in RBM3-/- lung ILCs shows global expression of critical cytokines, receptors, transcription factors, and survival transcripts is also significantly different compared to WT ILCs[258]. Matsuda *et al.* reported that RBM3 interacts with immunogenic DNA, CpG-B, a TLR9 activator in HEK293T and RAW264.7 cells. However, unexpectedly, no obvious phenotype was found in RBM3-/- mice for the DNA-mediated induction of cytokine genes. It is possibly due to compensatory effects from other proteins when RBM3 is completely lacking[264]. It was also found that the expression of "thermomiRs", miR-142–5p and miR-143, which target immune genes and further control fever, was significantly anti-correlated with RBM3 expression in THP-1-derived macrophages, and knock-down of RBM3 increases "thermomiRs" expression. However, most temperature-sensitive miRNAs are not regulated by RBM3, which raises the question how RBM3 targets these two "thermomiRs"[271].

5.3.3 Cell cycle

It seems that RBM3 has a cell-type specific function to control cell proliferation. A delayed proliferation and an increased G2/M-phase cell population are just found in the RBM3$^{-/-}$ MEFs, not in GM-CSF cultured bone marrow cells. Also, Wellmann *et al.* reported that the cell death

induced by siRNA-mediated RBM3 knock-down is not associated with cell cycle arrest in both HEK293 and K562[272]. The expression levels of cyclin B, cell division cycle 2 protein and essential regulators of the G2/M transition are normal in RBM3 deficient cells. Thus, how RBM3 modulates G2/M transition remains elusive. When RBM3 is over-expressed, hypoxia-induced cell cycle arrest in G0/G1 phase is relieved and more cells in S phase are observed. In RBM3 KO neural stem cells (NSCs), less BrdU-incorporation indicates a reduced number of cells in the S phase, while RBM3 overexpression increases proliferation rate of primary NSCs[264]. These data together clearly show a role of RBM3 in cell cycle control, but the mechanistic basis remains unknown.

5.3.4 Tumor

Several studies have reported that the expression of RBM3 is aberrant in a variety of cancers, and thus the occurrence and development of different tumors has been suggested to link to RBM3[273]. RBM3 protein can be detected in a variety of tumors, and it, as an RNA binding protein, may modulate alternative splicing of its targeting RNA molecules. Indeed, Yu Zeng *et al*. showed that RBM3 expresses at a very low level in human fetal prostate and in $CD133^+$ prostate epithelial cells, and its overexpression in prostate cancer cells attenuates cancer stem cell-like properties *in vitro* as well as tumorigenic potential *in vivo*. More interestingly, overexpression of RBM3 inhibits the generation of the CD44 alternative splicing variant v8-v10 and increases the major CD44 isoform production. Conversely, silencing RBM3 up-regulates the ratio of CD44 v8-v10 to major CD44 mRNA isoforms. Further mechanistic studies shows that elevating CD44 v8-v10 disrupts the MMP9-mediated sequential proteolytic cleavage of CD44, thereby the less released CD44 intracellular domain (CD44-ICD) translocates to the nucleus to activate gene transcription such as cyclin D1, and eventually cyclin D1 expression is supressed[274]. Taken together, these findings suggest that RBM3 can attenuate stem cell-like properties in prostate cancer by inhibiting the generation of CD44v8-v10 isoform. However, whether and how RBM3 directly regulates CD44 alternative splicing of CD44v8-v10 remains to be further investigated.

Overexpression of RBM3 in NIH3T3 mouse fibroblasts and SW480 human colon epithelial cells increases cell proliferation and development of compact multicellular spheroids, indicating that RBM3 can induce anchorage-independent cell growth. Knockdown of RBM3 not only decreases cellular growth in cell culture, but also results in the growth arrest of tumor xenografts[225]. At the molecular level, RBM3 facilities tumorigenesis through interacting with

the ARE region in the 3'UTR of COX-2, IL-8, and VEGF mRNAs, which increases mRNA stability and translation[225]. Dong *et al*. reported that stearoyl-CoA desaturase (SCD)-circRNA, derived from the 3'UTR of the SCD gene, was significantly upregulated in hepatocellular carcinoma **(**HCC) and correlated with poor patient prognosis. Meanwhile, they found that RBM3, an indicator of a short recurrence-free survival and poor overall survival for HCC patients, promotes HCC cell proliferation in a SCD-circRNA dependent manner. Deprivation of SCD-circRNA inhibits cell proliferation, while its upregulation promotes cell proliferation. RIP pulldown assays shows that SCD-circRNA interacts with RBM3[275]. However, whether RBM3 facilitates SCD-circRNA formation and how the RBM3-SCD-circRNA complex contributes to tumor cell growth remain unclear. More studies need to be done to answer how RBM3 selects SCD-circRNA, the interaction is sequence specific or not, whether RBM3 can also interact with other circRNAs, and whether the interaction is cell type specific. It has been shown that RBM3 interacts with 3'UTR of ARPC2 (actin-related protein 2/3 complex subunit 2) mRNA to stabilize it. Knock-down of ARPC2 represses proliferation and metastasis of the breast cell line, while its overexpression antagonizes the inhibitory effect[276]. RBM3 also interacts with the lncRNA DANCR, whose expression in NPC tumor tissues is significantly higher than that in adjacent normal tissues, to form DANCR/RBM3 complex. Meanwhile, the interaction between RBM3 and the 3'UTR of SOX2 mRNA, a transcription factor acting as an oncogene, also is observed, and this association can increase the stability of SOX2. Furthermore, silencing DANCR dramatically down-regulates SOX2 expression, indicating that DANCR/RBM3 complex interacts with SOX2 through RBM3 to stabilize itself, thereby activating SOX2-induced nasopharyngeal carcinoma (NPC) tumorigenesis. DANCR is significantly correlated with SOX2 and RBM3 expression in 100 clinical NPC tissues[277]. A. Bronisz *et al*. reported that the DICER complex, which is the major enzymatic complex involved in microRNA maturation, is aberrantly retained in the nucleus of the glioblastoma patient samples, thereby resulting in the downregulation of microRNAome. Intriguingly, RBM3 is the most abundant nuclear DICER-interacting protein but doesn't interact with cytosolic DICER. Subsequently, the circRNA circ2082, one of the most up-regulated circRNAs in glioblastoma, is identified to directly bind to RBM3 within the DICER, indicating that DICER/RBM3 can form complex with circ2082. Circ2082 deprivation via antisense oligonucleotides dramatically restores the abnormal nuclear localization of DICER in glioblastoma, leading to global microRNA upregulation[278].

Several signaling pathways are also involved in the cellular regulation of RBM3 in tumors. Ma *et al*. found that RBM3 was upregulated in radioresistant nasopharyngeal carcinoma (NPC) tissues and cells. RBM3 depletion in radioresistant NPC cells sensitizes cells to radiotherapy, showing increased DNA damage and apoptosis, while RBM3 overexpression in parental NPC cells significantly enhances radio-resistance. Inhibition of AKT signaling attenuates RBM3-mediated radio-resistance, and RBM3 directly interacts with PI3K subunit p85 in NPC cell lines. These data demonstrate that RBM3 facilitates radio-resistance through interacting with PI3K subunit P85 and triggering the downstream AKT/Bcl-2 signaling pathway to repress apoptosis[279]. Additional work indicates that RBM3 expression in spreading initiation centers and filopodia in B104 cells and primary myoblasts is capable of regulating cell polarity, spreading and migration. Reduction of RBM3 causes exaggerated spreading, increased RhoA expression, a loss of polarity, slowing migration and less protrusions, while overexpression of RBM3 enhances cell migration with extension of long protrusions. Thus, RBM3 is potentially prominent for tissue repair, metastasis, and development[280].

It was also reported that RBM3 could indirectly increase the activity of some transcription factors to promote cancer cell proliferation and enhance their stemness. Expression of RBM3 in both nucleus and cytoplasm is higher in hepatocellular carcinoma tissues compared to that in adjacent non-tumorous tissues shown by microarrays and immunohistochemistry. High nuclear RBM3 levels is highly correlated with larger tumor size and worse histological tumor grading. Additionally, RBM3 can facilitate YAP1 expression in HCC, and then induce proliferation of HCC cells. The effect can be abolished by Verteporfin, a YAP1 inhibitor. Thus, although it is not clear how RBM3 promotes hepatocellular carcinoma proliferation through YAP1, the RBM3/YAP1 axis provides a starting point to analyze the role of RBM3 in the development of HCC cells[281]. In doxycycline-inducible RBM3 overexpression cell lines, HCT 116 and DLD-1, nuclear *beta*-catenin as well as TCF/LEF transcriptional activity increase with RBM3 expression, indicating that RBM3 induces stemness in colorectal cancer cells through *beta*-catenin signaling. The detailed mechanisms how RBM3 increases stem cell characteristics needs to be further determined[282].

As RBM3 physiologically and widely expresses in an assortment of tumors, a lot of studies investigated the association between its expression with clinical outcome. Here, I summarize the published results (**Table 1**).

Table 1. Correlation between RBM3 and good clinical outcome in patient tumor samples

Association of RBM3 expression with good clinical outcomes		
Cancer type	**RBM3 expression**	**Good outcome**
Colorectal cancers, metastatic colorectal cancer	N/A	Positive[248,249]
Metastatic melanoma	Down-regulation	Positive[249]
Breast cancer	Up-regulation	Positive[250]
Non-small cell lung cancer	N/A	Positive[179]
Intestinal-type gastric cancer	Up-regulation	Positive[251]
Invasive breast cancer	N/A	Positive[252]
Esophageal cancer phenotype	N/A	Positive[253]
Non-seminomatous germ cell tumor	N/A	Positive[254]
Urothelial bladder cancer	N/A	Positive[255]
Adenocarcinomas	N/A	No correlation [179]
Squamous cell carcinomas	N/A	No correlation [179]
Aggressive and recurrent prostate cancer	Down-regulation	N/A[180]
Hepatocellular carcinoma tissues	Up-regulation	N/A[241]
Colitis-associated cancer	Up-regulation	Negative[256]

N/A means no data available in the paper. Positive good outcome indicates that patients with higher RBM3 expression in tumors have good clinical outcome.

Obviously, RBM3 functions distinctly in different tumors. Some published papers show that RBM3 facilitates cell proliferation in different immortal cancer cell lines or mouse models through a variety of mechanisms, and conversely it weakens tumorigenic potential and caner stem cell-like properties just in prostate cancer cells[274]. Moreover, another intriguing result is that high RBM3 expression in cancer patient samples is significantly correlated with good clinicopathological parameters (good outcomes) in the most of the clinical patient samples summarized in **Table 1**, although it promotes cell growth in most of the studies in cancer cell lines. There are several potential explanations for this discrepancy. Firstly, the environment where cancer cell lines are *ex vivo* cultured, is very different from the *in vivo* tumor environment[283]. Secondly, the phenotypes that RBM3 may be involved in the regulation of cell culture such as cell proliferation, migration, cancer stemness, and metastasis, are just some of the hallmarks of cancers. RBM3 possibly also modulates the other hallmarks of cancer, such as inflammatory, vascularization, and immune response, to eventually be beneficial for cancer patients[284-286]. Thirdly, the association between high expression of RBM3 and good outcomes in the clinic is just a correlation relationship and may be as well a passenger effect.

5.3.5 Others

RBM3 also is shown to play essential roles in other scenarios, such as ER stress, muscle growth, osteoblast differentiation, cardiomyocyte protection or hepatoprotection. Blocking RBM3 expression in HEK293 cells increases phosphorylation of PERK (Protein Kinase RNA-Like ER Kinase) and eIF2a (eukaryotic translation initiation factor 2a), while over-expression of RBM3 represses PERK-eIF2a-CHOP signaling under ER stress. In this scenario, nuclear factor 90 (NF90) that interacts with PERK, is essential for RBM3-mediated regulation of PERK[226]. In C2C12 cells, the upregulation of RBM3 results in 1.6 times larger myotubes and attenuates atrophy in myotubes exposed to dexamethasone, indicating that RBM3 is involved in hypertrophy modulation and attenuating atrophy. At the same time, overexpression of RBM3 in mice increases the cross-sectional area of muscle fibers[287]. Interestingly, RBM3 expression in skeletal muscle is significantly higher in Ames Dwarf and calorie restricted mice with extended lifespan compared to WT. It will be interesting to address if higher RBM3 expression is the cause or a result of lifespan extension, and how life span and RBM3 are linked in a molecular level[288]. Moreover, the muscle mass of hibernating animals does not decrease despite the lack of physical activity, reduction of protein synthesis and caloric intake. Given the potential functions of RBM3 in translation orchestration, RBM3 may function to reprogram translation to help hibernating animals to survive. RBM3 is also found to be upregulated in osteogenic conditions, and RBM3 knockdown significantly reduces the expression of osteogenic genes, such as Runx2 and osteocalcin in MC3T3-E1 cells. Further, RBM3 facilitates the phosphorylation of ERK and p38, which are upstream signals of Runx2. It seems that RBM3 contributes to osteoblast differentiation via the ERK-Runx2 signaling pathway[289]. Oxygen-glucose deprivation/reperfusion-induced oxidative stress in cardiomyocytes is attenuated by cooling, thereby preventing secondary apoptosis-driven myocardial cell death. However, it remains unknown which molecule plays a leading role although RBM3 was induced in the setting[290]. Significant hepatoprotection with 24hrs moderate (32°C) hypothermia is observed in acetaminophen-induced hepatocyte toxicity in the TAMH (transgenic mouse hepatocytes cell line) and L-02 (human liver hepatocytes cell line). RBM3 functions in the protection as knockdown of RBM3 dramatically attenuates cell viability and promptly abolishes the protection of hypothermia[291].

5.4 Therapeutic hypothermia

Although mild hypothermia (33°C or 35°C), along with upregulation of RBM3, significantly elevates survival rate in bovine embryos[292], it also can increase several cold-induced proteins as well. So far, to my knowledge, RBM3 is the only protein, which is thought to only have beneficial functions under hypothermia. For other cold induced proteins, such as CIRBP (cold-inducible RNA-binding protein) or RTN (Reticulon 3), it is still controversial whether their effect is beneficial or rather harmful[293]. CIRBP has been shown to be a mediator of sterile inflammation[294], a critical mechanism of the innate immune response in ischemia/reperfusion (I/R) injury[295]. RTN3 is thought to inhibit anti-virial responses[296], suppress hepatocellular carcinogenesis through mediating Chk2/p53 activation and inhibiting neuritic outgrowth after injury. Increased RTN3 leads to obesity and hypertriglyceridemia by interacting with Heat Shock Protein Family A (Hsp70) Member 5 (HSPA5)[297]. Over-expression of RTN3 enhances TRAIL-mediated apoptosis[298], inhibited the axonal transport of BACE1[299], and develops neuritic abnormalities with impairments in spatial learning and memory, as well as synaptic plasticity[300,301]; RTN3 KO also shows adverse effects on BACE1 activity and facilitated amyloid deposition[302].RTN3 is thought to inhibit anti-virial responses[296], suppress hepatocellular carcinogenesis through mediating Chk2/p53 activation and inhibiting neuritic outgrowth after injury. RTN3 associates with β-site amyloid precursor protein cleaving enzyme 1 (BACE1), which is involved in the generation of β-amyloid peptides (Aβ) to regulate its activity[302] through blocking access of BACE1 to amyloid precursor protein and reduce the cleavage of this protein[303]. Also, RTN3 was reported to inhibit prion protein clearance through autophagy inhibition[304], while it promotes the disposal of pathogenic prohormone aggregates including detergent-insoluble aggregates formed by Akita mutant proinsulin[305] through complexing with the ER transmembrane protein PGRMC1[306]. RTN3 is crucial for epidermal growth factor receptor (EGFR)/CD147-nonclathrin endocytic (NCE), promoting the creation of plasma membrane-ER contact sites for the formation and maturation of NCE[307]. Mice with overexpression or deficiency of RTN3 show differential deposition of Aβ[308]. Besides, the full length of RTN3 contributes to the ER-phagy via association with IL-3 with its N-terminal domain[309] and the ER transmembrane protein PGRMC1[310], and promotes the endosome maturation at the ER contract sites[311]. Increased RTN3 leads to obesity and hypertriglyceridemia by interacting with Heat Shock Protein Family A (Hsp70) Member 5 (HSPA5)[297]. Over-expression of RTN3 enhances TRAIL-mediated apoptosis[298], inhibites the axonal transport of BACE1[299], and develops neuritic abnormalities with impairments in spatial

learning and memory, as well as synaptic plasticity[300,301]; RTN3 KO also shows adverse effects on BACE1 activity and facilitates amyloid deposition[302].

Cooling is neuroprotective in OGD/R-injury with increased cell viability as well as induced gene expressions of cold shock proteins. However, as cooling alone leads to the upregulation of microglial activation, expression of proinflammatory cytokines, and a variety of cold-shock transcript expression, temperature management might have ambiguous effects in sterile inflammation[295].

Although the detailed protective molecular mechanisms of hypothermia remain elusive, several clinical trials have been performed to treat different diseases with therapeutic hypothermia in the past several years. Kim *et al*. meta-analyzed 14 high-quality randomized clinical trials including traumatic brain injury (9), serious infections (2), and stroke (3), and unexpectedly found that therapeutic hypothermia is highly correlated with higher mortality and found no positive good neurologic outcome and an increase in arrhythmias in comparison with normothermia in 2670 patients[312]. In the scenario of ST-elevation myocardial infarction, a systematic review also clearly points out that hypothermia benefits are only limited to the reduction of infarct size in patients with anterior wall, but no significant difference in mortality, recurrent myocardial infarction or heart failure/pulmonary oedema are observed. In this study, 6 randomized controlled clinical trials that 819 patients are involved in were comprehensively meta-analyzed[313]. Further, even though therapeutic hypothermia has been clinically used as a guideline in adult cardiac arrest and neonatal encephalopathy for several years, it is only partially effective (summarized in **Table 2** and **3**). The reason why the earliest clinical trials show good outcomes are possibly due to the small sample size and a suboptimal control group, which display rather elevated temperature. Thus, the positive outcome probably is on account of avoiding fever, instead of hypothermia. In the FROST-I trial, no statistically significant differences in neurological outcomes among the different levels of therapeutic hypothermia were observed[314]. Further, quicker cooling is also utilized to make hypothermia more efficient. In 6 clinical trials conducted during the last decades, where rapid infusion of cold solution was used in out-of-hospital cardiac arrest patients before they are admitted in hospital in the trial group (trial group), and after hospital admission (control group), both trial and control group are subject to hypothermia treatment recommended by international guidance. Unfortunately,

both mortality rate and good neurological outcome show no obviously statistical significance between two groups (**Table 4**).

Table 2. Clinical trials of therapeutic hypothermia in cardiac arrest

Year	2002	2002	2013	2015	2019	2021
Clinical trial name	HACA [315]	STEPHEN A. BERNARD *et al.* [316]	TTM [317]	THAPCA [318]	CRICS-TRIGGERSEP [319]	TTM2 [320]
Sample size	275	77	939	295	584	1861
Median age (Year) (Hypothermia *vs* Normatehrmia)	59	66.8/65	64	2.1/1.6	67	64
Disease	Cardiac arrest with ventricular	Out-of-hospital cardiac arrest	Out-of-hospital cardiac arrest	Out-of-hospital cardiac arrest	Cardiac arrest with nonshockable	Out-of-hospital cardiac arrest
Target T (℃) (Hypothermia *vs* Normatehrmia)	33 *vs* 37.5	33 *vs* 37	33 *vs* 36	33 *vs* 36.8	33 *vs* 37	33 *vs* 37
Time interval to target temperature (hours)	8	2	8	8	8	8
Duration (hours)	24	12	28	48	24	28
Mortality rate (%) (Hypothermia *vs* Normatehrmia)	**41 *vs* 55 P=0.02 At 6 months**	51 *vs* 68 P=0.145 At 1 month	No difference	No difference	No difference	No difference
Good neurological outcome (%) (Hypothermia *vs* Normatehrmia)	**39 *vs* 55 P=0.009**	**49 *vs* 26 P=0.046**	No difference	No difference	**10.2 *vs* 5.7 P=0.04**	No difference
Complication	No difference	No difference	More in Hypothermia	No difference	No difference	No difference
Complication	No difference	No difference	More in	No difference	No difference	No difference

Table 3. Clinical trials of therapeutic hypothermia in moderate or severe neonatal encephalopathy

Year	2005	2012	2014	2020	2021
Clinial trial name	the National Institute of Child Health and Human Development Neonatal Research Network[321]	the Eunice Kennedy Shriver NICHD Neonatal Research Network[322]	TOBY [323]	THIN [324]	HELIX (low-income and middle- income countries)[325]
Sample size	239	208	325	50	408
Median age Maternal (year)/Neonatal(hours)	27/<6	27/4.3	No/<6	No/<5	No/<6
Disease	Moderate or severe encephalopathy	Moderate or severe encephalopathy	Perinatal asphyxia	Moderate/severe hypoxic-ischaemic encephalopathy	Moderate or severe neonatal encephalopathy
Target Temperature (℃) **Duration time (hours)** **Time to start hypothermia (hours)**	33.5 72 N/A	33.5 72 N/A	33 to 34 72 <6	33.5±0.5 72 N/A	33·5 72 N/A
Mortality rate (%) Hypothermia *vs* Normathermia	Death or moderate or severe disability: 44 *vs* 62 (P=0.01) at 18 to 22 months	28 *vs* 44 P=0.04 at 6 to 7 years	No difference	No difference	Died or had a moderate or severe disability:50 *vs* 47 (p=0.55) Died: 42 *vs* 31 (P=0.022) at 18 to 22 months
Good neurological outcome (%)	the rate of cerebral palsy: No difference at 18 to 22 months	No difference	IQ>85: 52 *vs* 39 (P=0.04) Neurologic nornalities: 45 *vs* 28; risk of cerebral palsy: 21 *vs* 36 (P=0.03); risk of moderate or severe disability: 22 *vs* 37 (P=0.03)	More fractional anisotropy (FA) in the posterior limb of the internal capsule (PLIC) in hypothermia: P=0.023 at 5±1 days	No difference
Complication	No difference	No difference	No difference	No difference	No difference

Table 4. Clinical trials of therapeutic hypothermia with pre-hospital cooling in cardiac arrest

Year	2010	2012	2014	2014	2014	2016
Clinial trial name	RICH [326]	RICH [327]	Francis Kim *et al.* [328]	Francis Kim *et al.* [328]	Guillaume Debaty *et al.* [329]	RINSE [330]
Sample size	234	163	583	776	245	1198
Median age (Year) (Hypothermia *vs* Normothermia)	63.4/63	63.8/61.1	62.1	68.3/67.5	66/68.5	65.3/64.3
Disease	Out-of-hospital cardiac arrest with ventricular fibrillation	Non-ventricular fibrillation cardiac arrest	Out-of-hospital cardiac arrest With ventricular Fibrillation	Out-of-hospital cardiac arrest Without ventricular Fibrillation	Out-of-hospital cardiac arrest	Out-of-Hospital Cardiac Arrest
Cooling method (Pre-hospital *vs* Hospital)	Rapid infusion of 2 L of ice-cold lactated Ringer's solution *vs* cooling after hospital admission;0.8 (P=0.01);	Rapid infusion of up to two liter of Ice-cold Hartmann's solution *vs* cooling after hospital admission; 1.4 (P<0.001); 3.2hrs *vs* 4.8hrs; (P=0.0328)	Infusing up to 2 L of 4°C normal saline *vs* cooling after hospital admission	Infusing up to 2 L of 4°C normal saline *vs* cooling after hospital admission	Infusion of cold saline *vs* cooling after hospital admission	Rapid intravenous infusion of up to 2 L of cold saline
Mortality rate (%) (Pre-hospital *vs* Hospital)	52.5 *vs* 46.6 No difference at hospital discharge	86.6 *vs* 91.4 P=0.5 at hospital discharge with favorable outcome	37.3 *vs* 35.7 P=0.69 at hospital discharge	80.8 *vs* 83.7 P=0.3 at hospital discharge	94.3 *vs* 95.5 No difference at hospital discharge	89.8 *vs* 88.6 P=0.71 at hospital discharge
Good neurological outcome (%) (Pre-hospital *vs* Hospital)	N/A	12.2 *vs* 8.6 No difference at discharge home and rehabilitation	57.5 *vs* 61.9 P=0.69 at hospital discharge	14.4 *vs* 13.4 P=0.3 at hospital discharge	5.7 *vs* 4.1 No difference at one month	N/A

The results of clinical trials lead us to ask why the outcome of therapeutic outcomes are significantly distinct, showing relatively high effectiveness just in neonatal encephalopathy in developed countries. Certainly, there exist many potential reasons: 1) Neuroprotective effect of therapeutic hypothermia on different ages of patients are distinct, which is also found by Peretti *et al*., where AD (Alzheimer's disease) phenotype in old mice cannot be rescued under hypothermia, at least partially, due to the failure induction of RBM3 in old mice[265]. Clinically, the expression level of RBM3 in patients treated with therapeutic hypothermia isn't measured and thus remains elusive whether RBM3 is successfully induced under therapeutic hypothermia. Indeed, it has been shown that patients with shorter hypothermic time and older age have significantly higher probability to suffer from postoperative delirium in non-cardiac surgical patients (American Society of Anesthesiologists class I, II and III) with unplanned perioperative hypothermia. Interestingly, young patients, who have longer hypothermic time and suffer from more severe disease, get higher chance of postoperative delirium; while old patients, who have less hypothermic time and more severe disease, have higher opportunity suffering from postoperative delirium. This can be explained as RBM3 expression at basal level is high in young patients that the benefits of higher RBM3 is less than the longer complications caused by hypothermia. In contrast, basal RBM3 expression is reduced in old

patients, and hypothermia-induced RBM3 will contribute to neurological benefits[315]. The hypothesis need to be tested in the future. However, THAPCA trial for out-of-hospital cardiac arrest with coma at around 2-year-old kids also doesn't show significant good outcome. 2) Another potential reason is probably that it takes so long-time interval to reach the hypothermic temperature that RBM3 cannot be expressed in time to function in the emergency case. Although rapid infusion cold solution is utilized to lower the body temperature of patients, it doesn't shorten the time interval so much. 3) Hypothermia just can be performed for 1 to 3 days owing to its side effects, such as bradycardia, elevation of the blood pressure and hypotension, and thus RBM3 induction cannot be continued for a long time. Primary latent phase of cell injury after hypoxia and ischemia indeed lasts around 6 hrs showing that activation of neurotoxic cascades, and continues by a second phase of deterioration, which extends more than many days[316]. Thus, continuously protecting neurons seems compulsory to improve the outcome.

5.5 Outstanding questions

After reviewing extensive published scientific papers regarding RBM3, I found that there are several outstanding questions: 1) How is exactly RBM3 up-regulated under hypothermia as the response is prompt at both RNA level and protein level[243]. As the published molecular mechanisms, which focus on the RBM3 regulation at a transcriptional level, are based on the long-time hypothermia treatment in cell culture[241-245] (hypothermia treatment *in vivo* in mice is just 3hrs), do the short and long-time hypothermia treatment share the same mechanism? If not, there must be some other unknown mechanisms, which rapidly up-regulate RBM3 RNA at low temperature. Physiologically, RNA secondary structure, post-transcription regulation, or cold responsive protein (*e.g.*, kinase or phosphatase) may contribute to the fast response of RBM3 expression to temperature alternations. 2) Does hypothermia directly increase RBM3 protein expression? 3) How is RBM3 downregulated at normal or high temperature? 4) Why is RBM3 expression higher in infants than adults? This is intriguing as we can target the molecule or signaling pathway to up-regulate RBM3 in adults with pathological disease at normal temperature for the medication purpose if the clear mode of action is uncovered. 5) Why is the neurological outcome of therapeutic hypothermia treatment better in young individuals (see discussion above)? 6) Is the oligomerization of RBM3 correlated with its biological functions? In other words, is RBM3 protein at high temperature less active than at low temperature? What is the physiological function of RBM3 to form oligomerization?

6 Antisense oligonucleotide therapy

6.1 Types of ASO

Antisense oligonucleotide (ASO) is the synthesized single stranded nucleic acid with 8 to 50 nt in length, which can directly and specifically bind to RNA via Watson-Crick base paring. Different modifications of ASO can lead to totally distinct effects on the targeting RNA. Briefly, two groups of ASO have been mainly discovered so far: one is to sterically block the *trans*-acting factor or splicing machinery, which switches the splicing events; another one is to specifically bind to the targeting RNA sequence, that degrades the transcripts as the ASO contains central deoxynucleotides flanked by oxynucleotides (gapmer) and the ASO/RNA hybrid can induce RNase H-dependent degradation of RNA. Here, I just focus on the ASO causing splicing switch, while the ASO gapmers leading RNA degradation by RNase H will not be discussed.

Antisense oligonucleotide method to manipulate RNA was proposed since 1978, and the reasons why the scope of ASO has extraordinarily developed so rapidly in the last decades are as follows[317]. First, although symptomatic treatments (such as small molecules) have been clinically used in the treatment of neurodegenerative diseases, they are not highly efficient, also associated with undesirable side effects, and even cannot hinder the neurodegenerative disease progression in a dearth of scenarios. Second, many prominent targets, such as lncRNA accounting for up to 75% of the transcripts and pre-mRNA, are not traditionally druggable and not easy to be specifically targeted by small molecules. If we can specifically target the mutant genes, causive genes or beneficial genes, in principle we can address the problems. The influential CRISPR editing has its own limitations, at least so far, such as inversibility, off-target effect, ethics issue *etc*. Thus, ASOs are successfully developed to address unmet medical needs due to their own properties.

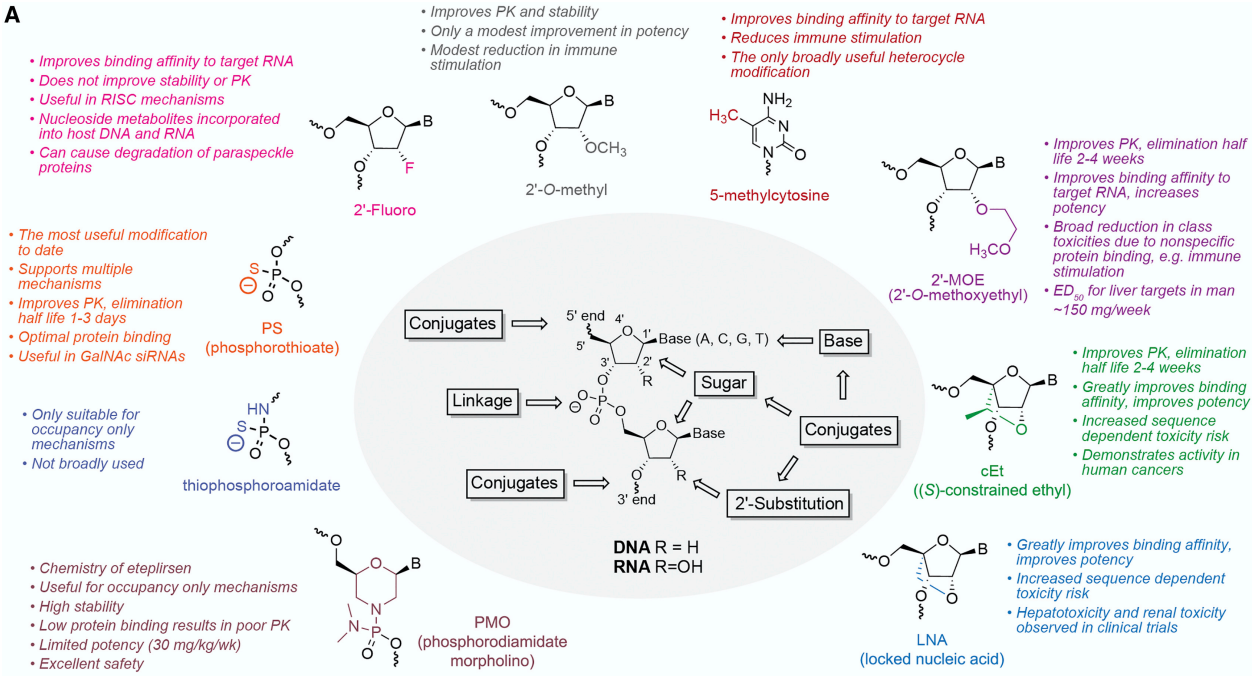

Figure 1.11 Characteristics of different modifications in chemistry of oligonucleotides. Reproduced from "RNA-Targeted Therapeutics"[317]

To obtain the potential ASOs used in clinic, chemists spare no efforts to modify the structure of ASO in the backbone, sugar and base in order to improve their potency, binding affinity and stability *in vivo* as the original structure of oligonucleotides bears poor pharmacological-like properties especially fast degradation rate[317] (**Fig. 1.11**). Phosphorothioate (PS) replacing a phosphodiester in the backbone linkage is the common way to reduce degradation by nuclease in the blood and tissue and to promote the binding of ASO with albumin and other blood proteins, thereby resulting in the retardation of renal clearance[318]. Another popular backbone linkage modification is phosphorodiamidate morpholino, which is frequently used in the lab research. PS modification is resistant to RNase H, whereas morpholino is not. The base modification, such as 5-methyl, 5-propynyl, 2-thio and 2,6-diaminopurine can adjust the binding affinity and specificity of ASO. In the sugar, 2'-O-Me, 2'-O-MOE, 2'-F can be adopted for the modifications to alter the nuclease resistance and binding affinity as the ASOs with these modifications favor an A-form or RNA-like conformation[319], and these 2'-modified ASOs are resistant to RNase H. Clinically, 2'-O-Me and 2'-O-MOE are the most seen modifications. Locked nucleic acid (LNA), tricyclo-DNA (tc-DNA) and constrained ethyl (cEt-BNA) chemistry introduce a ring to bridge the sugar, thereby enhancing their binding affinity to RNA. Naked 2'-O-MOE is effective when injected through numerous administration ways with half-life from 2 to 4 weeks[320].

6.2 Challenges and future directions

The very challenging part of ASO therapy is the delivery. How to specifically deliver ASO to the target tissue of interest, meanwhile reducing the off-target effect in other irrelevant tissues? Given that the high expression and rapid turnover of the asialoglycoprotein receptor (ASGR) in liver, GalNAc3 (shown in **Fig. 1.12**), a specific ligand of ASGR, has been conjugated to ASO to enhance the efficiency and septicity of liver target. To my knowledge, so far, GalNAc3-conjugated ASO is the most effective method to tackle the liver targeting issue with 60-fold increase in gene silence efficiency in hepatocytes[321,322], while the efficient methods of ASO delivery to other tissues are still on the way due to limited receptors with high density and high turnover rate. Crossing blood–brain barrier (BBB) is the most difficult obstacle for the delivery of ASO to CNS as after systemic administration just few ASOs can pass through the BBB to effectively act in the targeting area. Given the limitation, intracerebroventricular (ICV) injection or intrathecal administration has been used to directly deliver ASOs into central neural system.

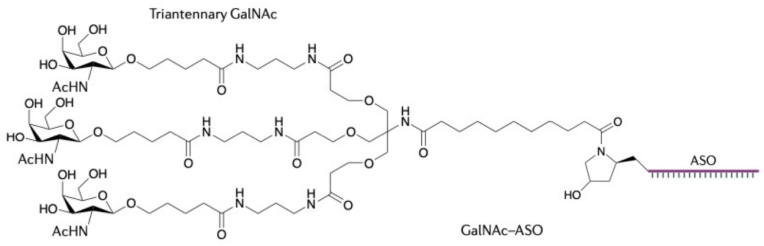

Figure 1.12 Structure of GalNAc conjugated ASO.

In the cellular level, when the naked ASO, nanoparticle-conjugated ASO or GalNAc3-conjugated ASO attach and absorb on the cell membrane, they will be internalized by endocytosis in a receptor dependent way or not, and then they will traffic in the complicated endosome network. It has been shown that different cell types have different ASO-binding affinities[323], showing that slow growing and differentiated cells are less efficiently to uptake ASOs in comparison with rapid growing cells, such as cancer cells[324]. Experimentally, immunostaining and other methods have demonstrated that post-transfected ASOs are in the PS-body-like, P-bodies, lysosome, late endosome, ER, Goligo-58K vesicle and XO6 *etc*[325-330]. Thus, ASOs in the membrane-bound compartment are separated from cytosol to nucleus. For the ASOs, which act to regulate pre-mRNA, should function in the nucleus. The intracellular distribution of ASOs influence the therapeutic efficacy of ASOs[331]. In this case, how to break

the endosome barrier is the key point to enhance the ASO delivery. Fortunately, some of the ASOs can naturally leak to cytosol during the fusion and fission of vesicles in the process of the complex endosome trafficking although the detailed mechanisms how ASOs are released from endosome remain unclear[332]. People used cationic lipids and polymers to coat with ASOs to destabilize the endosome membrane, which can release more ASOs to cytosol[333]. Finally, it is notable that ASOs are free to enter nucleus once they escape from endosome compartments[334,335]. The detailed mechanism of action how ASOs shuttle from nucleus to cytosol, what protein is responsible for the shuttling still remain elusive.

The delivery optimization of ASO with GalNAc3 conjugation and nanoparticle carrier has their own *pros* and *cons*. For example, GalNAc3 conjugates are single pure compounds, so it is easy to control the drug quality, while nanoparticle carrier is heterogenous in some ranges of size. In terms of uptake efficiency by cells, nanoparticles are more efficient as the cell can internalize numerous nanoparticles, while one GalNAc3 conjugate needs to bind one particular receptor to be endocytosed, which reduces internalization efficiency. Nanoparticle carrier is resistant to nuclease degradation, and GalNAc3 conjugates are not. The tissue specificity achieved by GalNAc3 conjugates cannot be accomplished by nanoparticles[331].

The conformation of ASOs and their binding proteins influence the cellular effect of ASOs. Interestingly, one phosphorothioate (PS) has two kinds of chiral conformations, R and S, so theoretically oligonucleotides with N bases have $2^{(n-1)}$ chirality conformations. Just few research investigate whether chirality influences the effect of ASO. Naoki Iwamoto *et al.* reported that S-configured PS linkages are more stable compared to R conformation, and thereby the pure S-configured ASO has higher efficacy[336].

It has been shown that many intracellular proteins can bind to ASO in live cells, such as Hsp90[337]. These interactions may promote or inhibit ASO binding to target RNAs[338-340], and may contribute to the side effects of therapeutic treatment in clinic. A better understanding how the ASO distribute in cells will help us to manipulate and modify ASO in chemistry to make ASO function in the active cellular compartments and alter their protein binding properties in differential cellular settings.

6.3 Therapeutic treatment of ASO

Broadly, ASO therapy is one rapidly developing type of nucleic acid treatments in the gene therapy field. Nowadays, several ASO-based drugs including 4 of 2'-O-methoxyethyl, 4 of

phosphorodiamidate morpholino and 1 of 2'-deoxy modification have been approved by FDA and EMA[341], and many of them mainly target genetic diseases to work efficiently in patients. Of course, many ASO drugs failed in the clinical trials due to different reasons. Several reviews have comprehensively summarized the approved drugs, including their chemistry modifications and mechanism of actions. Here, the splicing modulator Spinraza, the first FDA approved ASO to treat SMA (spinal muscular atrophy) in kids is taken as an example to describe how it functions in patients. In healthy individuals, SMN1 gene produces normal SMN protein, which is essential for motor neuron survival, and SMN2 gene generates truncated SMN protein due to the dominant exclusion of exon 7 caused by C to T mutation in exon 7 of SMN2 gene. In SMA patients, SMN1 gene is totally loss of function, cannot produce any functional SMN protein, and the SMN2 gene is not capable of producing enough SMN proteins to support the motor neuron survival[342]. Researchers identified the strong *cis*-regulatory repressor elements of exon 7, and then Spinraza as a ASO is designed to target the repressor to sterically block the recruitment of *trans* repressor, thereby promoting exon 7 inclusion to generate non-truncated functional SMN protein[343]. In cultured cells[343], *in vivo* mouse[344-346], and clinic patients[347], Spinraza can efficiently enhance the SMN expression. As the promising potentials of ASO, bewildering variety of pre-clinical experiments have been done in the lab to treat other diseases. For example, intraventricularly direct injection of antisense oligonucleotides targeting superoxide dismutase 1 (SOD1), one of the most abundant brain proteins, into mice significantly reduces SOD1 expression level at both protein and mRNA levels in the brain and spinal cord. This ASO injection slows the disease progression in a mouse model of ALS[348].

Results and discussion

1 Boosting endogenous RBM3 expression with antisense oligonucleotides.

In clinic, hypothermia has been a guideline in the cardiac arrest and moderate or severe neonatal encephalopathy to protect brains. Therapeutic hypothermia is limited by its long-time interval to target the cooling temperature, large and cumbersome device requirement, elongating hospital days, short-term treatment and other side effects. Importantly, some other proteins, besides RBM3, or signaling pathways, which are possibly not effective or even harmful, also can be induced, activated, or inhibited after body temperature is lowered. For instance, CIRBP, another cold-induced protein, has been identified as a damage-associated molecular pattern molecule, which leads to detrimental sterile inflammatory responses[349]. It was reported that extracellular CIRBP increases in ischemic stroke models, resulting in massive neuronal damage[350]. RTN3 is thought to inhibit anti-virial responses[296], suppress hepatocellular carcinogenesis through mediating Chk2/p53 activation and inhibiting neuritic outgrowth after injury. Increased RTN3 leads to obesity and hypertriglyceridemia by interacting with Heat Shock Protein Family A (Hsp70) Member 5 (HSPA5)[297]. Over-expression of RTN3 enhances TRAIL-mediated apoptosis[298], inhibits the axonal transport of BACE1[299], and develops neuritic abnormalities with impairments in spatial learning and memory, as well as synaptic plasticity[300,301]. It was also reported that just RBM3 not mild hypothermia can efficiently protect human SH-SY5Y neuroblastoma cells from neurotoxicity[351]. This is, at least one of the reasons, why in some pathological conditions, the outcome of therapeutic hypothermia is conflicting or not significantly beneficial to ameliorate diseases.

As a matter of fact, it is noteworthy that mortality rate is very high even in the case of neonatal encephalopathy, the most effective scenario treated with therapeutic hypothermia. A meta-analysis suggests an absolute reduction in risk of approximately 15%, from 61% to 46%, meaning that nearly half of infants die or survive with disability despite treatment with hypothermia[352]. Moreover, the neuroprotective effects of hypothermia have been shown to be attributed to decrease the metabolic rate, to reduce the generation of radicals, to ameliorate inflammation, to inhibit excitotoxicity and apoptosis. However, since its outcome is controversial in different scenarios, a common mechanism of action cannot explain all the

conflicts. To better utilize hypothermia to treat diseases, it has to be determined on a case-to-case basis to find the key beneficial factor and to avoid the exacerbating components .

Selectively and particularly increasing RBM3 expression at normothermia is a very promising approach for neuroprotection to avoid the unwanted side effects of therapeutic hypothermia. This would also solve the problem that hypothermia can only be used for a limited time span. It has been reported that post-insult hypothermia just delayed the brain damage from mild to moderate by more than a week, and then the damage was as severe as in normothermic animals[353]. Boosting RBM3 expression over a prolonged period could circumvent this drawback.

1.1 RBM3 intron 3 contains an evolutionary conserved heat-induced poison exon.

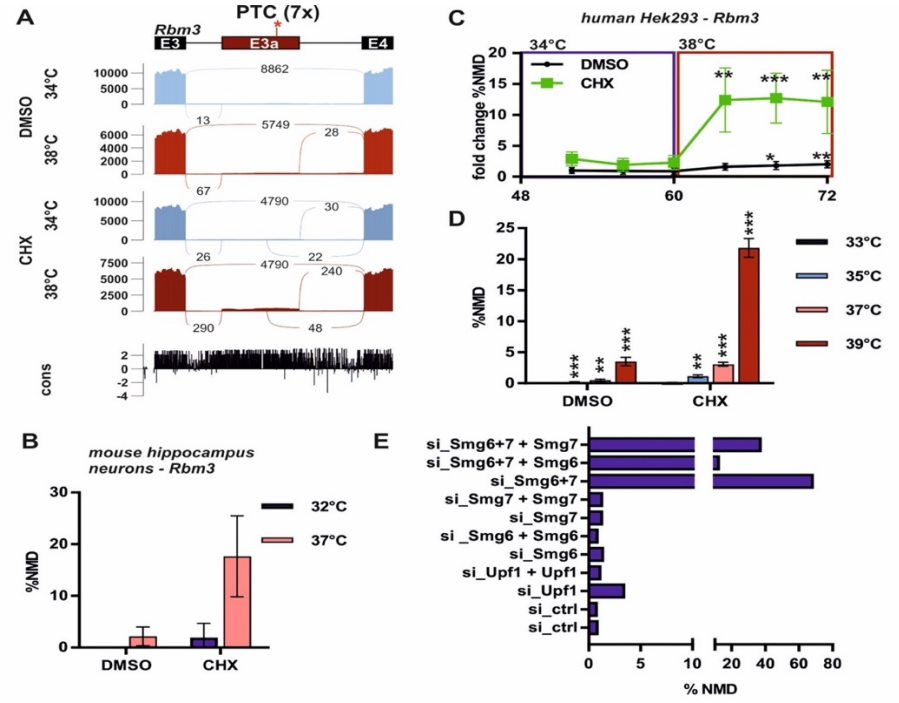

Courtesy from Marco

Figure 1.1 RBM3 intron 3 contains an evolutionary conserved heat-induced poison exon.
A. Sashimi blot identifying a novel exon (E3a; with 7 premature termination codons: PTC) within RBM3 intron 3. Mouse primary hepatocytes were incubated at 34°C or 38°C with or without the translation inhibitor cycloheximide (CHX, DMSO as solvent control) and analysed by RNA sequencing. Below the simplified exon-intron structure, the Sashimi plot shows the distribution of raw sequencing reads. Exon-Exon junction reads are indicated by the numbers connecting the exons. Note that exon 3a is mainly included at 38°C in CHX. At the bottom, high sequence conservation across placental species

is indicated. **B.** Radioactive splicing sensitive RT-PCRs confirm heat-induced and CHX-stabilized formation of the E3a containing isoform at warmer temperatures in primary hippocampal neurons (n=2, mean ± SD). **C, D.** RBM3 exon 3a regulation is conserved in humans. In **C**, HEK293 cells were pre-entrained with square-wave temperature cycles (12h 34°C/ 12h 38°C) for 48h. For the last 24h, cells were treated with DMSO or CHX every 4h and harvested after 4h and analyzed by splicing sensitive RT-PCR. In **D**, Cells were incubated at the indicated temperatures for 12h (DMSO/CHX last 4h). Statistical significance was determined by unpaired t-test and is indicated by asterisks: p values: *p<0.05, **p<0.01, ***p<0.001 (n=3, mean ± SD). **E.** RBM3 exon 3a stabilization in response to NMD factor knockdown and rescue experiments. Sequencing data were obtained from SRP083135[354].

With the cycloheximide (CHX) treatment dataset from EMBO Report[237], we found that the inclusion of a heat-induced "poison" exon, RBM3 exon 3a, which is non-annotated, significantly increased after CHX treatment at high temperature, not at low temperature (**Fig. 1.1A**), indicating that the RBM3 exon 3a may contribute to the NMD of RBM3 transcripts at high temperature as CHX can inhibit translation, and then represses translation-dependent NMD. This CHX-stabilized transcript with RBM3 exon 3a was also confirmed in mouse primary hippocampal cells (**Fig. 1.1B**). To check whether the CHX effect on RBM3 exon 3a is conserved in humans, we treated HEK293T cells with CHX at different time points, and the result shows that CHX stabilizes the RBM3 exon 3a in a time-dependent manner (**Fig. 1.1C**). Furthermore, knockdown of NMD core factors (UPF and SMG kinase) decreases the degradation of RBM3 exon 3a, while overexpression of NMD related factors in the knock-down samples rescues RBM3 exon 3a expression (**Fig. 1.1D**). Taken together, all the evidence suggest that the RBM3 exon 3a contributes to the NMD of RBM3 transcript at 37°C or higher temperature.

1.2 RBM3 exon 3a controls temperature dependent RBM3 expression.

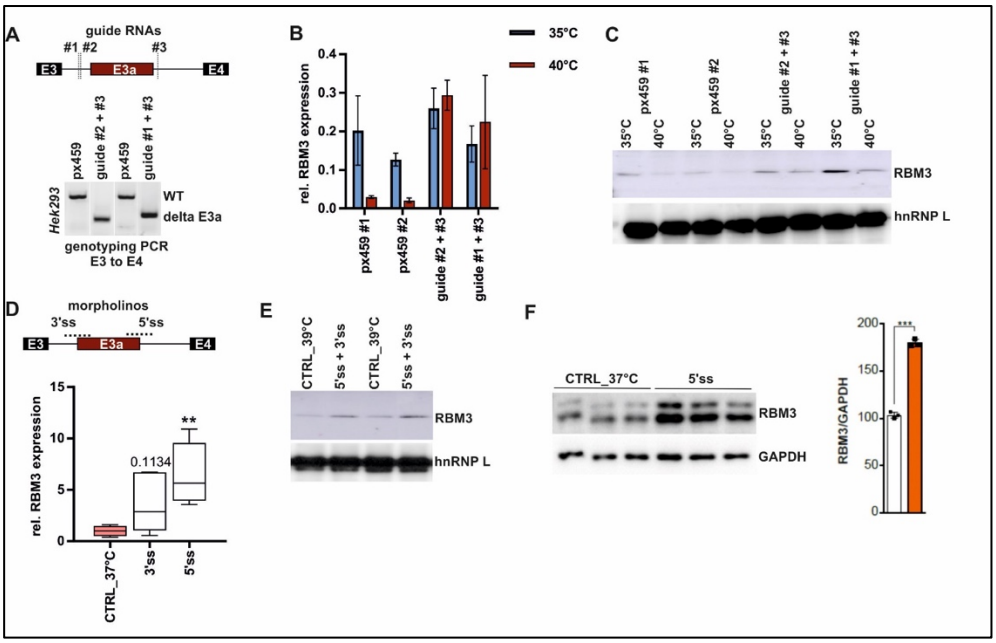

Courtesy from Marco

Figure 1.2 RBM3 exon 3a controls temperature-dependent RBM3 expression. A. CRISPR/CAS9 mediated removal of RBM3 exon 3a. One of two guide RNAs targeting the upstream intron (#1, #2) were co-transfected with a guide RNA targeting the downstream intron (#3). Below, genotyping PCR after clonal selection of Hek293. px459 transfected cells after clonal selection serve as a negative control. **B, C.** RT-qPCR (in B) and Western blot (in C) analysis of RBM3 levels in edited cell lines. Clonal cell lines from A were incubated at 35°C or 40°C for 24h. Isolated RNA was investigated by qPCR and Rbm3 expression is shown relative to GAPDH levels (n = 2-3). Lysates from an independent experiment were investigated for Rbm3 protein expression, hnRNP L served as a loading control. See also Figure S2a for 37°C samples. **D.** Manipulation of RBM3 exon 3a splicing directly controls RBM3 expression levels. HEK293 cells were transfected for 48h at 37°C with morpholinos blocking either the 3'SS or the 5'SS of exon 3a. RBM3 expression is shown relative to GAPDH levels and normalized to a non-targeting CTRL morpholino. Statistical significance was determined by unpaired t-test and is indicated by asterisks: p values: **p<0.01 (n>4). **E, F.** Blocking RBM3 exon 3a inclusion induces RBM3 protein levels. HEK293 cells (in E) or primary hippocampal neurons (in **F**) were transfected with the indicated morpholinos for 48 hours. HEK293 cells were shifted to 39°C for the last 24h. RBM3 protein levels were investigated by Western blotting. hnRNP L or GAPDH served as a loading control. For hippocampal neurons RBM3 levels were quantified relative to GAPDH levels (on the right; n=3; unpaired t-test derived p-value ***p<0.001).

Considering that most of the *cis*-regulatory enhancer elements are ESEs and the sequence conservation between humans and mice in the RBM3 exon, we deleted the exon 3a of RBM3 in the HEK293T genome with CRISPR-Cas9 editing (**Fig. 1.2A**). In the exon 3a KO cell line, at both mRNA and protein level, RBM3 expression significantly increases at high temperature (**Fig. 1.2B** and **Fig. 1.2C**). This indicates that the enhancer contributing to exon 3a inclusion at high temperature is indeed located in the exon 3a, and it dominantly functions at high temperature. To further confirm that the exon 3a responsible for NMD of RBM3 transcripts, morpholinos targeting 3'SS and 5'SS were used to block the spliceosome assembly in HEK293T cells. It showed that morpholino binding to 5'SS increases RBM3 expression (**Fig. 1.2D** and **1.2E**), whereas the effect of morpholino against 3'SS was not very strong. The morpholino targeting 5'SS also efficiently functions in primary neurons, showing around 1.75-fold enhancement in RBM3 protein expression. Taken together, these data further demonstrate that there should be *cis*-regulatory enhancer element located in exon 3a to promote exon 3a inclusion, and targeting the enhancer element in principle will repress the inclusion of RBM3, which boosts RBM3 expression.

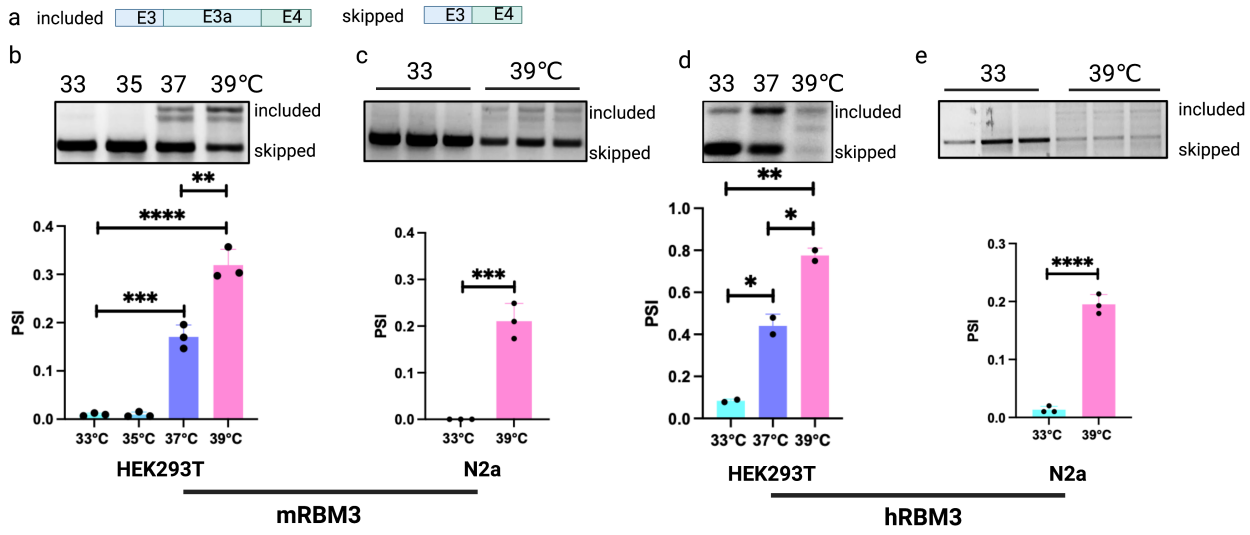

Figure 1.3 Poison exon 3a inclusion in mRBM3 and hRBM3 minigene is modulated by temperature. **a**, Schematic of two RBM3 isoforms. **b**, Alternative splicing of exon 3a in mRBM3 minigene is intricately controlled by temperature in HEK293T. n=3. **c**, Exon 3a inclusion of mRBM3 minigene is temperature sensitive in N2a. n=3. **d**, Exon 3a inclusion of hRBM3 minigene is controlled by temperature in HEK293T cells. n=2. **e**, Exon 3a inclusion of hRBM3 minigene is temperature sensitive in N2a cells. n=3. In each sub-figure, upper panel is the representative gel image of RT-PCR, and lower panel is the quantification result. All the mutants and WT mRBM3 and hRBM3 minigene were transfected into cells overnight, and then incubated in different temperatures for around 24hrs,

followed by RT-PCR. PSI: percentage of spliced in. Statistical significance was determined by unpaired t-test and is indicated by asterisks: unpaired t-test derived p-value **p<0.01, ***p<0.001. The other gel images for quantification are in the **App. Fig. 1**.

Considering that endogenous RBM3 transcripts containing exon 3a are degraded via NMD pathway, which makes difficult to detect the exon3a containing transcripts without CHX stabilizer, we cloned RBM3 minigene containing RBM3 exon 3, exon 4, exon 3a and its flanking upstream and downstream introns (**Fig. 1.3a**) to further investigate how temperature controls RBM3 exon 3a inclusion. It showed in both mRBM3 and hRBM3 minigene exon 3a inclusion is highly temperature sensitive at the range of 33°C to 39°C in both HEK293T and N2a cells, indicating that the cis-regulatory elements controlling heat-induced exon 3a are included in the minigenes, and the temperature-sensitive exon3a splicing event is conserved between humans and mice (**Fig.1.3 b to d**). The exon3a is almost fully skipped in both mRBM3 and hRBM3 minigene at low temperatures (33°C and 35°C), while its PSI significantly increases at 37°C and 39°C, showing in HEK293T around 0.2 (mRBM3) and 0.4 (hRBM3) at 37°C, 0.3 (mRBM3) and 0.8 (hRBM3) at 39°C; in N2a around 0.2 (mRBM3 and hRBM3) 39°C. These results indicate that at low temperature (33°C and 35°C) both mRBM3 and hRBM3 minigenes present similar inclusion in both N2a and HEK293T, while at high temperature the exon3a inclusion in both mRBM3 and hRBM3 minigenes is higher in HEK293T than that in N2a, suggesting that the differential *trans*-acting factor in both cells have different activities to control exon3a inclusion.

1.4 Mapping exonic *cis*-regulatory elements controlling RBM3 exon 3a inclusion.

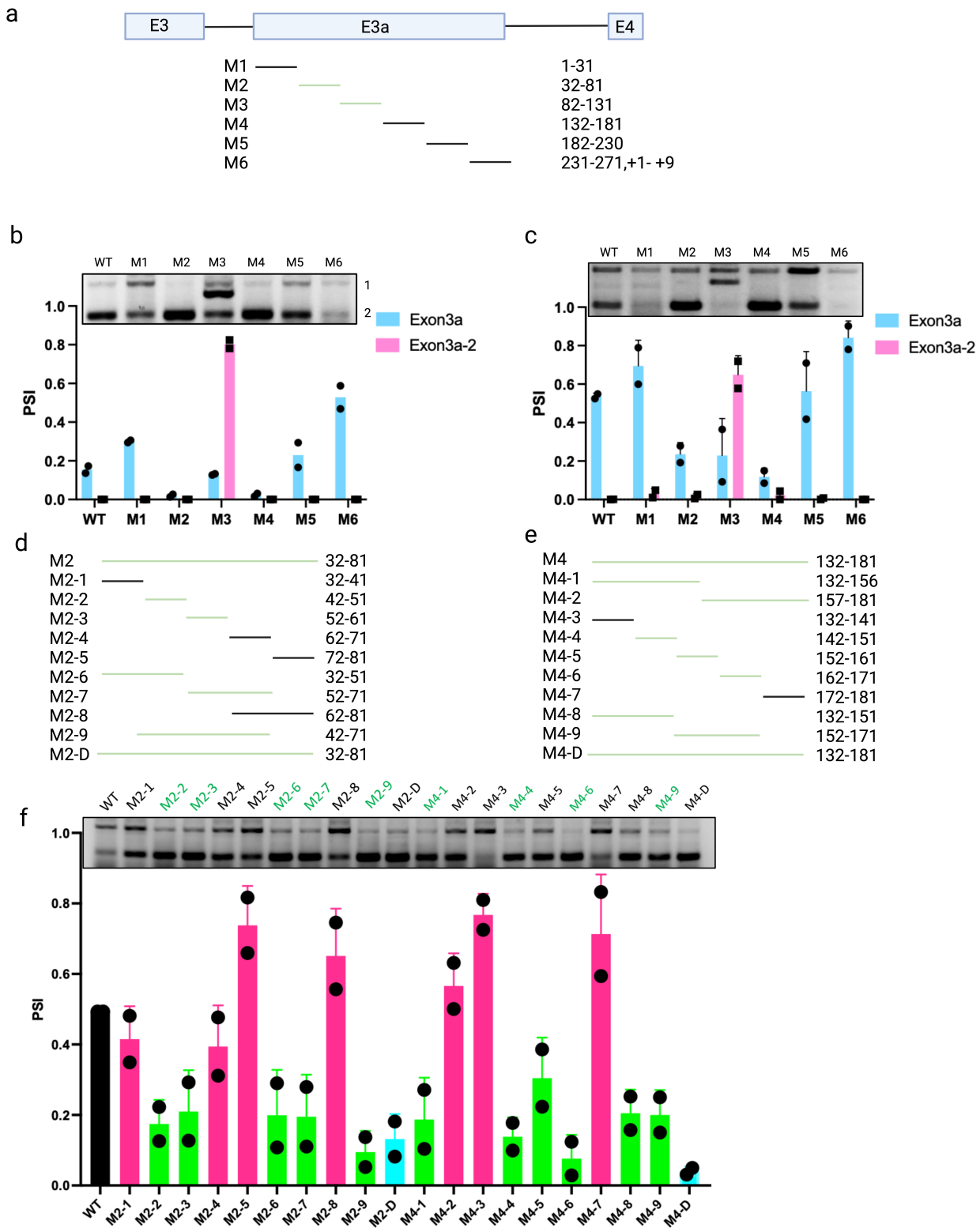

Figure 1.4 Mapping *cis*-regulatory elements controlling RBM3 exon 3a inclusion in HEK293T. a, Mutant (M1 to M6) schematic of mRBM3 minigene. **b and c**, M2 and M4 mutants

significantly abolish the exon 3a inclusion in HEK293T at 37℃ (**b**) and 39℃ (**c**). n=2. Upper panel is the representative RT-PCR gel image, and lower is the corresponding quantification result of each mutant. **d and e**, Sub-mutant (M2-1 to M2-9, M4-1 to M4-9, M2-D and M4-D) schematic of mRBM3 minigene. The indicated positions are replaced by human *beta*-globin sequences. M2-D and M4-D mean deletion of M2 and M4,repspectively. **f**, Mutagenesis screening of M2 and M4 indicates M2-9 and M4-5, M4-5 and 4-6 are the core *cis*-regulatory enhancer elements controlling exon 3a inclusion at 40℃. n=2. Upper panel is the representative RT-PCR gel image, and lower is the corresponding quantification result of each mutant. PSI: percentage of spliced in. All the cloning details are in the methods and materials. The detailed sequence information is also in the methods and materials. The other gel images for quantification are in the **App. Fig. 2**.

We next tried to identify the *cis*-regulatory enhancer elements to better understand the alternative splicing of RBM3 "poison" exon 3a. Importantly, it is speculated that antisense oligonucleotides which target the strong enhancer element via base-pairing to block the recruitment of *trans*-acting factors, can be utilized to inhibit exon 3a inclusion to therapeutically increase RBM3 expression.

Systematic mutagenesis (M1 to M6) of the "poison" exon 3a was performed in the mRBM3 minigene through the replacement of corresponding *cis* elements with *beta*-globin exon 2 element (the detailed replacement sequence is the method and material part.) (**Fig. 1.4a**). It shows that both M2 and M4 can significantly decrease the exon 3a inclusion (**Fig. 1.4b** and **1.4c**). M2-D and M4-D, in which the M2 and M4 sequence are fully deleted, also show less exon 3a inclusion (**Fig. 1.4f**), further confirming their enhancer activity in the regulation of "poison" exon 3a inclusion. Among these mutants, M5 caused dispensable effect. It is very intriguing that M1 and M6 significantly increase exon 3a inclusion, indicating that these two elements can strongly repress exon 3a inclusion (this will be discussed in the 2nd section, G4 story.). M3 is also interesting as the sequence mutagenesis activates another internal splice site, suggesting that the 3'SS is originally unused and masked by some reasons (it will be discussed in details in the 3rd section.).

Next, considering that the approved ASO drugs are around 20 nt and the mutant of M1 to M7 is approximately 50 nt, we tried to narrow down the enhancer element region to identify the core motif of *cis*-regulatory elements, and then several sub-mutants (M2-1 to M2-9, and M4-1 to M4-9), whose sequence are replaced by *beta*-globin exon sequence with the same length, were cloned on the basis of M2 and M4 position (**Fig. 1.4d** and **e**). For M2 located position,

the M2-9 (M2-2 and M2-3) is the strongest enhancer motif; M4-6 mutant almost abolishes RBM3 exon 3a inclusion (**Fig. 1.4f**).

1.4 Screening for MOE-based antisense oligonucleotides controlling RBM3 expression.

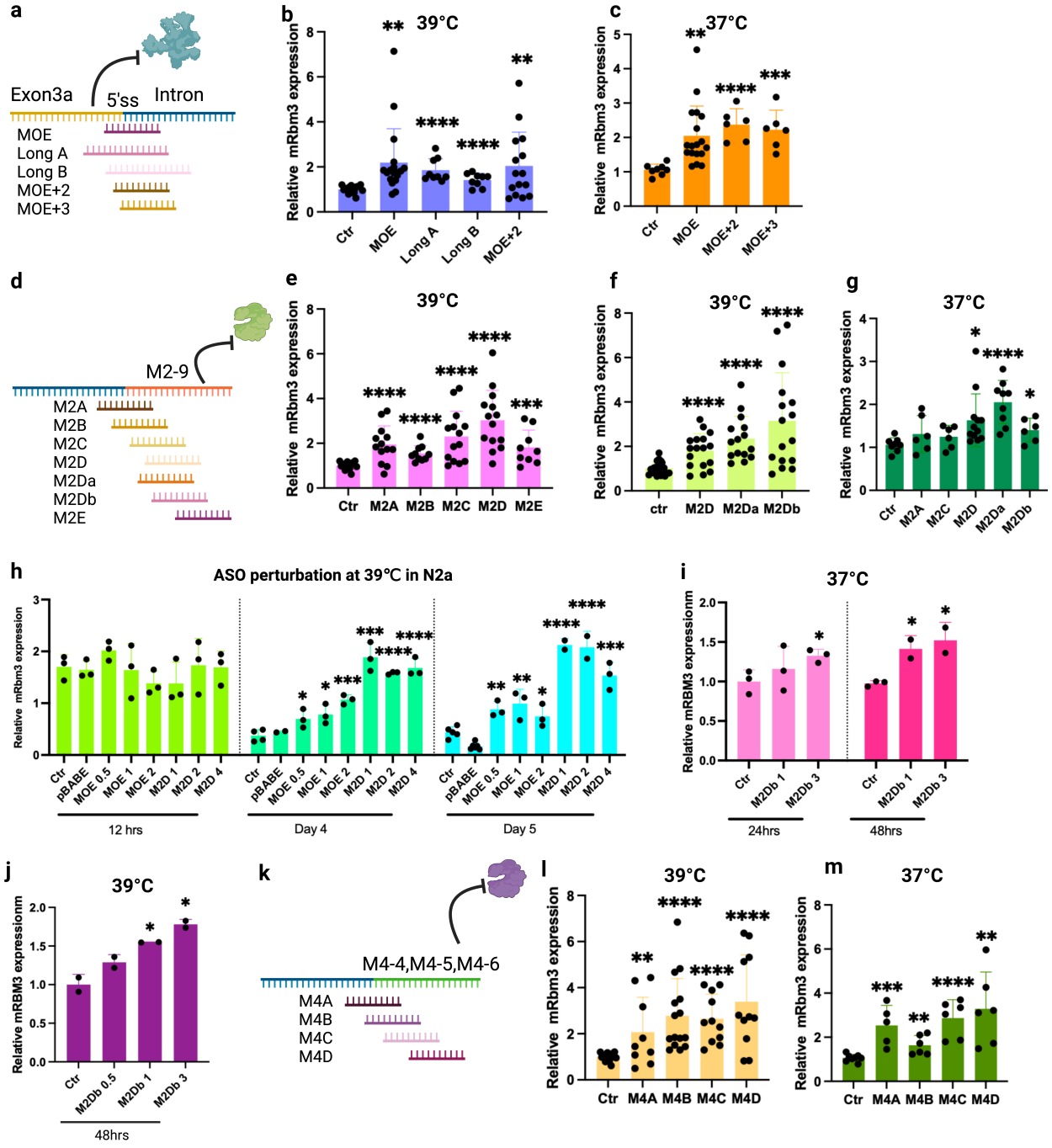

Figure 1.5 Screening for MOE-based antisense oligonucleotides controlling endogenous RBM3 expression in N2a. a, **d** and **k**, Schematic of ASO walking on the RNA. Different ASOs bind to the targeted RNA regions to prevent from the recruitment of U1-snRNP or *trans*-acting factors. The detailed information of position and targeting sequence of the ASO is in the methods and materials. **b**

and **c**, A series of ASOs targeting 5'SS increase mRBM3 expression at both 37℃ and 39℃ in N2a cells. **e**, ASOs binding to M2-9 significantly increase endogenous RBM3 expression, showing that M2D is the most potent. **f** and **g**, Optimized M2D ASOs further enhance endogenous RBM3 expression at both 37℃ and 39℃ in N2a cells. **h**, M2D increases RBM3 expression in a time-dependent manner. **i** and **j**, M2D morpholino increases RBM3 expression in a time and dosage dependent manner in N2a. **l** and **m**, ASOs targeting M4 enhancer augments endogenous RBM3 expression in N2a cells. n>3. Individual ASO or morpholino was transfected into N2a cells or HEK293T cells at 37℃ for around 4hrs, and then the cells were shifted into incubator at 37℃ or 39℃ for another 24hrs, followed by RT-PCR. For M2D and MOE kinetic assay, pBABE plasmid with puromycin resistance and M2D or MOE were co-transfected into N2a cells at 37℃ for around 4hrs, and then the cells were shifted to incubator at 39℃ culturing for different time durations. At day 2, puromycin (2mg/ml) was added into the medium to kill the non-transfected cells. At day 4 and Day 5, cells are harvested to do RNA extraction and RT-PCR. Statistical significance was determined by unpaired t-test and is indicated by asterisks: unpaired t-test derived p-value *p<0.01, **p<0.01, ***p<0.001.

As the potent *cis*-regulatory enhancer elements are identified in mRBM3 minigene, we next used antisense oligonucleotides (ASOs) to target the elements in the pre-mRNA, which can modulate alternative splicing of exon 3a to increase endogenous RBM3 expression. Considering that the poor pharmacokinetics (PK) and limited potency of morpholino *in vivo*, we first used 2'-O-MOE, which has improved PK, higher binding affinity to target RNA, and broad reduction in toxicity caused by nonspecific protein binding (low immune response), to target RBM3 exon 3a. Since overexpression of RBM3 has neuroprotective function and we planned to test the effective ASOs in vivo mice, we next performed the ASO screening in mouse neuroblastoma cells (N2a) to identify the most potent ASO increasing RBM3 expression. As previous morpholino against 5'SS of RBM3 exon 3a shows stronger effect on regulating of RBM3 exon 3a inclusion in comparison with 3'SS, we designed a series of MOEs-based on the sequence of exon 3a 5'SS with slight left- and right-shift of targeting position (**Fig. 1.5a**) given that the binding affinity is possibly influenced by the difference of binding sequences. These MOEs targeting 3'SS were first tested at higher temperature (39℃). All these MOEs can efficiently promote RBM3 expression up to around 2-fold increase (**Fig. 1.5b**). Further, it shows that ASOs with longer length in chemistry (Long A and Long B with 7 nt longer than MOE) cannot obviously further enhance the RBM3 expression compared to the shorter one (MOE) (**Fig. 1.5b**). Right shift of the binding site (MOE+2) slightly helps the enhancement of RBM3 expression (**Fig. 1.5b**) at 39℃. We further designed another ASO, MOE+3 to test it together with MOE, MOE+2 at 37℃, that is physiologically normal temperature in brain.

Obviously, MOE, MOE+2 and MOE+3 can efficiently boost RBM3 expression, presenting that MOE+2 has the highest potency at 37℃ among these ASOs targeting 5'SS.

Next, based on M2-9, the core enhancer element of M2 mutant, M2A to M2E series of ASOs were designed to target M2 element (**Fig. 1.5d**). M2D has the highest potency with around 3-fold increase of RBM3 in comparison to ctr ASO at 39℃ (**Fig. 1.5e**). Given that M2D showed the highest activity to increase RBM3 expression with just 2.5-fold change, while M2-9 mutant *cis*-regulatory element can almost 100% abolish RBM3 exon 3a inclusion, we asked whether increasing transfection efficiency could promote RBM3 expression more efficiently. We co-transfected pBABE-puromycin resistance plasmid with M2D and MOE ASO into N2a cells at 39℃, followed by puromycin selection at day 2. The result showed that RBM3 expression doesn't change at first 12hrs, but at day 4 and day 5 MOE targeting 5'SS can increase to around 2.8 times of RBM3 expression and M2D leads roughly 4 times increase of RBM3 expression (**Fig. 1.7h**). It further implicates that M2D functions to enhance RBM3 expression more efficiently with higher transfection efficiency and longer treatment time.

Encouraged by the M2D efficiency, we next designed M2Da and M2Db, whose binding site on pre-mRNA is 2 nt left-shift and 2nt right-shift of M2D targeting sequence, respectively (**Fig. 1.5d**), to achieve higher activity in M2 series. It shows that M2Da functions well in terms of consistency and potency of increasing endogenous RBM3 in N2a cells at 39℃ (**Fig. 1.5f**). To examine whether the M2D series ASOs function at 37℃, M2A, M2C, M2D, M2Da and M2Db were individually transfected into N2a cells, and M2Da still produces the best potency to increase RBM3 expression (**Fig. 1.5g**). In summary, M2Da has the highest activity to enhance RBM3 expression at both 37℃ and 39℃ in the M2 series ASO screening.

To further countercheck the efficiency of targeting M2D sequence, we designed PMO chemistry based ASOs to target the M2Db sequence. It showed that M2Db can effectively enhance RBM3 expression in a dosage and time dependent manner at both 37℃ and 39℃ in the N2a cells (**Fig. 1.5i** and **j**). These results further demonstrated that targeting M2D element is an effective strategy in the direction of increasing endogenous RBM3 expression.

As M4 has been also demonstrated as one of the potent *cis*-regulatory enhancers of RBM3 exon 3a inclusion and M4-4, M4-5 and M4-6 are the core elements maintaining the enhancer activity of M4 in the mutagenesis screening, M4 series of ASOs were designed on the ground of the M4-4 to M4-6 element (**Fig. 1.5k**). All of them could effectively promote RBM3

expression at both 37 and 39 ℃ in N2a cells (**Fig. 1.5l** and **m**), presenting that M4D has the highest potency.

In a word, the ASOs, which can be potentially used *in vivo*, directly targeting 5'SS, the core sequence of M2 and M4, can sufficiently enhance RBM3 expression at both 37℃ and 39℃ in N2a cells.

1.5 Conserved ASOs targeting enhancer of RBM3 exon 3a function in human cells.

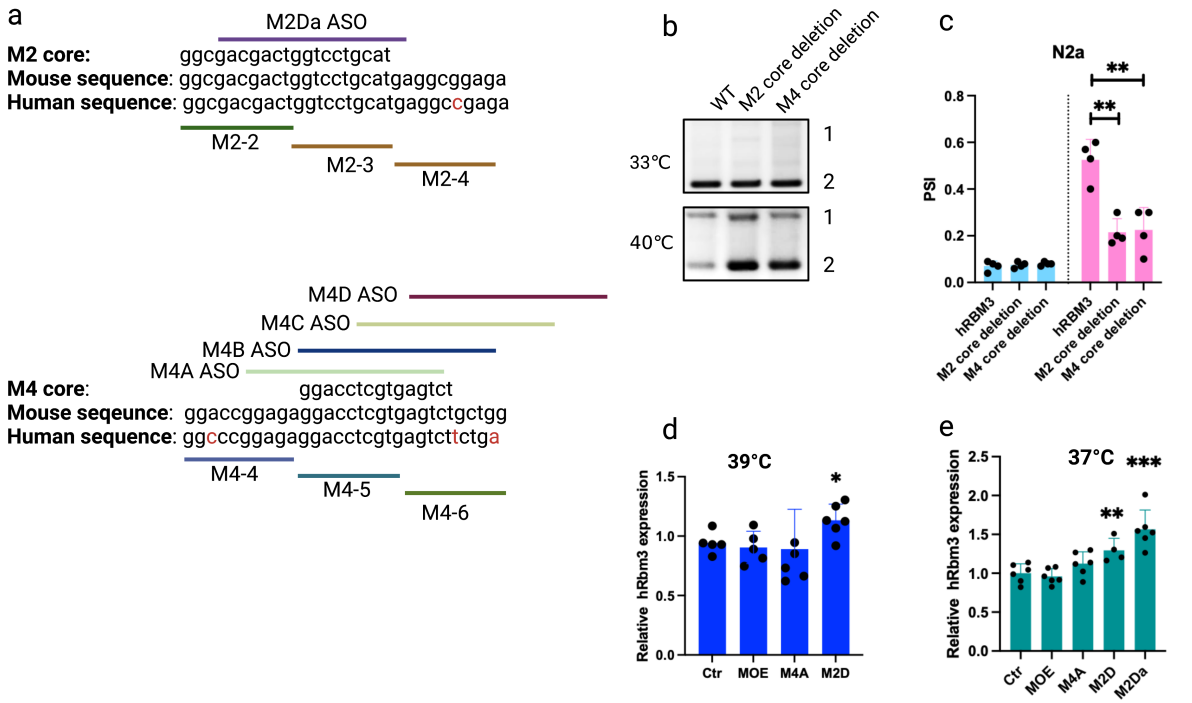

Figure 1.6 ASOs increase endogenous RBM3 expression in HEK293T. a, Schematic of M2 and M4 core sequence. **b and c**, M2 and M4 core *cis*-regulatory element deletion in hRBM3 minigene abolish 3 inclusion in N2a cells at high temperature. WT and mutant hRBM3 minigene were transfected into N2a cells overnight, respectively, and then they were shifted to different temperatures, 33 ℃ and 40 ℃, further culturing for around 24hrs, followed by RT-PCR. The representative RT-PCR results are in **b**, and the quantification results are in c. n=4. **d** and **e**, ASO M2Da and M2D significantly increase endogenous RBM3 expression in HEK293T. n=3. PSI: percentage spliced in. Statistical significance was determined by unpaired t-test and is indicated by asterisks: unpaired t-test derived p-value *p<0.01, **p<0.01, ***p<0.001, ****p<0.001. PSI: percentage of spliced in. The other gel images for quantification are in the **App. Fig. 3**.

As we have demonstrated that blocking 5'SS and *cis*-regulatory enhancer element M2 and M4 of RBM3 exon 3a could efficiently increase endogenous RBM3 expression in N2a cells, the

strategy can be potentially therapeutically used in clinic to protect neurons in different scenarios. We next examined whether deletion of the core element of M2 and M4 in hRBM3 minigene could efficiently reduce poison exon 3a inclusion. Considering that the conserved sequence between mice and humans), the result of mutagenesis assays and ASO perturbation assays, we deleted the core sequence of M2 and M4 as shown in the **Fig. 1.6a**. Briefly, M2-2 and M2-3 are conserved between humans and mice, and they contain 85% of M2Da ASO sequence, which is the ASO with highest potency and less variation in the M2 series. Thus, M2-2 and M2-3 are regarded as core sequence of M2 enhancer to be deleted in hRBM3 minigene. For M4 region, M4-5 is the central region of the conservative sequence between humans and mice, and the targeting central region of effective ASOs are M4-5 and part of M4-6. Therefore, M4-5 and the part of upstream sequence of M4-6 were deleted as core sequence of M4 mutant in hRBM3 minigene.

It was found both M2 core and M4 core deletion mutants can significantly reduce hRBM3 exon 3a inclusion in N2a at high temperature, indicating that the *cis*-regulatory elements modulating RBM3 exon 3a inclusion are conserved between humans and mice. Both M2 and M4-core deletion show identical effect on repressing exon 3a inclusion. We next tested the ASOs, which not only function in N2a, but also their targeting sequence are conserved between humans and mice, that are MOE, M4A, M2D and M2Da. Both M4A and MOE have no obvious effect on increasing endogenous hRBM3 expression, and M2D can increase hRBM3 expression at both 37℃ and 39℃ with ASO treatment for the 24hrs. M2Da significantly boosts hRBM3 expression even higher than M2D at 37℃, which is consistent to the data in N2a cells (**Fig. 1.8d** and **e**).

1.6 ASOs enhance endogenous RBM3 protein expression.

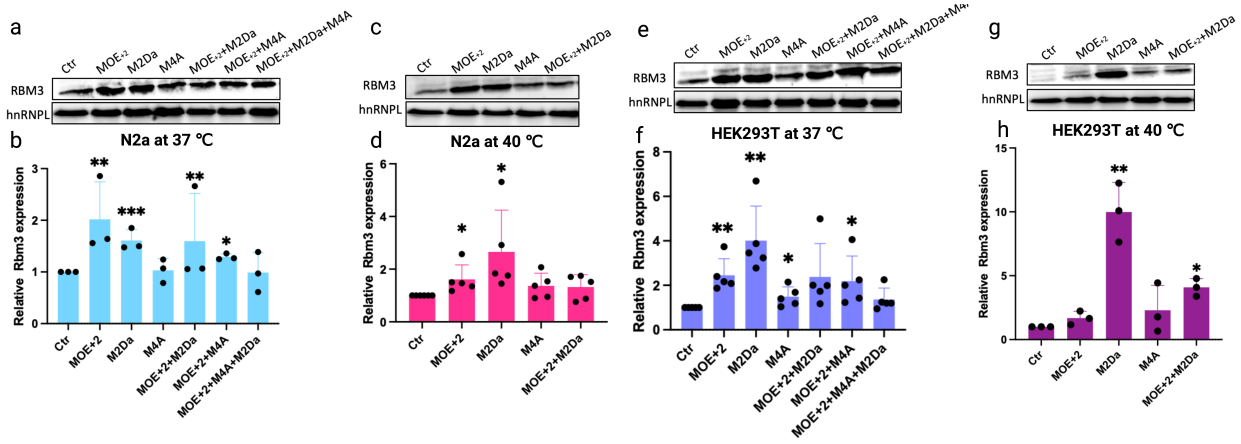

Figure 1.7 ASOs effectively increase endogenous RBM3 protein expression. **a** to **c**, ASOs efficiently increase RBM3 expression in N2a cells at 37℃ and 40℃. **b** and **d** are the quantification result. **e** to **h**, ASOs efficiently increase RBM3 expression in HEK293T cells at 37℃ and 40℃. Quantification results are in **f** and **h**. ASOs were transfected into N2a or HEK293T cells for around 4hrs, and then the cells were further incubated at 37℃ or 40℃ for 2 days. The samples were harvested for WB. Statistical significance was determined by unpaired t-test and is indicated by asterisks: unpaired t-test derived p-value *p<0.01, **p<0.01, ***p<0.001. The other gel images for quantification are in the **App. Fig. 4**.

Finally, we checked whether the effective ASOs could increase endogenous RBM3 protein expression. Given that the fold change of RBM3 mRNA caused by ASO is not very high with 24hrs treatment and the half-life of ASOs has been reported is more than one week, we treated the cells with ASOs for 2 days and then checked the RBM3 protein expression. MOE+2, M2Da and M4A were examined in N2a at both 37℃ and 40℃ given that MOE+2 showed highest potency in ASO series targeting 5'SS , M2Da and M4A are conserved between humans and mice and present high effect on increasing endogenous RBM3 mRNA expression. In N2a cells, M2Da only can significantly increase RBM3 protein expression to 1.5 folds at 37℃, and more than 2 folds at 40℃. As MOE+2 is not conserved between human and mouse, instead that MOE is conserved, so MOE was examined in HEK293T cells. Similarly, M2Da also shows the highest effect on increasing RBM3 expression in HEK293T cells (**Fig. 1.7**).

Interestingly, we found that the effect of M2Da on increasing RBM3 expression at 40℃ was much stronger than MOE series, especially in HEK293T cells. This is possibly because that high temperature treatment for longer time (around 2 days) makes the M2 *trans*-acting factor more active to enhance the exon 3a inclusion, while the accessibility of 5'SS is not influenced so much when the treatment time is elongated from 24hrs to 48hrs and the temperature increases from 39℃ to 40℃ if we compared the WB data with ASO perturbation data. We also noticed that the combination of different ASOs targeting M2, M4 and MOE couldn't significantly further enhance RBM3 expression compared to M2Da treatment only in both N2a and HEK293T cells at both 37℃ and 40℃ (**Fig. 1.7**). This is possibly because too much ASOs in the cells are toxic for cells for a long time treatment. In conclusion, the tested ASOs can enhance RBM3 protein expression in N2a and HEK293T cells, showing that M2Da has the highest potency to boost endogenous RBM3 expression.

1.8 Discussion

RBM3 is a well-known cold-induced protein, which also highly expresses in the brain of hibernating animals when the environmental temperature decreases[355]. However, the detailed mechanism how cold induces high RBM3 expression remains elusive although a few papers have shown that in a transcription level, some transcription factors, such as NF-κb, FAK/Scr and CREB, can drive more RBM3 transcription at low temperature. Also, it is almost impossible to therapeutically target the transcription factors to enhance RBM3 expression due to their broad effects on the regulation of gene expression. Here we present a novel mechanism how cold induces RBM3 expression in a posttranscription level. Importantly, this novel mechanism can be utilized to specifically increase endogenous RBM3 expression under normothermia.

A conserved heat-induced "poison" exon containing PTCs was determined in the RBM3 exon 3a, so the transcripts containing exon 3a will undergo NMD to be degraded[203-205,356-359]. Two strong *cis*-regulatory elements (M2 and M4) have been successfully identified to promote exon 3a inclusion in RBM3 at both normal (37℃) and high temperature (40℃), and we noticed that the activity of these two enhancers increased at high temperature in comparison to low temperature (33℃). At low temperature, M2 and M4 activity is too low to functionally promote RBM3 exon 3a inclusion. Sterically blocking the *trans*-acting factor of M2 and M4 binding to mRNA with modified antisense oligonucleotides (ASOs) can achieve the enhancement of RBM3 expression at normal temperature in both HEK293T and N2a cells. Meanwhile, ASO targeting 5'SS also can increase RBM3 expression at normal and high temperature even though they exert less efficacy compared to the ASO targeting M2 and M4. Taken together, targeting *cis*-regulatory element M2 or M4 is therapeutically promising to boost endogenous RBM3 expression.

Scientifically, several interesting questions can be asked in our study. How do M2 and M4 function together to promote RBM3 poison exon 3a inclusion? Why does RBM3 exon 3a need two strong ESE enhancer elements? M2 and M4 should act cooperatively to promote exon 3a inclusion as deletion of one of them can almost fully repress the exon 3a inclusion. In other words, they don't function synergistically, but it is required to maintain the enhancer activity of both M2 and M4 to efficiently enhance RBM3 exon 3a inclusion. Once the activity of one of them is inhibited, the effect on promoting exon 3a inclusion will be influenced. This is

demonstrated by mutagenesis and ASO perturbation assays. How they coordinate with each other needs to be further investigated.

1.9 Future plans

A therapeutically feasible approach of ASO-mediated transient enhancement of RBM3 is achieved in this study. It means that hypothermia “in a syringe” can be accomplished through injection of RBM3-based ASO at normal temperature in *ex vivo*. It is possible that only the tip of an iceberg was done for the clinical utilization of the ASO because the efficacy and toxicity of these ASOs in *vivo* need to be further tested. These effective ASOs should be tested in WT mouse and some neurodegenerative disease models to check their *in vivo* effects and toxicities. Identification and optimization of ASOs with minimal toxicity, maximal potency and efficacy should be further conducted in the future investigations.

2 RNA serves as direct thermosensors via spliceswitch formed by G-quadruplex in mammalian cells.

In most mammals including humans, core body temperature is tightly controlled to stay at ~37°C[360,361] with subtle circadian variations within a range of ~1-4°C[362]. This results in cells from most organs to be only exposed to a small temperature range. Some organs intricately and developmentally maintain differential temperatures showing lower temperature in skin and testis and gradient temperatures in the reproductive tract[362-364]. Pathologically, strong changes of core body temperature result in high morbidity and mortality[365,366]. Accidental hypothermia severely influence normal functions of physiological systems when the body temperature is reduced to below 35°C for a long period of time[367-369], while extreme hyperthermia causes heatstroke-induced cell death when the core body temperature rises above 40.5°C[370].

At the molecular level, various studies have investigated the response of cells to the temperature perturbation using heat-shock and cold-shock treatment. It is well-known that transient receptor potential (TRP) channels directly sense temperature alterations in human cells[371-374]. Besides, studies revealed that even small changes around 1-2°C in temperature are sufficient to impact RNA splicing, and these splicing changes could be regulated by phosphorylation of SR proteins[128,237]. Previously, we demonstrated that this regulation depends on the activity of CDC-like kinase (CLK), which is conferred by conformational rearrangements in the active center of the kinase at different temperatures[129]. In addition to the temperature-dependent splicing regulation arising from altered activity of kinases or channels, RNA itself may also serve as a sensor of temperature since it has diverse secondary structural conformations based on alternative base pairing and the structural stability could be impacted by temperature. Indeed, it has been shown that RNA could sense and respond to temperature changes to modulate alternative splicing in yeasts[135] and plants[136]. However, in mammals, the role of RNA secondary structures as thermo-sensors to control alternative splicing has not been investigated.

G-quadruplexes (G4) are stable secondary structures formed by Hoogsteen guanine base pairs (G-G) in different structural arrangements. Particularly, RNA G-quadruplexes (rG4s) have been implicated in many essential biological processes and contribute to multiple molecular functions[375]. For instance, in humans, rG4s could promote the alternative polyadenylation of LRP5 and FXR1 to produce shorter transcripts[183], be involved in PSD95 mRNA transport in neurites[184], contribute to the phase separation of RNA granules[185], and regulate translation[188,189].

In addition, it has been shown that rG4s could repress the recognition/definition of 5' splice sites through recruiting hnRNP H[175,176], enhance splicing to impede intron retention[177,178], and to promote exon inclusion through interacting with hnRNP F[179]. A recent genome-wide study suggested that rG4s are enriched near splice sites to promote exon inclusion possibly through enhancing binding of some RNA binding proteins in mammalian cells[32]. However, the involvement of rG4s in temperature-dependent RNA regulation at molecular level has not yet been explored.

2.1 rG4 motifs are significantly enriched around splice sites of cold-repressed cassette exons.

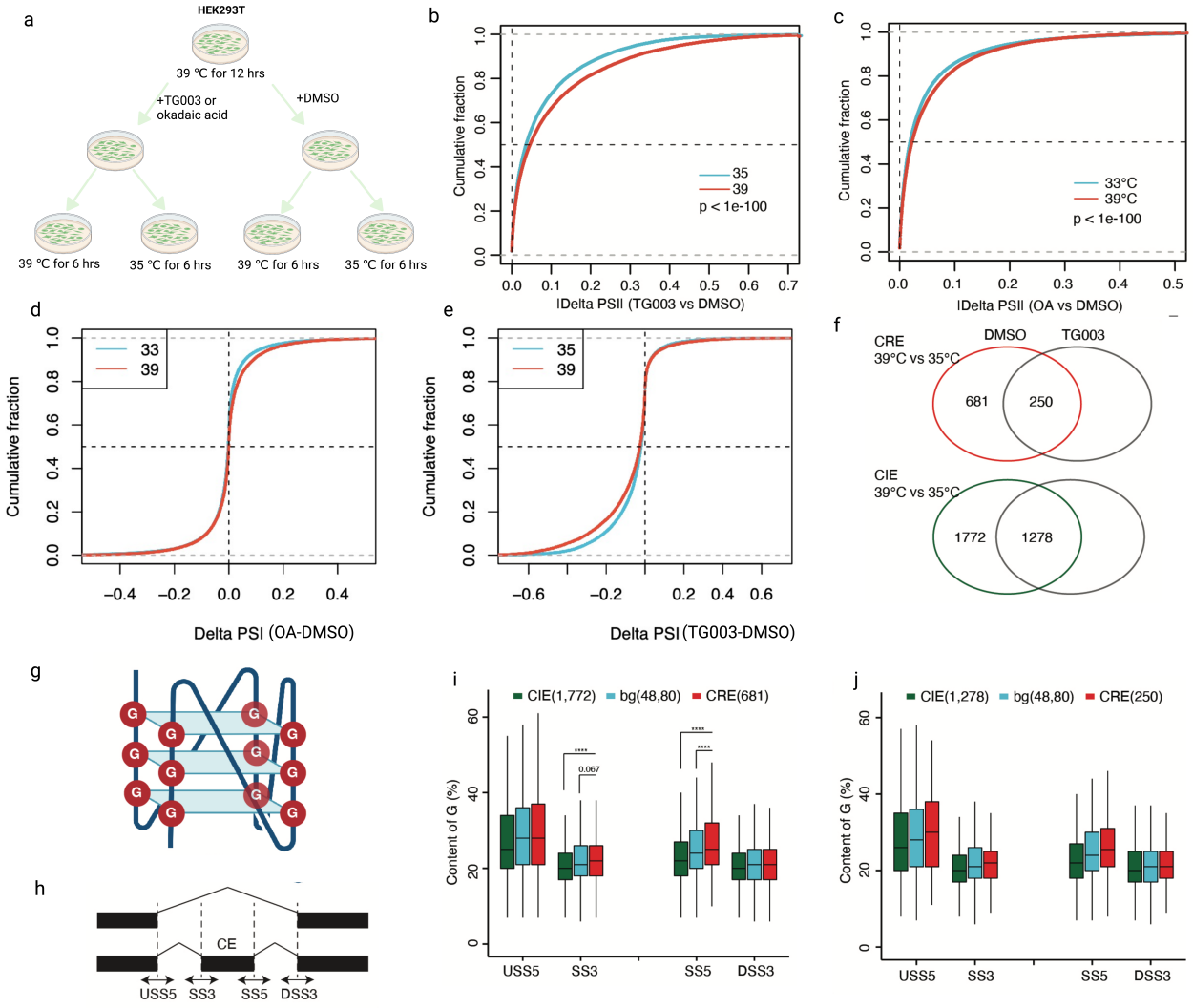

Figure 2.1 Cold-repressed exons are significantly G-rich near spice sites in HEK293T. a, Schematic diagram of HEK293T cells treatment in different conditions. HEK293T cells cultured at 37°C were shifted to 39°C incubator for 12hrs, followed by TG003 and DMSO treatment, respectively. Later, the treated cells were further cultured at 35°C for another 6hrs, and then subjected to RNA extraction and RNA-

seq. **b,** Cumulative fraction of absolute of delta PSI (TG003 *vs* DMSO) at 35℃ and 39℃ in HEK293T. **c,** Cumulative fraction of absolute of delta PSI (okadaic acid *vs* DMSO) at 35℃ and 39℃ in HEK293T. **d,** Cumulative fraction of delta PSI (TG003 *vs* DMSO) at 35℃ and 39℃ in HEK293T. **e,** Cumulative fraction of delta PSI (okadaic acid vs DMSO) at 35℃ and 39℃ in HEK293T. **f**, Venn diagram of CRE and CIE in TG003 and DMSO treated samples. **g**, Schematic of G-quadruplexes. **h**, Schematic diagram of bioinformatics analysis, SS3: 3'splice site flanking 50nt; SS5: 5' splice site flanking 50nt. **i**, CRE has higher G content near the 5'SS and 3'SS than CIE and background in TG003-independent temperature sensitive exons (CRE and CIE). **J**, CRE has higher G content near the 5'SS and 3'SS than CIE and background in TG003-dependent temperature sensitive exons (CRE and CIE). CIE: cold-induced exons. bg: non-temperature sensitive exons. CRE: cold-repressed exons. Statistical significance was determined by Wilcox test for boxplot (**c** and **d**) and is indicated by asterisks: p values: *p<0.05, **p<0.01, ***p<0.001. CRE: cold-repressed exons. CIE, cold-induced exons. bg: background (non-temperature sensitive exons). Cooperated and done with Bin ZHANG together.

Our previous studies have shown that the activity of kinases, CLK1/4, regulate temperature-dependent alternative splicing in mammalian cells. In that study we performed RNA sequencing on cells at different temperatures that were treated with DMSO and TG003 (a CLK specific inhibitor) (**Fig. 2.1a**). While around half of temperature-dependent splicing events (2453) did respond to CLK inhibition, a substantial proportion of them (1528) were not impacted by TG003[129](**Fig. 2.1f**). This points to the existence of other molecular mechanisms that are responsible for the modulation of temperature-dependent alternative splicing. Furthermore, we observed that pharmaceutical perturbation of phosphorylation via TG003 and okadaic acid (a broad phosphatase inhibitor) treatment has a greater influence on splicing at high temperature than that at low temperature (**Fig. 2.1b to e**), illustrating that phosphorylation-dependent splicing regulation is more profound at high temperature, and the unknown new mechanism might be less-phosphorylation dependent and preferentially impact splicing at low temperature.

As it has been reported RNA secondary structures could serve as molecular thermometers in yeasts and plants[67,135,136], we reasoned that rG4 structures, formed in guanine-rich nucleic acid sequences (**Fig. 2.1g**), which are known to dynamically control RNA processing events, would be well-suited to act as thermo-sensors in mammalian cells. To inspect this possibility, we first calculated G content for sequences around splice sites of each cassette exon and its upstream and downstream exons (**Fig. 2.1h**). Next, we classified the cassette exons into three categories, including cold-repressed exons (CREs), non-temperature sensitive exons (bg) and cold-

induced exons (CIEs) based on their percentage spliced in (PSI) at 35°C and 39°C in samples treated with TG003 or DMSO, respectively. We further defined CLK-dependent temperature-sensitive exons by requiring that CREs or CIEs specifically present in DMSO but not in TG003 treated samples, as well as CLK-independent ones using the overlapped CREs or CIEs between DMSO and TG003 treated samples (**Fig. 2.1f**).

We found that in both CLK-dependent and CLK-independent temperature-sensitive exons, G-content of sequences flanking the splice sites of CREs are significantly higher than that in CIEs and bg. Such differences were not observed for sequences flanking splice sites of their upstream and downstream exons, making a higher G-content around splice sites specific for cold-repressed cassette exons (**Fig. 2.1i and 2.1j**). As this holds true also for cold-repressed exons that are independent of CLK activity, these G-rich sequences may contribute to an alternative mechanism controlling temperature-sensitive alternative splicing.

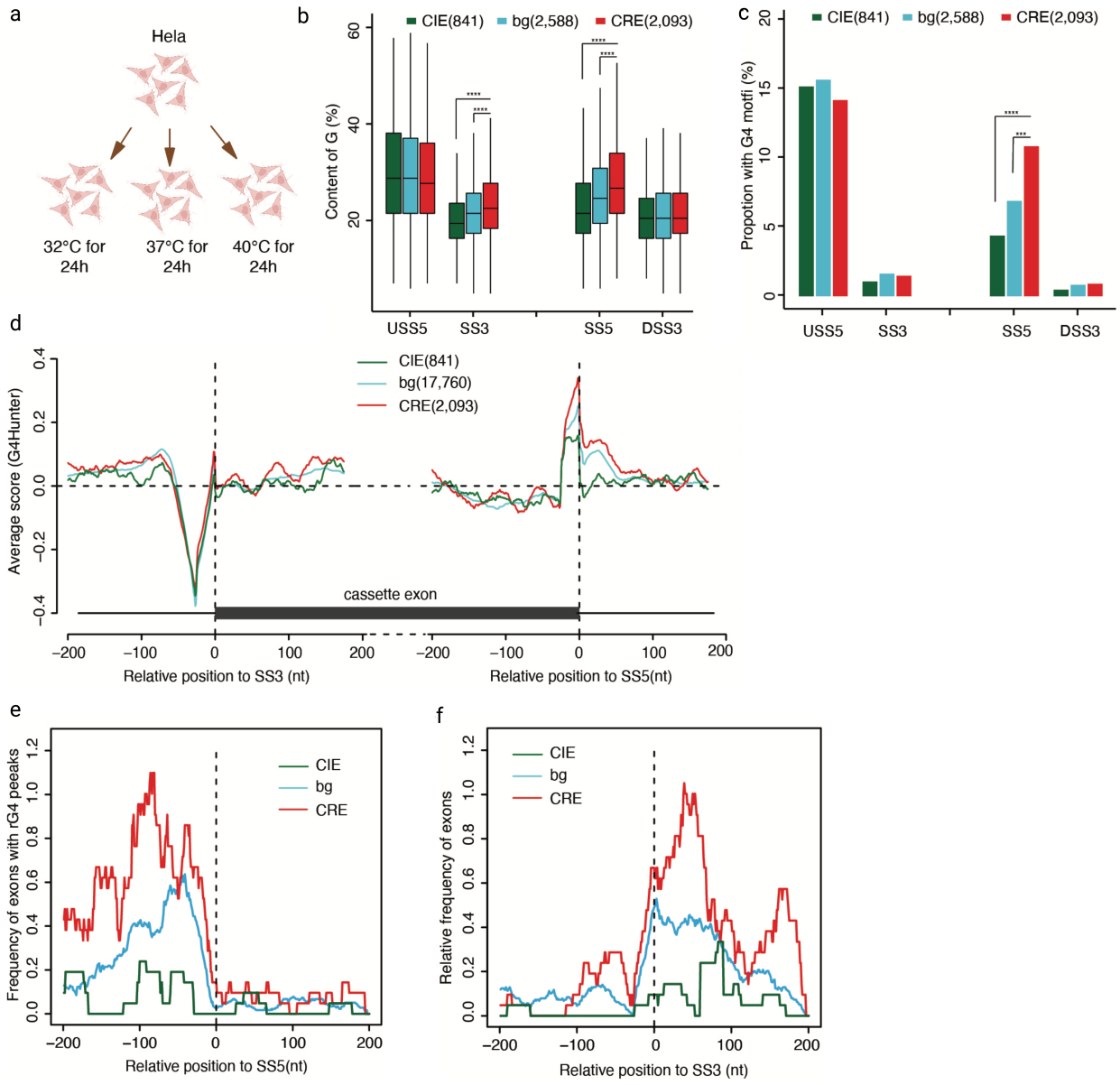

Figure 2.2 Cold-repressed exons have more RNA G-quadruplexes around 3'SS and 5'SS.

a, Schematic of Hela cells treatment in different conditions. Hela cells cultured at 32°C and 37°C for 24hrs were subject to RNA extraction and RNA-seq. **b**, G content is higher in CRE than CIE and background. **c**, Proportion of putative RNA G-quadruplex motif in CRE, CIE and bg shows that CREs have more G4 motifs than CIE and background. **d**, Highest G4 scores are located around the 5' splice site of cassette exons and is apparently higher for CREs than for CIEs and bg, predicted by G4hunter. **e and f**, CREs have more rG4 peaks than CIE and bg at both 5'SS (**e**) and 3'SS (**f**) supported by high-throughput rG4-seq screening datasets. Statistical significance was determined by Wilcox test for boxplot (**b** and **c**) is indicated by asterisks: p values: *p<0.05, **p<0.01, ***p<0.001. CRE: cold-repressed exons. CIE, cold-induced exons. bg: background (non-temperature sensitive exons). Cooperated and done with Bin ZHANG together.

To further validate these findings in a different cell culture model, we performed RNA-Seq in Hela cells at 32°C, 37°C and 40°C (**Fig. 2.2a**). With these RNA-seq data, we identified 2,093 CREs and 841 CIEs upon cold shock. Consistently, we observe a significantly higher G content in sequences flanking the splice sites of CREs compared with that of CIEs and bg (**Fig. 2.2b**). Next, for each cassette exon upon cold-shock, we searched for putative rG4s in the vicinity of its splice sites, or 5' splice site of the upstream and the 3' splice site of the downstream flanking exon[34]. Indeed, we observed a significantly higher frequency of rG4 motifs in sequence flanking splice sites of CREs compared to that from bg and CIEs. This trend is more evident for sequences flanking the 5' splice sites, showing that the percentage of sequences containing G4 motifs is higher (10% *vs* 7%) in CREs than that in bg and even doubled (10% *vs* 4.5%) compared with CIEs (**Fig. 2.2c**). To confirm this finding and to address the position of rG4 with respect to splice sites at single nucleotide resolution, we scanned sequences flanking each cassette exon with a 25nt window using G4Hunter[376]. Similar to the results from a previous study[174], the highest G4 scores are located around the 5' splice site of cassette exons and is apparently higher for CREs than for CIEs and bg (**Fig. 2.2d**). To further validate the in silico predictions, we analyzed RNA G-quadruplex sequencing (rG4-seq) data, which couples rG4-meditated reverse transcriptase stalling with high-throughput sequencing to map rG4 transcriptome wide[151]. Consistent with results from the in *silico* rG4 analysis, the occurrence frequency of rG4-seq peaks flanking splice sites of CREs is significantly higher than that of CIEs and bg (**Fig. 2.2e and 2.2f**).

Taken together, our analysis demonstrates that rG4 motifs are enriched around splice sites of CREs and depleted from splice sites of CIEs. These results indicate that rG4s could serve as widespread regulators of temperature-dependent alternative splicing. As RNA secondary structures are more stable at low temperature and may be disrupted at high temperature, we hypothesized that the formation of rG4 structures upon cold shock might mask splice sites thereby leading to exon exclusion. Based on this, the stability of rG4s should be negatively correlated with splicing of cassette exon.

2.2 G4 stabilizers effectively reduce the inclusion of cold-repressed exons.

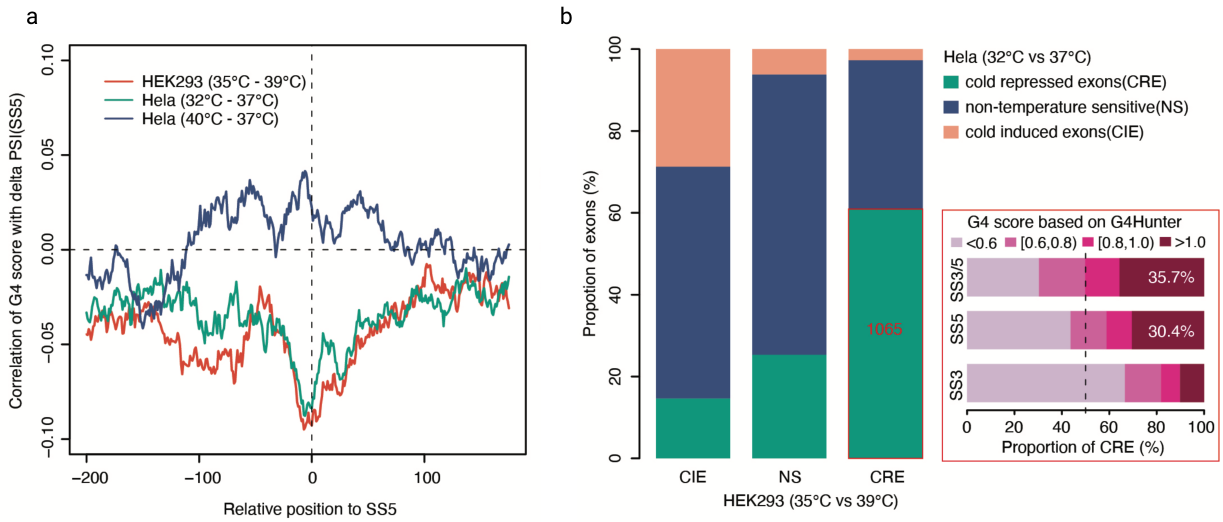

Figure 2.3 The predicted G4 score around 5' splice site of exon is negatively associated with delta PSI upon cold shock in both Hela and HEK293. **a,** Correlation of G4 score with delta PSI near 5'SS upon cold-shock and heat-shock in HEK293T and Hela cells. **b**, Overlapping of CREs between Hela and HEK293T. Cooperated and done with Bin ZHANG together.

Next, we investigate the impact of rG4 on temperature-dependent splicing globally by correlating the predicted rG4 scores with the PSI changes (delta PSI) of exons at different temperatures. Interestingly, we observed that the predicted G4 score around 5' splice site of exon is negatively associated with delta PSI upon cold shock in both Hela and HEK293 and slightly weaker positive correlations with delta PSI upon heat shock (**Fig. 2.3a**). As rG4s tend to be more stable at low temperature, this result suggests a general negative correlation between stability of rG4s around splice sites and the inclusion of the exon. To test this hypothesis, we firstly overlapped the identified CRE in Hela and HEK to exclude potential *trans*-effects. In total, 1065 overlapped CREs are identified and 35.7% of them contains predicted rG4 with G4 score more than 1 around the splice sites (**Fig. 2.3b**).

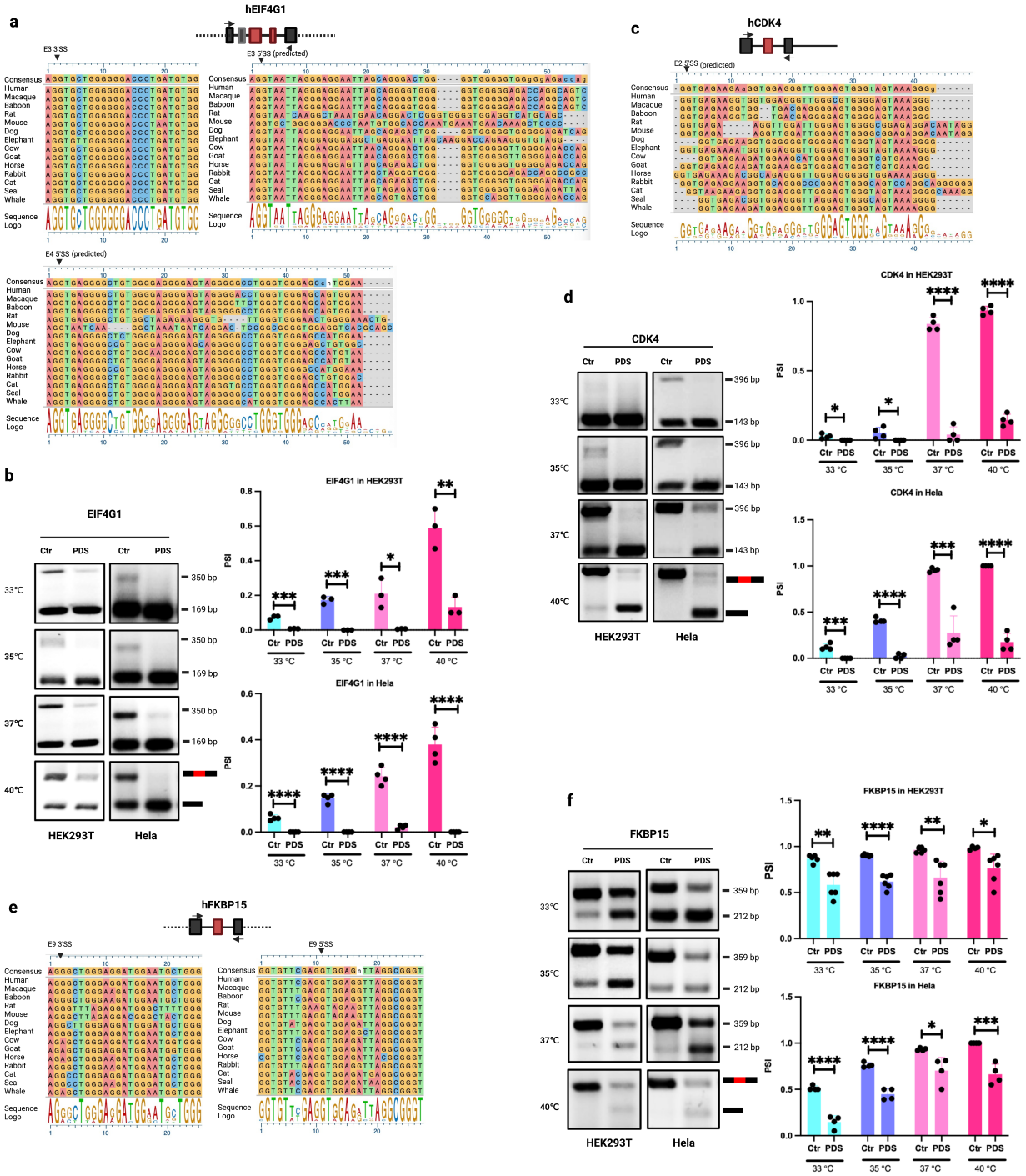

Figure 2.4 G4 stabilizer, PDS, reduces the inclusion of cold-repressed exons in both HEK293T and Hela. Different heat induced exons (hEIF4G1, CDK4 and FKBP15) with potential G4s were validated by PDS treatment at different temperatures. In each sub-figure, upper schematic (**a**, **c and e**) is the position of CREs in the corresponding genes. The evolutional conservation across different species of each potential G4 sequence is analyzed in the lower panel (**a,** **c** and **e**). Representative gel images of RT-PCR results are shown in the **b, d and f**. n>3. Quantified PSI of CREs at different temperatures with PDS or DMSO treatment is shown in the bar graph (**b**, **d and f**). HEK293T and Hela cells were treated with PDS and cultured at 33℃, 35℃, 37℃ and 40℃ for 24hrs,

followed by RT-PCR with gene specific primers. Amplified signal were detected by agarose gels, respectively. PSI: percentage of spliced in. All the calculated PSI indicate the PSI of heat induced exons. The black triangle indicates the splice site. Statistical significance was determined by unpaired t-test and is indicated by asterisks: p values: *p<0.05, **p<0.01, ***p<0.001. The other gel images used for quantification are in the **App. Fig. 5 (Fig. 2.1b) App. Fig. 6 (Fig. 2.1c) and App. Fi g. 7 (Fig. 2.1d)**.

Next, we selected three candidate genes containing the overlapped CRE and with predicted rG4 around the splice sites, including EIF4G1 and CDK4, and FKBP15. Sequence alignment shows that the G4 motifs surrounding CREs of these genes are conserved cross multiple mammals, indicating their importance in the gene regulation (**Fig. 2.4a, 2.4c and 2.4e**). By treating HEK293T and Hela cells with 10μM pyridostain (PDS), which is a well-known G4 stabilizer[157], we measured the splicing levels of CREs from these four genes at different temperatures (33, 35,37 and 40°C) with or without the PDS treatment.

EIF4G1 functions as molecular bridge between EIF4E and EIF4A to control translation[38], and there are two CREs in EIF4G1, the third (E3) and fourth (E4) exons, which encode distinct N termini of the EIF4G1 protein, suggesting altered functionalities of EIF4G1 at different temperatures. Both E3 and E4 showed apparent splicing changes at different temperatures, for which the PSI is around 50% at 40°C and it reduced to less than 5% at 33°C (**Fig. 2b**). Among the candidates, CDK4 exhibits the most drastic splicing changes upon cold shock, with gradually decreases PSI from more than 90% at 40°C to less than 10% at 33°C in both HEK293T and Hela (**Fig. 2.4d**). CDK4 is a catalytic subunit of the protein kinase complex in the cell cycle G1 phase, and promotes tumor growth by phosphorylation of tumor suppressor genes. The CRE E2 of CDK4 encodes the N terminal of CDK4 protein, which is required for the binding of ATP and D-type cyclin to maintain its catalytic activity. In line with our hypothesis, inclusion of both E2 from CDK4 and E3, E4 from EIF4G1 are almost abolished upon PDS treatment compared to the control at the four tested temperatures (**Fig. 2.4b and 2.4d**), suggesting that stabilizing rG4s by PDS indeed block the inclusion of cassette exon. On the other hand, FKBP15 shows similar splicing changes in Hela but the changes are almost neglect in HEK293 (**Fig. 2.4f**). As expected, a similar trend that G4 stabilizer PDS significantly reduce inclusion of CREs in FKBP15 at both low and high temperatures in both the two cell lines (**Fig. 2.4f**).

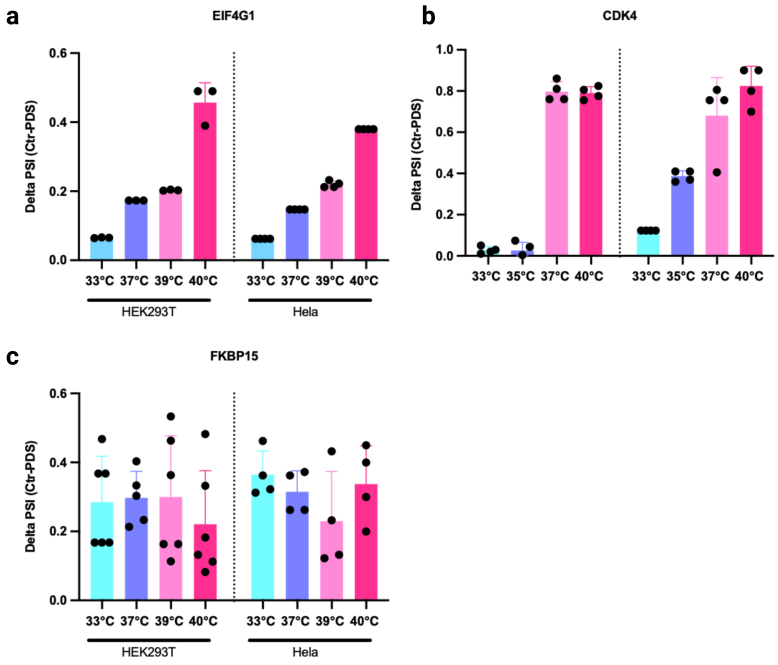

Figure 2.5 The reduced PSI caused by PDS is higher at high temperature than that at low temperature in EIF4G1 and CDK4, not in FKBP15

Additionally, we also observed that the reduced PSI caused by PDS treatment is generally higher at high temperature than that at low temperature (**Figure 2.5a**) in the CREs with high G4 score (>1,EIF4G1 and CDK4), suggesting that at low temperature rG4s might be stable enough, for which it become less sensitive to G4 stabilizer such as PDS. For the CRE with low G4 score (around 0.6, FKBP15), the delta PSI is similar in the temperature range from 33°C to 40°C), which further suggests that the G4 in FKBP15 is less stable even at 33°C, so PDS can more it more stable at that temperature. Taken together, our results demonstrate the robust effects of G4 stabilizer on repression the inclusion of CRE across different cell lines and temperatures, possibly through masking splice sites of these exons. These data also indicate that rG4 can act as sensors of temperature perturbation to control temperature-dependent alternative splicing, by modulating splice site accessibility.

2.3 Mapping putative *cis*-regulatory G-quadruplex elements repressing RBM3 exon 3a inclusion.

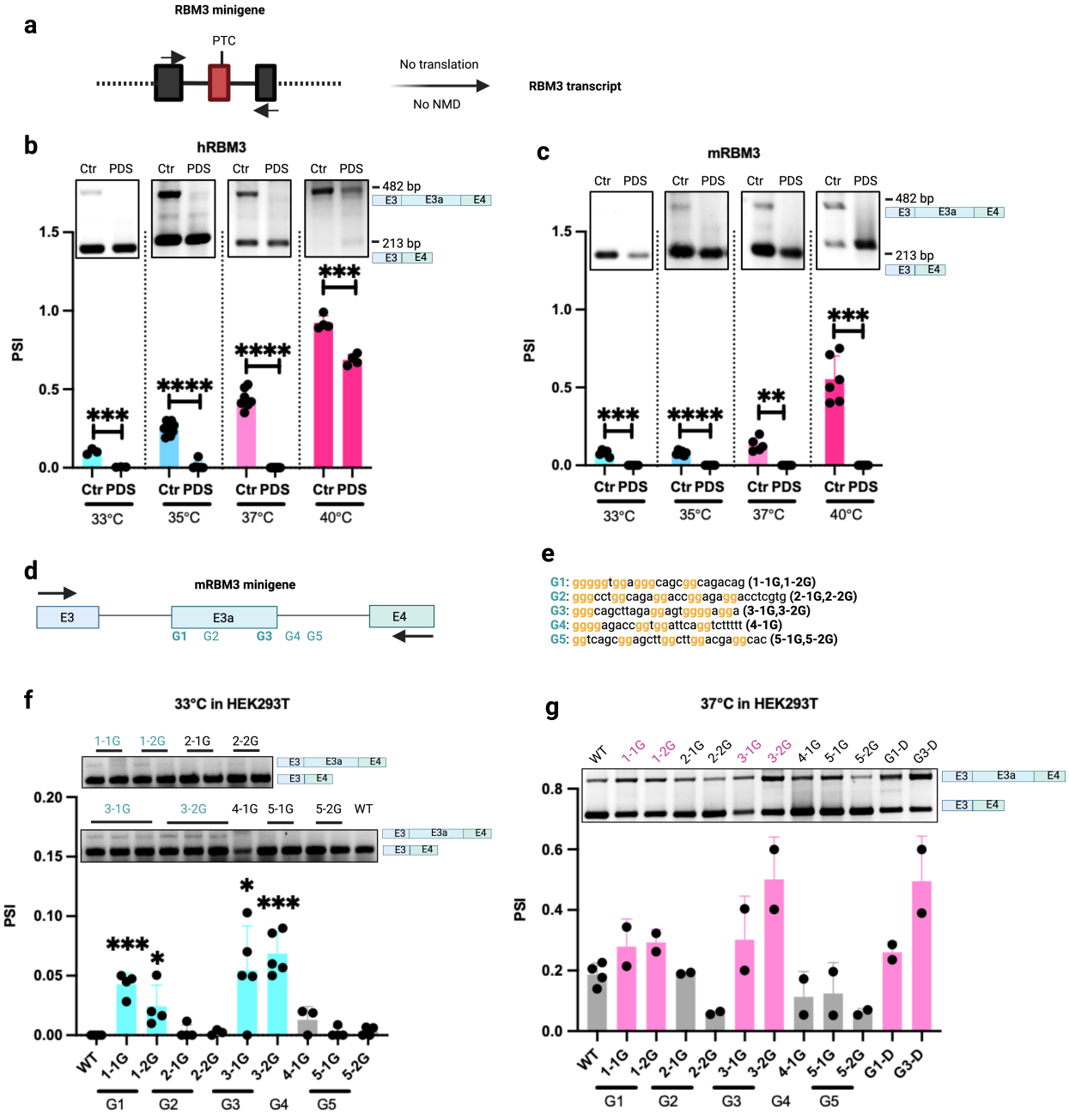

Figure 2.6 Fine-tuning mapping of repressive G-rich motifs via mutagenesis in RBM3 minigene. a, Schematic of RBM3 minigene. **b** and **c**, PDS dramatically reduces exon3a inclusion in both hRBM3 and mRBM3 minigene in HEk293T. Upper panels are the representative RT-PCR gels after DMSO and PDS treatment. The quantification results are in the lower panels. **d**, Schematic of different G mutant locations in mRBM3 minigene. **e**, Sequence of G1 to G5. **f** and **g**, RT- PCR results of multiple G-rich mutants at 33°C (**e**) and 37°C (**f**) resolved by agarose gels. Upper panels are the

representative RT-PCR gels, and the quantification results are in the lower panels. Plasmids were transfected into HEK293T or N2a cells, and then incubated at 37 °C overnight. All the cells were shifted into incubator at different temperatures to culture for another 24hrs, and then subject to RNA extraction, RT, and PCR. Statistical significance was determined by unpaired t-test and is indicated by asterisks: p values: *p<0.05, **p<0.01, ***p<0.001 (n>3, mean ± SD). PSI: percentage of spliced in. The other gel images used for quantification are in the **App. Fig. 8 (Fig. 2.6b** and **2.6c)** and **App. Fi g. 9a** and **9b (Fig. 2.6 f and 2.6g)**

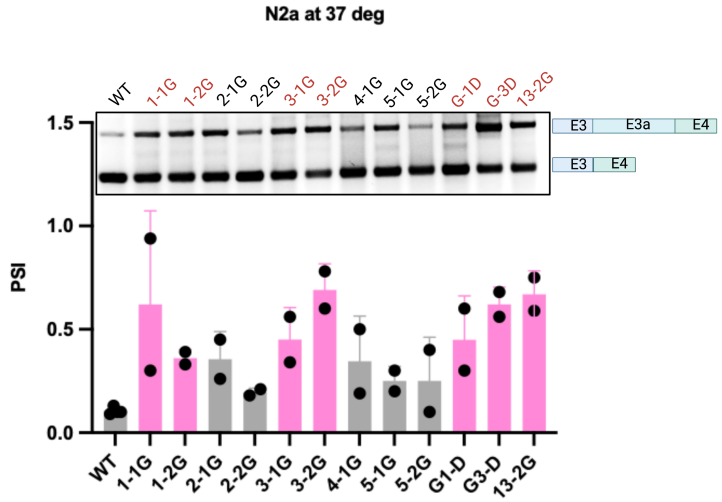

Figure 2.7 Fine-tuning mapping of putative G4 masking splice sites via mutagenesis in RBM3 minigene in N2a. RT-PCR result of different G-rich mutants of mRBM3 in N2a cells. Upper panel is the RT-PCR image and the quantification data is in the lower bar graph. PSI: percentage of spliced in. The other gel images used for quantification are in the **App. Fig. 9c.**

To provide a detailed proof of principle for the association of rG4 with temperature-dependent alternative splicing and its potential roles in cellular response to physiological temperature perturbations, we selected the cold-induced and neuroprotective protein RBM3[265] for more comprehensive investigation. Our recently study revealed that a heat-induced (cold-repressed) poison exon 3a controls temperature-dependent RBM3 expression. Interestingly, we noticed that this poison exon of RBM3 is one of CREs identified in Hela cells using RNA-seq with putative rG4s at both the 3'SS and 5'SS.

First, we aimed to identify rG4 structures/elements with splicing-repressive functions around exon 3a of RBM3. Since RBM3 transcripts containing exon 3a are physiologically degraded via NMD pathway, we cloned human RBM3 (hRBM3) and mouse RBM3 (mRBM3) minigenes consisting of the exon 3, exon 3a, exon 4, and the introns flanking exon 3a. The

RNA produced by two minigenes is not translated, and thereby will not be degraded by NMD (**Fig. 2.6a)**. In both the hRBM3 and mRBM3 minigenes, splicing of exon 3a preserved temperature sensitivity and PDS treatment strongly reduced exon 3a inclusion at four temperatures (**Fig. 2.6b and 2.6c**). At 33°C, 35°C and 37°C, the inclusion of exon 3a was almost fully blocked by PDS treatment, while the PSI was reduced by 30% (0.9 *vs* 0.6) at 40°C in hRBM3 minigene and by 100% (0.7 *vs* 0) in mRBM3. Next, we mutated each G-rich elements around the splice sites and within exon 3a that might impair the formation of rG4 (**Fig.2.6d and e**). It turned out that mutating rG1 and rG3 sequences increased exon 3a inclusion at both low and high temperatures in HEK293T and N2a cells (**Fig.2.6f, Fig. 2.6g and Fig. 2.7)**.

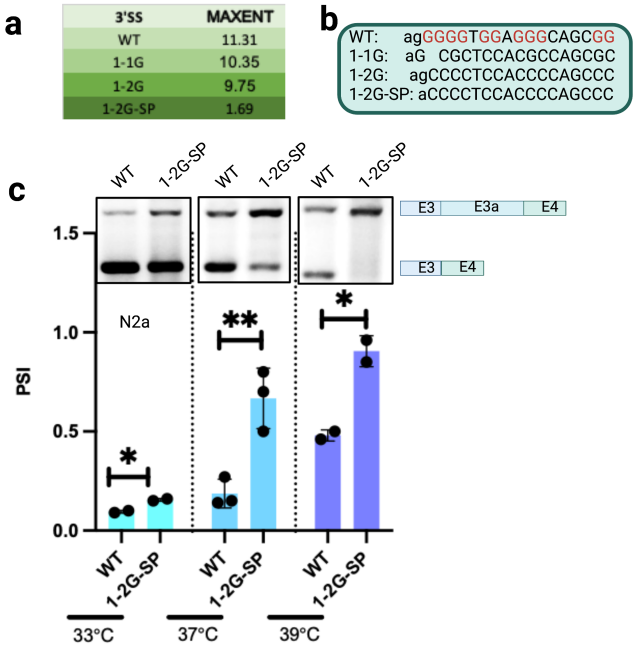

Figure 2.8 Reduction of 3'SS strength increases RBM3 exon 3a inclusion. a, splice site strength of 3'SS in WT and mutants analyzed by MaxEntScan. **b**, sequence of WT and G1 mutants. **c**, 1-2G-SP mutant with weak splice strength increases RBM3 exon 3a inclusion in HEK293T. Upper panel is the gel image of RT-PCR and lower is the quantification data. Plasmids were transfected into HEK293T or N2a cells overnight, and then they were shifted into different temperature for another 24hr culture, followed by RT-PCR and agarose gel resolving. Statistical significance was determined by unpaired t-test and is indicated by asterisks: p values: *p<0.05, **p<0.01, ***p<0.001 (n>3, mean ± SD) PSI: percentage of spliced in. The other gel images for quantification are in **App. Fig. 9d**.

To further exclude the possibility that the effect of the mutations in promoting exon 3a inclusion is caused by increasing of 3'SS strength, we computationally predicted the strength

of their splice sites (**Fig. 2.8a and b**) with MaxEntScan [377]. The mutant 1-2G-SP, in which the U2AF35 binding site "AG" was mutated to "AC" together with other G to C mutations, significantly promoted RBM3 exon 3a inclusion (**Fig. 2.8c**). The 3'SS strength slightly decrease in both the 1-1G and the 1-2G mutant in comparison with WT, and the 3'SS strength of 1-2G-SP was strongly reduced from 11.31 to around 1.69, consistent with the AG being crucial for the 3'SS in the AG-dependent splicing events. The decreased splice site strength (1-2G-SP) in principle will produce less exon 3a inclusion isoform in AG-dependent splicing events[378-380], but the splicing sensitive RT-PCR result was in a opposite way, suggesting that the recognition of 3'SS of RBM3 exon3a is AG-independent splicing events. We concluded that the increase of the RBM3 exon 3a isoform caused by G mutation is not due to altered splice site strength, but that it is rather controlled by disruption of rG1 and rG3, which may sterically block spliceosome assembly due to their proximity to splice sites. Collectively, the mutagenesis assays support the idea that rG1 and rG3 contribute to RBM3 exon 3a exclusion through sterically blocking spliceosome assembly or through masking splice sites.

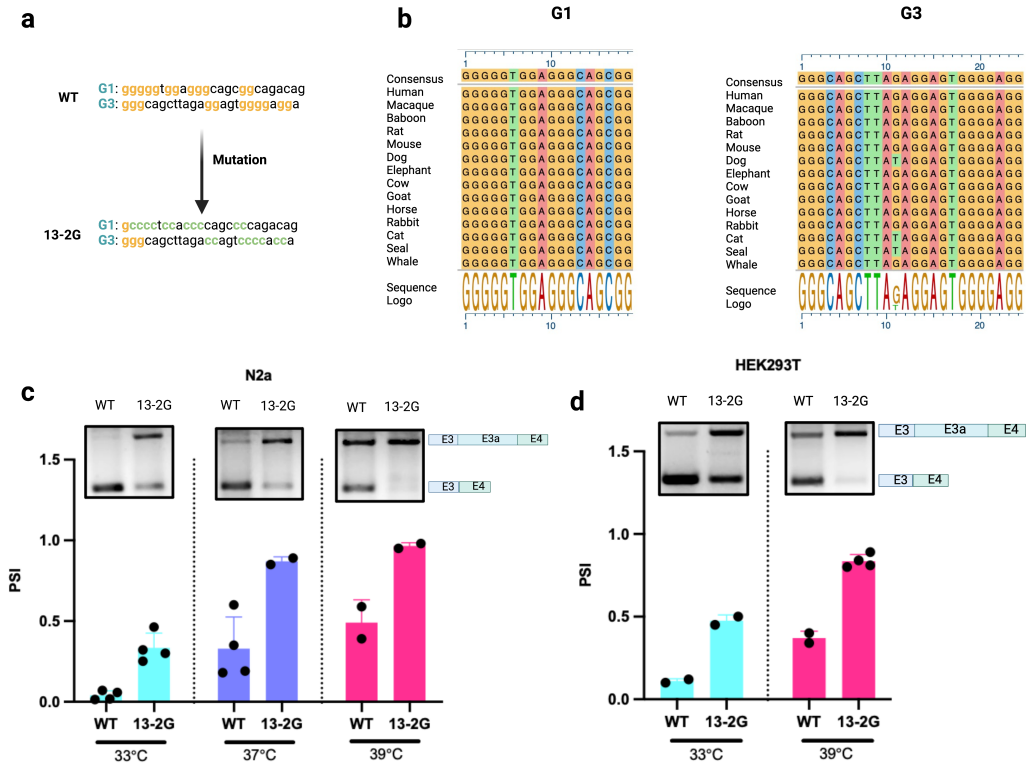

Figure 2.9 Disruption of potential G4s increases RBM3 exon 3a inclusion. a, Schematic of 13-2G mutation. **b**, rG1 and rG3 are evolutionally conserved cross multiple species. **c and d**, 13-2G mutant increases RBM3 exons3a inclusion at different temperatures in N2a (**b**) and HEK293T (**c**) cells. In **b** and **c**, Representative gel images in RT-PCR are shown in the upper panels, and quantification results are in the lower panel. The plasmids were transfected into cells overnight, and then were shifted

into incubators with different temperature to culture for around 24 hrs., followed by RT-PCR and agarose gel resolving. Statistical significance was determined by unpaired t-test and is indicated by asterisks: p values: *p<0.05, **p<0.01, ***p<0.001 (n>3, mean ± SD) PSI: percentage of spliced in. The other gel images used for quantification are in the **App. Fig. 10a** and **10b.**

We investigated whether these elements are evolutionally conserved in mammals via sequence alignament, and found that the four stretches of consecutive G residues in both G1 and G3, which are essential to form rG4 structure, are conserved from humans to whales (**Fig.2.9a**). As we hypothesized that rG1 and rG3 can individually mask one of the splice sites to repress splicing, their double mutants (**Fig. 2.9b)** might further reduce spliceosome accessibility, thereby strongly promoting RBM3 exon 3a inclusion. Indeed, double mutants (13-2G) further increases isoforms containing exon 3a in both HEK293T cells and N2a at low and high temperatures with a stronger effect than single mutant (**Fig. 2.9c and 2.9d).** Even at low temperature, the double mutants can increase the PSI to 0.5. Additionally, we observed that the double mutant (13-2G) still shows temperature sensitivity, suggesting rG4 elements are involved in setting basal inclusion levels and that other factors also contribute to the temperature sensitivity of exon 3a.

2.4 RNA G-quadruplex G1 in RBM3 is temperature sensitive shown by biophysical assays

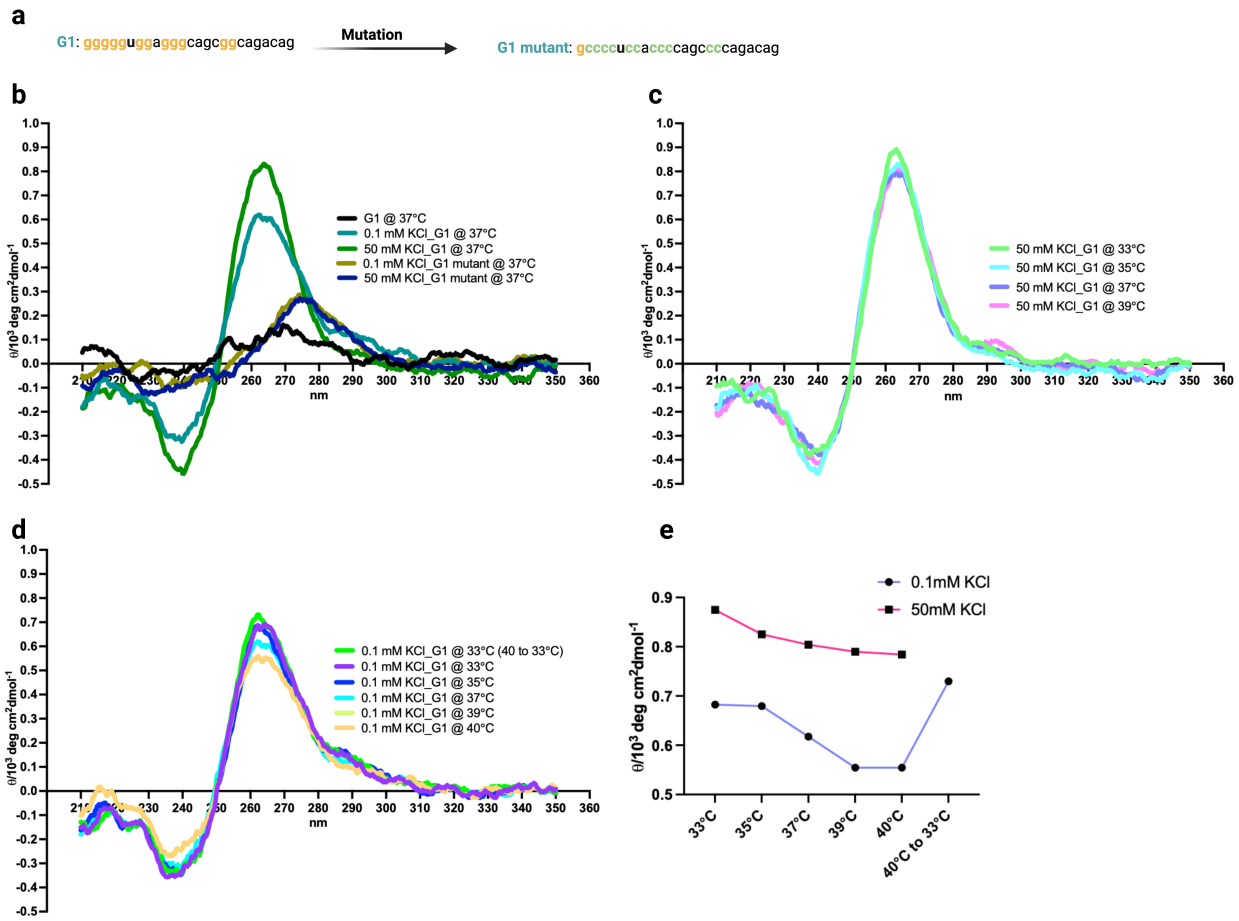

Figure 2.10 Biophysical assays show RNA G-quadruplex exists in rG1 *cis* element of RBM3. **a**, Sequence of synthesized G1 and G1 mutant RNA oligos. **b**, Circular dichroism (CD) signal of G1 significantly increases in high concentration of KCl, but G1 mutant has no response in high concentration of KCl at 37 °C. **c**, CD signal of G1 didn't significantly change in high concentration of KCl at different temperatures. **d**, CD signal of G1 decreases in low concentration of KCl at high temperature, and it was reversible. **e**, CD signal peak at 261nm at different temperatures in both low and high potassium concentration.

As our results demonstrate that G-rich elements around exon 3a are responsible to regulate RBM3 expression through modulating poison exon splicing, to prove that these G-rich elements can form rG4 structures, we synthesized an RNA oligo corresponding to the rG1 sequence and a mutant version (G1 mutant) by replacing the essential nucleotide G. We then performed circular dichroism (CD) spectroscopy, one of the standard methods to detect G4 structures. We observed a clear and strong signal with a peak at 262nm for the G1 oligo that was dependent on KCl, but not for G1mutant, which strongly supports the existence of an rG4

structure *in vitro* on the G1 oligo[381] (**Fig. 2.10b**). Furthermore, we checked whether the stability of this rG4 is temperature sensitive. In high KCl (50mM) buffer, rG4 was very stable, and showed less-temperature sensitivity (**Fig. 2.10c and e**). while the CD signal was obviously temperature sensitive in low KCl (0.1mM) buffer (**Fig. 2.10d and e**). Interestingly, the temperature-controlled changes in signal intensity were reversible when the RNA was first incubated at 40°C and then cooled down to 33°C, for which the rG4 signal returned to the similar level as that at 33°C without intermittent heating (**Fig. 2.10d**). These results suggest that the stability and temperature sensitivity of the rG4 structure is highly dependent on the concentration of G4 stabilizer (potassium) and that changes in the structure caused by alternations in temperature are dynamic and reversible.

2.5 Mutation of G1 and G3 abolishes the effect of G4 stabilizer on decreasing mRBM3 exon 3a inclusion.

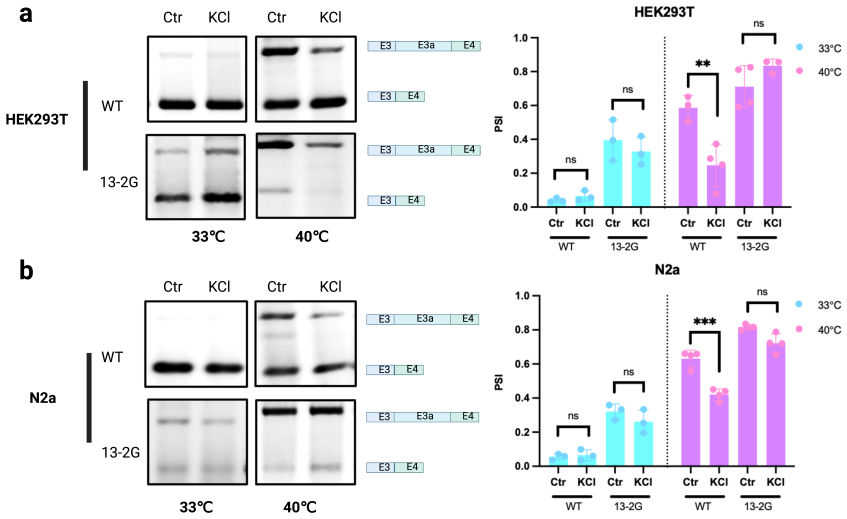

Figure 2.11 Mutation of G1 and G3 abolishes the effect of KCl on repression of RBM3 exon3a inclusion. a and b, KCl treatment significantly decreased RBM3 exon 3a inclusion in WT mRBM3 minigene, while 13-2G double mutant abolished the enhancement in both HEK293T (**a**) and N2a (**b**) cells at high temperature. Representative images of RT-PCR results are shown in the left side, and The quantification results are in the right panel. n≥3. Both WT and mutant plasmids were transfected into cells at 37°C overnight, 50 mM KCl was added into the medium, and then the cells were further incubated at different temperature for 24hrs, followed by RT-PCR and. PSI: percentage of spliced in. Statistical significance was determined by unpaired t-test and is indicated by asterisks: p values: *p<0.05, **p<0.01, ***p<0.001 (n>3, mean ± SD). The other gel images used for quantification are in the **App. Fig. 11**

We have demonstrated that the G1 sequence can form an rG4 structure *in vitro* which is likely also true for the G3. To confirm the relevance of rG4 structures for RBM3 expression in cells, we first tested the effect of endogenous G4 stabilizer K^+ on the mRBM3 minigene and the G4 double mutant (13-2G) in cells. In the WT mRBM3 minigene, K^+ treatment significantly decrease RBM3 exon 3a inclusion at high temperature, while it had no effect at low temperature in both HEK293T (**Fig. 2.11a**) and N2a cells (**Fig. 2.11b**). This is consistent with the *in vitro* data and again suggests higher stability of the rG4 structures, leading to reduced dependence on potassium, at lower temperature. In contrast, exon 3a inclusion in the double mutant (13-2G) didn't significantly change with KCl treatment at low and high temperature in both HEK293T (**Fig. 2.11a**) and N2a cells (**Fig. 2.11b**). These results support the hypothesis that the KCl-responsive elements in exon 3a are G1 and G3. All in all, these cellular data firmly implicate that G1 and G3 can form temperature-dependent rG4 structure in cells to repress exon inclusion, possibly through masking splice sites or through interfering in spliceosome assembly.

2.6 G4 stabilizers significantly increase endogenous RBM3 expression at both mRNA and protein level at high temperature.

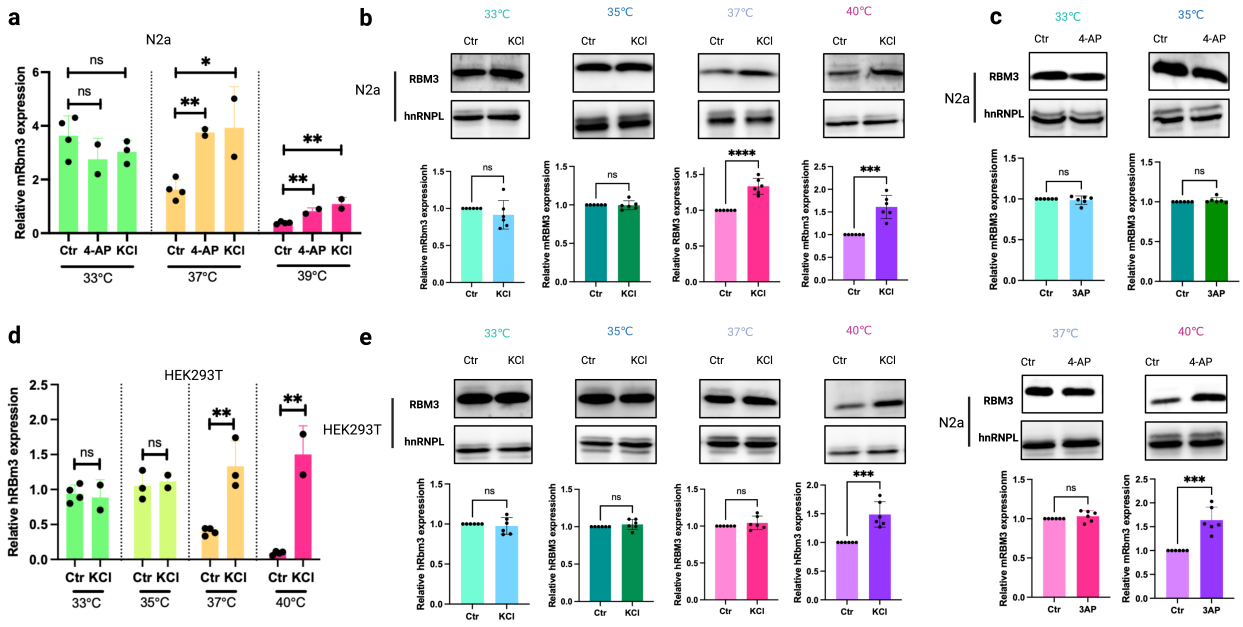

Figure 2.12 G4 stabilizers substantially increase endogenous RBM3 expression in both N2a and HEK293T cells at high temperature. a, b and c, KCl and 4-AP treatment increases endogenous RBM3 expression at high temperature, but not at low temperature in both RNA (**a**) and protein (**b** and **c**) levels in N2a cells. **d**, KCl treatment increases endogenous RBM3 expression at both RNA and protein level at high temperature, but not at low temperature in HEK293T cells. KCl (50 mM)

or 4-AP (0.3 mM) were added into cells, and then the cells were cultured at 33°C or 39°C for around 24hrs followed by WB. PSI: percentage of spliced in. Statistical significance was determined by unpaired t-test and is indicated by asterisks: p values: *p<0.05, **p<0.01, ***p<0.001 (mean ± SD). The other gel images used for quantification are in the **App. Fig. 15 (Fig 2.12b), App. Fig 18 (Fig. 2.12c)** and **App. Fig 12 (Fig. 2.12e)**

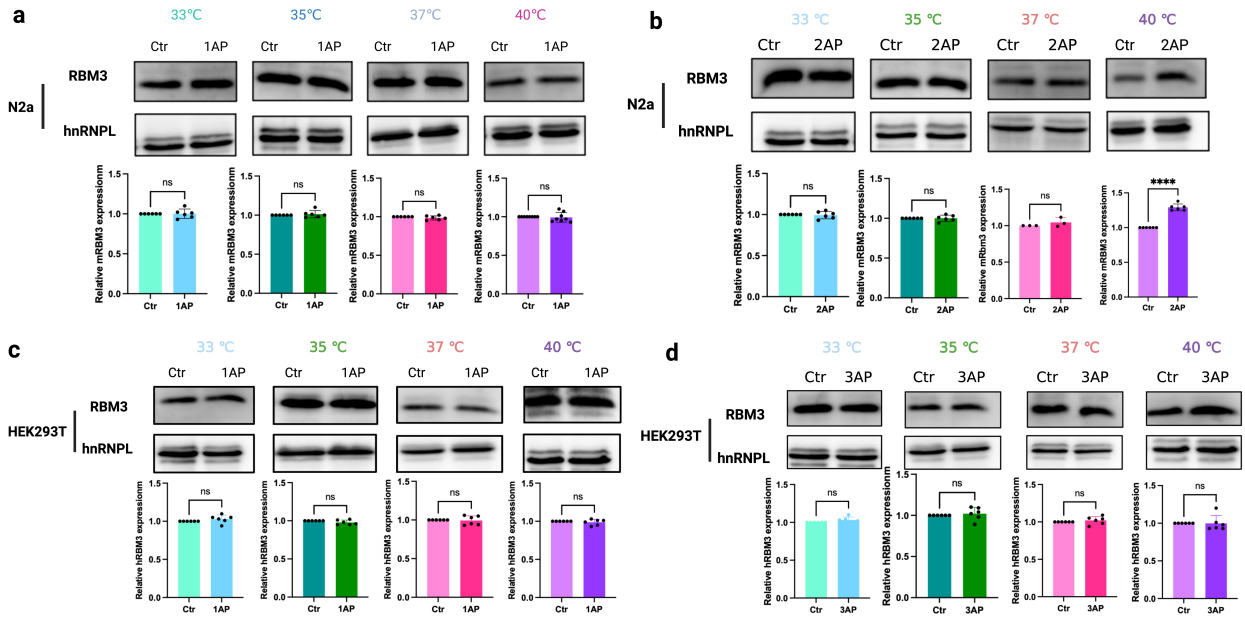

Figure 2.13 4-AP increases RBM3 expression in N2a cells in a dosage-dependent manner. **a** and **b**, 4-AP increases RBM3 expression in a dosage dependent manner at high temperature (40°C) in N2a cells. **c and d**, 4AP doesn't boost RBM3 expression in tested concentrations. For all the WB, the cells were treated with different concentrations of 4-AP at different temperature for around 30hrs. n>3. N2a were treated with 4-AP for 24hrs at different temperatures, followed by RT-qPCR. Statistical significance was determined by unpaired t-test and is indicated by asterisks: p values: *p<0.05, **p<0.01, ***p<0.001 (mean ± SD). 1AP means 0.1 mM of 4-AP treatment. 2AP indicates 2mM of 4-AP treatment. 3AP is the 3 mM of 4-AP treatment. The gel images for quantification are in the **App. Fig.13**, **App. Fig. 14**, **App. Fig. 16** and **App. Fig. 17**.

As exon 3a of RBM3 contains PTCs that trigger degradation of the transcript by NMD, inhibition of exon 3a inclusion increases RBM3 expression. Accordingly, stabilization of rG4s in exon 3a could increase RBM3 expression as it will repress exon 3a inclusion. Given that the toxicity of PDS to cells, we therefore checked whether artificially increasing intracellular potassium with KCl and 4-AP, a broad potassium voltage gated channel blocker, can increase RBM3 mRNA expression in living cells. RBM3 mRNA expression did not change at 33°C but is significantly enhanced at 37°C and 39°C with KCl or 4-AP treatment in N2a cells. Then, we

examined RBM3 protein expression with these two treatments. Indeed, KCl treatment could increase RBM3 protein expression at higher temperature (roughly 1.5 folds at 40°C in HEK293T cells, and around 1.25 fold at 37°C and 1.5 fold at 40°C in N2a cells), but not at low temperatures (33°C and 35°C) (**Fig. 2. 12a and b**). The differential response to KCl is possibly on account of differential stability of rG4s structure of mRBM3 (rG4 in N2a is less stable) or the distinct cell permeability of potassium (higher in N2a) in these two cell lines. Meanwhile, the 4-AP also could promote RBM3 expression at high temperature (40°C) to 1.5 times (**Fig. 2. 12a**), but not at low temperature. Importantly, the RBM3 enhancement caused by 4-AP in N2a is in a dosage-dependent manner, showing that 1 mM 4-AP had no effect on RBM3 expression (**Fig. 2. 13a and b**) and 2 mM 4-AP significantly enhanced RBM3 expression to 1.25-fold changes (**Fig. 2. 13a and b**). As a negative control that 4-AP cannot augment RBM3 expression in HEK293T cells in both low and high dosage of 4-AP treatment (**Fig. 2. 13b and c**) given that the potassium voltage gated channels are lacking in HEK293T cells. Taken together, this implicates that both low temperature and K^+ are capable of stabilizing G4s and shows again that at low temperature a further increase in intracellular potassium has no effect on exon 3a splicing and RBM3 expression.

Taken together, our results show that G-rich sequence around splice sites of RBM3 exon3a can form sufficiently stable rG4 structure to repress its inclusion at low temperature (33°C and 35°C), resulting in increased expression of RBM3 by escaping from NMD. Accordingly, rG4 may serve as physiological thermo-sensors to regulate alternative splicing, which we called spliceswitch, with impact on gene expression through modulating NMD.

2.7 Working model of RNA G-quadruplexes as evolutionally conserved physiological thermo-sensor via spliceswitch to modulate alternative splicing.

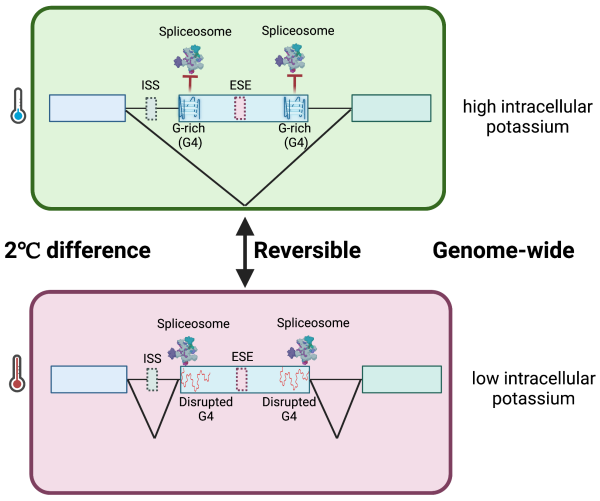

Figure 2.18 Working model of RNA G-quadruplexes as evolutionally conserved thermo-sensor modulating alternative splicing at a genome-wide scale. RNA G-quadruplexes serve as reversible temperature sensors synergistically and/or antagonistically modulating alternative splicing. At low temperature or high K^+, RNA G-quadruplexes surrounding 3'SS and 5'SS are stable enough and can sterically mask the splice sites. In this scenario, spliceosome complex, such as U1snRNP, the splicing factor U2AF[35], cannot be assembled on the pre-mRNA and thereby these splice sites aren't accessible, resulting in the skipping of the exon; At high temperature or low K^+, RNA G-quadruplexes are disrupted or not stable enough, leading to the exposure of splice sites to the spliceosome, and the exons containing RNA G-quadruplexes are efficiently spliced.

2.8 Discussion

Substantial studies have shown that alternative splicing is one of the most essential cellular events in gene regulation to accomplish the complex of transcriptome in mammalian cells. In most of the cases, dynamic modulation of alternative splicing is achieved via interplays between *trans*-acting factors and pre-mRNA sequences near or at splice sites. It has been shown that temperature alternation, as one of the crucial environmental factors, influences the choice of splice sites through changing the conformation or activity of *trans*-acting factors, eg. CLK1/4. Here, the spliceswitch we discovered, breaks the mechanistic mode as RNA can directly respond to temperature perturbations through the altered formation of rG4 structures in the vicinity of splice sites of cassette exons in mammalian cells, without the direct involvement of *trans*-acting proteins in mammalian cells.

RNA secondary structures function importantly in mammals since the second layer of genetic information is embedded in the RNA molecules in the form of differential structures[382]. The PARS (parallel analysis of RNA structure), a method with deep sequencing the *in vitro* RNA with structure specific enzymes to profile the RNA secondary structure, determined 1907 RNA structural change events caused by single nucleotide variants from 20,000 SNPs in a human family trio (mother, father, and their child), which is referred as riboSNitches. Furthermore, it showed that the riboSNitches influence genome-wide gene regulation[69]. In addition to riboSNitches, "m6A-switch", a PolyU elements in the stem region of RNA secondary structure, can regulate alternative splicing by modulating adenine methylation to control the accessibility of the elements for hnRNPC binding[74]. The spliceswitch, we reported, here revealed an unexpected mechanism to directly couple temperature perturbation with changes in RNA secondary structure, which causes differences in RNA processing and gene expression. Our

data showed that around 10-20% (G4 motif calculation) or 30% (G4-hunter prediction with G4 score>1) of exons that are repressed upon cold shock within physiological temperature ranges, contains putative rG4 motifs on sequence around their splice sites, suggesting a widespread effect of rG4 as thermo-sensor to confer spliceswitch in mammalian, including human cells.

The rG4 near splice sites may bind to a variety of RNA binding proteins to repress splicing upon cold shock. Although many *trans*-acting factors have consensus binding motifs from the *in vitro* SELEX enrichment or in cell profiling (such as iCLIP, PAR-CLIP *etc.*), not all enriched *cis* elements are associated with the respective *trans*-factors. Additionally, these high-throughput methods also give us some degenerate RBP binding motifs. The evidence indicate that the *cis* elements are necessary but are not sufficient for the *trans*-acting factor binding in some cases, and RNA secondary structure formed by *cis*-element sequence may contribute to the binding. Here, rG4 in the vicinity of splice sites, as a typical RNA secondary structure, might temperature-sensitively associate with their RBP binding, that at low temperature rG4 structure is stable to ensure the efficient binding of its corresponding binding protein to repress splicing, and at high temperature rG4 is less stable and dissolved so that its binding protein less productively associates with it. Recently, hnRNPH1 was identified to associated with G-rich motif near splice sites, showing high activity at low temperature and less active at high temperature to regulate alternative splicing with unknown mechanism. Here, we proposed that it is likely that at low temperature, the stable rG4s near splice sites of RBM3 exon 3a enable hnRNPH1 binding and at high temperature rG4s are less structured, leading to its less association with hnRNPH1.

We observed that repressive effects of G4 stabilizer on exon inclusion are distinct across different rG4 elements. For instance, PDS can almost fully block the splicing of CREs from EIF4G1 (**Fig. 2.4b**) and RBM3 minigenes (**Fig. 2.6b** and **2.6c**), but inclusion of CREs from CDK4 and FKBP15 (**Fig. 2.4d** and **2f**) were only partially impeded by the same concentration of PDS. It has been reported that PDS has different effects on different rG4s, but the molecular basis is unclear[383]. One possibility is that rG4s are not naked, and may associate with other trans-acting factors to repress alternative splicing of CREs. If these trans-acting factor are distinct for different CREs, they may respond differentially to G4 stabilizers.

Individually, some papers have experimentally demonstrated that G4 is involved in splicing regulation in different ways, such as repressing 5' splice sites through recruiting hnRNP H[175,176], enhancing splicing to impede intron retention[177,178], promoting exon inclusion through

interacting with hnRNP F[179]. In a genome-wide scale, however, until recently just one paper claimed that G4s are enriched near splice sites to promote exon inclusion possibly through binding to some RBPs in mammalian cells from the high-throughput DNA G4-seq[174]. Here, we first time show in physiological temperature range from 33°C to 40°C cold-repressed exons (CREs) occupy more G4 structures at the positions in proximity to splice sites and in the exons in a genome-wide scale. Importantly, the inclusion of these G4-dependent CREs is independent on the phosphorylation change of SR caused by different temperatures as G4s are also enriched in CREs in TG003 treated group and the percentage of G4 near splice sites is higher in TG003-independent CREs than that in TG003-dependent CREs, which indicate that G4s should be another novel mechanism to control temperature-sensitive alternative splicing. We proposed that at low temperature, G4s are stable enough to mask the splice sites, which leads exon exclusion; at high temperature, G4s are disrupted or less stable to expose the splice sites, thereby resulting in exon inclusion. The exchange of stable and less-stable status of G4s in response to temperature is reversible *in vitro*, and the sensitivity is high to 2°C difference in our hands. One of the reasons that people didn't pay attention to temperature sensitivity of G4s is possibly due to their high melting temperatures over physiological temperatures *in vitro* caused by the high concentration of KCl in the buffer stabilizing G4s in the melting curve experiments. In our case, G4s just show temperature sensitivity at low KCl condition. This can be explained as G4s are too stable at high KCl condition, so the temperature cannot alter its stability. Physiologically, the situation is more complex on the grounds that large amounts of stabilizer (K^+) and numerous unwinding helicases in cells. *In vivo*, it has been reported that genome-wide distributed G4s tend to unfold[151] at normal temperature, implicating that G4s are not stable enough in cellular contexts. Taken together, G4 may be less stable *in vivo* compared to *in vitro*, and this contributes to the temperature sensitivity of G4 in the physiological temperature range.

Furthermore, we ask why the G4s we discovered repress exon inclusion, while the Ilias Georgakopoulos-Soares *et al.* clearly claimed that G4s promoted exon inclusion. We noticed that the distance of G4s to splice sites may be the main contributor to this difference. They bioinformatically analyzed the whole genome sequence, that is 100nt window on both 5'SS and 3'SS, and we just focused on the 50nt motifs in proximity to splice sites. It is reasonable to assume that rG4s can easier mask the splice site the closer they are. Indeed, we individually checked the published validated rG4s controlling alternative splicing, and found that those rG4s potentially acted as enhancers are far away from splice sites, whereas those functioned as

repressors are closer to splice sites as summarized here: Enhancer: CD44[179] (84 nt to 5'SS); PAX 9[177] (821 nt to 5'SS); NAV2[174] (77 nt to 5'SS); SLC6A17[174] (50 nt to 5'SS); Repressor: BACE[33] (10 nt to 5'SS); EWSR1[176] (15 nt to 5'SS). Additionally, we find that in Georgakopoulos-Soares's paper, they also showed PSI obviously decreased after KCl treatment in a group of exons containing G4s, indicating these G4s potentially inhibit splicing although we cannot exclude that other mechanisms may contribute to the PSI change in the polarized neurons. However, at least the increased RBM3 mRNA after KCl treatment is not caused by the increasing of intracellular calcium, which is a well-known result in the depolarized cells with KCl treatment[384] because a calcium ionophore inhibits RBM3 expression at both 37°C and 32°C, indicating that increasing intracellular Ca^{2+} will attenuate RBM3 expression[244]. It has been reported that KCl depolarization can cause genome-wide spicing changes with increased exon inclusion or exclusion, but no one can comprehensively systematically explain the reasons[385]. Here, our model can comprehensively clarify how G4s function to modulate alternative splicing in different settings.

As physiological thermo-sensors, rG4s may contribute to the generation of tissue-specific alternative splicing pattern and differential gene expression in different tissues. Even though our core body temperature is normally relatively stable, some certain organs maintain differential temperatures. For instance, skin and testis have lower temperature in general. In testis, lower temperature makes G4s more stable to mask the splice sites, and thereby generates testis-specific splicing pattern. Deep body temperature in mammals is also not uniform even in a particular organ, and gradient temperatures in the reproductive tract have been determined in several mammals including humans[363,364,386-391]. Thus, temperature may intricately and developmentally modulate whole transcriptome, and the CREs could be also coupled with poison exons to developmentally degrade transcripts to physiologically regulate gene expression. As "poison" exons naturally widespread occur in the transcripts, revealing that 35% of alternative spliced exons and 23% of all isoforms contain poison exons[392-394]. For example, unproductive splicing of SR protein genes is associated with ultra-conserved DNA elements, which are called "poison exon", in different mammals. Once the SR transcripts are included with "poison exons", they will be degraded via NMD by virtue of the presence of PTCs in the "poison exons"[359]. We can speculate that temperature will influence gene expression through the alternation of G4 stability as some of the CREs are related to "poison exons"[237]. In the case of RBM3, the CRE exon 3a is indeed coupled to NMD, thereby influencing RBM3 expression.

If the CREs are coupled with “poison” exons, high temperature will promote the degradation of mRNA via NMD. This is possibly a cellular self-protection mechanism at moderate cold shock, that less transcripts are in a queue to wait for energy consuming translation. Indeed, embryos cultured at low temperature (35.5°C) showed slow “cleaving” embryos, poor-quality of blastocysts and even a higher expression of the apoptotic gene[395].

Pathologically, when the body temperature accidentally goes down to below 35°C, G4s are globally stabilized, thereby repressing exon inclusion, which will dysregulate alternative splicing networks. It is known that the accidental hypothermia is associated with significant morbidity and mortality[367,368] due to the influence in cardiovascular, hematology, neuromuscular, respiratory, renal and metabolic, gastrointestinal aspects[369]. The broad exon skipping caused by rG4 spliceswitch in the transcriptome may contribute to one of the pathological molecular mechanisms in the hypothermia.

2.9 Limitation of the work

How the temperature-sensitive rG4s repress splicing need to be teased out in the future. For instance, are they naked or associated with other proteins to influence splicing? If they are associated with proteins, what are these proteins? Do all the rG4s near the splice sites bind to the similar or same groups of proteins? Furthermore, *in vivo* RNA G4-seq in the different mammalian samples treated with different temperatures should be performed to directly check the rG4 signal at differential temperatures.

2.10 Future plans

It has been known that rG4s are enriched at R loop, 5’UTR and 3’UTR in mammalian cells, so it is reasonably speculated that the regulation of rG4s in these regions is also possibly temperature sensitive. Various temperature will influence the stability of R loop, and thereby it will result in temperature sensitive transcription in mammalian cells. For 5’UTR, at low temperature, G4s are more stable to sterically block the translation initiation complex to slow down or inhibit translation, which actually has been observed in microorganism[190]. For the 3’UTR, G4 enriched at downstream of 3’ polyadenylation site may also physically terminate transcription at low temperature, and the hindrance effect reduces at high temperature. Taken together, the thermo-stability of rG4 in mammals may regulate gene expression in several other layers, not only just in the alternative splicing. Further work also need to answer whether the other rG4s involved in the other layers of gene regulation, such as translation, and alternative

polyadenylation are temperature sensitive or not. Additionally, whether the thermo-sensor G4 plays a role in the setting that ambient temperature influencing sex determination in turtles needs to be further investigated[396].

3 A coordinated *cis*-regulatory network modulates the temperature-sensitive poison exon 3a inclusion of RBM3.

It has been shown that splice site selection must be intricately modulated at different molecular layers in cells. In myriads of studies have reconciled that, except for the loose consensus of 5'SS, 3'SS, branch point, polypyrimidine tract and their corresponding core splice factors (U1 to U6), the fine-tuning alternative splicing is highly dependent on the auxiliary factors, such as *cis*-regulatory element and its *trans*-acting binding factor, RNA secondary structure. These factors together contribute to the complex of transcriptome repertoire to further produce complicated proteome.

Temperature alternations are one of the crucial environmental factors. At the molecular level, alternative splicing, as an essential mechanism of gene regulation at the RNA level, has been shown to be one of the essential cellular events in response to temperature change. Conceivably, temperature remodels alternative splicing through acting on the factors, which influence the molecular processing of alternative splicing. However, it remains elusive how the activity of *cis*-regulatory element network responds to temperature change, thereby to achieve the temperature sensitive alternative splicing.

3.1 Systematic screening of *cis*-regulatory elements regulating alternative splicing of RBM3 exon 3a via CRISPR-dCasRx gRNA perturbation

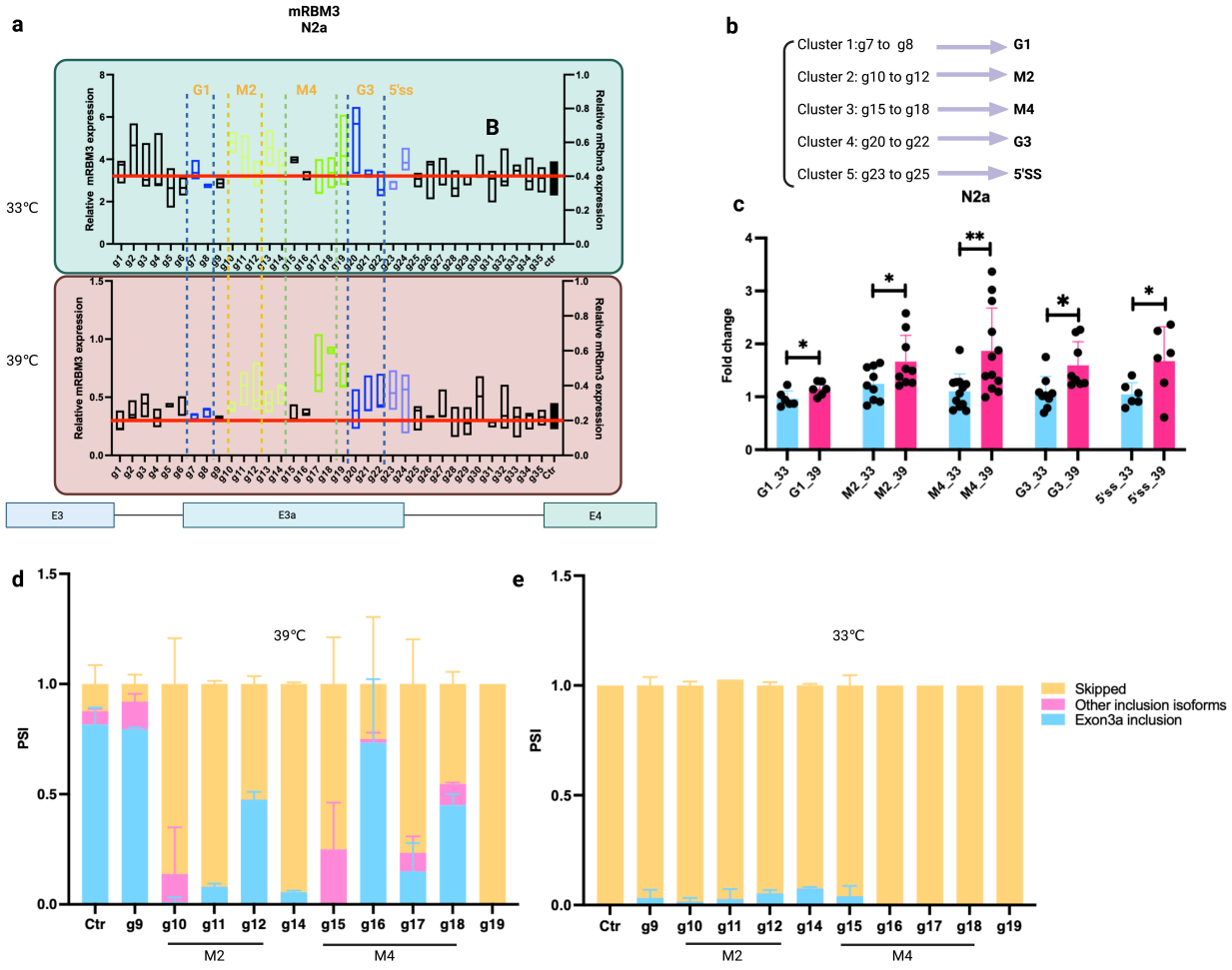

Figure 3.1 Systematic screening of *cis*-regulatory elements regulating alternative splicing of exon 3a of RBM3 via CRISPR-dCasRx gRNA perturbation in N2a cells. a, gRNA perturbation assay shows several clusters potentially enhancing endogenous RBM3 expression in N2a cells. **b and c**, Classification of different cluster gRNAs. **c**, Fold changes of gRNA clusters are higher at high temperature. **d and e**, gRNA cluster 2 and cluster 4 can efficiently decrease exon 3a inclusion at high temperature in N2a, but not in low temperature. Multiple gRNAs targeting the mRBM3 Exon 3a and its flanking region were individually co-transfected into N2a and HEK293T cells with dCasRx plasmid at both 33°C and 39°C for 2 days, followed by RT-qPCR. PSI: percentage of spliced in. All the gRNA cloning information in the methods and materials. Statistical significance was determined by unpaired t-test and is indicated by asterisks: unpaired t-test derived p-value *p<0.01, **p<0.01, ***p<0.001. The gel images for quantification are in the **App. Fig. 19**.

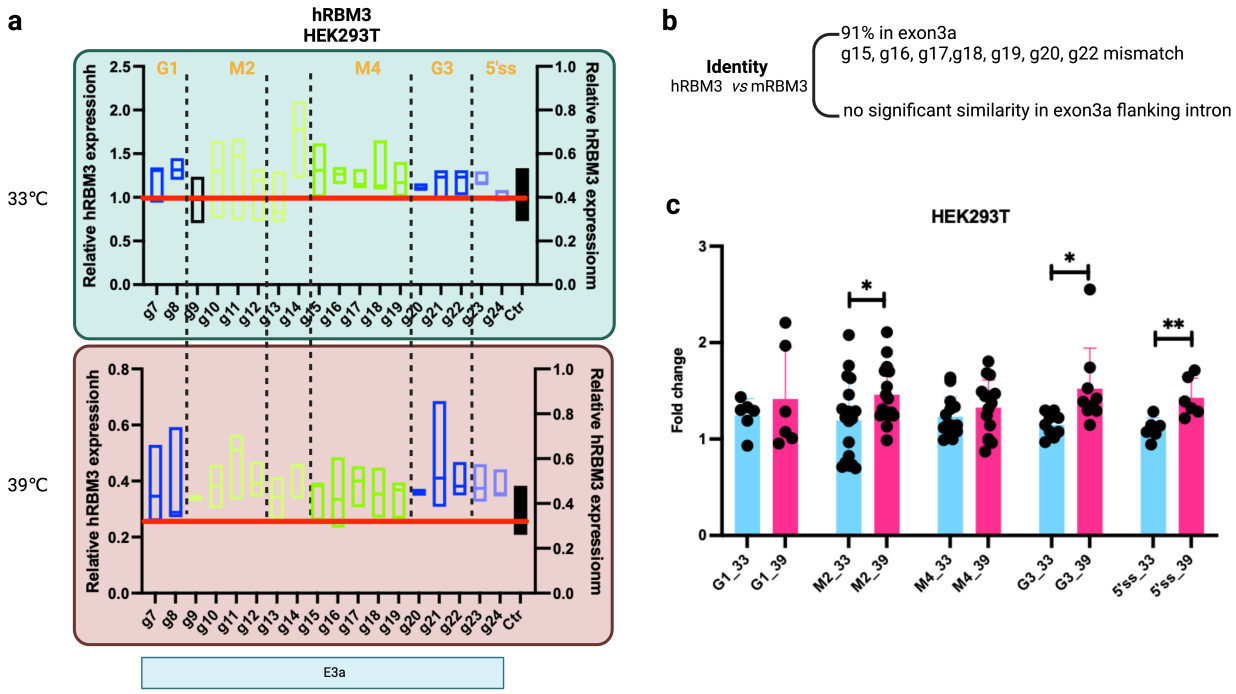

Figure 3.2 Systematic screening of *cis*-regulatory elements regulating alternative splicing of exon 3a of RBM3 via CRISPR-dCasRx gRNA perturbation in HEK293T. a, gRNA perturbation shows several clusters potentially enhancing RBM3 expression in HEK293T cells. **b**, Identity of exon 3a and its flanking region between hRBM3 and mRBM3.**c**, The fold change of endogenous RBM3 caused by M2, G3 and 5'SS gRNAs is higher at high temperature in comparison with low temperature. gRNAs targeting the hRBM3 Exon 3a and its flanking region were individually co-transfected into N2a and HEK293T cells with dCasRx plasmid at both 33°C and 39°C for 2 days, followed by RT-qPCR PSI: percentage of spliced in. Statistical significance was determined by unpaired t-test and is indicated by asterisks: unpaired t-test derived p-value *p<0.01, **p<0.01, ***p<0.001.

We previously identified a non-annotated poison exon, exon 3a, which is highly included at normal and high temperature, and majorly exclusive at low temperature, in RBM3, a well-known cold-induced protein with neuroprotective function. Exon 3a contains several premature stop codons, which lead to the non-sense mediated decay (NMD) of RBM3 mRNA transcripts, and thereby facilitating exon 3a skipping will enhance endogenous RBM3 expression. Meanwhile, two strong ESE elements (in the 1st section) and RNA G-quadruplex elements nearby the 5'SS and 3'SS (in the 2nd section) were successfully identified in the exon 3a. We here asked whether there exist other cis-regulatory elements contributing to the temperature sensitivity of exon 3a alternative splicing in the flanking intron, and how these cis-regulatory elements coordinate to accomplish this temperature sensitive alternative splicing event.

RNA-targeting type VI-D CRISPR effectors, known as Cas13, have been utilized to efficiently and specifically recognize single-stranded RNA to reprogram transcriptome[397-401]. CRISPR-Cas13 complex requires a minimum 22 nucleotide spacer, which is complementary to the target RNA, in guide RNA (gRNA), and is intolerant to mismatches, especially in the central complementary region. These characteristics make a modified dCasRx, which lacks cleavage activity but remains its targeting activity to RNA, as a robust and sensitive tool to target the *cis*-regulatory elements, which potentially modulate alternative splicing through the recruitment of *trans*-acting factors[397]. Therefore, the dCasRx complex can compete with the *trans*-acting factors to manipulate alternative splicing.

To systematically discover the potential enhancer and repressor regulating the alternative splicing of RBM3 exon 3a, we designed a series of 22-nt gRNA targeting exon 3a and its flanking intronic region based on the mouse RBM3 gene. The gRNA perturbation assay clearly shows that 5 clusters, G1, M2, M4, G3 and 5'SS, can enhance endogenous RBM3 expression in two cell types (**Fig. 3.1** and **3.2**). Interestingly, in comparison with control, the fold changes that gRNA cluster caused at high temperature is significantly higher than that at low temperature in N2a (**Fig. 3.1)**. Since the exonic region of RBM3 exon 3a has 91% identity with mouse RBM3, showing the M4 region bears several mismatches while the flanking intronic region has no significant similarity, just gRNAs targeting exon 3a were examined in HEK293T cells. The result shows that gRNAs targeting M2, G3 and 5'SS can enhance RBM3 expression more effectively at high temperature than that at low temperature, whereas M4 presents no difference and 3'SS shows similar fold change at both temperatures. The high mismatch in M4 region between humans and mice may result in no significant difference at both temperatures as the binding of gRNAs to mRNA is disrupted by the intolerance to mismatch at both temperatures. No significant difference at different temperatures in G1 region is possibly caused by the transfection efficiency because the increasing trend was still observed at high temperature.

As we have demonstrated that G1 and G3 are potential G4 repressive elements, which can form stable RNA secondary structure (G4) at lower temperature in the 2nd section of the thesis, and thus gRNAs targeting G1 and G3 region are less accessible. At high temperature, the G4s are disrupted, and the gRNAs have more access to target the G3 region to block the spliceosome assembly, which thereby inhibits RBM3 exon 3a inclusion and further enhances endogenous RBM3 expression. For the M2 and M4, these data strongly indicate that M2 and M4 *cis*-

regulatory elements present higher enhancing activity at higher temperature than lower temperature. Even the gRNAs against 5'splice sites show stronger effect at high temperature, suggesting that 5'splice sites are less accessible at low temperature. Taken together, the dCasRx gRNA perturbation assay implicated that both splice sites, M2 and M4 are easier to be recognized or show higher activity at high temperature.

To further demonstrate that the change of endogenous RBM3 expression is correlated to the alternation of RBM3 exon 3a inclusion, we also transfected mRBM3 minigenes with gRNAs and dCasRx plasmids together in N2a cells to check the PSI of exon 3a because the exon 3a is coupled to the NMD, thereby leading to the degradation of endogenous transcripts, and thus the endogenous transcripts containing exon 3a are difficult to be detected. The gRNAs targeting M2 (g10 to g12) and M4 (g15 to g18) region indeed can reduce the inclusion of RBM3 exon 3a (**Fig. 3.1d** and **e**).

Furthermore, we also observed that some of the gRNAs targeting the intron region also influenced the endogenous RBM3 expression. However, it is noticed that the signal is not clustered, instead that individual gRNA shows distinct effects on the RBM3 expression (**Fig. 3.1a**). It can be explained with several reasons, such as spatially in proximity of two *cis*-regulatory elements bearing distinct effects on modulating alternative splicing, the low binding affinity of gRNAs to the intronic region or the limited accessibility of gRNAs to secondary RNA structure in introns.

3.2 Mapping intronic *cis*-regulatory elements of RBM3 exon 3a via mutagenesis.

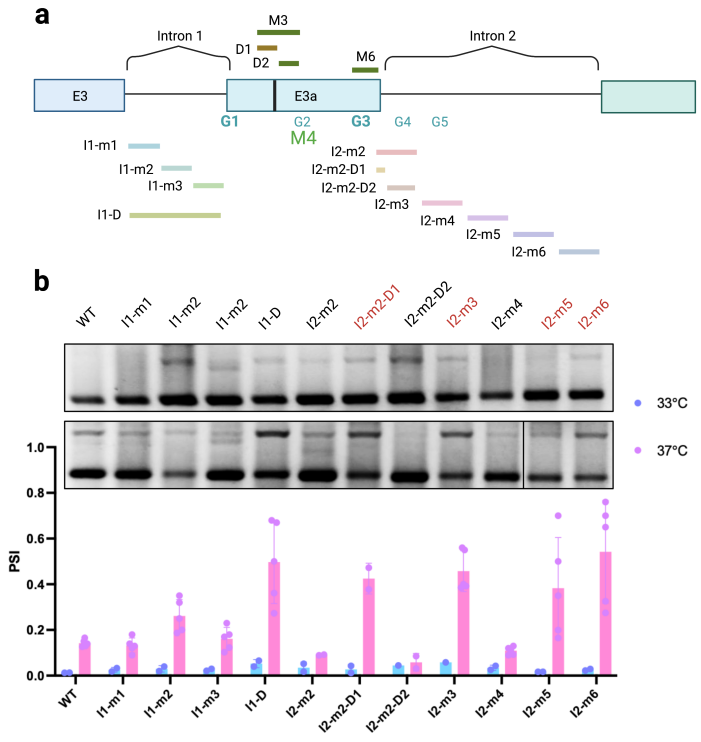

Figure 3.3 Fine-tuning mapping of *cis*-regulatory elements of RBM3 exon 3a via mutagenesis. **a**, Schematic of different mutants of mRBM3 minigene. **b**, Multiple intronic *cis*-regulatory element mutants change exon 3a inclusion. Upper panel is gel image of the RT-PCR result, and quantification data is in the lower panel. Plasmids were transfected into HEK293T cells, and then incubated at 37°C overnight. All the cells were shifted into incubator at 33°C or 37°C to culture for another 24hrs, and then subject to RT-PCR. PSI: percentage of spliced in. All the cloning information in the methods and materials. The gel images for quantification are in the **App. Fig. 20**.

To further dissect the intronic *cis*-regulatory elements involved in the regulation of RBM3 exon 3a inclusion, we next performed mutagenesis in the intronic region to identify the ISE or ISS (**Fig. 3.3a**). Mutagenesis assay shows that at low temperature many of mutants in intron and exon in vicinity to intron have slight influence in the inclusion of RBM3 exon 3a, whereas at high temperature I2-m2-D1, I2-m3 and I2-m6 significantly increase RBM3 exon 3a inclusion. Meanwhile, I2-m2-D2 and I2-m4 mutants are potential ISEs to enhance RBM3 exon 3a inclusion at high temperature (**Fig. 3.3b** and **c**). I2-m3 and I2-m4 are spatially close to each other, suggesting that the proximity of two distinct *cis*-regulatory elements may result in less efficiency in the dCasRx gRNA perturbation assay. Among these mutants, I2-m6 is in proximity to the 3'SS of exon 4, and thus it may influence the 3'SS strength. Further, we noticed that the repressor element I2-

m2-D1 is closed to G3 element, double mutations (M6) of I2-m2-D1 and G3 can significantly enhance RBM3 inclusion to 100% at even 33 ℃ in both N2a and HEK293T cells (**Fig. 3.4d**), indicating that I2-m2-D1 and G3 synergistically function to repress exon 3a inclusion. Importantly, I2-m2-D1, I2-m2-D2 and I2-m4 are evolutionally conserved across different species, which suggest their importance to manipulate RBM3 exon 3a inclusion (**Fig. 3.4c** and **d**).

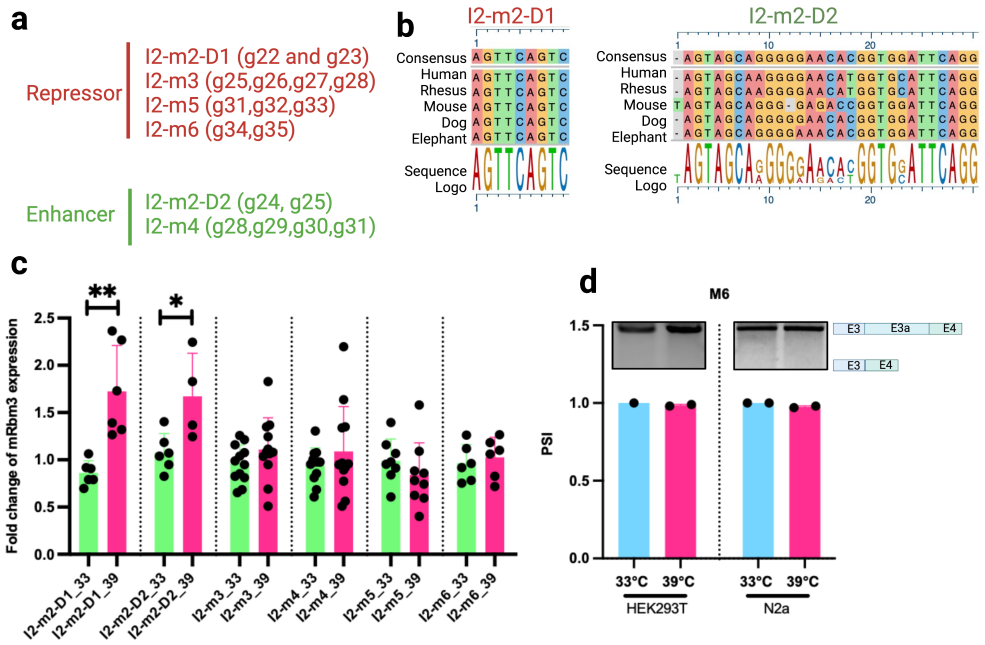

Figure 3.4 Temperature sensitive and evolutionally conserved *cis*-regulatory elements. a, gRNA cluster summary of potential repressor and enhancer. **b**, Evolutional conservation of intronic I2-m2-D1 and I2-m2-D2, **c**, Fold change of mRBM3 expression caused by gRNA cluster of I2-m2-D1 and I2-m2-D2 is higher at high temperature than that at low temperature in N2a cells. **d**, M6 mutant increases exon 3a inclusion in both HEK293T and N2a cells at 33°C. The gel images for quantification are in the **App. Fig. 21.b**.

In accordance with the result of mutagenesis assay, we also artificially grouped the gRNA targeting intron region to different clusters even though in the CRISPR-dCasRx perturbation assay no obvious clusters were observed, referring to the position of gRNA targeting (**Fig. 3.1a** and **Fig. 3.4a**). The fold change caused by I2-m2-D1 and I2-m2-D2 gRNA is higher at high temperature than that at low temperature. This is due to higher accessibility of 5'SS at high temperature demonstrated in the G4 story. Although I2-m2-D1 has been identified as a potential repressor via mutagenesis, gRNA targeting I2-m2-D1 also can influence the recognition of 5'SS because it is spatially close to 5'SS. The higher expression caused by gRNAs targeting I2-m2-D2 is due to the blockage of enhancer *trans*-acting factor by dCasRx

and/or the influence of spliceosome assembly at 5'SS. These data indicate that the interpretation of dCasRx perturbation should be integrated with mutagenesis assay together. I2-m2-D1 and I2-m2-D2 are temperature sensitive cis-regulatory element to control the inclusion of RBM3 exon 3a.

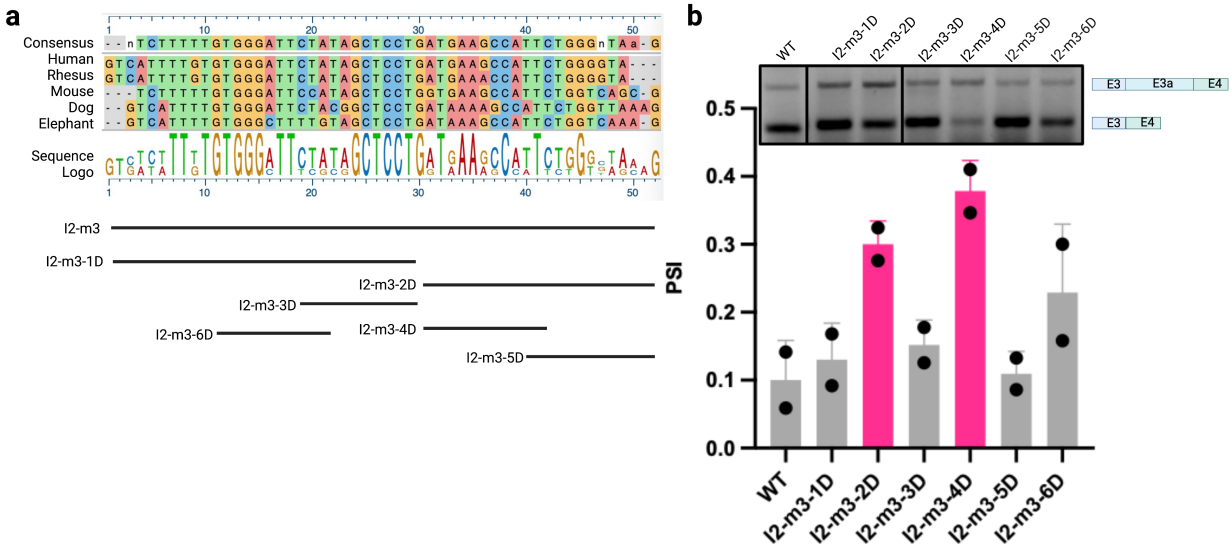

Fig 3.5 I2-m3 is an effective repressor of RBM3 exon 3a inclusion. a, Sequence alignment of I2-m3 and schematic of mutation in I2-m3. **b**, I2-m3-3D and I2-m3-5D enhance exon 3a inclusion at 37°C in HEK293T cells. Both WT and mutant plasmids were transfected into cells at 37 °C overnight, and then continue to culture for another 24hrs, followed by RT-PCR and agarose gel resolving. n=2. PSI: percentage of spliced in. All the cloning info in the methods and materials. The gel images for quantification are in the **App. Fig. 21a**.

As I2-m3 is a potent repressor, we decided to identify the core elements in the motif via mutagenesis. Obviously, the I2-m3-3D and I2-m3-5D significantly enhance RBM3 inclusion (**Fig. 3.5b**). More interestingly, the I2-m3-3D and I2-m3-5D sequence is conserved between humans and mice, which implicates that they are evolutionally essential for RBM3 exon 3a inclusion.

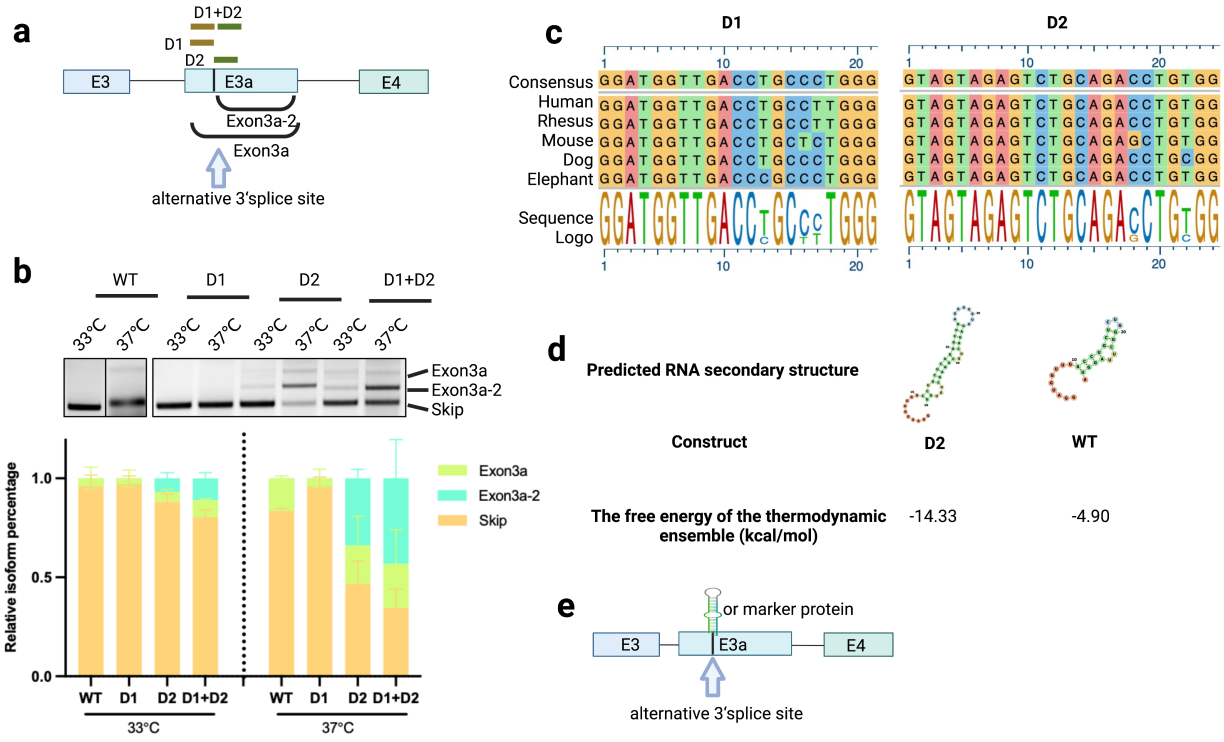

Figure 3.6 D2 mutant masks an alternative 3'SS in the exonic region of exon 3a. a, Schematic of D1, D2 and D1+D2 mutant position and exon 3a and exon 3a-2 isoform. **b**, D2 mutant significantly increases the usage of alternative splice site in the exon 3a. Upper panel is the image gel of RT-PCR result, and lower panel is the quantification result. **c**, D1 and D2 are evolutionally conserved cross different species. **d**, D2 mutant makes the predicted RNA secondary structure less stable. **e**, Proposed model how D2 masks the alternative 3'SS in exon 3a. Both WT and mutant plasmids were transfected into cells at 37°C overnight, and then the cells were shifted into the incubators with different temperatures to culture for around 24hrs, followed by RT-PCR and agarose gel resolving. n>3. PSI: percentage of spliced in. All the cloning info in the methods and materials. The gel images for quantification are in the **App. Fig. 21c**.

We observed that a potential alternative splice site is in the exon 3a of RBM3 (M3 mutant) in the 1st section, and thus we deleted the surrounding sequence of the alternative splice site to generate D1 and D2 mutant. Apparently, the D2 deletion can significantly increase the usage of the alternative splice site at both 33°C and 37°C, while D1 shows slightly enhancer activity at both low and high temperatures (**Fig. 3.6b**). Evolutionally, D1 and D2 are conserved from humans to elephants (**Fig. 3.6c**), illuminating their importance in the regulation of alternative 3'SS utilization. All the evidence together implicate that D2 element can impede the usage of alternative splice site especially at high temperature as deletion of D2 enhance the percentage of Exon3a-2 isoform. RNA secondary structure prediction shows the sequence surrounding the alternative splice sites can potentially form RNA secondary structure, and D2 deletion can significantly increase the ensemble

free energy, indicating that D2 deletion potentially causes the RNA secondary structure less stable. This is one of the possible reasons that D2 deletion increases the utilization of alternative splice site. Another reason is that D2 can specifically recruit one "masker protein", thereby masking the alternative splice sites (**Fig. 3.6e**).

3.3 RNA G-quadruplexes, G1 and G3, cooperate with other *cis*-regulatory elements to regulate RBM3 exon 3a inclusion.

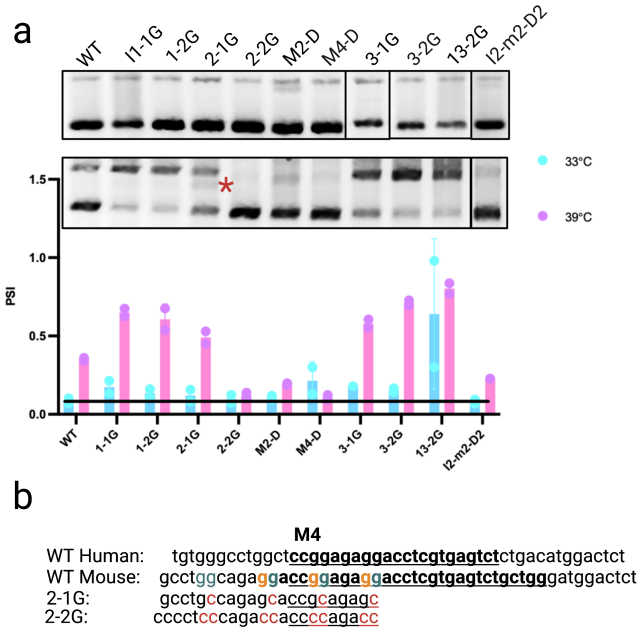

Figure 3.7 Point mutation of M4 can effectively abolish its enhancer activity. a, 2-2G abolishes exon 3a inclusion at 39°C. Upper panel is the image gel of RT-PCR result, and lower panel is the quantification result **b**, Two Gs are essential to maintain the enhancer activity of M4. Both WT and mutant plasmids were transfected into cells at 37°C overnight, and then the cells were shift into the incubators with different temperatures to culture for around 24hrs, followed by RT-PCR and agarose gel resolving. PSI: percentage of spliced in. n=3. The gel images for quantification are in the **App. Fig. 21d**.

Next, considering the G4 and exonic mutants together, we noticed that 2-2G abolishes the exon 3a inclusion, while 2-1G almost presents no inhibitory effect (**Fig. 3.7**). Aligning the sequence of humans and mice, we found that these two Gs were essential to main the enhancer activity of M4 in the conserved **G**GAGA**G**GA sequence. Another interesting finding is that that 2-1G mutant can promote the usage of alternative splice site in the exon 3a (the band is marked by red star in the **Fig. 3.7a**). As 2-1G is in proximity to the alternative splice site, it is conceivable that the *trans*-acting factor of M4 can not only enhance the inclusion of RBM3 exon 3a, but also sterically mask

the internal (alternative) splice site of exon 3a as 2-1G mutant decreases the binding affinity of *trans*-acting factor to the *cis*-regulatory elements. 2-2G fully disrupts the recruitment of M4 *trans*-acting factor, resulting in the decreased exon 3a inclusion possibly due to the less efficient spliceosome assembly at splice sites for RBM3 exon 3a inclusion (**Fig. 3.7**). Taken together, as an ESE, the M4 may not only enhance 5'SS of exon 3a usage on account of its short distance to 5'SS, but also block the alternative 3'SS of exon 3a through steric hindrance to inhibit the recruitment of U1snRNP. This evidence supports that there exists a "masker protein" to repress alternative splice site usage of RBM3 exon 3a.

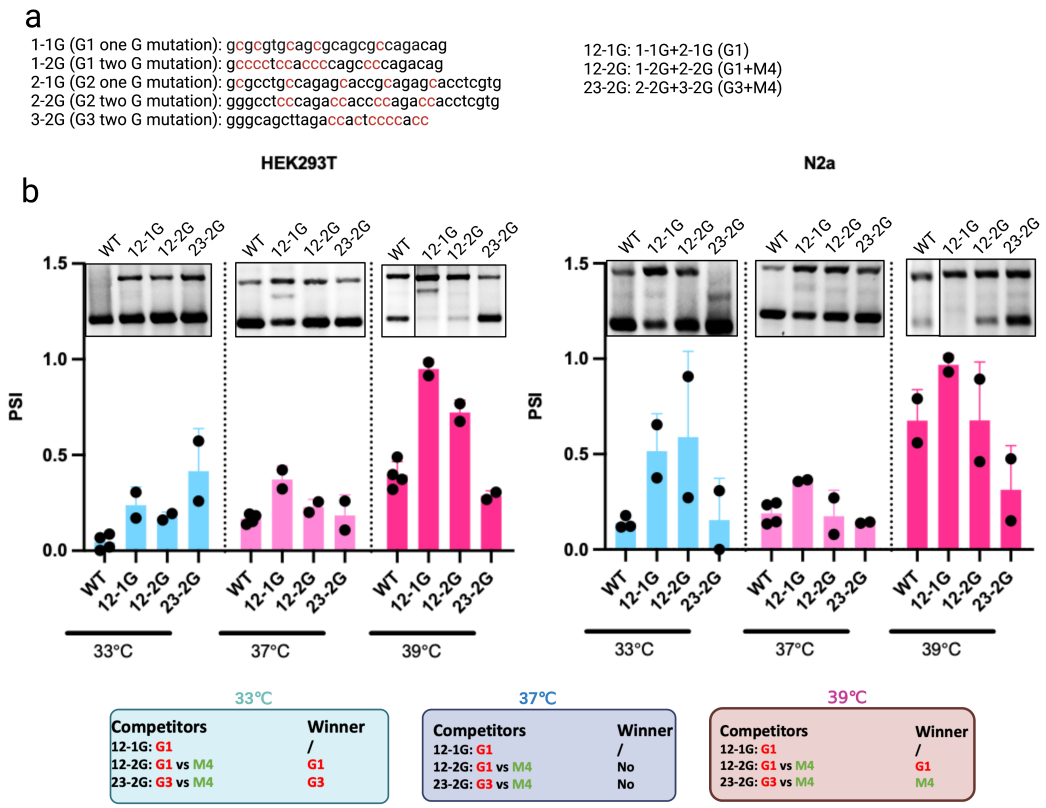

Figure 3.8 M4 coordinates with G1 and G3 elements to modulate alternative splicing of RBM3 exon 3a. a, Sequence of different mutants. **b**, G1 and G3 is dominant at 33 °C, and M4 is more active at high temperature. At 37 °C, repressive activity of G1, G3 and enhancing activity is similar. Upper panel is the gel image of RT-PCR result, middle is the quantification result, and lower panel is the summary result of G1, G3 and M4 competition. Both WT and mutant plasmids were transfected into cells at 37°C overnight, and then the cells were shifted into the incubators with different temperatures to culture for around 24hrs, followed by RT-PCR and agarose gel resolving. n>3. PSI: percentage of spliced in. The gel images for quantification are in the **App. Fig. 22**.

Since several enhancer and repressor *cis*-regulatory elements have been identified to be involved in the modulation of RBM3 exon 3a alternative splicing, we asked how these *cis*-regulatory elements cooperate each other. We next focused on the M4, G1 and G3, considering their strong activities to regulate the exon 3a inclusion. To simplify the model, we ignored the M2 here as mutation of anyone of M2 and M4 abolishes their enhancer activity shown in the 1st section of the thesis. Double mutants (12-2G: G1+M4 and 23-2G:G3+M4) were cloned to observe which *cis*-regulatory element is dominant to modulate exon3a inclusion at different temperatures. The results show that at 33°C G1 and G3 were always dominant as the PSI of exon 3a is higher in both 12-2G and 23-2G mutants than WT (**Fig. 3.8b**). At 37°C, the double mutants have the similar PSI of exon 3a to WT, indicating that the repressive activity of G1 or G3 and enhancer activity of M4 is identical at 37°C. Apparently, 12-2G still shows repressive activity in comparison with WT at 39°C, indicating that the inhibitory activity of G1 is still stronger than the boosting effect of M4 on exon 3a inclusion. Interestingly, the 23-2G mutant presents the enhancer activity at 39°C, suggesting that the repressive activity of G3 is less strong than M4 at high temperature. Taken together, the repressive *cis* regulatory element, G1 and G3, can compete with M4 enhancer to modulate the exon 3a inclusion (**Fig. 3.8**). At low temperature, G1 and G3 are dominant to control exon 3a inclusion, while M4 is more powerful to increase exon 3a inclusion at high temperature. It is because that G1 and G3 can form RNA G-quadruplexes to mask the splice sites, and they are less stable at high temperature. The reason why M4 shows higher activity at high temperature remain elusive.

3.4 Phosphorylation plays a prominent role to main the temperature sensitivity of RBM3 exon 3a inclusion at high temperature, but not at low temperature.

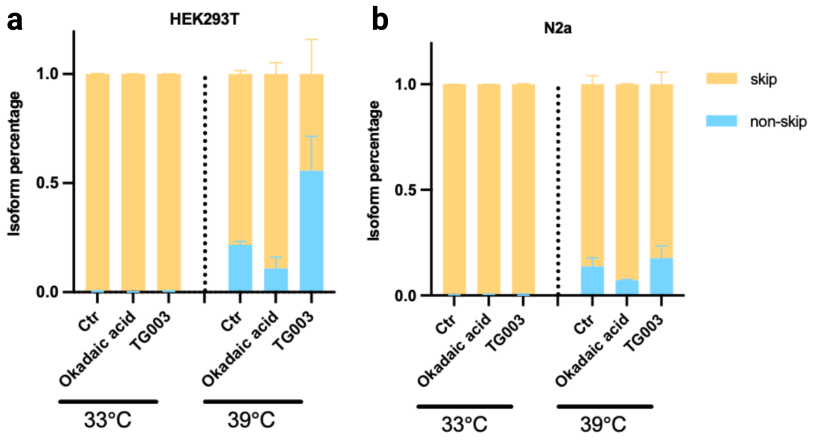

Figure 3.9 Phosphatase inhibitor reduces exon 3a inclusion, while CLK inhibitor increases exon 3a inclusion at high temperature, but not at low temperature. Exon 3a inclusion changes in

okadaic acid (20 nM) and TG003 (20 μM) treatment in HEK293T cells and N2a cells. mRBM3 minigenes were transfected into cells at 37°C overnight, and then the cells were treated with different concentrations of okadaic acid and TG003, and then were shifted into the incubators with different temperatures to culture for another around 24hrs, followed by RT-PCR and agarose gel resolving. n=2. The gel images for quantification are in the **App. Fig. 23**.

As we have demonstrated that the differential activity of G1 and G3 at different temperatures is caused by the disrupted structure of G-quadruplex, we next asked what contributes to the differential activity of those cis-regulatory elements (G1, G3, M2 and M4). Marco Preußner *et al.* showed that circadian rhythm of body temperature drives SR protein phosphorylation in cycles to control alternative splicing events[127]. James Manley group also revealed that dramatic dephosphorylation of SRSF10 after heat shock[128]. Later, Tom Haltenhof *et al.* further demonstrated that evolutionarily conserved CLK kinase was the key kinase with differential activities in response to temperature change for the phosphorylation of SR proteins from reptiles to mammals[128]. Therefore, we next examine whether phosphorylation is responsible for the temperature sensitivity of alternative splicing of exon3a. We treated cells with phosphatase inhibitor okadaic acid and CLK specific inhibitor TG003 to check the RBM3 exon 3a inclusion, respectively. In both HEK293T and N2a cells, at low temperature the exon 3a inclusion doesn't change in these treatments, while the RBM3 isoform containing exon 3a significantly changes at high temperature, showing that TG003 increases RBM3 exon 3a inclusion and okadaic acid reduces the percentage of RBM3 isoforms containing exon 3a (**Fig. 3.9**). This suggests that at low temperature the RBM3 inclusion or exclusion is mainly not dependent on the phosphorylation, while at high temperature less phosphorylation promotes exon 3a inclusion.

3.5 Working model of cis-regulatory element network regulating alternative splicing of RBM3 exon 3a

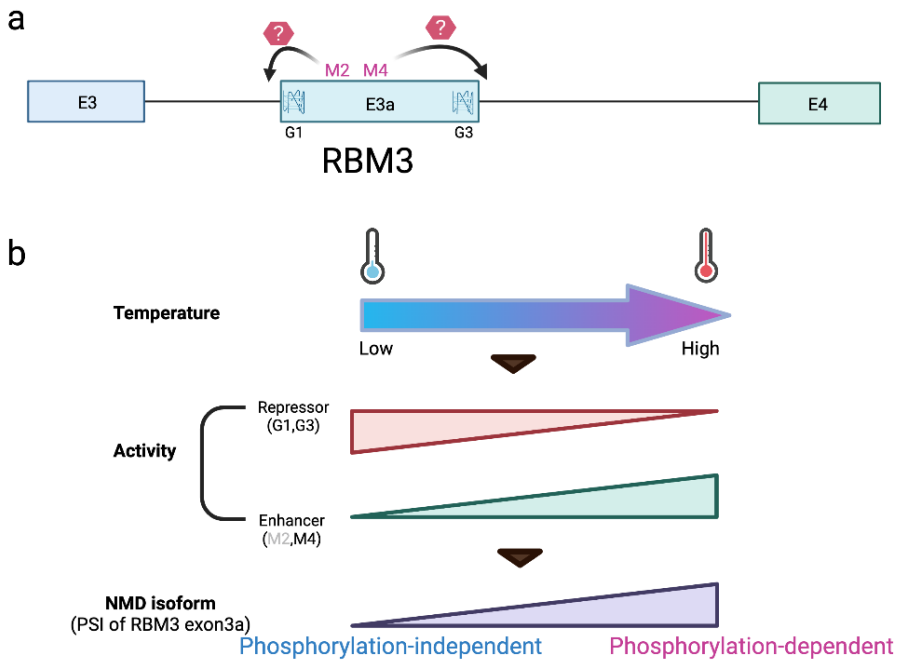

Figure 3.10 Working model of temperature regulating RBM3 exon 3a inclusion. a, Simplified working model how *cis*-regulatory element controlling exon 3a inclusion. M2 and M4 are the most active enhancer elements to modulate alternative splicing of exon 3a, and G1 and G3 are dominant repressive *cis*-regulatory element to inhibit RBM3 exon 3a inclusion. **b**, Proposed simplified model how temperature controls RBM3 exon 3a inclusion. As temperature increases, the repressive activity of G1 and G3 decreases, while the enhancer activity of M2 and M4 enhances, which result in more exon 3a inclusion. At low temperature, the splicing machinery is phosphorylation-independent, and it highly relies on the phosphorylation at high temperature.

Through systematic screening via CRISPR-dCasRx gRNA perturbation tiling on the RBM3 exon 3a and its flanking region and mutagenesis screening, the effective *cis*-regulatory enhancers and repressors are efficiently identified for the modulation of RBM3 exon 3a inclusion. To simplify the coordinated network, we took the strongest repressive *cis*-regulatory element (G1 and G3) and enhancer (M4) as examples, and demonstrated that the representative repressor, G1 and G3, cooperate with the typical enhancer element M4 at both low and high temperatures, resulting in the higher exon 3a inclusion at high temperature (**Fig. 3.10**).

3.6 Discussion

Massively parallel CRISPR-Cas13-based screening has been leveraged in many scenarios to specifically and robustly knockdown genes without altering the genome[402]. The catalytically inactive dCas13 can be utilized to systematically identify novel undetermined *cis*-regulatory elements modulating alternative splicing[203]. Here, we showed that CRISPR-dCasRx gRNA tilling, to some extent, is capable of efficiently identifying the *cis*-regulatory elements, especially the strong enhancer and repressor *cis*-regulatory elements, which overlap with the mutagenesis results in the 1st and 2nd section. Then, the remaining potential intronic *cis*-regulatory elements are further validated via mutagenesis. It shows that the resolution of dCasRx gRNA tilling assay is not high enough if different *cis*-regulatory elements are in proximity to each other in distance possibly because the dCasRx protein is too big to sterically produce hindrance in a broad range of gRNA targeting sequence. Additionally, some of the *cis* elements, such as I2-m2-D1, shows opposite effect between gRNA perturbation and mutagenesis assay due to the proximity of *cis*-regulatory element to 5'SS, presenting that the dCasRx complex not only can compete with the *trans*-acting factor of I2-m2-D1, but also sterically blocks spliceosome assembly at the 5'SS. These results suggest that CRISPR-dCasRx gRNA perturbation assay is less efficient to identify the functional cis-regulatory that is close to the splice sites. The CRISPR-dCasRx gRNA perturbation is also limited to target the highly structured region as the gRNA just recognizes the single-stranded RNA. Of course, this characteristic can be utilized as an alternative strategy to demonstrate an RNA region is structured or not. In summary, CRISPR-dCasRx gRNA perturbation is an efficient strategy to identify potential *cis*-regulatory elements, but its resolution is not high enough in some conditions.

In the case of RBM3, the exon 3a inclusion is intricately modulated by several *cis*-regulatory elements including repressors and enhancers. Guide RNA tilling assay presents several clusters increasing endogenous RBM3 expression, which can be experimentally validated that the increased RBM3 expression is due to the less exon 3a inclusion. Additionally, a *cis* element was determined via mutagenesis to mask the alternative splice site in the exon 3a, and it is possibly caused by a masker protein binding to the *cis* element. In a genome-wide scale, we can speculate that some alternative splice sites in the exon or intron also is masked a masker protein to prevent from the usage of "cryptic" splice site. More investigations should be done in this direction.

More interestingly, to our knowledge, we first demonstrated how the activity of different *cis*-regulatory elements coordinately responds to temperature changes. The activity of repressive *cis*

element (G4) is down-regulated, while *cis* enhancer activity is up-regulated as the temperature increases. Finally, these two pathways achieve heat-induced poison exon 3a inclusion of RBM3.

3.7 Future plans

Taken together, we systematically identified extensive cross-regulation of *cis*-regulatory element network controlling alternative splicing of heat-induced "poison" RBM3 exon 3a and found several temperature-sensitive *cis*-regulatory elements, which intricately cooperate to achieve the temperature sensitivity of RBM3 exon 3a. To our knowledge, this is the first-time deliberated identification of temperature sensitive *cis*-regulatory element controlling exon inclusion. It is conceivable that there exist a plenty of other exon inclusion event sharing the similar mechanism that several temperature-sensitive motifs are interactively (synergistically and/or antagonistically) coupled in the alternative splicing. Future work is to identify the corresponding *trans*-acting factors of *cis*-regulatory elements to deeply understand how cold induces RBM3 expression.

Material and Method

Bioinformatics analysis and data analysis

Cassette exons were classified into three groups, including cold-repressed exons (CRE), cold-induced exons (CIE), and the background (bg), based on the percentage spliced in (PSI) values at 35℃ and 38℃ for the HEK293T dataset; 32℃, 37℃ and 40℃ for the Hela dataset. For HEK293T dataset, CIE: p value_35℃ vs 39℃ < 0.05 & ΔPSI_35℃ vs 39℃ > 0.1; CRE: p value_35℃ vs 39℃ < 0.05; ΔPSI_35℃ vs 39℃ < -0.1; bg: (p value_35℃ vs 39℃ > 0.1 & abs (ΔPSI_35℃ vs 39℃) < 0.1). For Hela dataset, CIE: p value_32℃ *vs* 37℃ < 0.05 & p value_37℃ *vs* 40℃ < 0.05 & ΔPSI_32℃ *vs* 37℃ * ΔPSI_37℃ *vs* 40℃ > 0 & ΔPSI_32℃ *vs* 37℃ + ΔPSI_37℃ *vs* 40℃ > 0.1; CRE: p value_32℃ *vs* 37℃ < 0.05 & p value_37℃ *vs* 40℃ < 0.05 & ΔPSI_32℃ *vs* 37℃ * ΔPSI_37℃ *vs* 40℃ > 0 & ΔPSI_32℃ *vs* 37℃ + ΔPSI_37℃ *vs* 40℃ < -0.1; bg: (p value_32℃ *vs* 37℃ > 0.1 & abs(ΔPSI_32℃ *vs* 37℃) < 0.1) or (p value_37℃ vs 40℃ > 0.1 & abs(ΔPSI _37℃ *vs* 40℃) < 0.1). For **g**, CIE: p value_37 ℃ *vs* 40 ℃<0.05, ΔPSI_32℃ *vs* 37℃>0.1; CRE: p value_37 ℃ *vs* 40 ℃<0.05, ΔPSI_32℃ *vs* 37℃<0.1; bg: (p value_37℃ vs 40℃ > 0.1 & abs (ΔPSI_37℃ *vs* 40℃) < 0.1).

Then, the sequence of each cassette exon, and the around splice sites as well as the upstream and downstream exons were extracted using bedtools[403]. We further predicted G4 in these sequences by searching motifs from the previous study*[150],* and using pqsfinder*[404]*, and G4Hunter[376], rG4-seq[151], respectively. All the bar graphs were generated by Prism 9, and schematic and working model were made by Bio-render.

Cell culture

HEK293T and Hela cells were cultured on uncoated plastic flasks or plates in the DMEM medium (4.5 g glucose/L, supplied with GlutaMAX L-glutamine, Gibco,10566) supplemented with 10% fetal bovine serum (Biochrom) and penicillin-streptomycin (1:100 from a stock of 10000 U/mL, Gibco, 15140122) in the incubator with 5% CO2 at 37℃ except for unless explicitly stated. N2a cells were cultured also on the plastic flasks or plates in the medium with half DMEM and half opti-MEM supplemented with 10% fetal bovine serum (Biochrom) and penicillin-streptomycin (1:00 from a stock of 10000 U/mL, Gibco, 15140122). At roughly 80% confluency, the cells were sub-cultured using a 0.25% trypsin solution (1:10 dilution of 2.5% stock, Gibco,15090046) in phosphate buffered saline.

Cloning

All the cloning were used ClonExpress II One Step Cloning kit from Vazyme (C112). Briefly, the mutated DNA fragments were generated from PCR, and then the fragment and enzyme digested vector were incubated for 30min, and then the reaction solution was directly added into DH5apha competent cells on ice for another 30min, followed by heat shock around 1min at 42 ℃. Then, the heat shocked bacteria were immediately put on the ice for 5min, followed by adding 300ul of LB medium without antibiotics. These bacteria were then cultured at 37℃ for another 1hrs, and then they are stripped on the agar plate with corresponding antibiotics resistance. The sequences of mutants and gRNA are shown below:

Mutant	**Target region** exon3a: 1 to 278 upstream flanking intron of exon3a: "-119 to -1" downstream flanking intron of exon3a: "+1 to +228"	**WT sequence**	**Replacement seqeunce**
M1	0 to 31	ggggtggagggcagcggcagacagagccggg	TCTATTTTCCCACCCTTAGGCTGCTGGTGGTCTACCCTTGGACCCAGA
M2	32 to 81	ctgcctgggaggcgacgactggtcctgcatgaggcggagaagccacctgt	CCCAGAGGTTCTTTGAGTCCTTTGGGGATCTGTCCACTCCTGATGCTGTT
M3	82 to 131	ggatggttgacctgctctgggcttaggtagtagagtctgcagagctgtgg	CTATTGGTCTATTTTCCCACCCTTAGGCTGCTGGTGGTCTACCCTTGGAC
M4	132 to 181	gcctggcagaggaccggagaggacctcgtgagtctgctgggatggactct	CCCAGAGGTT CTTTGAGTCCTTTGG GGATCTGTCCACTCCTGATGCTGTT
M5	182 to 230	gaagcctcagaccgagagaggtgtctagccctaatagtcgggcagctta	CCCAGAGGTTCTTTGAGTCCTTTGGGGATCTGTCCACTCCTGATGCTGTT
M6	231 to 271, "+1 to +9"	gaggagtggggaggatacgtcagcctgagttcagtcaagatgtaagtagt	GGCACTGTGACAAGCTGCATGTGGATCCTGAGAACTTCAAGGTGAGTCCAG
M2-D	32 to 81	ctgcctgggaggcgacgactggtcctgcatgaggcggagaagccacctgt	deletion
M2-1	32 to 41	ctgcctggga	CCCAGAGGTT
M2-2	42 to 51	ggcgacgact	CTTTGAGTCC
M2-3	52 to 61	ggtcctgcat	TTTGGGGATC
M2-4	62 to 71	gaggcggaga	TGTCCACTCC
M2-5	72 to 81	aagccacctgt	TGATGCTGTT
M2-6	32 to 51	ctgcctgggaggcgacgact	CCCAGAGGTTCTTTGAGTCC
M2-7	52 to 71	ggcgacgactggtcctgcat	TTTGGGGATCTGTCCACTCC
M2-8	62 to 81	gaggcggagaagccacctgt	TGTCCACTCCTGATGCTGTT
M2-9	42 to 71	ggcgacgactggtcctgcatgaggcggaga	CTTTGAGTCCTTTGGGGATCTGTCCACTCC
M4-D	132 to 181	gcctggcagaggaccggagaggacctcgtgagtctgctgggatggactct	deletion
M4-1	132 to 156	gcctggcagaggaccggagaggacc	CCCAGAGGTTCTTTGAGTCCTTTGG
M4-2	157 to 181	tcgtgagtctgctgggatggactc	GGATCTGTCCACTCCTGATGCTGTT
M4-3	132 to 141	gcctggcaga	CCCAGAGGTT
M4-4	142 to 151	ggaccggaga	CTTTGAGTCC
M4-5	152 to 161	ggacctcgtg	TTTGGGGATC
M4-6	162 to 171	agtctgctgg	TGTCCACTCC
M4-7	172 to 181	gatggactct	TGATGCTGTT
M4-8	132 to 151	gcctggcagaggaccggaga	CCCAGAGGTTCTTTGAGTCC
M4-9	152 to 171	ggacctcgtgagtctgctgg	TTTGGGGATCTGTCCACTCC
M2 core	42 to 61	ggcgacgactggtcctgcat	deletion
M4 core	146 to 160	ggacctcgtgagtct	deletion

gRNA name	Target region exon3a: 1 to 278 upstream flanking intron of exon3a: "-119 to -1" downstream flanking intron of exon3a: "+1 to +228"	Target sequence	gRNA sequence
gRNA1	"-119 to -98"	tcctgcctgcacaggggccgtc	GACGGCCCCTGTGCAGGCAGGA
gRNA2	"-81 to -102"	ccgtctccctgtctgccacttt	AAAGTGGCAGACAGGGAGACGG
gRNA3	"-64 to -85"	actttcttcgttctttctgttt	AAACAGAAAGAACGAAGAAAGT
gRNA4	"-47 to -67"	tgttttccctctatgtctgcca	TGGCAGACATAGAGGGAAAACA
gRNA5	"-30 to -51"	tgccaggggcagcgtggccact	AGTGGCCACGCTGCCCCTGGCA
gRNA6	"-13 to -34"	ccactcacaggagcatgactgc	GCAGTCATGCTCCTGTGAGTGG
gRNA7	"-16 to -1" to "1 to 6"	actgccttctgttctagggggt	ACCCCCTAGAACAGAAGGCAGT
gRNA8	1 to 22	gggtggagggcagcggcagaca	TGTCTGCCGCTGCCCTCCACCC
gRNA9	19 to 40	agacagagccgggctgcctggg	CCCAGGCAGCCCGGCTCTGTCT
gRNA10	36 to 57	ctgggaggcgacgactggtcct	AGGACCAGTCGTCGCCTCCCAG
gRNA11	53 to 74	gtcctgcatgaggcggagaagc	GCTTCTCCGCCTCATGCAGGAC
gRNA12	70 to 91	gaagccacctgtggatggttga	TCAACCATCCACAGGTGGCTTC
gRNA13	87 to 108	gttgacctgctctgggcttagg	CCTAAGCCCAGAGCAGGTCAAC
gRNA14	104 to 125	ttaggtagtagagtctgcagag	CTCTGCAGACTCTACTACCTAA
gRNA15	121 to 142	cagagctgtgggcctggcagag	CTCTGCCAGGCCCACAGCTCTG
gRNA16	138 to 159	cagaggaccggagaggacctcg	CGAGGTCCTCTCCGGTCCTCTG
gRNA17	155 to 176	cctcgtgagtctgctgggatgg	CCATCCCAGCAGACTCACGAGG
gRNA18	172 to 193	gatggactctgaagcctcagac	GTCTGAGGCTTCAGAGTCCATC
gRNA19	189 to 210	cagaccgagagaggtgtctagc	GCTAGACACCTCTCTCGGTCTG
gRNA20	206 to 227	ctagccctaatagtcgggcagc	GCTGCCCGACTATTAGGGCTAG
gRNA21	223 to 244	gcagcttagaggagtggggagg	CCTCCCCACTCCTCTAAGCTGC
gRNA22	257 to 278	ggaggatacgtcagcctgagtt	AACTCAGGCTGACGTATCCTCC
gRNA23	"257 to 271" to "+1 to +7"	gagttcagtcaagatgtaagta	TACTTACATCTTGACTGAACTC
gRNA24	"+3 to +24"	aagtagtagcaggggagaccgg	CCGGTCTCCCCTGCTACTACTT
gRNA25	"+20 to +21"	accggtggattcaggtcttttt	AAAAAGACCTGAATCCACCGGT
gRNA26	"+37 to +58"	tttttgtgggattccatagctc	GAGCTATGGAATCCCACAAAAA
gRNA27	"+54 to +75"	agctcctggtgaagccattctg	CAGAATGGCTTCACCAGGAGCT
gRNA28	"+71 to +92"	ttctggtcagcggagcttggct	AGCCAAGCTCCGCTGACCAGAA
gRNA29	"+88 to +109"	tggcttggacgaggcacccaga	TCTGGGTGCCTCGTCCAAGCCA
gRNA30	"+105 to +126"	ccagaatttggtgcccagcagg	CCTGCTGGGCACCAAATTCTGG
gRNA31	"+122 to +143"	gcaggaatttctgggctcttgc	GCAAGAGCCCAGAAATTCCTGC
gRNA32	"+139 to +160"	cttgcctacacctacctgcctg	CAGGCAGGTAGGTGTAGGCAAG
gRNA33	"+156 to +177"	gcctgtgcccattcttccctca	TGAGGGAAGAATGGGCACAGGC
gRNA34	"+190 to +211"	cctcatccctactgtgactgac	GTCAGTCACAGTAGGGATGAGG
gRNA35	"+190 to +211"	ctgacaattccttgtgtctgtc	GACAGACACAAGGAATTGTCAG
gRNA36	"+207 to +228"	ctgtctccttcccatacctagT	ACTAGGTATGGGAAGGAGACAG

Transfection

Roti-fect was used as a carrier to transfect plasmids into cells. Briefly, around 800 ng plasmid per well (12 well plate) was mixed with 100 µl of opti-MEM, and 2 µl of Roti-fect was added into another tube containing 100 µl of opti-MEM. These two mixture solutions were put at room temperature for around 5min, and then they were mixed to incubate at room temperature for another 20min. The mixed 200ul solution was slowing added into cells. MOE antisense oligonucleotides (1ul, 100 ng/µl) were purchased from Mycrosynth and transfected into N2A

cells (3*106 cells per well on a 12-well plate) via Rotifect. The sequence of antisense oligonucleotides is shown in the following table:

ASO name	Target region exon3a: 1 to 278 upstream flanking intron of exon3a: "-119 to -1" downstream flanking intron of exon3a: "+1 to +228"	Target sequence	ASO sequence
MOE	"267 to 271" to "+1 to +13"	aagatgtaagtagtagca	TGCTACTACTTACATCTT
MOE+2	"269 to 271" to "+1 to +15"	gatgtaagtagtagcaggg	CCCTGCTACTACTTACATC
MOE+3	"270 to 271" to "+1 to +17"	atgtaagtagtagcagggg	CCCCTGCTACTACTTACAT
LongA	"268 to 271" to "+1 to +21"	agatgtaagtagtagcaggggagac	GTCTCCCCTGCTACTACTTACATCT
LongB	"261 to 271" to "+1 to +14"	tcagtcaagatgtaagtagtagcag	CTGCTACTACTTACATCTTGACTGA
M2A	32 to 50	ctgcctgggaggcgacgac	GTCGTCGCCTCCCAGGCAG
M2B	37 to 55	tgggaggcgacgactggtc	GACCAGTCGTCGCCTCCCA
M2C	42 to 60	ggcgacgactggtcctgca	TGCAGGACCAGTCGTCGCC
M2D	47 to 65	cgactggtcctgcatgagg	CCTCATGCAGGACCAGTCG
M2Da	45 to 63	gacgactggtcctgcatga	TCATGCAGGACCAGTCGTC
M2Db	49 to 67	actggtcctgcatgaggcg	CGCCTCATGCAGGACCAGT
M2E	52 to 70	ggtcctgcatgaggcggag	CTCCGCCTCATGCAGGACC
M4A	147 to 165	ggagaggacctcgtgagtc	GACTCACGAGGTCCTCTCC
M4B	152 to 170	ggacctcgtgagtctgctg	CAGCAGACTCACGAGGTCC
M4C	157 to 175	tcgtgagtctgctgggatg	CATCCCAGCAGACTCACGA
M4D	162 to 180	agtctgctgggatggactc	GAGTCCATCCCAGCAGACT

RNA extraction, RT-PCR, and qPCR

Trizol was used for RNA extraction. Shortly, Trizol was directly added into the cells with medium removal to lysis the cells. Then, 1/5 CH_3Cl was mixed with Trizol solution, followed by 13000g centrifuge for around 30min. The supernatant was carefully pipetted to mix with isopropanol with 1:1 ratio, and then the mixture was subjected into 13000g centrifuge for around 30min to pellet the RNA. The RNA pellet was washed with 70% ethanol (diluted with DEPC-treated water), and dried at room temperature for 1min. Then the dried RNA is subjected to DNAse digestion at 37 for at least 30min, followed by PCI adding with 1:1 and centrifuging for 10min. Then, the supernatant was removed to 1:1 mix with ethanol containing 0.12M Sodium Acetate. The mixture was then centrifuged for 30min, followed by 70% ethanol washing the pellet and drying for 1min at room temperature. to get the pure RNA.

For reverse transcription (RT), 1000 ng RNA, 2 ng/μl RT primer and 5X hybridization buffer were mixed to incubator in RT program with continuous ramp-down the temperature to make the RT primer anneal with RNA, and then the M-MLV Reverse Transcriptase with RT buffer

was added into the mixture to incubate for 30min at 43℃ followed by 95 ℃ for 2min to inactivate reverse transcriptase. cDNA from RT was directly used for PCR with home-made Taq polymerase following the standard PCR protocol. cDNA from RT was mixed with 2X SYBRGREEN, then the mixture was subjected into 3 step qPCR program in accordance with the manufacture protocol.

Primer name	Primer seqeunce	Primer purpose
mRBM3_E2/3_qF	AAGGGAAACTCTTCGTAG	qPCR mouse
mRBM3_E3_qR	GACAACAACCACCTCAGAGATAG	qPCR mouse
HPRT_qF	CAACGGGGGACATAAAAGTTATTGGTGGA	qPCR mouse
HPRT_qR	TGCAACCTTAACCATTTTGGGGCTGT	qPCR mouse
hRBM3_E2/3_qF	AAGGAAAGCTCTTCGTGGGA	qPCR human
hRBM3_E3_qR	GACAACGACCACCTCAGAGA	qPCR human
mRbm3_E3_F4	TGGTTGTTGTCAAGGACCGGG	RT-PCR for mRBM3 minigene
mRbm3_E4_R	CTCTAGAGTAACTGCGACCAC	RT-PCR for mRBM3 minigene
hRbm3_E3_F4	TGGTCGTTGTCAAGGACCGGG	RT-PCR for hRBM3 minigene
hRbm3_E4_R	CTCTAGAGTAGCTGCGACCAC	RT-PCR for hRBM3 minigene

CD spectroscopy

Briefly, the CD spectroscopy was performed using Jasco J-1500 CD spectrophotometer and a 0.1-cm path length quartz cuvette (Hellma Analytics) was employed in a volume of 200 µl. Samples with 5 µM RNA (final concentration) were prepared in 50mM KCl or 0.1mM KCl in 50mM Tris-HCl pH7.5. Each of the RNA samples was then thoroughly mixed and denatured by heating at 95 °C for 5 min and cooled to room temperature overnight for renaturation. The RNA samples were excited and scanned from 220–310 nm at different temperature and spectra were acquired every 1 nm. All spectra reported were an average of 3 scans with a response time of 0.5 s/nm. They were then normalized to molar residue ellipticity.

Protein extraction and western blot

Whole-cell extracts were prepared with lysis buffer (20mM Tris (pH 8.0), 2% NP-40 (v/v), 0,01% sodium deoxycholate (w/v), 4mM EDTA and 200mM NaCl) supplemented with protease inhibitor mix (Aprotinin, Leupeptin, Vanadat and PMSF). Concentrations were determined using by BCA assay (23225 Pierce™ BCA Protein Assay Kit, Thermofisher) according to manufacturer's instructions. SDS-PAGE and Western blotting followed standard procedures. Western blots were quantified using the ImageQuant TL software. The following

antibodies were used for Western blotting: hnRNPL (4D11, Santa Cruz), RBM3 (14363-1-AP, Proteintech), Gapdh (GT239, GeneTex).

Reference

1 *Grabowski, P. J., Padgett, R. A. & Sharp, P. A. Messenger RNA splicing in vitro: an excised intervening sequence and a potential intermediate. Cell **37**, 415-427 (1984). https://doi.org:10.1016/0092-8674(84)90372-6*

2 *Padgett, R. A., Konarska, M. M., Grabowski, P. J., Hardy, S. F. & Sharp, P. A. Lariat RNA's as intermediates and products in the splicing of messenger RNA precursors. Science **225**, 898-903 (1984). https://doi.org:10.1126/science.6206566*

3 *Ruskin, B., Krainer, A. R., Maniatis, T. & Green, M. R. Excision of an intact intron as a novel lariat structure during pre-mRNA splicing in vitro. Cell **38**, 317-331 (1984). https://doi.org:10.1016/0092-8674(84)90553-1*

4 *Chapman, K. B. & Boeke, J. D. Isolation and characterization of the gene encoding yeast debranching enzyme. Cell **65**, 483-492 (1991). https://doi.org:10.1016/0092-8674(91)90466-c*

5 *Hesselberth, J. R. Lives that introns lead after splicing. Wiley Interdiscip Rev RNA **4**, 677-691 (2013). https://doi.org:10.1002/wrna.1187*

6 *Mironov, A. A., Fickett, J. W. & Gelfand, M. S. Frequent alternative splicing of human genes. Genome Res **9**, 1288-1293 (1999). https://doi.org:10.1101/gr.9.12.1288*

7 *Baralle, F. E. & Giudice, J. Alternative splicing as a regulator of development and tissue identity. Nat Rev Mol Cell Biol **18**, 437-451 (2017). https://doi.org:10.1038/nrm.2017.27*

8 *Johnson, J. M. et al. Genome-wide survey of human alternative pre-mRNA splicing with exon junction microarrays. Science **302**, 2141-2144 (2003). https://doi.org:10.1126/science.1090100*

9 *Kan, Z., Rouchka, E. C., Gish, W. R. & States, D. J. Gene structure prediction and alternative splicing analysis using genomically aligned ESTs. Genome Res **11**, 889-900 (2001). https://doi.org:10.1101/gr.155001*

10 *Nilsen, T. W. & Graveley, B. R. Expansion of the eukaryotic proteome by alternative splicing. Nature **463**, 457-463 (2010). https://doi.org:10.1038/nature08909*

11 *Reid, D. C. et al. Next-generation SELEX identifies sequence and structural determinants of splicing factor binding in human pre-mRNA sequence. RNA **15**, 2385-2397 (2009). https://doi.org:10.1261/rna.1821809*

12 *Lee, F. C. Y. & Ule, J. Advances in CLIP Technologies for Studies of Protein-RNA Interactions. Mol Cell **69**, 354-369 (2018). https://doi.org:10.1016/j.molcel.2018.01.005*

13 *Shepard, P. J. & Hertel, K. J. The SR protein family. Genome Biol **10**, 242 (2009). https://doi.org:10.1186/gb-2009-10-10-242*

14 *Stamm, S. Regulation of alternative splicing by reversible protein phosphorylation. J Biol Chem **283**, 1223-1227 (2008). https://doi.org:10.1074/jbc.R700034200*

15 *Staley, J. P. & Guthrie, C. Mechanical devices of the spliceosome: motors, clocks, springs, and things. Cell **92**, 315-326 (1998). https://doi.org:10.1016/s0092-8674(00)80925-3*

16 *Smith, C. W. & Valcarcel, J. Alternative pre-mRNA splicing: the logic of combinatorial control. Trends Biochem Sci **25**, 381-388 (2000). https://doi.org:10.1016/s0968-0004(00)01604-2*

17 *Wang, J. & Manley, J. L. Regulation of pre-mRNA splicing in metazoa. Curr Opin Genet Dev **7**, 205-211 (1997). https://doi.org:10.1016/s0959-437x(97)80130-x*

18 *Rosenberg, A. B., Patwardhan, R. P., Shendure, J. & Seelig, G. Learning the sequence determinants of alternative splicing from millions of random sequences. Cell **163**, 698-711 (2015). https://doi.org:10.1016/j.cell.2015.09.054*

19 *Wong, M. S., Kinney, J. B. & Krainer, A. R. Quantitative Activity Profile and Context Dependence of All Human 5' Splice Sites. Mol Cell **71**, 1012-1026 e1013 (2018). https://doi.org:10.1016/j.molcel.2018.07.033*

20 *Schaal, T. D. & Maniatis, T. Selection and characterization of pre-mRNA splicing enhancers: identification of novel SR protein-specific enhancer sequences. Mol Cell Biol **19**, 1705-1719 (1999). https://doi.org:10.1128/MCB.19.3.1705*

21 *Fairbrother, W. G., Yeh, R. F., Sharp, P. A. & Burge, C. B. Predictive identification of exonic splicing enhancers in human genes. Science **297**, 1007-1013 (2002). https://doi.org:10.1126/science.1073774*

22 *Wang, Z. et al. Systematic identification and analysis of exonic splicing silencers. Cell **119**, 831-845 (2004). https://doi.org:10.1016/j.cell.2004.11.010*

23 *Pandit, S. et al. Genome-wide analysis reveals SR protein cooperation and competition in regulated splicing. Mol Cell **50**, 223-235 (2013). https://doi.org:10.1016/j.molcel.2013.03.001*

24 *Gonatopoulos-Pournatzis, T. et al. Genome-wide CRISPR-Cas9 Interrogation of Splicing Networks Reveals a Mechanism for Recognition of Autism-Misregulated Neuronal Microexons. Mol Cell **72**, 510-524 e512 (2018). https://doi.org:10.1016/j.molcel.2018.10.008*

25 *Ule, J. et al. An RNA map predicting Nova-dependent splicing regulation. Nature **444**, 580-586 (2006). https://doi.org:10.1038/nature05304*

26 *Blencowe, B. J. Exonic splicing enhancers: mechanism of action, diversity and role in human genetic diseases. Trends Biochem Sci **25**, 106-110 (2000). https://doi.org:10.1016/s0968-0004(00)01549-8*

27 *Sanford, J. R., Longman, D. & Caceres, J. F. Multiple roles of the SR protein family in splicing regulation. Prog Mol Subcell Biol **31**, 33-58 (2003). https://doi.org:10.1007/978-3-662-09728-1_2*

28 *Cartegni, L. & Krainer, A. R. Disruption of an SF2/ASF-dependent exonic splicing enhancer in SMN2 causes spinal muscular atrophy in the absence of SMN1. Nat Genet **30**, 377-384 (2002). https://doi.org:10.1038/ng854*

29 *Hofmann, Y., Lorson, C. L., Stamm, S., Androphy, E. J. & Wirth, B. Htra2-beta 1 stimulates an exonic splicing enhancer and can restore full-length SMN expression to survival motor neuron 2 (SMN2). Proc Natl Acad Sci U S A **97**, 9618-9623 (2000). https://doi.org:10.1073/pnas.160181697*

30 *Rothrock, C. R., House, A. E. & Lynch, K. W. HnRNP L represses exon splicing via a regulated exonic splicing silencer. EMBO J **24**, 2792-2802 (2005). https://doi.org:10.1038/sj.emboj.7600745*

31 *Chen, C. D., Kobayashi, R. & Helfman, D. M. Binding of hnRNP H to an exonic splicing silencer is involved in the regulation of alternative splicing of the rat beta-tropomyosin gene. Genes Dev **13**, 593-606 (1999). https://doi.org:10.1101/gad.13.5.593*

32 *Bashaw, G. J. & Baker, B. S. The msl-2 dosage compensation gene of Drosophila encodes a putative DNA-binding protein whose expression is sex specifically regulated by Sex-lethal. Development **121**, 3245-3258 (1995). https://doi.org:10.1242/dev.121.10.3245*

33 *Kelley, R. L. et al. Expression of msl-2 causes assembly of dosage compensation regulators on the X chromosomes and female lethality in Drosophila. Cell **81**, 867-877 (1995). https://doi.org:10.1016/0092-8674(95)90007-1*

34 *Zhou, S. et al. Male-specific lethal 2, a dosage compensation gene of Drosophila, undergoes sex-specific regulation and encodes a protein with a RING finger and a metallothionein-like cysteine cluster. EMBO J **14**, 2884-2895 (1995). https://doi.org:10.1002/j.1460-2075.1995.tb07288.x*

35 *Boggs, R. T., Gregor, P., Idriss, S., Belote, J. M. & McKeown, M. Regulation of sexual differentiation in D. melanogaster via alternative splicing of RNA from the transformer gene. Cell **50**, 739-747 (1987). https://doi.org:10.1016/0092-8674(87)90332-1*

36 *Keppetipola, N., Sharma, S., Li, Q. & Black, D. L. Neuronal regulation of pre-mRNA splicing by polypyrimidine tract binding proteins, PTBP1 and PTBP2. Crit Rev Biochem Mol Biol **47**, 360-378 (2012). https://doi.org:10.3109/10409238.2012.691456*

37 *Spellman, R. et al. Regulation of alternative splicing by PTB and associated factors. Biochem Soc Trans **33**, 457-460 (2005). https://doi.org:10.1042/BST0330457*

38 *Xue, Y. et al. Direct conversion of fibroblasts to neurons by reprogramming PTB-regulated microRNA circuits. Cell **152**, 82-96 (2013). https://doi.org:10.1016/j.cell.2012.11.045*

39 *Qian, H. et al. Reversing a model of Parkinson's disease with in situ converted nigral neurons. Nature **582**, 550-556 (2020). https://doi.org:10.1038/s41586-020-2388-4*

40 *Zhou, H. et al. Glia-to-Neuron Conversion by CRISPR-CasRx Alleviates Symptoms of Neurological Disease in Mice. Cell **181**, 590-603 e516 (2020). https://doi.org:10.1016/j.cell.2020.03.024*

41 *Wollerton, M. C., Gooding, C., Wagner, E. J., Garcia-Blanco, M. A. & Smith, C. W. Autoregulation of polypyrimidine tract binding protein by alternative splicing leading to nonsense-mediated decay. Mol Cell **13**, 91-100 (2004). https://doi.org:10.1016/s1097-2765(03)00502-1*

42 *Zheng, S. et al. PSD-95 is post-transcriptionally repressed during early neural development by PTBP1 and PTBP2. Nat Neurosci **15**, 381-388, S381 (2012). https://doi.org:10.1038/nn.3026*

43 *Yano, M., Hayakawa-Yano, Y., Mele, A. & Darnell, R. B. Nova2 regulates neuronal migration through an RNA switch in disabled-1 signaling. Neuron **66**, 848-858 (2010). https://doi.org:10.1016/j.neuron.2010.05.007*

44 *Forch, P. et al. The apoptosis-promoting factor TIA-1 is a regulator of alternative pre-mRNA splicing. Mol Cell **6**, 1089-1098 (2000). https://doi.org:10.1016/s1097-2765(00)00107-6*

45 *Del Gatto-Konczak, F. et al. The RNA-binding protein TIA-1 is a novel mammalian splicing regulator acting through intron sequences adjacent to a 5' splice site. Mol Cell Biol **20**, 6287-6299 (2000). https://doi.org:10.1128/MCB.20.17.6287-6299.2000*

46 *Huh, G. S. & Hynes, R. O. Regulation of alternative pre-mRNA splicing by a novel repeated hexanucleotide element. Genes Dev **8**, 1561-1574 (1994). https://doi.org:10.1101/gad.8.13.1561*

47 *Black, D. L. Activation of c-src neuron-specific splicing by an unusual RNA element in vivo and in vitro. Cell **69**, 795-807 (1992). https://doi.org:10.1016/0092-8674(92)90291-j*

48 *Guo, N. & Kawamoto, S. An intronic downstream enhancer promotes 3' splice site usage of a neural cell-specific exon. J Biol Chem **275**, 33641-33649 (2000). https://doi.org:10.1074/jbc.M005597200*

49 *Kuroyanagi, H. Fox-1 family of RNA-binding proteins. Cell Mol Life Sci **66**, 3895-3907 (2009). https://doi.org:10.1007/s00018-009-0120-5*

50 *Calarco, J. A. et al. Regulation of vertebrate nervous system alternative splicing and development by an SR-related protein. Cell **138**, 898-910 (2009). https://doi.org:10.1016/j.cell.2009.06.012*

51 *Raj, B. et al. A global regulatory mechanism for activating an exon network required for neurogenesis. Mol Cell **56**, 90-103 (2014). https://doi.org:10.1016/j.molcel.2014.08.011*

52 *Quesnel-Vallieres, M., Irimia, M., Cordes, S. P. & Blencowe, B. J. Essential roles for the splicing regulator nSR100/SRRM4 during nervous system development. Genes Dev* ***29****, 746-759 (2015).* https://doi.org:10.1101/gad.256115.114

53 *Rouskin, S., Zubradt, M., Washietl, S., Kellis, M. & Weissman, J. S. Genome-wide probing of RNA structure reveals active unfolding of mRNA structures in vivo. Nature* ***505****, 701-705 (2014).* https://doi.org:10.1038/nature12894

54 *Sanchez de Groot, N. et al. RNA structure drives interaction with proteins. Nat Commun* ***10****, 3246 (2019).* https://doi.org:10.1038/s41467-019-10923-5

55 *Ding, Y. et al. In vivo genome-wide profiling of RNA secondary structure reveals novel regulatory features. Nature* ***505****, 696-700 (2014).* https://doi.org:10.1038/nature12756

56 *Shilo, A., Tosto, F. A., Rausch, J. W., Le Grice, S. F. J. & Misteli, T. Interplay of primary sequence, position and secondary RNA structure determines alternative splicing of LMNA in a pre-mature aging syndrome. Nucleic Acids Res* ***47****, 5922-5935 (2019).* https://doi.org:10.1093/nar/gkz259

57 *Gosai, S. J. et al. Global analysis of the RNA-protein interaction and RNA secondary structure landscapes of the Arabidopsis nucleus. Mol Cell* ***57****, 376-388 (2015).* https://doi.org:10.1016/j.molcel.2014.12.004

58 *Talkish, J., May, G., Lin, Y., Woolford, J. L., Jr. & McManus, C. J. Mod-seq: high-throughput sequencing for chemical probing of RNA structure. RNA* ***20****, 713-720 (2014).* https://doi.org:10.1261/rna.042218.113

59 *Liu, Z. et al. In vivo nuclear RNA structurome reveals RNA-structure regulation of mRNA processing in plants. Genome Biol* ***22****, 11 (2021).* https://doi.org:10.1186/s13059-020-02236-4

60 *Raker, V. A., Mironov, A. A., Gelfand, M. S. & Pervouchine, D. D. Modulation of alternative splicing by long-range RNA structures in Drosophila. Nucleic Acids Res* ***37****, 4533-4544 (2009).* https://doi.org:10.1093/nar/gkp407

61 *Fedorova, O. et al. Small molecules that target group II introns are potent antifungal agents. Nat Chem Biol* ***14****, 1073-1078 (2018).* https://doi.org:10.1038/s41589-018-0142-0

62 *Mandal, M., Boese, B., Barrick, J. E., Winkler, W. C. & Breaker, R. R. Riboswitches control fundamental biochemical pathways in Bacillus subtilis and other bacteria. Cell* ***113****, 577-586 (2003).* https://doi.org:10.1016/s0092-8674(03)00391-x

63 *Kubodera, T. et al. Thiamine-regulated gene expression of Aspergillus oryzae thiA requires splicing of the intron containing a riboswitch-like domain in the 5'-UTR. FEBS Lett* ***555****, 516-520 (2003).* https://doi.org:10.1016/s0014-5793(03)01335-8

64 *Cheah, M. T., Wachter, A., Sudarsan, N. & Breaker, R. R. Control of alternative RNA splicing and gene expression by eukaryotic riboswitches. Nature* ***447****, 497-500 (2007).* https://doi.org:10.1038/nature05769

65 *Croft, M. T., Moulin, M., Webb, M. E. & Smith, A. G. Thiamine biosynthesis in algae is regulated by riboswitches. Proc Natl Acad Sci U S A* ***104****, 20770-20775 (2007).* https://doi.org:10.1073/pnas.0705786105

66 *Bocobza, S. et al. Riboswitch-dependent gene regulation and its evolution in the plant kingdom. Genes Dev* ***21****, 2874-2879 (2007).* https://doi.org:10.1101/gad.443907

67 *Wachter, A. et al. Riboswitch control of gene expression in plants by splicing and alternative 3' end processing of mRNAs. Plant Cell* ***19****, 3437-3450 (2007).* https://doi.org:10.1105/tpc.107.053645

68 *Li, S. & Breaker, R. R. Eukaryotic TPP riboswitch regulation of alternative splicing involving long-distance base pairing. Nucleic Acids Res* ***41****, 3022-3031 (2013).* https://doi.org:10.1093/nar/gkt057

69 *Wan, Y. et al. Landscape and variation of RNA secondary structure across the human transcriptome. Nature **505**, 706-709 (2014). https://doi.org:10.1038/nature12946*

70 *Kalmykova, S. et al. Conserved long-range base pairings are associated with pre-mRNA processing of human genes. Nat Commun **12**, 2300 (2021). https://doi.org:10.1038/s41467-021-22549-7*

71 *Lev-Maor, G. et al. Intronic Alus influence alternative splicing. PLoS Genet **4**, e1000204 (2008). https://doi.org:10.1371/journal.pgen.1000204*

72 *Miriami, E., Margalit, H. & Sperling, R. Conserved sequence elements associated with exon skipping. Nucleic Acids Res **31**, 1974-1983 (2003). https://doi.org:10.1093/nar/gkg279*

73 *Konig, J. et al. iCLIP reveals the function of hnRNP particles in splicing at individual nucleotide resolution. Nat Struct Mol Biol **17**, 909-915 (2010). https://doi.org:10.1038/nsmb.1838*

74 *Liu, N. et al. N(6)-methyladenosine-dependent RNA structural switches regulate RNA-protein interactions. Nature **518**, 560-564 (2015). https://doi.org:10.1038/nature14234*

75 *Jacquenet, S. et al. Conserved stem-loop structures in the HIV-1 RNA region containing the A3 3′ splice site and its cis-regulatory element: possible involvement in RNA splicing. Nucleic Acids Res **29**, 464-478 (2001). https://doi.org:10.1093/nar/29.2.464*

76 *Spitale, R. C. et al. Structural imprints in vivo decode RNA regulatory mechanisms. Nature **519**, 486-490 (2015). https://doi.org:10.1038/nature14263*

77 *Loeb, D. D., Mack, A. A. & Tian, R. A secondary structure that contains the 5′ and 3′ splice sites suppresses splicing of duck hepatitis B virus pregenomic RNA. J Virol **76**, 10195-10202 (2002). https://doi.org:10.1128/jvi.76.20.10195-10202.2002*

78 *Howe, K. J. & Ares, M., Jr. Intron self-complementarity enforces exon inclusion in a yeast pre-mRNA. Proc Natl Acad Sci U S A **94**, 12467-12472 (1997). https://doi.org:10.1073/pnas.94.23.12467*

79 *Libri, D., Stutz, F., McCarthy, T. & Rosbash, M. RNA structural patterns and splicing: molecular basis for an RNA-based enhancer. RNA **1**, 425-436 (1995).*

80 *Graveley, B. R. Mutually exclusive splicing of the insect Dscam pre-mRNA directed by competing intronic RNA secondary structures. Cell **123**, 65-73 (2005). https://doi.org:10.1016/j.cell.2005.07.028*

81 *Yang, Y. et al. RNA secondary structure in mutually exclusive splicing. Nat Struct Mol Biol **18**, 159-168 (2011). https://doi.org:10.1038/nsmb.1959*

82 *Clouet d'Orval, B. et al. RNA secondary structure repression of a muscle-specific exon in HeLa cell nuclear extracts. Science **252**, 1823-1828 (1991). https://doi.org:10.1126/science.2063195*

83 *Solnick, D. Alternative splicing caused by RNA secondary structure. Cell **43**, 667-676 (1985). https://doi.org:10.1016/0092-8674(85)90239-9*

84 *Cote, J. & Chabot, B. Natural base-pairing interactions between 5′ splice site and branch site sequences affect mammalian 5′ splice site selection. RNA **3**, 1248-1261 (1997).*

85 *Blanchette, M. & Chabot, B. Modulation of exon skipping by high-affinity hnRNP A1-binding sites and by intron elements that repress splice site utilization. EMBO J **18**, 1939-1952 (1999). https://doi.org:10.1093/emboj/18.7.1939*

86 *Lovci, M. T. et al. Rbfox proteins regulate alternative mRNA splicing through evolutionarily conserved RNA bridges. Nat Struct Mol Biol **20**, 1434-1442 (2013). https://doi.org:10.1038/nsmb.2699*

87 *Chou, M. Y., Underwood, J. G., Nikolic, J., Luu, M. H. & Black, D. L. Multisite RNA binding and release of polypyrimidine tract binding protein during the regulation of c-*

src neural-specific splicing. Mol Cell ***5****, 949-957 (2000).* https://doi.org:10.1016/s1097-2765(00)80260-9

88 *Taube, J. R. et al. PMD patient mutations reveal a long-distance intronic interaction that regulates PLP1/DM20 alternative splicing. Hum Mol Genet* ***23****, 5464-5478 (2014).* https://doi.org:10.1093/hmg/ddu271

89 *Zychlinski, D. et al. Limited complementarity between U1 snRNA and a retroviral 5' splice site permits its attenuation via RNA secondary structure. Nucleic Acids Res* ***37****, 7429-7440 (2009).* https://doi.org:10.1093/nar/gkp694

90 *Liu, H. X., Goodall, G. J., Kole, R. & Filipowicz, W. Effects of secondary structure on pre-mRNA splicing: hairpins sequestering the 5' but not the 3' splice site inhibit intron processing in Nicotiana plumbaginifolia. EMBO J* ***14****, 377-388 (1995).* https://doi.org:10.1002/j.1460-2075.1995.tb07012.x

91 *Muro, A. F., Iaconcig, A. & Baralle, F. E. Regulation of the fibronectin EDA exon alternative splicing. Cooperative role of the exonic enhancer element and the 5' splicing site. FEBS Lett* ***437****, 137-141 (1998).* https://doi.org:10.1016/s0014-5793(98)01201-0

92 *Buratti, E. et al. RNA folding affects the recruitment of SR proteins by mouse and human polypurinic enhancer elements in the fibronectin EDA exon. Mol Cell Biol* ***24****, 1387-1400 (2004).* https://doi.org:10.1128/MCB.24.3.1387-1400.2004

93 *Muro, A. F. et al. Regulation of fibronectin EDA exon alternative splicing: possible role of RNA secondary structure for enhancer display. Mol Cell Biol* ***19****, 2657-2671 (1999).* https://doi.org:10.1128/MCB.19.4.2657

94 *Singh, N. N., Singh, R. N. & Androphy, E. J. Modulating role of RNA structure in alternative splicing of a critical exon in the spinal muscular atrophy genes. Nucleic Acids Res* ***35****, 371-389 (2007).* https://doi.org:10.1093/nar/gkl1050

95 *Miyaso, H. et al. An intronic splicing enhancer element in survival motor neuron (SMN) pre-mRNA. J Biol Chem* ***278****, 15825-15831 (2003).* https://doi.org:10.1074/jbc.M209271200

96 *Donahue, C. P., Muratore, C., Wu, J. Y., Kosik, K. S. & Wolfe, M. S. Stabilization of the tau exon 10 stem loop alters pre-mRNA splicing. J Biol Chem* ***281****, 23302-23306 (2006).* https://doi.org:10.1074/jbc.C600143200

97 *Varani, L. et al. Structure of tau exon 10 splicing regulatory element RNA and destabilization by mutations of frontotemporal dementia and parkinsonism linked to chromosome 17. Proc Natl Acad Sci U S A* ***96****, 8229-8234 (1999).* https://doi.org:10.1073/pnas.96.14.8229

98 *Grover, A. et al. 5' splice site mutations in tau associated with the inherited dementia FTDP-17 affect a stem-loop structure that regulates alternative splicing of exon 10. J Biol Chem* ***274****, 15134-15143 (1999).* https://doi.org:10.1074/jbc.274.21.15134

99 *Hutton, M. et al. Association of missense and 5'-splice-site mutations in tau with the inherited dementia FTDP-17. Nature* ***393****, 702-705 (1998).* https://doi.org:10.1038/31508

100 *D'Souza, I. et al. Missense and silent tau gene mutations cause frontotemporal dementia with parkinsonism-chromosome 17 type, by affecting multiple alternative RNA splicing regulatory elements. Proc Natl Acad Sci U S A* ***96****, 5598-5603 (1999).* https://doi.org:10.1073/pnas.96.10.5598

101 *Spillantini, M. G. et al. Mutation in the tau gene in familial multiple system tauopathy with presenile dementia. Proc Natl Acad Sci U S A* ***95****, 7737-7741 (1998).* https://doi.org:10.1073/pnas.95.13.7737

102 *Young, J. J., Lavakumar, M., Tampi, D., Balachandran, S. & Tampi, R. R. Frontotemporal dementia: latest evidence and clinical implications. Ther Adv Psychopharmacol* ***8****, 33-48 (2018).* https://doi.org:10.1177/2045125317739818

103 *Yadegari, H. et al. Intron retention resulting from a silent mutation in the VWF gene that structurally influences the 5′ splice site. Blood* ***128****, 2144-2152 (2016).* https://doi.org:10.1182/blood-2016-02-699686

104 *Charpentier, B. & Rosbash, M. Intramolecular structure in yeast introns aids the early steps of in vitro spliceosome assembly. RNA* ***2****, 509-522 (1996).*

105 *Tomezsko, P. J. et al. Determination of RNA structural diversity and its role in HIV-1 RNA splicing. Nature* ***582****, 438-442 (2020).* https://doi.org:10.1038/s41586-020-2253-5

106 *Gahura, O., Hammann, C., Valentova, A., Puta, F. & Folk, P. Secondary structure is required for 3′ splice site recognition in yeast. Nucleic Acids Res* ***39****, 9759-9767 (2011).* https://doi.org:10.1093/nar/gkr662

107 *Goguel, V., Wang, Y. & Rosbash, M. Short artificial hairpins sequester splicing signals and inhibit yeast pre-mRNA splicing. Mol Cell Biol* ***13****, 6841-6848 (1993).* https://doi.org:10.1128/mcb.13.11.6841-6848.1993

108 *Deshler, J. O. & Rossi, J. J. Unexpected point mutations activate cryptic 3′ splice sites by perturbing a natural secondary structure within a yeast intron. Genes Dev* ***5****, 1252-1263 (1991).* https://doi.org:10.1101/gad.5.7.1252

109 *Estes, P. A., Cooke, N. E. & Liebhaber, S. A. A native RNA secondary structure controls alternative splice-site selection and generates two human growth hormone isoforms. J Biol Chem* ***267****, 14902-14908 (1992).*

110 *Dhir, A., Buratti, E., van Santen, M. A., Luhrmann, R. & Baralle, F. E. The intronic splicing code: multiple factors involved in ATM pseudoexon definition. EMBO J* ***29****, 749-760 (2010).* https://doi.org:10.1038/emboj.2009.397

111 *Chen, Y. & Stephan, W. Compensatory evolution of a precursor messenger RNA secondary structure in the Drosophila melanogaster Adh gene. Proc Natl Acad Sci U S A* ***100****, 11499-11504 (2003).* https://doi.org:10.1073/pnas.1932834100

112 *Hiller, M., Zhang, Z., Backofen, R. & Stamm, S. Pre-mRNA secondary structures influence exon recognition. PLoS Genet* ***3****, e204 (2007).* https://doi.org:10.1371/journal.pgen.0030204

113 *Warf, M. B. & Berglund, J. A. MBNL binds similar RNA structures in the CUG repeats of myotonic dystrophy and its pre-mRNA substrate cardiac troponin T. RNA* ***13****, 2238-2251 (2007).* https://doi.org:10.1261/rna.610607

114 *Damgaard, C. K., Tange, T. O. & Kjems, J. hnRNP A1 controls HIV-1 mRNA splicing through cooperative binding to intron and exon splicing silencers in the context of a conserved secondary structure. RNA* ***8****, 1401-1415 (2002).* https://doi.org:10.1017/s1355838202023075

115 *Shi, H., Hoffman, B. E. & Lis, J. T. A specific RNA hairpin loop structure binds the RNA recognition motifs of the Drosophila SR protein B52. Mol Cell Biol* ***17****, 2649-2657 (1997).* https://doi.org:10.1128/MCB.17.5.2649

116 *Buckanovich, R. J. & Darnell, R. B. The neuronal RNA binding protein Nova-1 recognizes specific RNA targets in vitro and in vivo. Mol Cell Biol* ***17****, 3194-3201 (1997).* https://doi.org:10.1128/MCB.17.6.3194

117 *Brugiolo, M., Herzel, L. & Neugebauer, K. M. Counting on co-transcriptional splicing. F1000Prime Rep* ***5****, 9 (2013).* https://doi.org:10.12703/P5-9

118 *Schor, I. E., Rascovan, N., Pelisch, F., Allo, M. & Kornblihtt, A. R. Neuronal cell depolarization induces intragenic chromatin modifications affecting NCAM alternative*

splicing. Proc Natl Acad Sci U S A ***106****, 4325-4330 (2009).* *https://doi.org:10.1073/pnas.0810666106*

119 *Kadener, S. et al. Antagonistic effects of T-Ag and VP16 reveal a role for RNA pol II elongation on alternative splicing. EMBO J* ***20****, 5759-5768 (2001).* *https://doi.org:10.1093/emboj/20.20.5759*

120 *de la Mata, M., Lafaille, C. & Kornblihtt, A. R. First come, first served revisited: factors affecting the same alternative splicing event have different effects on the relative rates of intron removal. RNA* ***16****, 904-912 (2010).* *https://doi.org:10.1261/rna.1993510*

121 *Nogues, G., Kadener, S., Cramer, P., Bentley, D. & Kornblihtt, A. R. Transcriptional activators differ in their abilities to control alternative splicing. J Biol Chem* ***277****, 43110-43114 (2002).* *https://doi.org:10.1074/jbc.M208418200*

122 *Howe, K. J., Kane, C. M. & Ares, M., Jr. Perturbation of transcription elongation influences the fidelity of internal exon inclusion in Saccharomyces cerevisiae. RNA* ***9****, 993-1006 (2003).* *https://doi.org:10.1261/rna.5390803*

123 *Munoz, M. J. et al. DNA damage regulates alternative splicing through inhibition of RNA polymerase II elongation. Cell* ***137****, 708-720 (2009).* *https://doi.org:10.1016/j.cell.2009.03.010*

124 *Eperon, L. P., Graham, I. R., Griffiths, A. D. & Eperon, I. C. Effects of RNA secondary structure on alternative splicing of pre-mRNA: is folding limited to a region behind the transcribing RNA polymerase? Cell* ***54****, 393-401 (1988).* *https://doi.org:10.1016/0092-8674(88)90202-4*

125 *Lin, S., Xiao, R., Sun, P., Xu, X. & Fu, X. D. Dephosphorylation-dependent sorting of SR splicing factors during mRNP maturation. Mol Cell* ***20****, 413-425 (2005).* *https://doi.org:10.1016/j.molcel.2005.09.015*

126 *Ling, Y., Mahfouz, M. M. & Zhou, S. Pre-mRNA alternative splicing as a modulator for heat stress response in plants. Trends Plant Sci* ***26****, 1153-1170 (2021).* *https://doi.org:10.1016/j.tplants.2021.07.008*

127 *Preussner, M. et al. Body Temperature Cycles Control Rhythmic Alternative Splicing in Mammals. Mol Cell* ***67****, 433-446 e434 (2017).* *https://doi.org:10.1016/j.molcel.2017.06.006*

128 *Shi, Y., Nishida, K., Campigli Di Giammartino, D. & Manley, J. L. Heat shock-induced SRSF10 dephosphorylation displays thermotolerance mediated by Hsp27. Mol Cell Biol* ***31****, 458-465 (2011).* *https://doi.org:10.1128/MCB.01123-10*

129 *Haltenhof, T. et al. A Conserved Kinase-Based Body-Temperature Sensor Globally Controls Alternative Splicing and Gene Expression. Mol Cell* ***78****, 57-69 e54 (2020).* *https://doi.org:10.1016/j.molcel.2020.01.028*

130 *Geuens, T., Bouhy, D. & Timmerman, V. The hnRNP family: insights into their role in health and disease. Hum Genet* ***135****, 851-867 (2016).* *https://doi.org:10.1007/s00439-016-1683-5*

131 *Wan, Y. et al. Genome-wide measurement of RNA folding energies. Mol Cell* ***48****, 169-181 (2012).* *https://doi.org:10.1016/j.molcel.2012.08.008*

132 *Lu, Z. J., Turner, D. H. & Mathews, D. H. A set of nearest neighbor parameters for predicting the enthalpy change of RNA secondary structure formation. Nucleic Acids Res* ***34****, 4912-4924 (2006).* *https://doi.org:10.1093/nar/gkl472*

133 *Lorenz, R. et al. ViennaRNA Package 2.0. Algorithms Mol Biol* ***6****, 26 (2011).* *https://doi.org:10.1186/1748-7188-6-26*

134 *Chursov, A., Kopetzky, S. J., Bocharov, G., Frishman, D. & Shneider, A. RNAtips: Analysis of temperature-induced changes of RNA secondary structure. Nucleic Acids Res* ***41****, W486-491 (2013).* *https://doi.org:10.1093/nar/gkt486*

135 *Meyer, M., Plass, M., Perez-Valle, J., Eyras, E. & Vilardell, J. Deciphering 3'ss selection in the yeast genome reveals an RNA thermosensor that mediates alternative splicing. Mol Cell **43**, 1033-1039 (2011). https://doi.org:10.1016/j.molcel.2011.07.030*

136 *Broft, P., Rosenkranz, R., Schleiff, E., Hengesbach, M. & Schwalbe, H. Structural analysis of temperature-dependent alternative splicing of HsfA2 pre-mRNA from tomato plants. RNA Biol **19**, 266-278 (2022). https://doi.org:10.1080/15476286.2021.2024034*

137 *Dominguez, C. E., Cunningham, D., Venkataramany, A. S. & Chandler, D. S. Heat increases full-length SMN splicing: promise for splice-augmenting therapies for SMA. Hum Genet **141**, 239-256 (2022). https://doi.org:10.1007/s00439-021-02408-7*

138 *Sidaway-Lee, K., Costa, M. J., Rand, D. A., Finkenstadt, B. & Penfield, S. Direct measurement of transcription rates reveals multiple mechanisms for configuration of the Arabidopsis ambient temperature response. Genome Biol **15**, R45 (2014). https://doi.org:10.1186/gb-2014-15-3-r45*

139 *Svoboda, P. & Di Cara, A. Hairpin RNA: a secondary structure of primary importance. Cell Mol Life Sci **63**, 901-908 (2006). https://doi.org:10.1007/s00018-005-5558-5*

140 *Schudoma, C., May, P., Nikiforova, V. & Walther, D. Sequence-structure relationships in RNA loops: establishing the basis for loop homology modeling. Nucleic Acids Res **38**, 970-980 (2010). https://doi.org:10.1093/nar/gkp1010*

141 *Hermann, T. & Patel, D. J. RNA bulges as architectural and recognition motifs. Structure **8**, R47-54 (2000). https://doi.org:10.1016/s0969-2126(00)00110-6*

142 *Ben-Asouli, Y., Banai, Y., Pel-Or, Y., Shir, A. & Kaempfer, R. Human interferon-gamma mRNA autoregulates its translation through a pseudoknot that activates the interferon-inducible protein kinase PKR. Cell **108**, 221-232 (2002). https://doi.org:10.1016/s0092-8674(02)00616-5*

143 *Huang, L. & Lilley, D. M. J. The Kink Turn, a Key Architectural Element in RNA Structure. J Mol Biol **428**, 790-801 (2016). https://doi.org:10.1016/j.jmb.2015.09.026*

144 *Diamond, J. M., Turner, D. H. & Mathews, D. H. Thermodynamics of three-way multibranch loops in RNA. Biochemistry **40**, 6971-6981 (2001). https://doi.org:10.1021/bi0029548*

145 *Wang, X. W., Liu, C. X., Chen, L. L. & Zhang, Q. C. RNA structure probing uncovers RNA structure-dependent biological functions. Nat Chem Biol **17**, 755-766 (2021). https://doi.org:10.1038/s41589-021-00805-7*

146 *Piazza, A. et al. Short loop length and high thermal stability determine genomic instability induced by G-quadruplex-forming minisatellites. EMBO J **34**, 1718-1734 (2015). https://doi.org:10.15252/embj.201490702*

147 *Guedin, A., Gros, J., Alberti, P. & Mergny, J. L. How long is too long? Effects of loop size on G-quadruplex stability. Nucleic Acids Res **38**, 7858-7868 (2010). https://doi.org:10.1093/nar/gkq639*

148 *Fay, M. M., Lyons, S. M. & Ivanov, P. RNA G-Quadruplexes in Biology: Principles and Molecular Mechanisms. J Mol Biol **429**, 2127-2147 (2017). https://doi.org:10.1016/j.jmb.2017.05.017*

149 *Chambers, V. S. et al. High-throughput sequencing of DNA G-quadruplex structures in the human genome. Nat Biotechnol **33**, 877-881 (2015). https://doi.org:10.1038/nbt.3295*

150 *Gong, J. Y. et al. G-quadruplex structural variations in human genome associated with single-nucleotide variations and their impact on gene activity. Proc Natl Acad Sci U S A **118** (2021). https://doi.org:10.1073/pnas.2013230118*

151 *Kwok, C. K., Marsico, G., Sahakyan, A. B., Chambers, V. S. & Balasubramanian, S. rG4-seq reveals widespread formation of G-quadruplex structures in the human transcriptome. Nat Methods* ***13****, 841-844 (2016).* https://doi.org:10.1038/nmeth.3965

152 *Lyu, K., Chow, E. Y., Mou, X., Chan, T. F. & Kwok, C. K. RNA G-quadruplexes (rG4s): genomics and biological functions. Nucleic Acids Res* ***49****, 5426-5450 (2021).* https://doi.org:10.1093/nar/gkab187

153 *Miglietta, G., Russo, M. & Capranico, G. G-quadruplex-R-loop interactions and the mechanism of anticancer G-quadruplex binders. Nucleic Acids Res* ***48****, 11942-11957 (2020).* https://doi.org:10.1093/nar/gkaa944

154 *Zhang, J. Y., Zheng, K. W., Xiao, S., Hao, Y. H. & Tan, Z. Mechanism and manipulation of DNA:RNA hybrid G-quadruplex formation in transcription of G-rich DNA. J Am Chem Soc* ***136****, 1381-1390 (2014).* https://doi.org:10.1021/ja4085572

155 *Sen, D. & Gilbert, W. A sodium-potassium switch in the formation of four-stranded G4-DNA. Nature* ***344****, 410-414 (1990).* https://doi.org:10.1038/344410a0

156 *Bhattacharyya, D., Mirihana Arachchilage, G. & Basu, S. Metal Cations in G-Quadruplex Folding and Stability. Front Chem* ***4****, 38 (2016).* https://doi.org:10.3389/fchem.2016.00038

157 *Liu, L. Y., Ma, T. Z., Zeng, Y. L., Liu, W. & Mao, Z. W. Structural Basis of Pyridostatin and Its Derivatives Specifically Binding to G-Quadruplexes. J Am Chem Soc* ***144****, 11878-11887 (2022).* https://doi.org:10.1021/jacs.2c04775

158 *Sexton, A. N. & Collins, K. The 5′ guanosine tracts of human telomerase RNA are recognized by the G-quadruplex binding domain of the RNA helicase DHX36 and function to increase RNA accumulation. Mol Cell Biol* ***31****, 736-743 (2011).* https://doi.org:10.1128/MCB.01033-10

159 *Lattmann, S., Stadler, M. B., Vaughn, J. P., Akman, S. A. & Nagamine, Y. The DEAH-box RNA helicase RHAU binds an intramolecular RNA G-quadruplex in TERC and associates with telomerase holoenzyme. Nucleic Acids Res* ***39****, 9390-9404 (2011).* https://doi.org:10.1093/nar/gkr630

160 *Lattmann, S., Giri, B., Vaughn, J. P., Akman, S. A. & Nagamine, Y. Role of the amino terminal RHAU-specific motif in the recognition and resolution of guanine quadruplex-RNA by the DEAH-box RNA helicase RHAU. Nucleic Acids Res* ***38****, 6219-6233 (2010).* https://doi.org:10.1093/nar/gkq372

161 *Chakraborty, P. & Grosse, F. Human DHX9 helicase preferentially unwinds RNA-containing displacement loops (R-loops) and G-quadruplexes. DNA Repair (Amst)* ***10****, 654-665 (2011).* https://doi.org:10.1016/j.dnarep.2011.04.013

162 *Zhang, F. et al. Fragile X mental retardation protein modulates the stability of its m6A-marked messenger RNA targets. Hum Mol Genet* ***27****, 3936-3950 (2018).* https://doi.org:10.1093/hmg/ddy292

163 *Biffi, G., Di Antonio, M., Tannahill, D. & Balasubramanian, S. Visualization and selective chemical targeting of RNA G-quadruplex structures in the cytoplasm of human cells. Nat Chem* ***6****, 75-80 (2014).* https://doi.org:10.1038/nchem.1805

164 *Belotserkovskii, B. P., Tornaletti, S., D'Souza, A. D. & Hanawalt, P. C. R-loop generation during transcription: Formation, processing and cellular outcomes. DNA Repair (Amst)* ***71****, 69-81 (2018).* https://doi.org:10.1016/j.dnarep.2018.08.009

165 *Lee, C. Y. et al. R-loop induced G-quadruplex in non-template promotes transcription by successive R-loop formation. Nat Commun* ***11****, 3392 (2020).* https://doi.org:10.1038/s41467-020-17176-7

166 *Bugaut, A. & Balasubramanian, S. 5′-UTR RNA G-quadruplexes: translation regulation and targeting. Nucleic Acids Res* ***40****, 4727-4741 (2012).* https://doi.org:10.1093/nar/gks068

167 *Lee, D. S. M., Ghanem, L. R. & Barash, Y. Integrative analysis reveals RNA G-quadruplexes in UTRs are selectively constrained and enriched for functional associations. Nat Commun **11**, 527 (2020). https://doi.org:10.1038/s41467-020-14404-y*

168 *Guo, J. U. & Bartel, D. P. RNA G-quadruplexes are globally unfolded in eukaryotic cells and depleted in bacteria. Science **353** (2016). https://doi.org:10.1126/science.aaf5371*

169 *Wells, S. E., Hughes, J. M., Igel, A. H. & Ares, M., Jr. Use of dimethyl sulfate to probe RNA structure in vivo. Methods Enzymol **318**, 479-493 (2000). https://doi.org:10.1016/s0076-6879(00)18071-1*

170 *Caterino, M. & Paeschke, K. Action and function of helicases on RNA G-quadruplexes. Methods **204**, 110-125 (2022). https://doi.org:10.1016/j.ymeth.2021.09.003*

171 *Liu, Y., Zhu, X., Wang, K., Zhang, B. & Qiu, S. Corrigendum: The Cellular Functions and Molecular Mechanisms of G-Quadruplex Unwinding Helicases in Humans. Front Mol Biosci **8**, 833430 (2021). https://doi.org:10.3389/fmolb.2021.833430*

172 *Yang, X. et al. RNA G-quadruplex structures exist and function in vivo in plants. Genome Biol **21**, 226 (2020). https://doi.org:10.1186/s13059-020-02142-9*

173 *Yang, S. Y. et al. Transcriptome-wide identification of transient RNA G-quadruplexes in human cells. Nat Commun **9**, 4730 (2018). https://doi.org:10.1038/s41467-018-07224-8*

174 *Georgakopoulos-Soares, I. et al. Alternative splicing modulation by G-quadruplexes. Nat Commun **13**, 2404 (2022). https://doi.org:10.1038/s41467-022-30071-7*

175 *Fisette, J. F., Montagna, D. R., Mihailescu, M. R. & Wolfe, M. S. A G-rich element forms a G-quadruplex and regulates BACE1 mRNA alternative splicing. J Neurochem **121**, 763-773 (2012). https://doi.org:10.1111/j.1471-4159.2012.07680.x*

176 *Neckles, C. et al. HNRNPH1-dependent splicing of a fusion oncogene reveals a targetable RNA G-quadruplex interaction. RNA **25**, 1731-1750 (2019). https://doi.org:10.1261/rna.072454.119*

177 *Ribeiro, M. M. et al. G-quadruplex formation enhances splicing efficiency of PAX9 intron 1. Hum Genet **134**, 37-44 (2015). https://doi.org:10.1007/s00439-014-1485-6*

178 *Marcel, V. et al. G-quadruplex structures in TP53 intron 3: role in alternative splicing and in production of p53 mRNA isoforms. Carcinogenesis **32**, 271-278 (2011). https://doi.org:10.1093/carcin/bgq253*

179 *Huang, H., Zhang, J., Harvey, S. E., Hu, X. & Cheng, C. RNA G-quadruplex secondary structure promotes alternative splicing via the RNA-binding protein hnRNPF. Genes Dev **31**, 2296-2309 (2017). https://doi.org:10.1101/gad.305862.117*

180 *Didiot, M. C. et al. The G-quartet containing FMRP binding site in FMR1 mRNA is a potent exonic splicing enhancer. Nucleic Acids Res **36**, 4902-4912 (2008). https://doi.org:10.1093/nar/gkn472*

181 *Blice-Baum, A. C. & Mihailescu, M. R. Biophysical characterization of G-quadruplex forming FMR1 mRNA and of its interactions with different fragile X mental retardation protein isoforms. RNA **20**, 103-114 (2014). https://doi.org:10.1261/rna.041442.113*

182 *Weldon, C. et al. Identification of G-quadruplexes in long functional RNAs using 7-deazaguanine RNA. Nat Chem Biol **13**, 18-20 (2017). https://doi.org:10.1038/nchembio.2228*

183 *Beaudoin, J. D. & Perreault, J. P. Exploring mRNA 3'-UTR G-quadruplexes: evidence of roles in both alternative polyadenylation and mRNA shortening. Nucleic Acids Res **41**, 5898-5911 (2013). https://doi.org:10.1093/nar/gkt265*

184 *Subramanian, M. et al. G-quadruplex RNA structure as a signal for neurite mRNA targeting. EMBO Rep **12**, 697-704 (2011). https://doi.org:10.1038/embor.2011.76*

185 *Fay, M. M., Anderson, P. J. & Ivanov, P. ALS/FTD-Associated C9ORF72 Repeat RNA Promotes Phase Transitions In Vitro and in Cells. Cell Rep* ***21****, 3573-3584 (2017).* https://doi.org:10.1016/j.celrep.2017.11.093

186 *Conlon, E. G. et al. The C9ORF72 GGGGCC expansion forms RNA G-quadruplex inclusions and sequesters hnRNP H to disrupt splicing in ALS brains. Elife* ***5*** *(2016).* https://doi.org:10.7554/eLife.17820

187 *Wolfe, A. L. et al. RNA G-quadruplexes cause eIF4A-dependent oncogene translation in cancer. Nature* ***513****, 65-70 (2014).* https://doi.org:10.1038/nature13485

188 *Benhalevy, D. et al. The Human CCHC-type Zinc Finger Nucleic Acid-Binding Protein Binds G-Rich Elements in Target mRNA Coding Sequences and Promotes Translation. Cell Rep* ***18****, 2979-2990 (2017).* https://doi.org:10.1016/j.celrep.2017.02.080

189 *Kumari, S., Bugaut, A., Huppert, J. L. & Balasubramanian, S. An RNA G-quadruplex in the 5′ UTR of the NRAS proto-oncogene modulates translation. Nat Chem Biol* ***3****, 218-221 (2007).* https://doi.org:10.1038/nchembio864

190 *Wieland, M. & Hartig, J. S. RNA quadruplex-based modulation of gene expression. Chem Biol* ***14****, 757-763 (2007).* https://doi.org:10.1016/j.chembiol.2007.06.005

191 *Yi, Z., Sanjeev, M. & Singh, G. The Branched Nature of the Nonsense-Mediated mRNA Decay Pathway. Trends Genet* ***37****, 143-159 (2021).* https://doi.org:10.1016/j.tig.2020.08.010

192 *Gupta, P. & Li, Y. R. Upf proteins: highly conserved factors involved in nonsense mRNA mediated decay. Mol Biol Rep* ***45****, 39-55 (2018).* https://doi.org:10.1007/s11033-017-4139-7

193 *Boehm, V. et al. SMG5-SMG7 authorize nonsense-mediated mRNA decay by enabling SMG6 endonucleolytic activity. Nat Commun* ***12****, 3965 (2021).* https://doi.org:10.1038/s41467-021-24046-3

194 *Yamashita, A., Ohnishi, T., Kashima, I., Taya, Y. & Ohno, S. Human SMG-1, a novel phosphatidylinositol 3-kinase-related protein kinase, associates with components of the mRNA surveillance complex and is involved in the regulation of nonsense-mediated mRNA decay. Genes Dev* ***15****, 2215-2228 (2001).* https://doi.org:10.1101/gad.913001

195 *Metze, S., Herzog, V. A., Ruepp, M. D. & Muhlemann, O. Comparison of EJC-enhanced and EJC-independent NMD in human cells reveals two partially redundant degradation pathways. RNA* ***19****, 1432-1448 (2013).* https://doi.org:10.1261/rna.038893.113

196 *Buchwald, G. et al. Insights into the recruitment of the NMD machinery from the crystal structure of a core EJC-UPF3b complex. Proc Natl Acad Sci U S A* ***107****, 10050-10055 (2010).* https://doi.org:10.1073/pnas.1000993107

197 *Zhang, Z. & Krainer, A. R. Involvement of SR proteins in mRNA surveillance. Mol Cell* ***16****, 597-607 (2004).* https://doi.org:10.1016/j.molcel.2004.10.031

198 *Lindeboom, R. G. H., Vermeulen, M., Lehner, B. & Supek, F. The impact of nonsense-mediated mRNA decay on genetic disease, gene editing and cancer immunotherapy. Nat Genet* ***51****, 1645-1651 (2019).* https://doi.org:10.1038/s41588-019-0517-5

199 *Ge, Z., Quek, B. L., Beemon, K. L. & Hogg, J. R. Polypyrimidine tract binding protein 1 protects mRNAs from recognition by the nonsense-mediated mRNA decay pathway. Elife* ***5*** *(2016).* https://doi.org:10.7554/eLife.11155

200 *Kishor, A., Ge, Z. & Hogg, J. R. hnRNP L-dependent protection of normal mRNAs from NMD subverts quality control in B cell lymphoma. EMBO J* ***38*** *(2019).* https://doi.org:10.15252/embj.201899128

201 *Kebaara, B. W. & Atkin, A. L. Long 3′-UTRs target wild-type mRNAs for nonsense-mediated mRNA decay in Saccharomyces cerevisiae. Nucleic Acids Res* ***37****, 2771-2778 (2009).* https://doi.org:10.1093/nar/gkp146

202 *Pervouchine, D. et al. Integrative transcriptomic analysis suggests new autoregulatory splicing events coupled with nonsense-mediated mRNA decay. Nucleic Acids Res **47**, 5293-5306 (2019). https://doi.org:10.1093/nar/gkz193*

203 *Leclair, N. K. et al. Poison Exon Splicing Regulates a Coordinated Network of SR Protein Expression during Differentiation and Tumorigenesis. Mol Cell **80**, 648-665 e649 (2020). https://doi.org:10.1016/j.molcel.2020.10.019*

204 *Carvill, G. L. & Mefford, H. C. Poison exons in neurodevelopment and disease. Curr Opin Genet Dev **65**, 98-102 (2020). https://doi.org:10.1016/j.gde.2020.05.030*

205 *Garcia-Moreno, J. F. & Romao, L. Perspective in Alternative Splicing Coupled to Nonsense-Mediated mRNA Decay. Int J Mol Sci **21** (2020). https://doi.org:10.3390/ijms21249424*

206 *Hu, Z., Yau, C. & Ahmed, A. A. A pan-cancer genome-wide analysis reveals tumour dependencies by induction of nonsense-mediated decay. Nat Commun **8**, 15943 (2017). https://doi.org:10.1038/ncomms15943*

207 *Lindeboom, R. G., Supek, F. & Lehner, B. The rules and impact of nonsense-mediated mRNA decay in human cancers. Nat Genet **48**, 1112-1118 (2016). https://doi.org:10.1038/ng.3664*

208 *Popp, M. W. & Maquat, L. E. Leveraging Rules of Nonsense-Mediated mRNA Decay for Genome Engineering and Personalized Medicine. Cell **165**, 1319-1322 (2016). https://doi.org:10.1016/j.cell.2016.05.053*

209 *Kertesz, S. et al. Both introns and long 3'-UTRs operate as cis-acting elements to trigger nonsense-mediated decay in plants. Nucleic Acids Res **34**, 6147-6157 (2006). https://doi.org:10.1093/nar/gkl737*

210 *Nyiko, T., Sonkoly, B., Merai, Z., Benkovics, A. H. & Silhavy, D. Plant upstream ORFs can trigger nonsense-mediated mRNA decay in a size-dependent manner. Plant Mol Biol **71**, 367-378 (2009). https://doi.org:10.1007/s11103-009-9528-4*

211 *Tan, K., Stupack, D. G. & Wilkinson, M. F. Nonsense-mediated RNA decay: an emerging modulator of malignancy. Nat Rev Cancer **22**, 437-451 (2022). https://doi.org:10.1038/s41568-022-00481-2*

212 *Hug, N., Longman, D. & Caceres, J. F. Mechanism and regulation of the nonsense-mediated decay pathway. Nucleic Acids Res **44**, 1483-1495 (2016). https://doi.org:10.1093/nar/gkw010*

213 *Lou, C. H. et al. Nonsense-Mediated RNA Decay Influences Human Embryonic Stem Cell Fate. Stem Cell Reports **6**, 844-857 (2016). https://doi.org:10.1016/j.stemcr.2016.05.008*

214 *Han, X. et al. Nonsense-mediated mRNA decay: a 'nonsense' pathway makes sense in stem cell biology. Nucleic Acids Res **46**, 1038-1051 (2018). https://doi.org:10.1093/nar/gkx1272*

215 *Ryu, I. et al. eIF4A3 Phosphorylation by CDKs Affects NMD during the Cell Cycle. Cell Rep **26**, 2126-2139 e2129 (2019). https://doi.org:10.1016/j.celrep.2019.01.101*

216 *Hwang, J. & Maquat, L. E. Nonsense-mediated mRNA decay (NMD) in animal embryogenesis: to die or not to die, that is the question. Curr Opin Genet Dev **21**, 422-430 (2011). https://doi.org:10.1016/j.gde.2011.03.008*

217 *Bhuvanagiri, M., Schlitter, A. M., Hentze, M. W. & Kulozik, A. E. NMD: RNA biology meets human genetic medicine. Biochem J **430**, 365-377 (2010). https://doi.org:10.1042/BJ20100699*

218 *Derry, J. M., Kerns, J. A. & Francke, U. RBM3, a novel human gene in Xp11.23 with a putative RNA-binding domain. Hum Mol Genet **4**, 2307-2311 (1995). https://doi.org:10.1093/hmg/4.12.2307*

219 *Hiller, M. et al. Widespread occurrence of alternative splicing at NAGNAG acceptors contributes to proteome plasticity. Nat Genet* ***36****, 1255-1257 (2004).* https://doi.org:10.1038/ng1469

220 *Xing, D. & Li, Q. Q. Alternative polyadenylation: a mechanism maximizing transcriptome diversity in higher eukaryotes. Plant Signal Behav* ***4****, 440-442 (2009).* https://doi.org:10.1104/pp.108.129817

221 *Zhu, X., Buhrer, C. & Wellmann, S. Cold-inducible proteins CIRP and RBM3, a unique couple with activities far beyond the cold. Cell Mol Life Sci* ***73****, 3839-3859 (2016).* https://doi.org:10.1007/s00018-016-2253-7

222 *Maris, C., Dominguez, C. & Allain, F. H. The RNA recognition motif, a plastic RNA-binding platform to regulate post-transcriptional gene expression. FEBS J* ***272****, 2118-2131 (2005).* https://doi.org:10.1111/j.1742-4658.2005.04653.x

223 *Roy, S. et al. Structural and dynamic studies of the human RNA binding protein RBM3 reveals the molecular basis of its oligomerization and RNA recognition. FEBS J (2021).* https://doi.org:10.1111/febs.16301

224 *Dignon, G. L., Best, R. B. & Mittal, J. Biomolecular Phase Separation: From Molecular Driving Forces to Macroscopic Properties. Annu Rev Phys Chem* ***71****, 53-75 (2020).* https://doi.org:10.1146/annurev-physchem-071819-113553

225 *Sureban, S. M. et al. Translation regulatory factor RBM3 is a proto-oncogene that prevents mitotic catastrophe. Oncogene* ***27****, 4544-4556 (2008).* https://doi.org:10.1038/onc.2008.97

226 *Zhu, X., Zelmer, A., Kapfhammer, J. P. & Wellmann, S. Cold-inducible RBM3 inhibits PERK phosphorylation through cooperation with NF90 to protect cells from endoplasmic reticulum stress. FASEB J* ***30****, 624-634 (2016).* https://doi.org:10.1096/fj.15-274639

227 *Smart, F. et al. Two isoforms of the cold-inducible mRNA-binding protein RBM3 localize to dendrites and promote translation. J Neurochem* ***101****, 1367-1379 (2007).* https://doi.org:10.1111/j.1471-4159.2007.04521.x

228 *Pilotte, J., Cunningham, B. A., Edelman, G. M. & Vanderklish, P. W. Developmentally regulated expression of the cold-inducible RNA-binding motif protein 3 in euthermic rat brain. Brain Res* ***1258****, 12-24 (2009).* https://doi.org:10.1016/j.brainres.2008.12.050

229 *Chip, S. et al. The RNA-binding protein RBM3 is involved in hypothermia induced neuroprotection. Neurobiol Dis* ***43****, 388-396 (2011).* https://doi.org:10.1016/j.nbd.2011.04.010

230 *Danno, S., Itoh, K., Matsuda, T. & Fujita, J. Decreased expression of mouse Rbm3, a cold-shock protein, in Sertoli cells of cryptorchid testis. Am J Pathol* ***156****, 1685-1692 (2000).* https://doi.org:10.1016/S0002-9440(10)65039-0

231 *Ushio, A. & Eto, K. The Expression of the Cold Shock Protein RNA Binding Motif Protein 3 is Transcriptionally Responsive to Organ Temperature in Mice. Protein Pept Lett* ***28****, 270-275 (2021).* https://doi.org:10.2174/0929866527666200924144424

232 *Jackson, T. C., Janesko-Feldman, K., Carlson, S. W., Kotermanski, S. E. & Kochanek, P. M. Robust RBM3 and beta-klotho expression in developing neurons in the human brain. J Cereb Blood Flow Metab* ***39****, 2355-2367 (2019).* https://doi.org:10.1177/0271678X19878889

233 *Danno, S. et al. Increased transcript level of RBM3, a member of the glycine-rich RNA-binding protein family, in human cells in response to cold stress. Biochem Biophys Res Commun* ***236****, 804-807 (1997).* https://doi.org:10.1006/bbrc.1997.7059

234 *Jackson, T. C. et al. Cold stress protein RBM3 responds to temperature change in an ultra-sensitive manner in young neurons. Neuroscience* ***305****, 268-278 (2015).* https://doi.org:10.1016/j.neuroscience.2015.08.012

235 *Williams, D. R. et al. Seasonally hibernating phenotype assessed through transcript screening. Physiol Genomics* ***24****, 13-22 (2005).* https://doi.org:10.1152/physiolgenomics.00301.2004

236 *Xia, W., Su, L. & Jiao, J. Cold-induced protein RBM3 orchestrates neurogenesis via modulating Yap mRNA stability in cold stress. J Cell Biol* ***217****, 3464-3479 (2018).* https://doi.org:10.1083/jcb.201801143

237 *Neumann, A. et al. Alternative splicing coupled mRNA decay shapes the temperature-dependent transcriptome. EMBO Rep* ***21****, e51369 (2020).* https://doi.org:10.15252/embr.202051369

238 *Chappell, S. A., Owens, G. C. & Mauro, V. P. A 5′ Leader of Rbm3, a Cold Stress-induced mRNA, Mediates Internal Initiation of Translation with Increased Efficiency under Conditions of Mild Hypothermia. J Biol Chem* ***276****, 36917-36922 (2001).* https://doi.org:10.1074/jbc.M106008200

239 *Chappell, S. A. & Mauro, V. P. The internal ribosome entry site (IRES) contained within the RNA-binding motif protein 3 (Rbm3) mRNA is composed of functionally distinct elements. J Biol Chem* ***278****, 33793-33800 (2003).* https://doi.org:10.1074/jbc.M303495200

240 *Baranick, B. T. et al. Splicing mediates the activity of four putative cellular internal ribosome entry sites. Proc Natl Acad Sci U S A* ***105****, 4733-4738 (2008).* https://doi.org:10.1073/pnas.0710650105

241 *Peretti, D. et al. TrkB signaling regulates the cold-shock protein RBM3-mediated neuroprotection. Life Sci Alliance* ***4*** *(2021).* https://doi.org:10.26508/lsa.202000884

242 *Ushio, A. & Eto, K. RBM3 expression is upregulated by NF-kappaB p65 activity, protecting cells from apoptosis, during mild hypothermia. J Cell Biochem* ***119****, 5734-5749 (2018).* https://doi.org:10.1002/jcb.26757

243 *Yuan, X. et al. Expression regulation of cold-inducible protein RBM3 by FAK/Src signaling for neuroprotection against rotenone under mild hypothermia. Biochem Biophys Res Commun* ***534****, 240-247 (2021).* https://doi.org:10.1016/j.bbrc.2020.11.105

244 *Fujita, T. et al. TRPV4-dependent induction of a novel mammalian cold-inducible protein SRSF5 as well as CIRP and RBM3. Sci Rep 7, 2295 (2017).* https://doi.org:10.1038/s41598-017-02473-x

245 *Fujita, T. et al. Involvement of TRPV3 and TRPM8 ion channel proteins in induction of mammalian cold-inducible proteins. Biochem Biophys Res Commun* ***495****, 935-940 (2018).* https://doi.org:10.1016/j.bbrc.2017.11.136

246 *Nilius, B., Vriens, J., Prenen, J., Droogmans, G. & Voets, T. TRPV4 calcium entry channel: a paradigm for gating diversity. Am J Physiol Cell Physiol* ***286****, C195-205 (2004).* https://doi.org:10.1152/ajpcell.00365.2003

247 *Wie, M. B. et al. BAPTA/AM, an intracellular calcium chelator, induces delayed necrosis by lipoxygenase-mediated free radicals in mouse cortical cultures. Prog Neuropsychopharmacol Biol Psychiatry* ***25****, 1641-1659 (2001).* https://doi.org:10.1016/s0278-5846(01)00202-0

248 *Fang, M. et al. Long Noncoding RNA AFAP1-AS1 Is a Critical Regulator of Nasopharyngeal Carcinoma Tumorigenicity. Front Oncol* ***10****, 601055 (2020).* https://doi.org:10.3389/fonc.2020.601055

249 *Ma, R. et al. Inhibition of cell proliferation and radioresistance by miR-383-5p through targeting RNA binding protein motif (RBM3) in nasopharyngeal carcinoma. Ann Transl Med* ***9****, 123 (2021).* https://doi.org:10.21037/atm-20-6881

250 *Tian, Y., Xia, S., Ma, M. & Zuo, Y. LINC00096 Promotes the Proliferation and Invasion by Sponging miR-383-5p and Regulating RBM3 Expression in Triple-Negative Breast Cancer. Onco Targets Ther* ***12****, 10569-10578 (2019).* https://doi.org:10.2147/OTT.S229659

251 *Wang, S., Chen, X. & Qiao, T. Long noncoding RNA MIR44352HG promotes the progression of head and neck squamous cell carcinoma by regulating the miR3835p/RBM3 axis. Oncol Rep* ***45*** *(2021).* https://doi.org:10.3892/or.2021.8050

252 *Elkon, R., Ugalde, A. P. & Agami, R. Alternative cleavage and polyadenylation: extent, regulation and function. Nature Reviews Genetics* ***14****, 496-506 (2013).* https://doi.org:10.1038/nrg3482

253 *Gruber, A. J. & Zavolan, M. Alternative cleavage and polyadenylation in health and disease. Nat Rev Genet* ***20****, 599-614 (2019).* https://doi.org:10.1038/s41576-019-0145-z

254 *Tian, B. & Manley, J. L. Alternative polyadenylation of mRNA precursors. Nat Rev Mol Cell Biol* ***18****, 18-30 (2017).* https://doi.org:10.1038/nrm.2016.116

255 *Pilotte, J., Dupont-Versteegden, E. E. & Vanderklish, P. W. Widespread regulation of miRNA biogenesis at the Dicer step by the cold-inducible RNA-binding protein, RBM3. PLoS One* ***6****, e28446 (2011).* https://doi.org:10.1371/journal.pone.0028446

256 *Dresios, J. et al. Cold stress-induced protein Rbm3 binds 60S ribosomal subunits, alters microRNA levels, and enhances global protein synthesis. Proc Natl Acad Sci U S A* ***102****, 1865-1870 (2005).* https://doi.org:10.1073/pnas.0409764102

257 *Liu, Y. et al. Cold-induced RNA-binding proteins regulate circadian gene expression by controlling alternative polyadenylation. Sci Rep* ***3****, 2054 (2013).* https://doi.org:10.1038/srep02054

258 *Badrani, J. H. et al. RNA-binding protein RBM3 intrinsically suppresses lung innate lymphoid cell activation and inflammation partially through CysLT1R. Nat Commun* ***13****, 4435 (2022).* https://doi.org:10.1038/s41467-022-32176-5

259 *Cristofari, G. & Darlix, J. L. The ubiquitous nature of RNA chaperone proteins. Progress in Nucleic Acid Research and Molecular Biology, Vol 72* ***72****, 223-268 (2002).* https://doi.org:Doi *10.1016/S0079-6603(02)72071-0*

260 *Park, S. et al. Dynamic interactions between the RNA chaperone Hfq, small regulatory RNAs, and mRNAs in live bacterial cells. Elife* ***10*** *(2021).* https://doi.org:ARTN *e64207 10.7554/eLife.64207*

261 *Bae, W., Jones, P. G. & Inouye, M. CspA, the major cold shock protein of Escherichia coli, negatively regulates its own gene expression. Journal of Bacteriology* ***179****, 7081-7088 (1997).* https://doi.org:DOI *10.1128/jb.179.22.7081-7088.1997*

262 *Caballero, C. J. et al. The regulon of the RNA chaperone CspA and its auto-regulation in Staphylococcus aureus. Nucleic Acids Research* ***46****, 1345-1361 (2018).* https://doi.org:10.1093/nar/gkx1284

263 *Karnatovskaia, L. V., Wartenberg, K. E. & Freeman, W. D. Therapeutic hypothermia for neuroprotection: history, mechanisms, risks, and clinical applications. Neurohospitalist* ***4****, 153-163 (2014).* https://doi.org:10.1177/1941874413519802

264 *Matsuda, A. et al. Generation of mice deficient in RNA-binding motif protein 3 (RBM3) and characterization of its role in innate immune responses and cell growth. Biochem Biophys Res Commun* ***411****, 7-13 (2011).* https://doi.org:10.1016/j.bbrc.2011.06.038

265 *Peretti, D. et al. RBM3 mediates structural plasticity and protective effects of cooling in neurodegeneration. Nature* ***518****, 236-239 (2015). https://doi.org:10.1038/nature14142*

266 *Bastide, A. et al. RTN3 Is a Novel Cold-Induced Protein and Mediates Neuroprotective Effects of RBM3. Curr Biol* ***27****, 638-650 (2017). https://doi.org:10.1016/j.cub.2017.01.047*

267 *Zhuang, R. J. et al. Cold-Inducible Protein RBM3 Protects UV Irradiation-Induced Apoptosis in Neuroblastoma Cells by Affecting p38 and JNK Pathways and Bcl2 Family Proteins. J Mol Neurosci* ***63****, 142-151 (2017). https://doi.org:10.1007/s12031-017-0964-3*

268 *Yang, H. J. et al. RNA-binding protein RBM3 prevents NO-induced apoptosis in human neuroblastoma cells by modulating p38 signaling and miR-143. Sci Rep* ***7****, 41738 (2017). https://doi.org:10.1038/srep41738*

269 *Zhang, L. et al. Mild therapeutic hypothermia improves neurological outcomes in a rat model of cardiac arrest. Brain Res Bull* ***173****, 97-107 (2021). https://doi.org:10.1016/j.brainresbull.2021.05.014*

270 *Zhu, X. et al. RBM3 promotes neurogenesis in a niche-dependent manner via IMP2-IGF2 signaling pathway after hypoxic-ischemic brain injury. Nat Commun* ***10****, 3983 (2019). https://doi.org:10.1038/s41467-019-11870-x*

271 *Wong, J. J. et al. RBM3 regulates temperature sensitive miR-142-5p and miR-143 (thermomiRs), which target immune genes and control fever. Nucleic Acids Res* ***44****, 2888-2897 (2016). https://doi.org:10.1093/nar/gkw041*

272 *Wellmann, S. et al. The RNA-binding protein RBM3 is required for cell proliferation and protects against serum deprivation-induced cell death. Pediatr Res* ***67****, 35-41 (2010). https://doi.org:10.1203/PDR.0b013e3181c13326*

273 *Li, Z. et al. The RNA-Binding Motif Protein Family in Cancer: Friend or Foe? Front Oncol* ***11****, 757135 (2021). https://doi.org:10.3389/fonc.2021.757135*

274 *Zeng, Y. et al. Stress-response protein RBM3 attenuates the stem-like properties of prostate cancer cells by interfering with CD44 variant splicing. Cancer Res* ***73****, 4123-4133 (2013). https://doi.org:10.1158/0008-5472.CAN-12-1343*

275 *Dong, W. et al. The RNA-binding protein RBM3 promotes cell proliferation in hepatocellular carcinoma by regulating circular RNA SCD-circRNA 2 production. EBioMedicine* ***45****, 155-167 (2019). https://doi.org:10.1016/j.ebiom.2019.06.030*

276 *Chen, P., Yue, X., Xiong, H., Lu, X. & Ji, Z. RBM3 upregulates ARPC2 by binding the 3'UTR and contributes to breast cancer progression. Int J Oncol* ***54****, 1387-1397 (2019). https://doi.org:10.3892/ijo.2019.4698*

277 *Li, Q. et al. Long Noncoding RNA DANCR Regulates Cell Proliferation by Stabilizing SOX2 mRNA in Nasopharyngeal Carcinoma. Am J Pathol* ***190****, 2343-2354 (2020). https://doi.org:10.1016/j.ajpath.2020.09.005*

278 *Bronisz, A. et al. The nuclear DICER-circular RNA complex drives the deregulation of the glioblastoma cell microRNAome. Sci Adv* ***6*** *(2020). https://doi.org:10.1126/sciadv.abc0221*

279 *Ma, R. et al. RNA binding motif protein 3 (RBM3) drives radioresistance in nasopharyngeal carcinoma by reducing apoptosis via the PI3K/AKT/Bcl-2 signaling pathway. Am J Transl Res* ***10****, 4130-4140 (2018).*

280 *Pilotte, J. et al. Morphoregulatory functions of the RNA-binding motif protein 3 in cell spreading, polarity and migration. Sci Rep* ***8****, 7367 (2018). https://doi.org:10.1038/s41598-018-25668-2*

281 *Miao, X. B. & Zhang, N. Role of RBM3 in the regulation of cell proliferation in hepatocellular carcinoma. Experimental and Molecular Pathology* ***117*** *(2020). https://doi.org:ARTN 104546*

10.1016/j.yexmp.2020.104546

282 *Venugopal, A. et al. RNA binding protein RBM3 increases beta-catenin signaling to increase stem cell characteristics in colorectal cancer cells. Mol Carcinog* ***55****, 1503-1516 (2016). https://doi.org:10.1002/mc.22404*

283 *Quail, D. F. & Joyce, J. A. Microenvironmental regulation of tumor progression and metastasis. Nat Med* ***19****, 1423-1437 (2013). https://doi.org:10.1038/nm.3394*

284 *Hanahan, D. & Weinberg, R. A. Hallmarks of cancer: the next generation. Cell* ***144****, 646-674 (2011). https://doi.org:10.1016/j.cell.2011.02.013*

285 *Fouad, Y. A. & Aanei, C. Revisiting the hallmarks of cancer. Am J Cancer Res* ***7****, 1016-1036 (2017).*

286 *Hanahan, D. & Weinberg, R. A. The hallmarks of cancer. Cell* ***100****, 57-70 (2000). https://doi.org:10.1016/s0092-8674(00)81683-9*

287 *Van Pelt, D. W., Confides, A. L., Judge, A. R., Vanderklish, P. W. & Dupont-Versteegden, E. E. Cold shock protein RBM3 attenuates atrophy and induces hypertrophy in skeletal muscle. J Muscle Res Cell Motil* ***39****, 35-40 (2018). https://doi.org:10.1007/s10974-018-9496-x*

288 *Hettinger, Z. R. et al. Skeletal muscle RBM3 expression is associated with extended lifespan in Ames Dwarf and calorie restricted mice. Exp Gerontol* ***146****, 111214 (2021). https://doi.org:10.1016/j.exger.2020.111214*

289 *Kim, D. Y., Kim, K. M., Kim, E. J. & Jang, W. G. Hypothermia-induced RNA-binding motif protein 3 (RBM3) stimulates osteoblast differentiation via the ERK signaling pathway. Biochem Biophys Res Commun* ***498****, 459-465 (2018). https://doi.org:10.1016/j.bbrc.2018.02.209*

290 *Tong, G. et al. Post-TTM Rebound Pyrexia after Ischemia-Reperfusion Injury Results in Sterile Inflammation and Apoptosis in Cardiomyocytes. Mediators Inflamm* ***2019****, 6431957 (2019). https://doi.org:10.1155/2019/6431957*

291 *Tan, Y. L., Tey, S. M. & Ho, H. K. Moderate Hypothermia Effectively Alleviates Acetaminophen-Induced Liver Injury With Prolonged Action Beyond Cooling. Dose Response* ***18****, 1559325820970846 (2020). https://doi.org:10.1177/1559325820970846*

292 *Ishii, T. et al. Mild hypothermia promotes the viability of in vitro-produced bovine blastocysts and their transcriptional expression of the cold-inducible transcription factor Rbm3 during in vitro culture. J Reprod Dev* ***65****, 275-280 (2019). https://doi.org:10.1262/jrd.2018-142*

293 *Zhong, P., Peng, J., Yuan, M., Kong, B. & Huang, H. Cold-inducible RNA-binding protein (CIRP) in inflammatory diseases: Molecular insights of its associated signalling pathways. Scand J Immunol* ***93****, e12949 (2021). https://doi.org:10.1111/sji.12949*

294 *Tan, C., Gurien, S. D., Royster, W., Aziz, M. & Wang, P. Extracellular CIRP Induces Inflammation in Alveolar Type II Cells via TREM-1. Front Cell Dev Biol* ***8****, 579157 (2020). https://doi.org:10.3389/fcell.2020.579157*

295 *Lucht, J. et al. Cooling and Sterile Inflammation in an Oxygen-Glucose-Deprivation/Reperfusion Injury Model in BV-2 Microglia. Mediators Inflamm* ***2021****, 8906561 (2021). https://doi.org:10.1155/2021/8906561*

296 *Yang, Z. et al. RTN3 inhibits RIG-I-mediated antiviral responses by impairing TRIM25-mediated K63-linked polyubiquitination. Elife* ***10*** *(2021). https://doi.org:10.7554/eLife.68958*

297 Xiang, R. et al. Increased Reticulon 3 (RTN3) Leads to Obesity and Hypertriglyceridemia by Interacting With Heat Shock Protein Family A (Hsp70) Member 5 (HSPA5). Circulation **138**, 1828-1838 (2018). https://doi.org:10.1161/CIRCULATIONAHA.117.030718

298 Lee, J. T., Lee, T. J., Kim, C. H., Kim, N. S. & Kwon, T. K. Over-expression of Reticulon 3 (RTN3) enhances TRAIL-mediated apoptosis via up-regulation of death receptor 5 (DR5) and down-regulation of c-FLIP. Cancer Lett **279**, 185-192 (2009). https://doi.org:10.1016/j.canlet.2009.01.035

299 Deng, M. et al. Increased expression of reticulon 3 in neurons leads to reduced axonal transport of beta site amyloid precursor protein-cleaving enzyme 1. J Biol Chem **288**, 30236-30245 (2013). https://doi.org:10.1074/jbc.M113.480079

300 Hu, X. et al. Transgenic mice overexpressing reticulon 3 develop neuritic abnormalities. EMBO J **26**, 2755-2767 (2007). https://doi.org:10.1038/sj.emboj.7601707

301 Shi, Q. et al. Preventing formation of reticulon 3 immunoreactive dystrophic neurites improves cognitive function in mice. J Neurosci **33**, 3059-3066 (2013). https://doi.org:10.1523/JNEUROSCI.2445-12.2013

302 Shi, Q. et al. Impact of RTN3 deficiency on expression of BACE1 and amyloid deposition. J Neurosci **34**, 13954-13962 (2014). https://doi.org:10.1523/JNEUROSCI.1588-14.2014

303 He, W. et al. Reticulon family members modulate BACE1 activity and amyloid-beta peptide generation. Nat Med **10**, 959-965 (2004). https://doi.org:10.1038/nm1088

304 Chen, R. et al. Reticulon 3 attenuates the clearance of cytosolic prion aggregates via inhibiting autophagy. Autophagy **7**, 205-216 (2011). https://doi.org:10.4161/auto.7.2.14197

305 Cunningham, C. N. et al. Cells Deploy a Two-Pronged Strategy to Rectify Misfolded Proinsulin Aggregates. Mol Cell **75**, 442-456 e444 (2019). https://doi.org:10.1016/j.molcel.2019.05.011

306 Knupp, J. et al. The ER transmembrane protein PGRMC1 recruits misfolded proteins for reticulophagic clearance. Autophagy **18**, 228-230 (2022). https://doi.org:10.1080/15548627.2021.1997062

307 Caldieri, G. et al. Reticulon 3-dependent ER-PM contact sites control EGFR nonclathrin endocytosis. Science **356**, 617-624 (2017). https://doi.org:10.1126/science.aah6152

308 Sharoar, M. G. & Yan, R. Effects of altered RTN3 expression on BACE1 activity and Alzheimer's neuritic plaques. Rev Neurosci **28**, 145-154 (2017). https://doi.org:10.1515/revneuro-2016-0054

309 Grumati, P. et al. Full length RTN3 regulates turnover of tubular endoplasmic reticulum via selective autophagy. Elife **6** (2017). https://doi.org:10.7554/eLife.25555

310 Chen, Y. J. et al. PGRMC1 acts as a size-selective cargo receptor to drive ER-phagic clearance of mutant prohormones. Nat Commun **12**, 5991 (2021). https://doi.org:10.1038/s41467-021-26225-8

311 Wu, H. & Voeltz, G. K. Reticulon-3 Promotes Endosome Maturation at ER Membrane Contact Sites. Dev Cell **56**, 52-66 e57 (2021). https://doi.org:10.1016/j.devcel.2020.12.014

312 Sadan, O. Therapeutic Hypothermia in Critically Ill Patients: The Role of Hypothermia in the Critical Care Toolbox. Crit Care Med **48**, 1089-1090 (2020). https://doi.org:10.1097/CCM.0000000000004389

313 Villablanca, P. A. & Mookadam, F. Therapeutic hypothermia in ST-elevation myocardial infarction (STEMI): targeting the appropriate STEMI. J Thorac Dis **8**, E1540-E1542 (2016). https://doi.org:10.21037/jtd.2016.11.98

314 *Lopez-de-Sa, E. et al. A multicentre randomized pilot trial on the effectiveness of different levels of cooling in comatose survivors of out-of-hospital cardiac arrest: the FROST-I trial. Intensive Care Med* ***44****, 1807-1815 (2018).* https://doi.org:10.1007/s00134-018-5256-z

315 *Wagner, D., Hooper, V., Bankieris, K. & Johnson, A. The Relationship of Postoperative Delirium and Unplanned Perioperative Hypothermia in Surgical Patients. J Perianesth Nurs* ***36****, 41-46 (2021).* https://doi.org:10.1016/j.jopan.2020.06.015

316 *Gunn, A. J. et al. Therapeutic hypothermia translates from ancient history in to practice. Pediatr Res* ***81****, 202-209 (2017).* https://doi.org:10.1038/pr.2016.198

317 *Crooke, S. T., Witztum, J. L., Bennett, C. F. & Baker, B. F. RNA-Targeted Therapeutics. Cell Metab* ***29****, 501 (2019).* https://doi.org:10.1016/j.cmet.2019.01.001

318 *Eckstein, F. Phosphorothioates, essential components of therapeutic oligonucleotides. Nucleic Acid Ther* ***24****, 374-387 (2014).* https://doi.org:10.1089/nat.2014.0506

319 *Smith, C. I. E. & Zain, R. Therapeutic Oligonucleotides: State of the Art. Annu Rev Pharmacol Toxicol* ***59****, 605-630 (2019).* https://doi.org:10.1146/annurev-pharmtox-010818-021050

320 *Geary, R. S., Norris, D., Yu, R. & Bennett, C. F. Pharmacokinetics, biodistribution and cell uptake of antisense oligonucleotides. Adv Drug Deliv Rev* ***87****, 46-51 (2015).* https://doi.org:10.1016/j.addr.2015.01.008

321 *Prakash, T. P. et al. Targeted delivery of antisense oligonucleotides to hepatocytes using triantennary N-acetyl galactosamine improves potency 10-fold in mice. Nucleic Acids Res* ***42****, 8796-8807 (2014).* https://doi.org:10.1093/nar/gku531

322 *Juliano, R. L., Ming, X. & Nakagawa, O. Cellular uptake and intracellular trafficking of antisense and siRNA oligonucleotides. Bioconjug Chem* ***23****, 147-157 (2012).* https://doi.org:10.1021/bc200377d

323 *Vlassov, V. V., Vlassova, I. E. & Pautova, L. V. Oligonucleotides and polynucleotides as biologically active compounds. Prog Nucleic Acid Res Mol Biol* ***57****, 95-143 (1997).* https://doi.org:10.1016/s0079-6603(08)60279-2

324 *Iversen, P. L., Zhu, S., Meyer, A. & Zon, G. Cellular uptake and subcellular distribution of phosphorothioate oligonucleotides into cultured cells. Antisense Res Dev* ***2****, 211-222 (1992).* https://doi.org:10.1089/ard.1992.2.211

325 *Stein, C. A. et al. Efficient gene silencing by delivery of locked nucleic acid antisense oligonucleotides, unassisted by transfection reagents. Nucleic Acids Res* ***38****, e3 (2010).* https://doi.org:10.1093/nar/gkp841

326 *Lorenz, P., Baker, B. F., Bennett, C. F. & Spector, D. L. Phosphorothioate antisense oligonucleotides induce the formation of nuclear bodies. Mol Biol Cell* ***9****, 1007-1023 (1998).* https://doi.org:10.1091/mbc.9.5.1007

327 *Marcusson, E. G., Bhat, B., Manoharan, M., Bennett, C. F. & Dean, N. M. Phosphorothioate oligodeoxyribonucleotides dissociate from cationic lipids before entering the nucleus. Nucleic Acids Res* ***26****, 2016-2023 (1998).* https://doi.org:10.1093/nar/26.8.2016

328 *Zelphati, O. & Szoka, F. C., Jr. Mechanism of oligonucleotide release from cationic liposomes. Proc Natl Acad Sci U S A* ***93****, 11493-11498 (1996).* https://doi.org:10.1073/pnas.93.21.11493

329 *Tarkanyi, I. et al. Inhibition of human telomerase by oligonucleotide chimeras, composed of an antisense moiety and a chemically modified homo-oligonucleotide. FEBS Lett* ***579****, 1411-1416 (2005).* https://doi.org:10.1016/j.febslet.2005.01.041

330 *Castanotto, D. et al. A cytoplasmic pathway for gapmer antisense oligonucleotide-mediated gene silencing in mammalian cells. Nucleic Acids Res* ***43****, 9350-9361 (2015).* https://doi.org:10.1093/nar/gkv964

331 *Juliano, R. L. The delivery of therapeutic oligonucleotides. Nucleic Acids Res **44**, 6518-6548 (2016). https://doi.org:10.1093/nar/gkw236*

332 *Yang, B. et al. High-throughput screening identifies small molecules that enhance the pharmacological effects of oligonucleotides. Nucleic Acids Res **43**, 1987-1996 (2015). https://doi.org:10.1093/nar/gkv060*

333 *Yang, L. et al. Efficient Delivery of Antisense Oligonucleotides Using Bioreducible Lipid Nanoparticles In Vitro and In Vivo. Mol Ther Nucleic Acids **19**, 1357-1367 (2020). https://doi.org:10.1016/j.omtn.2020.01.018*

334 *Lorenz, P., Misteli, T., Baker, B. F., Bennett, C. F. & Spector, D. L. Nucleocytoplasmic shuttling: a novel in vivo property of antisense phosphorothioate oligodeoxynucleotides. Nucleic Acids Res **28**, 582-592 (2000). https://doi.org:10.1093/nar/28.2.582*

335 *Sixou, S. et al. Intracellular oligonucleotide hybridization detected by fluorescence resonance energy transfer (FRET). Nucleic Acids Res **22**, 662-668 (1994). https://doi.org:10.1093/nar/22.4.662*

336 *Iwamoto, N. et al. Control of phosphorothioate stereochemistry substantially increases the efficacy of antisense oligonucleotides. Nat Biotechnol **35**, 845-851 (2017). https://doi.org:10.1038/nbt.3948*

337 *Liang, X. H. et al. Hsp90 protein interacts with phosphorothioate oligonucleotides containing hydrophobic 2'-modifications and enhances antisense activity. Nucleic Acids Res **44**, 3892-3907 (2016). https://doi.org:10.1093/nar/gkw144*

338 *Brown, D. A. et al. Effect of phosphorothioate modification of oligodeoxynucleotides on specific protein binding. J Biol Chem **269**, 26801-26805 (1994).*

339 *Crooke, S. T., Wang, S., Vickers, T. A., Shen, W. & Liang, X. H. Cellular uptake and trafficking of antisense oligonucleotides. Nat Biotechnol **35**, 230-237 (2017). https://doi.org:10.1038/nbt.3779*

340 *Wang, S., Sun, H., Tanowitz, M., Liang, X. H. & Crooke, S. T. Annexin A2 facilitates endocytic trafficking of antisense oligonucleotides. Nucleic Acids Res **44**, 7314-7330 (2016). https://doi.org:10.1093/nar/gkw595*

341 *Kulkarni, J. A. et al. The current landscape of nucleic acid therapeutics. Nat Nanotechnol **16**, 630-643 (2021). https://doi.org:10.1038/s41565-021-00898-0*

342 *Monani, U. R. Spinal muscular atrophy: a deficiency in a ubiquitous protein; a motor neuron-specific disease. Neuron **48**, 885-896 (2005). https://doi.org:10.1016/j.neuron.2005.12.001*

343 *Hua, Y., Vickers, T. A., Baker, B. F., Bennett, C. F. & Krainer, A. R. Enhancement of SMN2 exon 7 inclusion by antisense oligonucleotides targeting the exon. PLoS Biol **5**, e73 (2007). https://doi.org:10.1371/journal.pbio.0050073*

344 *Hua, Y. et al. Peripheral SMN restoration is essential for long-term rescue of a severe spinal muscular atrophy mouse model. Nature **478**, 123-126 (2011). https://doi.org:10.1038/nature10485*

345 *Passini, M. A. et al. Antisense oligonucleotides delivered to the mouse CNS ameliorate symptoms of severe spinal muscular atrophy. Sci Transl Med **3**, 72ra18 (2011). https://doi.org:10.1126/scitranslmed.3001777*

346 *Hua, Y., Vickers, T. A., Okunola, H. L., Bennett, C. F. & Krainer, A. R. Antisense masking of an hnRNP A1/A2 intronic splicing silencer corrects SMN2 splicing in transgenic mice. Am J Hum Genet **82**, 834-848 (2008). https://doi.org:10.1016/j.ajhg.2008.01.014*

347 *Finkel, R. S. et al. Nusinersen versus Sham Control in Infantile-Onset Spinal Muscular Atrophy. N Engl J Med **377**, 1723-1732 (2017). https://doi.org:10.1056/NEJMoa1702752*

348 *Smith, R. A. et al. Antisense oligonucleotide therapy for neurodegenerative disease. J Clin Invest* ***116****, 2290-2296 (2006).* https://doi.org:10.1172/JCI25424
349 *Qiang, X. et al. Cold-inducible RNA-binding protein (CIRP) triggers inflammatory responses in hemorrhagic shock and sepsis. Nat Med* ***19****, 1489-1495 (2013).* https://doi.org:10.1038/nm.3368
350 *Zhou, M., Yang, W. L., Ji, Y., Qiang, X. & Wang, P. Cold-inducible RNA-binding protein mediates neuroinflammation in cerebral ischemia. Biochim Biophys Acta* ***1840****, 2253-2261 (2014).* https://doi.org:10.1016/j.bbagen.2014.02.027
351 *Yang, H. J. et al. Cold Shock Induced Protein RBM3 but Not Mild Hypothermia Protects Human SH-SY5Y Neuroblastoma Cells From MPP(+)-Induced Neurotoxicity. Front Neurosci* ***12****, 298 (2018).* https://doi.org:10.3389/fnins.2018.00298
352 *Gunn, A. J. & Battin, M. Towards faster studies of neonatal encephalopathy. Lancet Neurol* ***18****, 21-22 (2019).* https://doi.org:10.1016/S1474-4422(18)30370-3
353 *Trescher, W. H., Ishiwa, S. & Johnston, M. V. Brief post-hypoxic-ischemic hypothermia markedly delays neonatal brain injury. Brain Dev* ***19****, 326-338 (1997).* https://doi.org:10.1016/s0387-7604(97)00027-2
354 *Colombo, M., Karousis, E. D., Bourquin, J., Bruggmann, R. & Mühlemann, O. Transcriptome-wide identification of NMD-targeted human mRNAs reveals extensive redundancy between SMG6- and SMG7-mediated degradation pathways. RNA (New York, N.Y.)* ***23****, 189-201 (2017).* https://doi.org:10.1261/rna.059055.116
355 *Logan, S. M. & Storey, K. B. Cold-inducible RNA-binding protein Cirp, but not Rbm3, may regulate transcript processing and protection in tissues of the hibernating ground squirrel. Cell Stress Chaperones* ***25****, 857-868 (2020).* https://doi.org:10.1007/s12192-020-01110-3
356 *Anko, M. L., Morales, L., Henry, I., Beyer, A. & Neugebauer, K. M. Global analysis reveals SRp20- and SRp75-specific mRNPs in cycling and neural cells. Nat Struct Mol Biol* ***17****, 962-970 (2010).* https://doi.org:10.1038/nsmb.1862
357 *Jumaa, H. & Nielsen, P. J. The splicing factor SRp20 modifies splicing of its own mRNA and ASF/SF2 antagonizes this regulation. EMBO J* ***16****, 5077-5085 (1997).* https://doi.org:10.1093/emboj/16.16.5077
358 *Anko, M. L. et al. The RNA-binding landscapes of two SR proteins reveal unique functions and binding to diverse RNA classes. Genome Biol* ***13****, R17 (2012).* https://doi.org:10.1186/gb-2012-13-3-r17
359 *Lareau, L. F., Inada, M., Green, R. E., Wengrod, J. C. & Brenner, S. E. Unproductive splicing of SR genes associated with highly conserved and ultraconserved DNA elements. Nature* ***446****, 926-929 (2007).* https://doi.org:10.1038/nature05676
360 *Robertshaw, D. Temperature regulation and the thermal environment. Dukes' physiology of domestic animals, 962-973 (2004).*
361 *Clarke, A. & Rothery, P. Scaling of body temperature in mammals and birds. Functional Ecology* ***22****, 58-67 (2008).* https://doi.org:10.1111/j.1365-2435.2007.01341.x
362 *Buhr, E. D., Yoo, S. H. & Takahashi, J. S. Temperature as a universal resetting cue for mammalian circadian oscillators. Science* ***330****, 379-385 (2010).* https://doi.org:10.1126/science.1195262
363 *Bahat, A. et al. Thermotaxis of mammalian sperm cells: a potential navigation mechanism in the female genital tract. Nat Med* ***9****, 149-150 (2003).* https://doi.org:10.1038/nm0203-149
364 *Bahat, A., Eisenbach, M. & Tur-Kaspa, I. Periovulatory increase in temperature difference within the rabbit oviduct. Hum Reprod* ***20****, 2118-2121 (2005).* https://doi.org:10.1093/humrep/dei006

365 Watts, N. et al. The 2020 report of The Lancet Countdown on health and climate change: responding to converging crises. Lancet **397**, 129-170 (2021). https://doi.org:10.1016/S0140-6736(20)32290-X
366 Paal, P. et al. Accidental Hypothermia: 2021 Update. Int J Environ Res Public Health **19** (2022). https://doi.org:10.3390/ijerph19010501
367 Paal, P. et al. Accidental hypothermia-an update : The content of this review is endorsed by the International Commission for Mountain Emergency Medicine (ICAR MEDCOM). Scand J Trauma Resusc Emerg Med **24**, 111 (2016). https://doi.org:10.1186/s13049-016-0303-7
368 Brown, D. J., Brugger, H., Boyd, J. & Paal, P. Accidental hypothermia. N Engl J Med **367**, 1930-1938 (2012). https://doi.org:10.1056/NEJMra1114208
369 Mallet, M. L. Pathophysiology of accidental hypothermia. QJM **95**, 775-785 (2002). https://doi.org:10.1093/qjmed/95.12.775
370 Yuan, F. et al. Z-DNA binding protein 1 promotes heatstroke-induced cell death. Science **376**, 609-615 (2022). https://doi.org:10.1126/science.abg5251
371 Voets, T. et al. The principle of temperature-dependent gating in cold- and heat-sensitive TRP channels. Nature **430**, 748-754 (2004). https://doi.org:10.1038/nature02732
372 Brauchi, S., Orio, P. & Latorre, R. Clues to understanding cold sensation: thermodynamics and electrophysiological analysis of the cold receptor TRPM8. Proc Natl Acad Sci U S A **101**, 15494-15499 (2004). https://doi.org:10.1073/pnas.0406773101
373 Song, K. et al. The TRPM2 channel is a hypothalamic heat sensor that limits fever and can drive hypothermia. Science **353**, 1393-1398 (2016). https://doi.org:10.1126/science.aaf7537
374 Patapoutian, A., Peier, A. M., Story, G. M. & Viswanath, V. ThermoTRP channels and beyond: mechanisms of temperature sensation. Nat Rev Neurosci **4**, 529-539 (2003). https://doi.org:10.1038/nrn1141
375 Varshney, D., Spiegel, J., Zyner, K., Tannahill, D. & Balasubramanian, S. The regulation and functions of DNA and RNA G-quadruplexes. Nat Rev Mol Cell Biol **21**, 459-474 (2020). https://doi.org:10.1038/s41580-020-0236-x
376 Bedrat, A., Lacroix, L. & Mergny, J. L. Re-evaluation of G-quadruplex propensity with G4Hunter. Nucleic Acids Res **44**, 1746-1759 (2016). https://doi.org:10.1093/nar/gkw006
377 Yeo, G. & Burge, C. B. Maximum entropy modeling of short sequence motifs with applications to RNA splicing signals. J Comput Biol **11**, 377-394 (2004). https://doi.org:10.1089/1066527041410418
378 Guth, S., Martinez, C., Gaur, R. K. & Valcarcel, J. Evidence for substrate-specific requirement of the splicing factor U2AF(35) and for its function after polypyrimidine tract recognition by U2AF(65). Mol Cell Biol **19**, 8263-8271 (1999). https://doi.org:10.1128/MCB.19.12.8263
379 Guth, S., Tange, T. O., Kellenberger, E. & Valcarcel, J. Dual function for U2AF(35) in AG-dependent pre-mRNA splicing. Mol Cell Biol **21**, 7673-7681 (2001). https://doi.org:10.1128/MCB.21.22.7673-7681.2001
380 Fu, Y., Masuda, A., Ito, M., Shinmi, J. & Ohno, K. AG-dependent 3'-splice sites are predisposed to aberrant splicing due to a mutation at the first nucleotide of an exon. Nucleic Acids Res **39**, 4396-4404 (2011). https://doi.org:10.1093/nar/gkr026
381 Del Villar-Guerra, R., Trent, J. O. & Chaires, J. B. G-Quadruplex Secondary Structure Obtained from Circular Dichroism Spectroscopy. Angew Chem Int Ed Engl **57**, 7171-7175 (2018). https://doi.org:10.1002/anie.201709184

382 *Wan, Y., Kertesz, M., Spitale, R. C., Segal, E. & Chang, H. Y. Understanding the transcriptome through RNA structure. Nat Rev Genet* ***12****, 641-655 (2011). https://doi.org:10.1038/nrg3049*

383 *Weldon, C. et al. Specific G-quadruplex ligands modulate the alternative splicing of Bcl-X. Nucleic Acids Res* ***46****, 886-896 (2018). https://doi.org:10.1093/nar/gkx1122*

384 *Collins, F., Schmidt, M. F., Guthrie, P. B. & Kater, S. B. Sustained increase in intracellular calcium promotes neuronal survival. J Neurosci* ***11****, 2582-2587 (1991).*

385 *An, P. & Grabowski, P. J. Exon silencing by UAGG motifs in response to neuronal excitation. PLoS Biol* ***5****, e36 (2007). https://doi.org:10.1371/journal.pbio.0050036*

386 *Grinsted, J., Blendstrup, K., Andreasen, M. P. & Byskov, A. G. Temperature measurements of rabbit antral follicles. J Reprod Fertil* ***60****, 149-155 (1980). https://doi.org:10.1530/jrf.0.0600149*

387 *Hunter, R. H., Bogh, I. B., Einer-Jensen, N., Muller, S. & Greve, T. Pre-ovulatory graafian follicles are cooler than neighbouring stroma in pig ovaries. Hum Reprod* ***15****, 273-283 (2000). https://doi.org:10.1093/humrep/15.2.273*

388 *Ng, K. Y. B., Mingels, R., Morgan, H., Macklon, N. & Cheong, Y. In vivo oxygen, temperature and pH dynamics in the female reproductive tract and their importance in human conception: a systematic review. Hum Reprod Update* ***24****, 15-34 (2018). https://doi.org:10.1093/humupd/dmx028*

389 *Grinsted, J., Kjer, J. J., Blendstrup, K. & Pedersen, J. F. Is low temperature of the follicular fluid prior to ovulation necessary for normal oocyte development? Fertil Steril* ***43****, 34-39 (1985). https://doi.org:10.1016/s0015-0282(16)48314-7*

390 *Leese, H. J., Baumann, C. G., Brison, D. R., McEvoy, T. G. & Sturmey, R. G. Metabolism of the viable mammalian embryo: quietness revisited. Mol Hum Reprod* ***14****, 667-672 (2008). https://doi.org:10.1093/molehr/gan065*

391 *Hunter, R. H. Temperature gradients in female reproductive tissues. Reprod Biomed Online* ***24****, 377-380 (2012). https://doi.org:10.1016/j.rbmo.2011.12.007*

392 *Lewis, B. P., Green, R. E. & Brenner, S. E. Evidence for the widespread coupling of alternative splicing and nonsense-mediated mRNA decay in humans. Proc Natl Acad Sci U S A* ***100****, 189-192 (2003). https://doi.org:10.1073/pnas.0136770100*

393 *Green, R. E. et al. Widespread predicted nonsense-mediated mRNA decay of alternatively-spliced transcripts of human normal and disease genes. Bioinformatics* ***19 Suppl 1****, i118-121 (2003). https://doi.org:10.1093/bioinformatics/btg1015*

394 *Zhang, X. et al. Cell-Type-Specific Alternative Splicing Governs Cell Fate in the Developing Cerebral Cortex. Cell* ***166****, 1147-1162 e1115 (2016). https://doi.org:10.1016/j.cell.2016.07.025*

395 *Moriyama, D. F. et al. The effects of temperature variation treatments on embryonic development: a mouse study. Sci Rep* ***12****, 2489 (2022). https://doi.org:10.1038/s41598-022-06158-y*

396 *Weber, C. et al. Temperature-dependent sex determination is mediated by pSTAT3 repression of Kdm6b. Science* ***368****, 303-306 (2020). https://doi.org:10.1126/science.aaz4165*

397 *Konermann, S. et al. Transcriptome Engineering with RNA-Targeting Type VI-D CRISPR Effectors. Cell* ***173****, 665-676 e614 (2018). https://doi.org:10.1016/j.cell.2018.02.033*

398 *Zhang, Y. et al. Optimized RNA-targeting CRISPR/Cas13d technology outperforms shRNA in identifying functional circRNAs. Genome Biol* ***22****, 41 (2021). https://doi.org:10.1186/s13059-021-02263-9*

399 *Yang, L. Z. et al. Dynamic Imaging of RNA in Living Cells by CRISPR-Cas13 Systems. Mol Cell* ***76****, 981-997 e987 (2019). https://doi.org:10.1016/j.molcel.2019.10.024*

400 *Li, S. et al. Screening for functional circular RNAs using the CRISPR-Cas13 system. Nat Methods* ***18****, 51-59 (2021).* https://doi.org:10.1038/s41592-020-01011-4

401 *Abudayyeh, O. O. et al. C2c2 is a single-component programmable RNA-guided RNA-targeting CRISPR effector. Science* ***353****, aaf5573 (2016).* https://doi.org:10.1126/science.aaf5573

402 *Wessels, H. H. et al. Massively parallel Cas13 screens reveal principles for guide RNA design. Nat Biotechnol* ***38****, 722-727 (2020).* https://doi.org:10.1038/s41587-020-0456-9

403 *Quinlan, A. R. & Hall, I. M. BEDTools: a flexible suite of utilities for comparing genomic features. Bioinformatics* ***26****, 841-842 (2010).* https://doi.org:10.1093/bioinformatics/btq033

404 *Hon, J., Martinek, T., Zendulka, J. & Lexa, M. pqsfinder: an exhaustive and imperfection-tolerant search tool for potential quadruplex-forming sequences in R. Bioinformatics* ***33****, 3373-3379 (2017).* https://doi.org:10.1093/bioinformatics/btx413

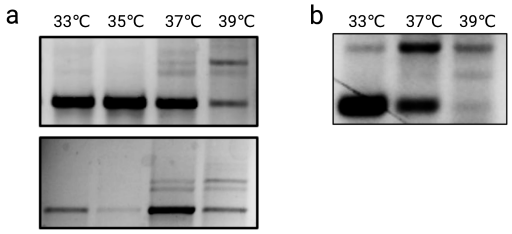

App. Fig. 1. **a**, Other gel images for the quantification of Fig. 1.3a. **b**, Other gel images for the quantification of Fig. 1.3d

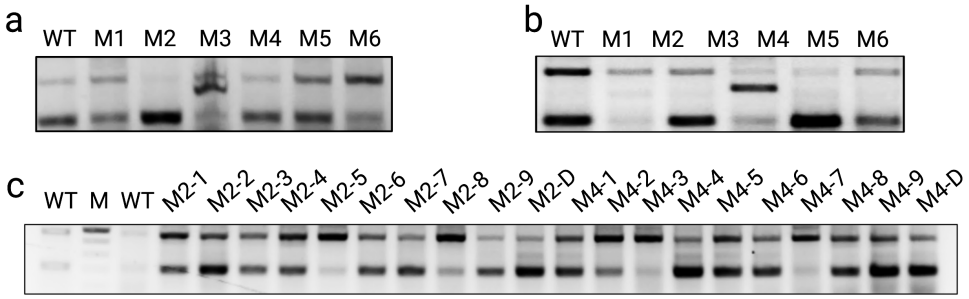

App. Fig. 2. **a**, Other gel images for the quantification of Fig. 1.4b. **b**, Other gel images for the quantification of Fig. 1.4c. Other gel images for the quantification of Fig. 1.4f

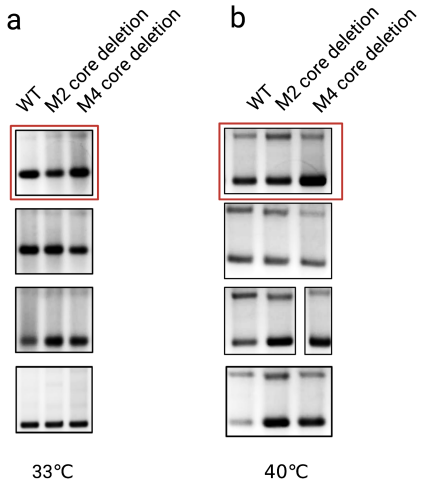

App. Fig. 3. a, Gel images for the quantification of Fig. 1.6c.

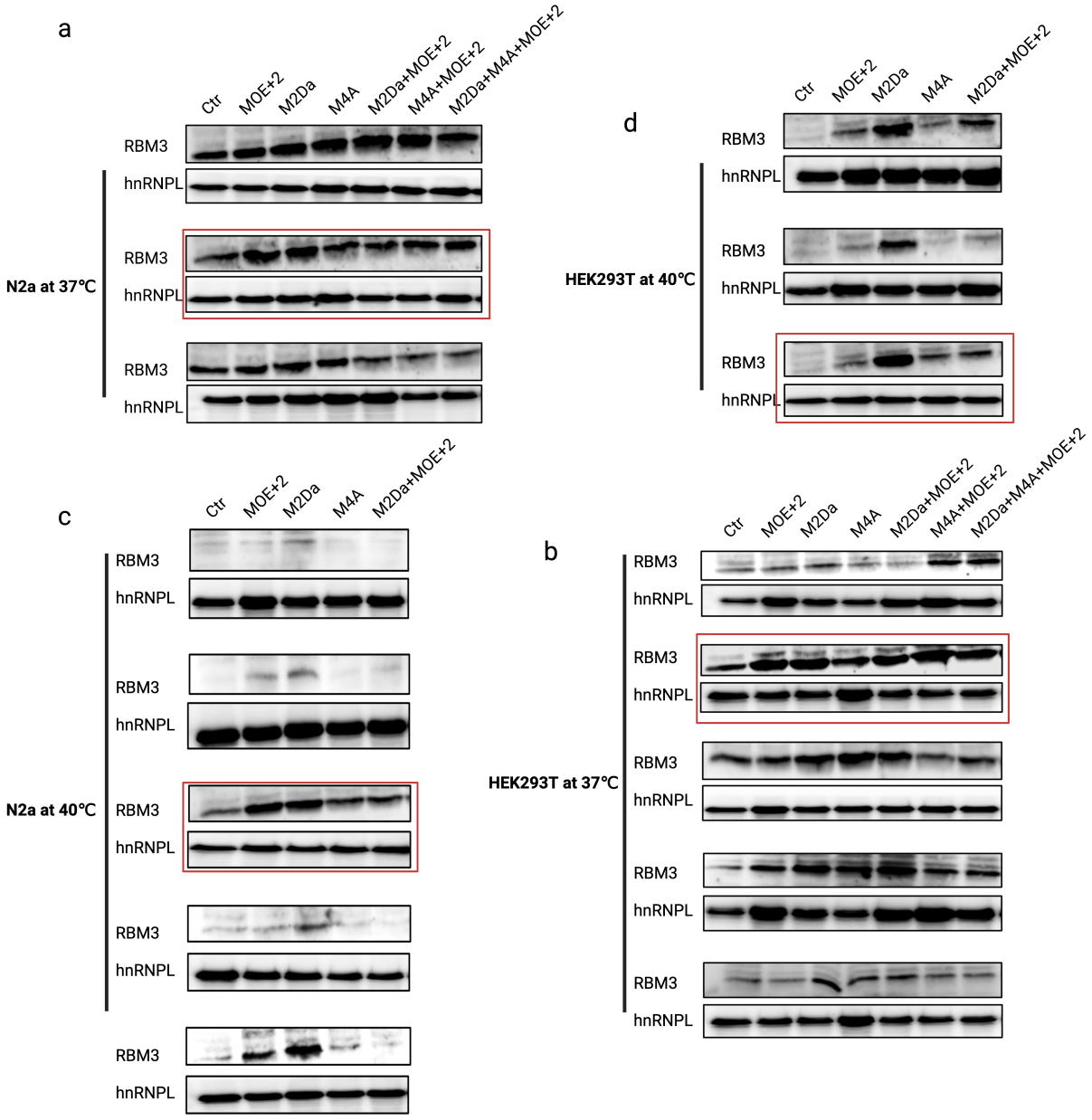

App. Fig. 4. Gel images for the quantification of Fig. 1.7.

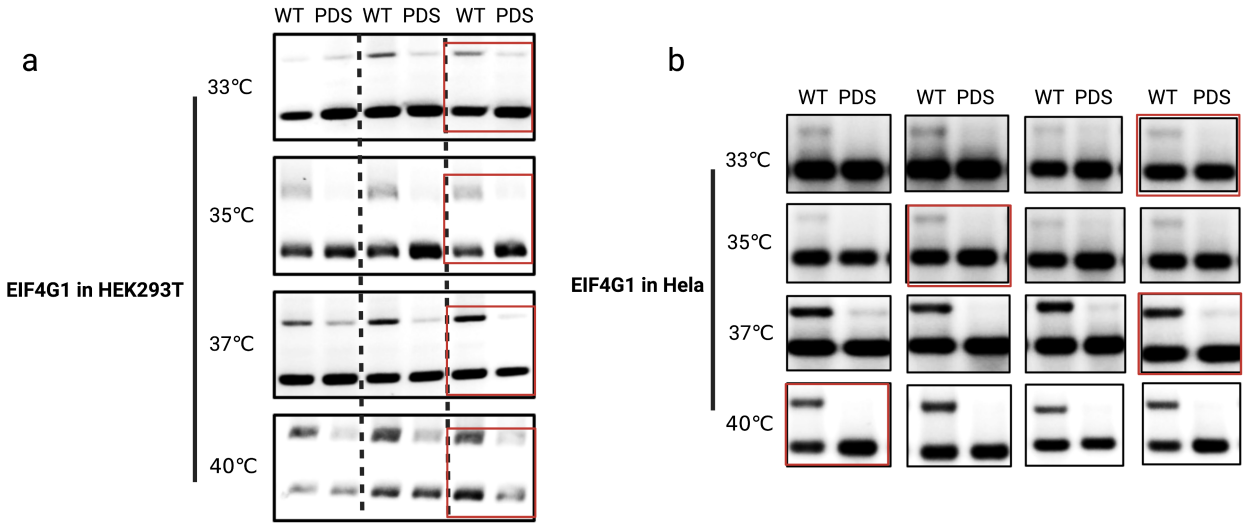

App. Fig. 5 Gel images for the quantification of Fig. 2.4b. The images marked by the red rectangle are the representative images in the main figures.

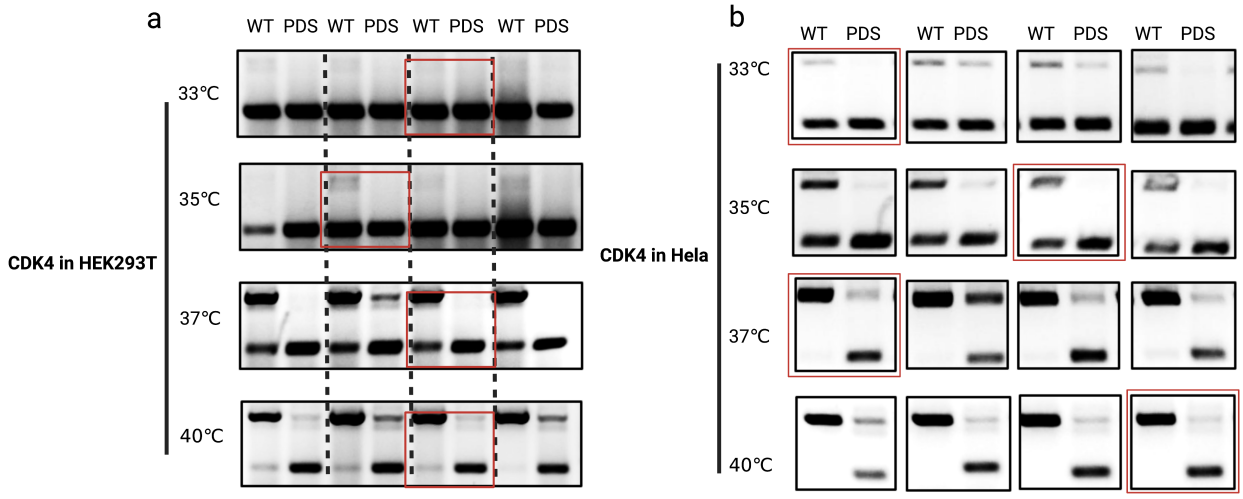

App. Fig. 6 Gel images for the quantification of Fig. 2.4c. The images marked by the red rectangle are the representative images in the main figures.

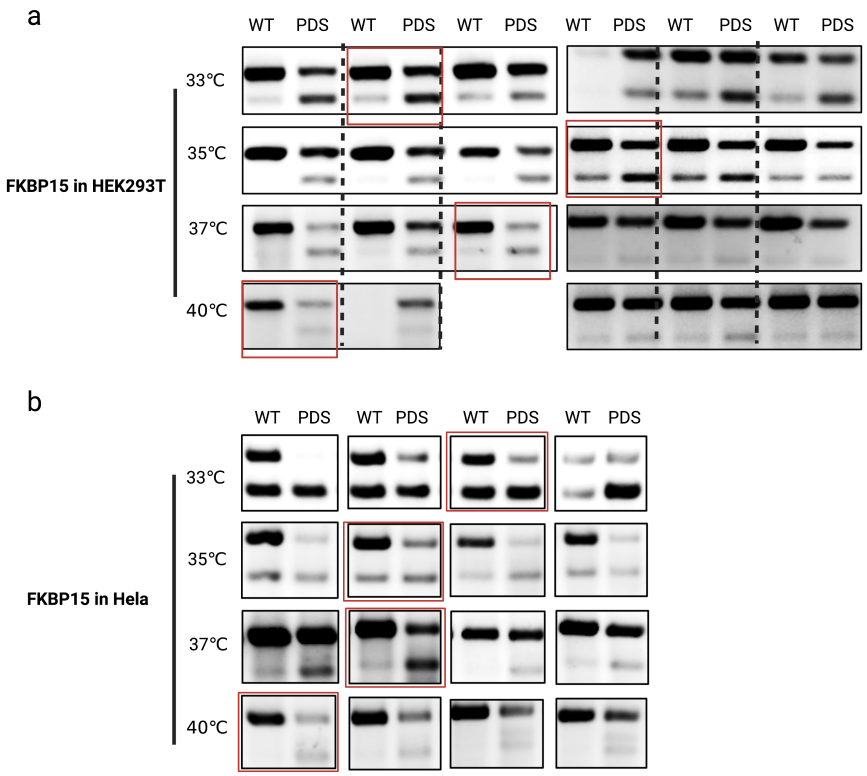

App. Fig. 7 Gel images for the quantification of Fig. 2.4d. The images marked by the red rectangle are the representative images in the main figures.

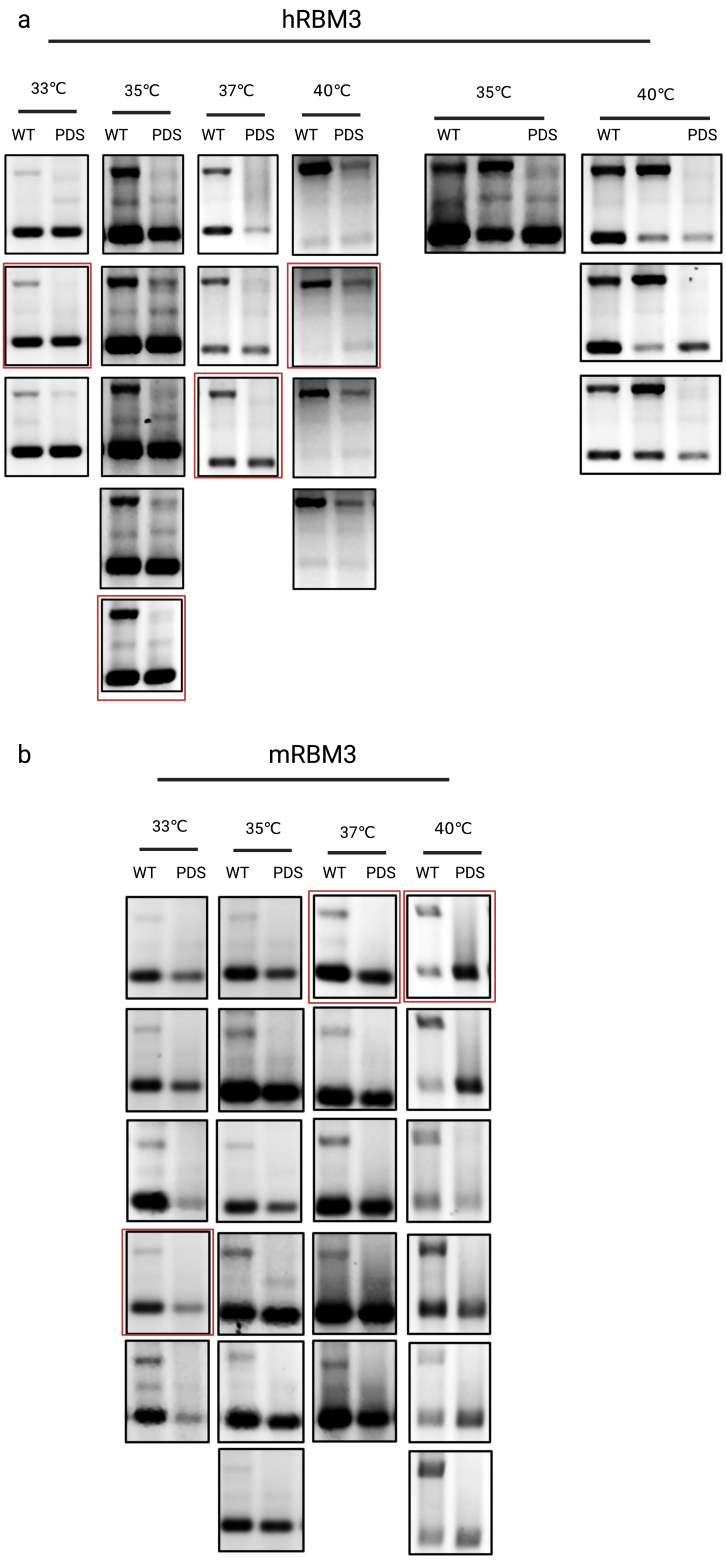

App. Fig. 8 Gel images for the quantification of Fig. 2.6b and 2.6c. The images marked by the red rectangle are the representative images in the main figures.

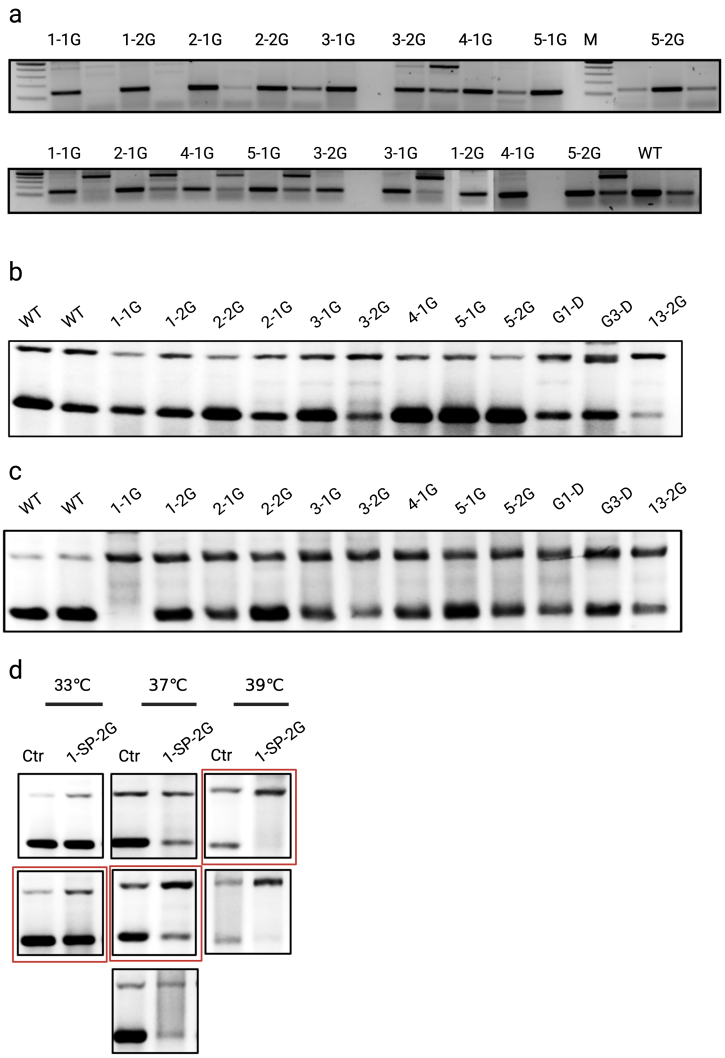

App. Fig. 9 Gel images for the quantification of Fig. 2.6e (**a**) , 2.6f (**b**), Fig. 2.7 (**c**) and Fig. 2.8 (**d**). The images marked by the red rectangle are the representative images in the main figures.

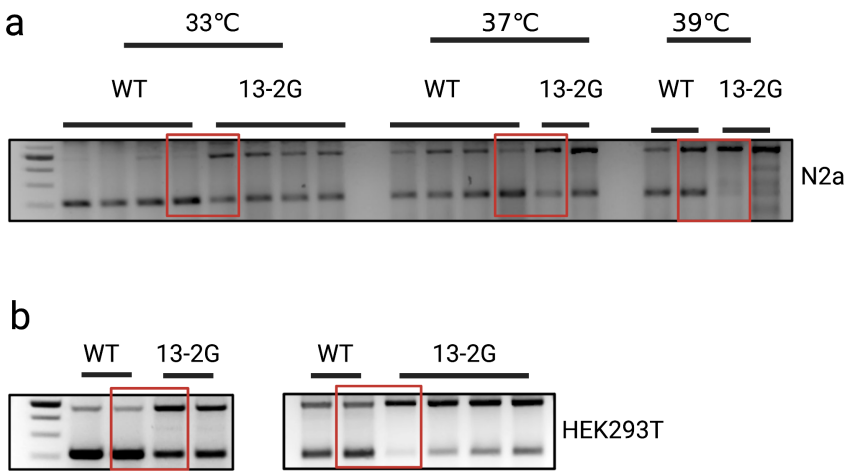

App. Fig. 10. Gel images for the quantification of Fig. 2.9. The images marked by the red rectangle are the representative images in the main figures.

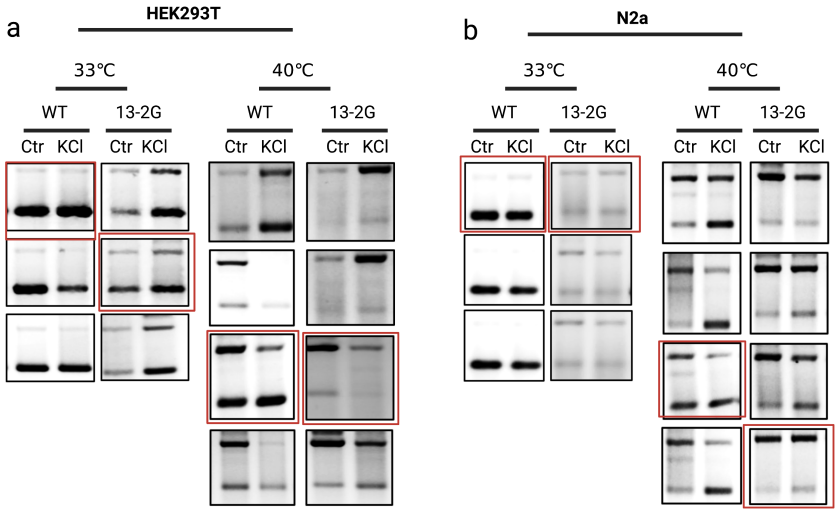

App. Fig. 11. Gel images for the quantification of Fig. 2.11. The images marked by the red rectangle are the representative images in the main figures.

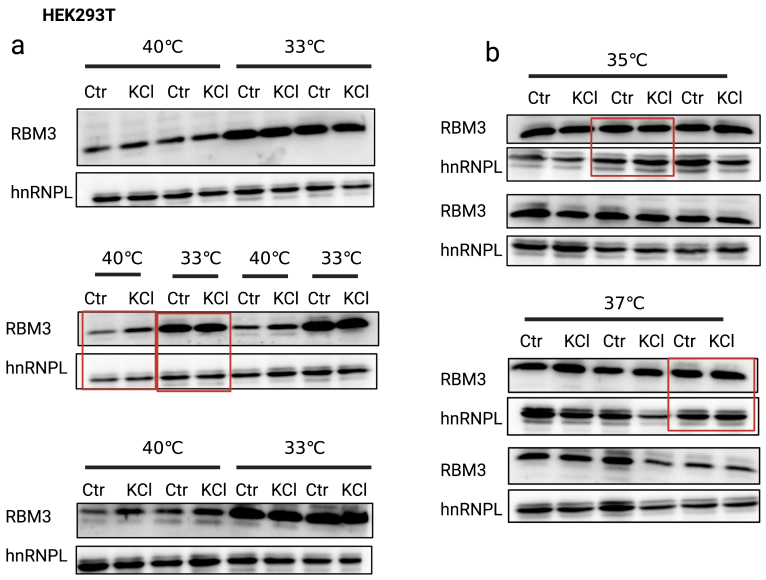

App. Fig. 12. Gel images for the quantification of Fig. 2.12. The images marked by the red rectangle are the representative images in the main figures.

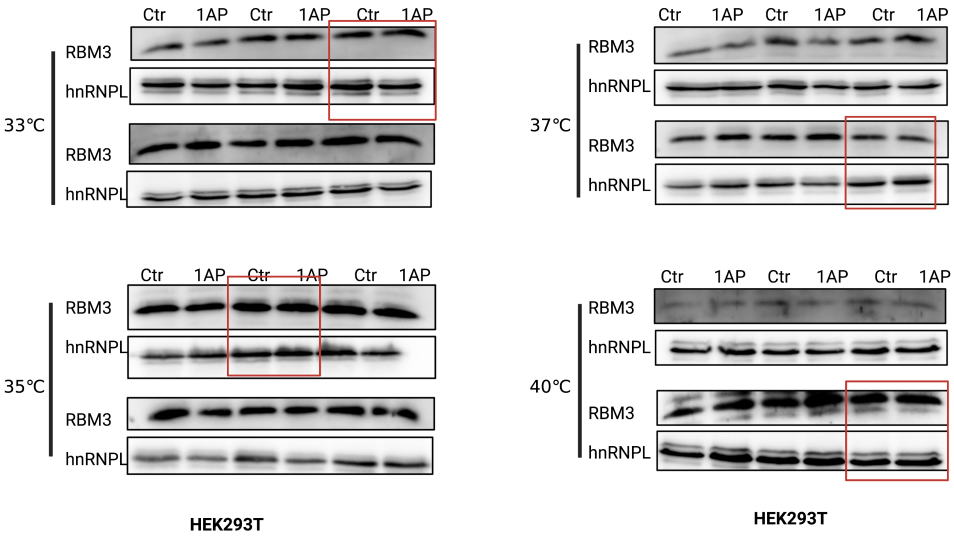

App. Fig. 13. Gel images for the quantification of Fig. 2.13. The images marked by the red rectangle are the representative images in the main figures.

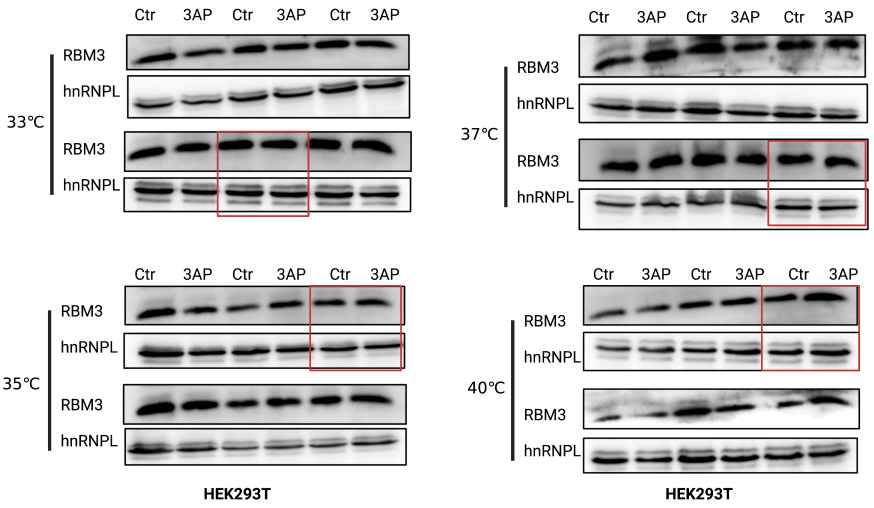

App. Fig. 14. Gel images for the quantification of Fig. 2.12. The images marked by the red rectangle are the representative images in the main figures.

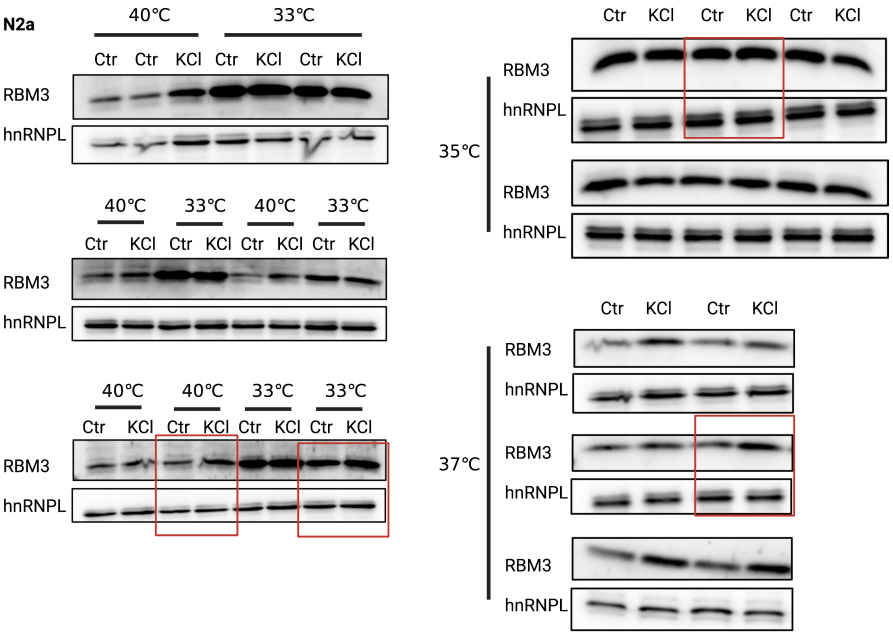

App. Fig. 15. Gel images for the quantification of Fig. 2.12. The images marked by the red rectangle are the representative images in the main figures.

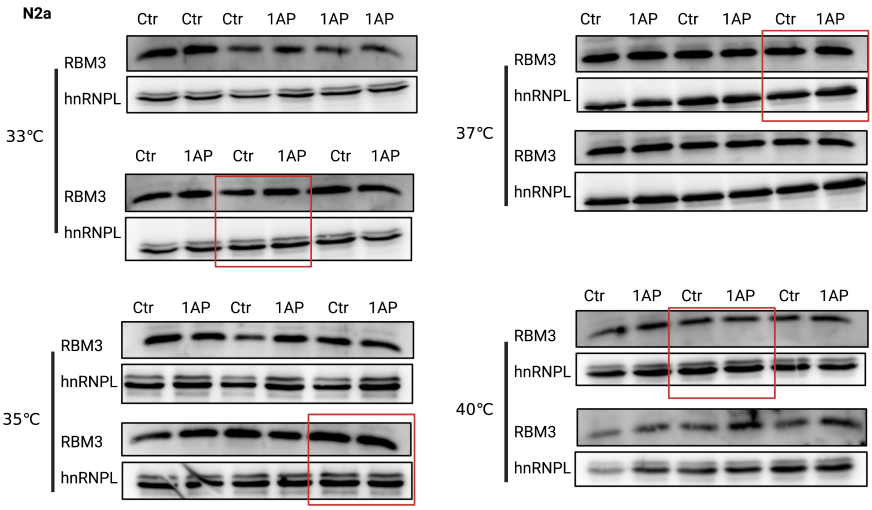

App. figure 16. Gel images for the quantification of Fig. 2.13. The images marked by the red rectangle are the representative images in the main figures.

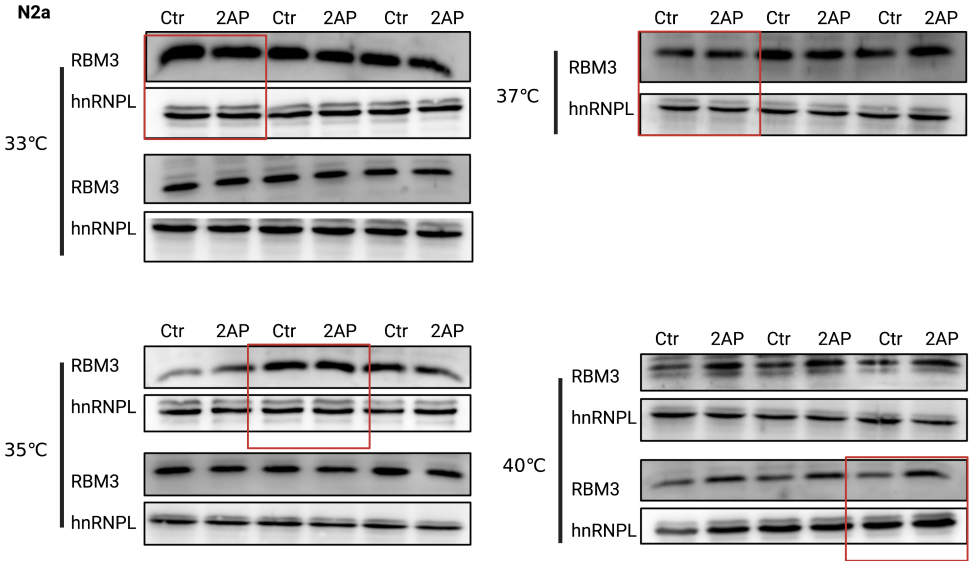

App. Fig. 17. Gel images for the quantification of Fig. 2.13. The images marked by the red rectangle are the representative images in the main figures.

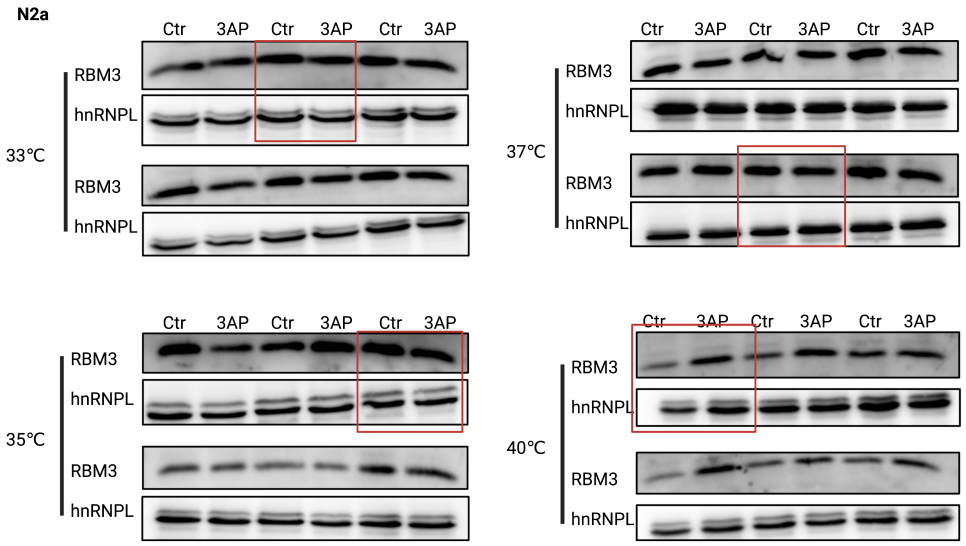

App. Fig. 18. Gel images for the quantification of Fig. 2.12. The images marked by the red rectangle are the representative images in the main figures.

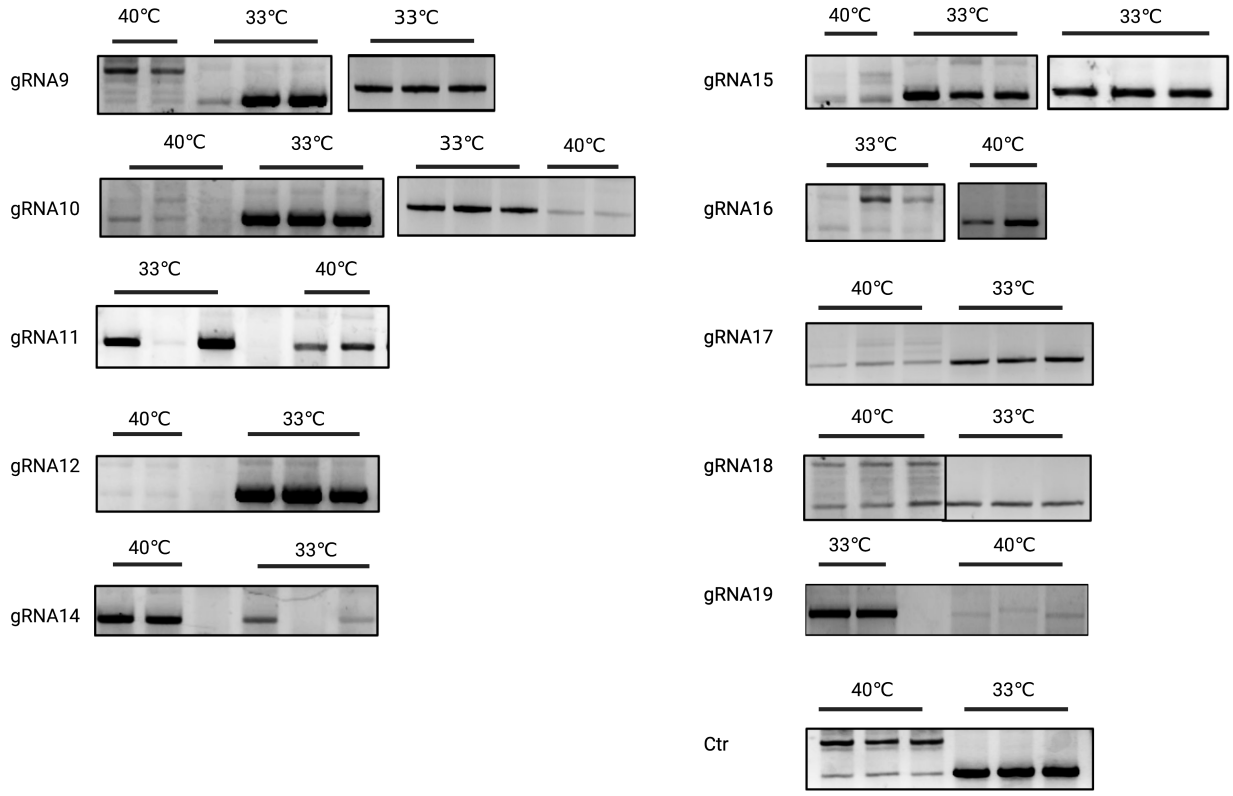

App. Fig. 19 Gel images for the quantification of Fig. 3.1c and 3.1d. The images marked by the red rectangle are the representative images in the main figures.

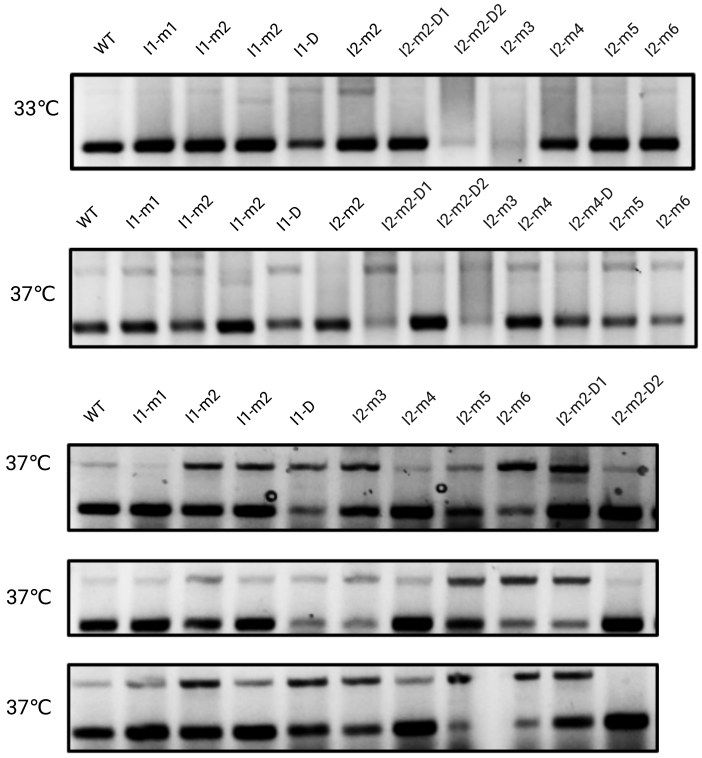

App. Fig. 20 The remaining gel images for the quantification of Fig. 3.3b.

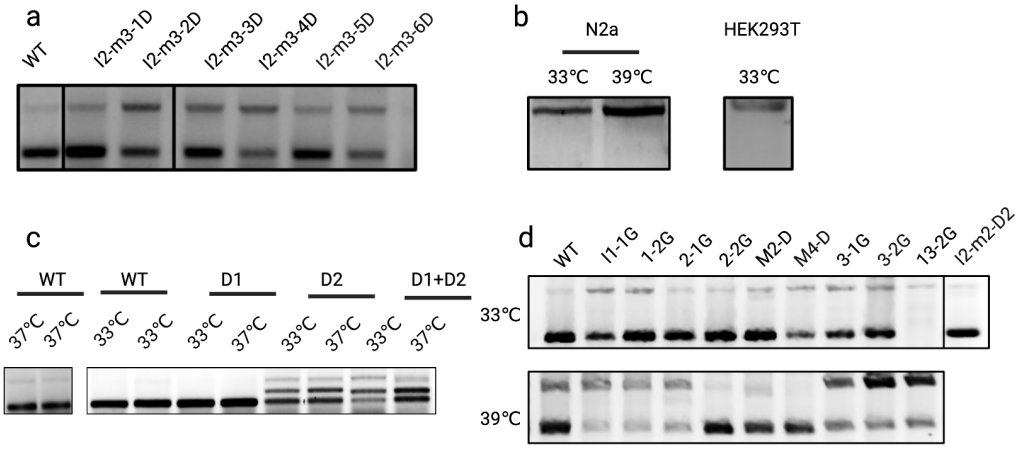

App. Fig. 21 The remaining gel images for the quantification of Fig. 3.5b (**a**), Fig. 3.4d (**b**), Fig. 3.6b (**c**) and Fig.3.7 (**d**).

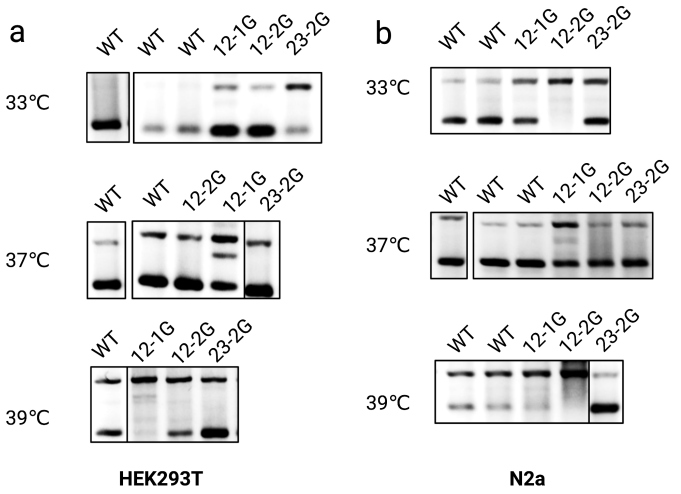

App. Fig. 22 The remaining gel images for the quantification of Fig. 3.8

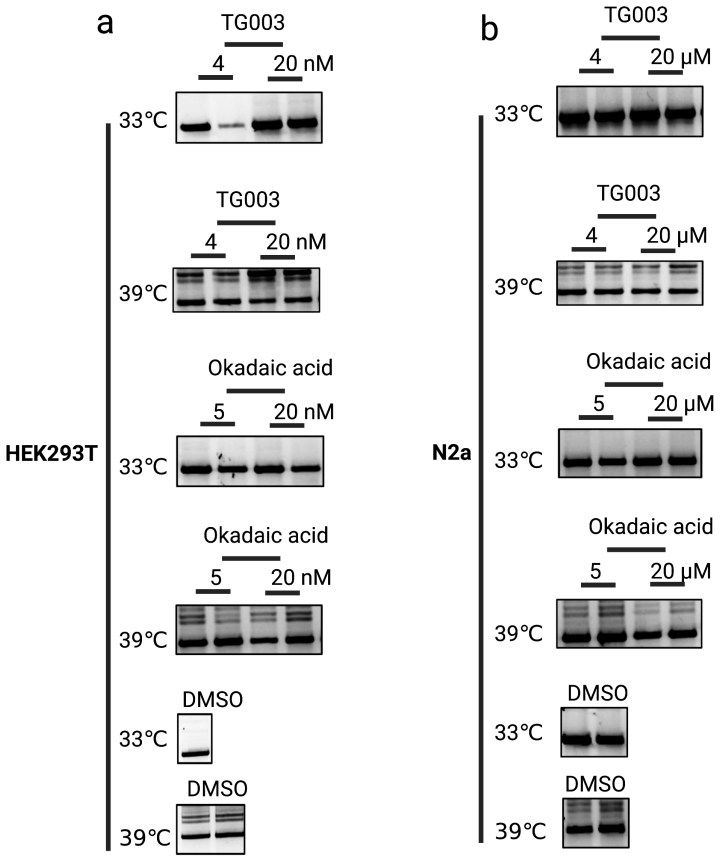

App. Fig. 23 The gel images for the quantification of Fig. 3.9